

Trace Element Geochemistry and
Geochronology of an IOCG Mineral
System: A Case Study from the Vulcan
Prospect, South Australia

Thesis submitted in accordance with the requirements of the University of
Adelaide for an Honours Degree in Geology/Geophysics

Caelan Charles Grooby

November 2020



THE UNIVERSITY
of ADELAIDE

ABSTRACT

The Vulcan prospect is a hematite-rich brecciated iron-oxide copper-gold (IOCG) prospect within the eastern Gawler Craton, South Australia, 30 km from the ca. 1590 Ma Olympic Dam IOCG system. Apatite is abundant within metamorphic clasts and in altered and mineralised rock. In-situ geochronology and trace element analyses of gangue minerals including apatite, florencite and hematite from 41 thin sections from the Vulcan prospect were investigated to determine timing of mineralising events, changes in fluid chemistry, and to evaluate similarities and differences between Vulcan and similar deposits within the eastern Gawler Craton.

Apatite petrography revealed three grain populations. Coarse-grained apatite from hematite-sericite dominated lithologies produced 461 ± 9 Ma, 510 ± 8 Ma and 544 ± 46 Ma ages coincident with the Delamarian orogeny, representing cooling during this period. Fine-grained vein-hosted apatite within hematite lithologies produced 985 ± 18 Ma and 1095 ± 10 Ma ages, coeval with late stages of the Musgravian Orogeny indicating a thermal control on the Gawler Craton. Apatite associated with magnetite-chlorite lithologies produced ages of 1522 ± 42 Ma, 1543 ± 25 Ma and 1611 ± 24 Ma within error of ca. 1580 Ma Hiltaba Suite felsic magmatism and ca. 1586 Ma molybdenite mineralisation which has an association to Cu-Au. Hematite and zircon in-situ geochronology was attempted but for a variety of reasons, failed.

Trace element analysis indicates early apatite grains are light rare earth element (LREE) enriched and this shifts to LREE-depleted, middle REE-enriched in late apatite growths. Evidence suggests LREE remobilised into florencite grains, possibly attributed to a shift from alkaline to acidic fluid conditions as documented at Olympic Dam. Hematite pseudomorphs and elemental maps of apatite support this shift. Comparison of trace element behaviour in apatite and geochronological constraints between Vulcan and Olympic Dam suggest the two mineralising systems share a similar history.

KEYWORDS

Vulcan, IOCG, Apatite, Hematite, Florencite, U-Pb Geochronology, Trace Elements.

TABLE OF CONTENTS

Abstract.....	1
Keywords.....	1
List of Figures.....	4
List of Tables.....	6
1. Introduction.....	7
2. Geological Setting.....	11
3. Methods.....	15
3.1 Sampling Procedure.....	15
3.2 Petrography.....	16
3.3 Scanning Electron Microscope (SEM).....	16
3.4 Laser Ablation Coupled Plasma Mass Spectrometry (LA-ICP-MS).....	17
Apatite.....	17
Hematite.....	18
Florencite.....	18
Zircon.....	18
3.5 Data Reduction.....	19
Geochronology.....	19
Trace Elements.....	20
4. Observations and Results.....	21
4.1 Vulcan Sample Petrography.....	21
Hematite-Rich Breccias.....	21
Magnetite-Rich Breccias.....	21
Gneissic/Mylonitic Clasts.....	22
4.2 Standards.....	26
4.3 Apatite.....	26
Apatite 1.....	26
Petrography.....	26
Trace Elements.....	27
U-Pb Geochronology.....	28
Maps.....	30
Apatite 2.....	32

Petrography.....	32
Trace Elements	32
U-Pb Geochronology	33
Apatite 3	34
Petrography.....	34
Trace Elements	35
U-Pb Geochronology	36
4.4 Hematite	38
Petrography	38
Trace Elements	38
U-Pb Geochronology.....	38
Maps	39
4.5 Magnetite	40
Petrography	40
4.6 Zircon.....	41
Petrography	41
Geochronology	42
4.7 Florencite	42
Petrography	42
Trace Elements	43
5. Discussion	44
5.1 Apatite 1 – Metamorphic Clast-hosted Apatite	44
Trace Element Signature	44
Elemental Mapping	45
Timing of Apatite Growth.....	46
5.2 Apatite 2 – Hematite-hosted Hydrothermal Apatite	47
Trace Element Signature	47
Timing of Apatite Growth.....	48
5.3 Apatite 3 – Magnetite-hosted Hydrothermal Apatite.....	48
Trace Element Signature	48
Timing of Apatite Growth.....	49
5.4 Florencite	49
Trace Element Signature	49

5.5 Hematite and Magnetite	50
Petrography	50
Trace Element Signature	51
Elemental Mapping	51
Mineralisation Timing within the Olympic Cu-Au Province.....	54
5 Conclusions and Outlook	55
Acknowledgments	56
References	56
Appendix A: Sample Descriptions	62
Appendix B: Petrography	66
Appendix C: Standards for U-Pb Geochronology.....	97
Appendix D: Apatite Trace Element Data.....	99
Appendix E: Apatite U-Pb Geochronology Data	140
Appendix F: Additional Elemental Maps.....	155
Appendix G: Hematite Trace Element Data.....	182
Appendix H: Hematite U-Pb Geochronology Data.....	195
Appendix I: Zircon U-Pb Geochronology Data	201
Appendix J: Florencite Trace Element Data.....	203

LIST OF FIGURES

Figure 1: Regional Geology Map of the Olympic Cu-Au Province within the Eastern Gawler Craton, South Australia. Geology modified from Fairclough et al. (2003) is overlain on a map of the Gawler Craton. Inset is the location of the Gawler Craton with respect to the other cratons within Australia. Modified from (Reid et al., 2013).....	9
Figure 2: Residual gravity image over the Vulcan prospect showing the distance of Vulcan from other Eastern Gawler Craton deposits. Modified from (Reid et al., 2013).	14
Figure 3: Core photos from the Vulcan prospect highlighting various textures in the prospect. a) Massive hematite breccias in VUD009. b) Blebby sulphides within a hematite-rich core from VUD009. c) Potassic alteration of host in a magnetite-rich section of core from VUD007. d) A chlorite altered clast as well as suspended metamorphic clasts within a magnetite-rich section of core from VUD007. e) Clasts of sericite-altered metamorphic material within potassic altered hematite in VUD009. f) Massive sulphides, chalcopyrite and pyrite, from VUD003. Abbreviations: Ser: sericite, MM: metamorphic, chl: chlorite, Hm: Hematite, Mg: Magnetite	23
Figure 4: Reflected light (RL) and transmitted light (TL) images of hematite and apatite textures. a) VUD009 – Sample 801: TL image of apatite grains within a metamorphic clast surrounded by massive hematite. b) VUD009 – Sample 1020: TL image of apatite	

grain with zoned inclusions surrounded by a sericite mush but bounded by bladed hematite. c) VUD009 – Sample 852: RL image of apatite 2 veins within massive hematite displaying classic bladed textures. d) VUD003 – Sample 894: RL image of granular hematite with small pyrite crystals. e) VUD016 – Sample 1091: RL image of late hematite-rich fluids overprinting grains of the host apatite. f) VUD007 – Sample 1192: RL image of magnetite-rich cores with hematite rims suggesting overprinting. Abbreviations: Qtz: quartz, Hem: hematite, Mag: magnetite, Py: pyrite, Apa: Apatite, Alb: albite, Ser: sericite 25

Figure 5: Chondrite-normalised REE plots for apatite 1 samples from laser ablation for a) 1488 samples (red). b) 801 samples (green). c) 973 samples (blue). Chondrite values are from (Boynton, 1984). 27

Figure 6: Tera-Wasserburg plots and corresponding ages of apatite 1 samples from laser ablation session. Apatite samples are as follows: a) 801. b) 1488. c) 973. The line represents the line of best fit used to calculate the common lead line. The sample population for each plot is represented by the corresponding n=..... 29

Figure 7: Elemental maps of apatite highlighting the distribution of trace elements within apatite grains from sample 801. All three apatite grains are hosted within a clast of metamorphic material, mainly quartz and albite. Maps of grain A) and B) depict euhedral apatite grains within these clasts whereas grain C) depicts apatite that is forming a vein structure within the clast. All values are in ppm unless otherwise specified..... 32

Figure 8: Chondrite-normalised REE plot for apatite 2 samples from laser ablation for a) 852 samples (light blue). b) 973 samples (pink). Chondrite values are from (Boynton, 1984). 33

Figure 9: Tera-Wasserburg plots and corresponding ages of apatite 2 samples from laser ablation. Apatite samples are as follows: a) 852. b) 973. The line represents the line of best fit used to calculate the common lead line. The sample population for each plot is represented by the corresponding n=..... 34

Figure 10: Chondrite-normalised REE plot for apatite 3 samples from laser ablation session for a) 1084 samples (red). b) 1183 samples (green). c) 1210 samples (dark blue). Chondrite values are from (Boynton, 1984). 35

Figure 11: Tera-Wasserburg plots and corresponding ages of apatite 3 samples from laser ablation. Apatite samples are as follows: a) 1084. b) 1183. c) 1210. The line represents the line of best fit used to calculate the common lead line. The sample population for each plot is represented by the corresponding n=..... 37

Figure 12: Elemental maps of hematite highlighting the distribution of trace elements within hematite grains from sample 994 and 973. Grain A depicts hematite from sample 994 and is defined by multiple stages of growth intergrown with metamorphic material. Grain B depicts a hematite grain from Sample 973 that has formed within a hematite, albite, quartz, apatite breccia. All values are in ppm unless otherwise specified..... 40

Figure 13: BSE images of florencite and zircon grains from SEM analyses. a) intergrown florencite and quartz grains from sample 801. b) Florencite infill of a fracture within massive hematite associated with barite from sample 852. c) A zircon grain that has crystallised inside a metamorphic fragment of quartz with an apatite grain from sample 801. d) A zircon grain within a hematite-rich breccia from sample 973. Abbreviations: Flo: florencite, Bar: barite, Zir: zircon, Hem: hematite, Apa: apatite.... 41

Figure 14: Chondrite-normalised REE plots for florencite samples from laser ablation for a) 801 samples (red). b) 852 samples (green). c) 973 samples (blue). Chondrite values are from (Boynton, 1984). 44

Figure 15: Time space plot of geochronology data from prospects and deposits within the Olympic Cu-Au Province. Geochronology from Vulcan, Olympic Dam, Acropolis, Wirrda Well and Oak Dam is displayed. Vulcan: Cambrian apatite recorded dates of 461.78 ± 16.29 Ma, 525.0 ± 82.10 Ma, 520.39 ± 12.89 Ma (this study), Late Mesoproterozoic apatite had ages of 1087.04 ± 12.61 Ma, 981.10 ± 31.30 Ma (this study), and Middle Mesoproterozoic apatite recorded ages of 1546.10 ± 39.20 Ma, 1627.50 ± 36.30 Ma, 1546.40 ± 59.90 Ma (this study). Re-Os dating of molybdenite showed an age of ~ 1586 from (Reid et al., 2013). SHRIMP U-Pb analysis of zircon grains from across the Vulcan prospect recorded ages of ~ 1820 Ma, ~ 1920 Ma, ~ 1980 Ma, ~ 2190 Ma (Jagodzinski, 2005). Olympic Dam: Fluroapatite, ~ 1.59 Ga (Apukhtina et al., 2017), ~ 0.82 Ga (Apukhtina et al., 2016; Huang et al., 2015), ~ 0.44 - 0.48 Ga (Kamenetsky et al., 2015). Chalcopyrite dated at ~ 1.26 Ga by Re-Os (McInnes et al., 2008). Hematite U-Pb at ~ 1.59 - 1.58 Ga (Apukhtina et al., 2017; Ciobanu et al., 2013; L. Courtney-Davies et al., 2019). U-Pb dating of magnetite revealed ~ 1.76 Ga (Courtney-Davies et al., 2020; L. Courtney-Davies et al., 2019); ~ 1.59 Ga magmatic hematite inferred from dating of surrounding minerals (Apukhtina et al., 2017). Vein hosted xenotime at ~ 1.08 Ga (Cherry et al., 2017). Hydrothermal monazite dated at ~ 0.44 - 0.48 Ga (Kamenetsky et al., 2015). U-Pb dating of zircon revealed hydrothermal and magmatic zircon at ~ 1.59 Ga; hydrothermal zircon at ~ 1.14 Ga and other zircon grains at 0.49 Ga (Jagodzinski, 2014). Uraninite at OD is dated at ~ 1.59 Ga (Apukhtina et al., 2017), ~ 1.4 - 1.3 Ga, ~ 1.22 Ga, ~ 0.83 Ga and ~ 0.57 Ga (Johnson, 1993). Acropolis: Monazite U-Pb dating reveals two ages at acropolis at ~ 0.43 - 0.53 Ga and ~ 1.37 - 1.44 Ga (Cherry et al., 2018). U-Pb dating of hematite produced a date of ~ 1.59 Ga (L. Courtney-Davies et al., 2019). U-Pb dating of apatite at Acropolis dates apatite at ~ 1.59 Ga (Cherry et al., 2018). Xenotime dated at ~ 1.38 Ga (Cherry et al., 2018). TIMS zircon dating shows dates of ~ 1.59 Ga for Acropolis (McPhie et al., 2020). Wirrda Well: Hematite U-Pb dating gains an age of ~ 1.62 Ga (L. Courtney-Davies et al., 2019).
 Caption modified from (Maas et al., 2020). 53

LIST OF TABLES

Table 1: Parameters used for SEM sessions that were completed during this study..... 17
 Table 2: Parameters used during the LA-ICP-MS sessions for Apatite, Hematite, Florencite, Zircon and elemental maps. Parameters in red were used for Florencite trace element analysis spots. Standards in bold were used as the primary standards. 19
 Table 3: Vulcan Prospect samples used for SEM and LA-ICP-MS analysis within this project and the mineralogy and alteration assemblage of each. 24

1. INTRODUCTION

Iron-Oxide Copper-Gold (IOCG) deposits are defined by mineralisation containing >10% of low-Ti Fe-oxides correlated with elevated contents of copper, gold, rare earth elements (REEs), phosphorous, uranium, silver, and cobalt (Barton, 2014; Groves et al., 2010). IOCG deposits span a wide range in ages from Archean to Cenozoic (Barton, 2014; Barton & Johnson, 1996). IOCG deposits are formed by hydrothermal processes resulting in intense brecciation and structurally controlled deposit styles, as well as disseminated and in massive lenses (Barton, 2014; Groves et al., 2010; Mumin et al., 2007; Ruiz & Ericksen, 1962; Sillitoe, 2003; Simon et al., 2018; Williams et al., 2005). The origin of hydrothermal ore fluids in the formation of IOCG deposits remains poorly constrained. Various studies suggest an involvement in meteoric, evaporitic, and magmatic-hydrothermal fluids, or a combination of these (Barton, 2014; Simon et al., 2018; Williams et al., 2005). IOCGs exhibit a large variation in geological settings and mineralising fluid compositions (Barton, 2014; Groves et al., 2010). Some districts contain Cu-poor magnetite ores with adjacent shallow hematite ores, more commonly known as Iron-Oxide Apatite (IOA) deposits (Barton & Johnson, 2000; Parak, 1975).

In the Gawler Craton, South Australia, many IOCG style deposits including Olympic Dam (OD), Prominent Hill, Carrapateena and Oak Dam make up the “Olympic Cu-Au Province” (Figure 1; Reid et al., 2013; Skirrow et al., 2007; Skirrow et al., 2002).

Within the province, deposits share comparable mineralogy, fluid composition and geochronology (Reid et al., 2013; Skirrow et al., 2007; Skirrow et al., 2002). The presence of these deposits link the region to lithospheric scale magmatic-hydrothermal

system which formed due to dominantly felsic magmas of the Gawler Range Volcanics and Hiltaba Suite (Hand et al., 2007; Reid et al., 2013).

Little geochronology and trace element geochemistry on ore and gangue minerals has been undertaken on these Gawler Craton IOCG-style deposits, with the exception of a considerable body of work at OD (Apukhtina et al., 2016; L. Courtney-Davies et al., 2019; Krneta, 2017; Reid et al., 2013; Verdugo-Ihl et al., 2017). Therefore there is a lack of understanding of mineralisation ages and fluid chemistry across the Olympic Cu-Au Province.

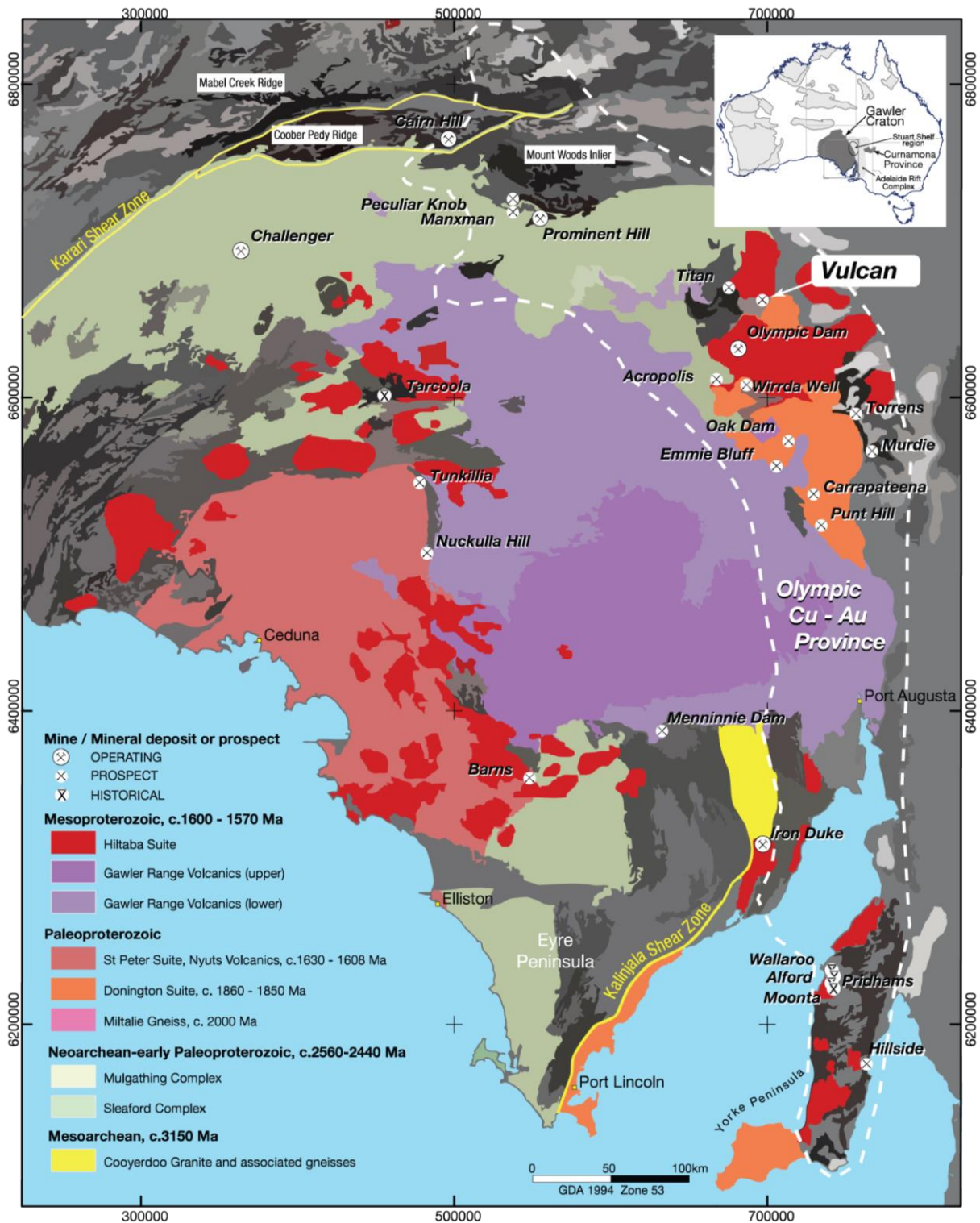


Figure 1: Regional Geology Map of the Olympic Cu-Au Province within the Eastern Gawler Craton, South Australia. Geology modified from Fairclough et al. (2003) is overlain on a map of the Gawler Craton. Inset is the location of the Gawler Craton with respect to the other cratons within Australia. Modified from (Reid et al., 2013).

Apatite, a calcium phosphate mineral is prevalent in both magmatic, sedimentary and metamorphic rocks (Chew et al., 2014; Kirkland et al., 2018). Coupled with its ability to host uranium (U) apatite is useful as both a U-Pb geochronometer and thermochronometer (Chew & Spikings, 2015; Corfu & Stone, 1998; Kirkland et al., 2017; Kirkland et al., 2018; Mark et al., 2016; Schoene & Bowring, 2007). Apatite has a typical closure temperature of around 375-600° and therefore can provide information on retrograde or low-temperature processes (Cochrane et al., 2014; Schoene & Bowring, 2007). Apatite can accommodate high concentrations of REEs, U, Th, Sr, and Mn as well as other trace elements (Fleet & Pan, 1997; Gawęda et al., 2014; Kirkland et al., 2018; Mao et al., 2016; Piccoli & Candela, 2002). This ability makes it a powerful mineral in understanding the trace element chemistry of low temperature fluids and constraining the source of minerals (Fleet & Pan, 1997; Gawęda et al., 2014; Kirkland et al., 2018; Mao et al., 2016; Piccoli & Candela, 2002). Apatite trace element work at OD by S. Krneta et al. (2017) concluded that apatite geochemistry, evolution and petrography can play a key role in characterising the development of the ore system.

Hematite is a common Fe-oxide in many ore systems and most abundant in IOCG, IOA and banded iron deposits (Barton, 2014; Groves et al., 2010). Uranium bearing hematite from OD was recently dated via the laser-ablation inductively-coupled plasma mass spectrometry (LA-ICP-MS) U-Pb method through the use of a new hydrated ferric oxide (HFO) standard. Providing absolute constraints on timing of Fe-oxides at the deposit (Apukhtina et al., 2017; Ciobanu et al., 2013; Cook et al., 2016; Liam Courtney-Davies et al., 2019; Courtney-Davies et al., 2016; Verdugo-Ihl et al., 2017). Hematite is also commonly zoned with OD samples zoned in REE, U, Sn, W and Mo as well as

other trace elements thus providing insight into the evolution of fluid over time (Liam Courtney-Davies et al., 2019; Verdugo-Ihl et al., 2017).

Vulcan (Figure 1) is a hematite breccia-rich Cu-Au prospect within the Eastern Gawler Craton which is located 30 km northeast of OD (Reid et al., 2013). Reid et al. (2013) utilised Re-Os dating of molybdenite to constrain timing of sulphide deposition at ca. 1586 Ma. Little is known about the prospect regarding the timing of post ore events and the chemistry of the ore bearing fluids.

In this study apatite and hematite U-Pb geochronology and trace element analysis were undertaken to derive the timing of apatite and hematite mineralisation and changes in fluid chemistry for hematite and magnetite-rich endmember alteration systems at Vulcan. Using the data gained from apatite and hematite U-Pb geochronology and trace element analysis this study aims to explore similarities and differences between Vulcan, OD and other deposits within the Olympic Cu-Au Province.

2. GEOLOGICAL SETTING

The Gawler Craton is the major crustal province within southern Australia, composed of rocks ranging from Late Archean to the Mesoproterozoic (Hand et al., 2007). Younger Neoproterozoic and Phanerozoic sediments overlie much of the older Archean and Mesoproterozoic units within the craton, leaving little accessible geological evidence in some parts of the craton for the older events.

The development of the Gawler Craton can be separated into two major phases (Hand et al., 2007):

1. A Late Archean complex 'nucleus' (2550–2500 Ma).

Late Archean rocks form a ‘nucleus’ within the Gawler Craton and have been divided into two separate complexes, the Mulgathing in the central-west of the craton and the Sleaford in the south (Hand et al., 2007; Payne et al., 2008; Greg Swain et al., 2005).

These complexes are dominated by aluminous metasedimentary, volcanic and granite–greenstone lithologies (2560–2500 Ma) (Hand et al., 2007; Payne et al., 2008; Greg Swain et al., 2005) that were both deformed during the ca. 2460–2430 Ma Sleafordian Orogeny (Daly, 1998; Hand et al., 2007; McFarlane, 2006; Payne et al., 2008).

Between and around these two complexes, the Gawler Craton records stable geological activity with a period of an essentially unchanging cratonic system from 2400–2000 Ma (Hand et al., 2007). The only known geologic event is the ca 2000 Ma Miltalie Gneiss in the east (Daly, 1998; C. Fanning et al., 2007; Hand et al., 2007; Howard, 2006; Payne et al., 2008).

2. Late Paleoproterozoic and Early Mesoproterozoic (1900–1450 Ma) felsic magmatism.

The majority of material within the Gawler Craton is of Late Proterozoic or Early Mesoproterozoic age, and largely intrude and overlie the Archean core (Hand et al., 2007). Deposition of the Hutchison Group unconformably overlies the Miltalie Gneiss indicating the maximum age of deposition to be 2000 Ma in the eastern Gawler Craton (Daly, 1998; C. Fanning et al., 2007; Hand et al., 2007; Payne et al., 2008). This was followed by the ca. 1850 Ma Donington Suite intrusion and Cornian Orogeny (Hand et al., 2007; Payne et al., 2008; Reid et al., 2006) and then subsequent onset of magmatism and deformation due to the Kimban Orogeny from ca. 1730–1690 Ma (Daly, 1998; Ferris et al., 2002; Hand et al., 2007; Payne et al., 2008; GM Swain et al., 2005; Vassallo & Wilson, 2001, 2002). After these orogenic events there was a subsequent

period of sedimentary deposition across the eastern Gawler Craton which included the ca. 1760–1740 Ma Wallaroo Group (Daly, 1998; Hand et al., 2007; J. L. Payne et al., 2006; Payne et al., 2008). Sedimentation was followed by late to post-tectonic magmatism of the ca. 1690–1670 Ma Tunkillia Suite (Ferris, 2001; Hand et al., 2007; J. Payne et al., 2006; Payne et al., 2008) and development of ca. 1630–1615 Ma arc-like magmatism of the St Peter Suite, which dominates the south-western section of the Gawler Craton (Hand et al., 2007; Payne et al., 2008). Extensive felsic magmatism of the Gawler Range Volcanics ca. 1590 Ma and Hiltaba Suite ca. 1595–1575 Ma was emplaced across the eastern Gawler Craton (Allen et al., 2003; Creaser, 1995; Hand et al., 2007; Payne et al., 2008).

The eastern Gawler Craton hosts multiple IOCG deposits including, OD, Oak Dam, Acropolis, Carrapateena and Prominent Hill as well as many other prospects. The presence of these systems are used to support the hypothesis of a N-S trending Olympic Cu-Au province (Skirrow et al., 2002). This province is generally accepted to be spatially and temporally associated with a magmatic event termed the Gawler Silicic Large Igneous Province consisting of extrusive and intrusive magmatism at approximately 1600–1580 Ma which includes the Hiltaba Suite and Gawler Range Volcanics units (Allen et al., 2008; Blissett et al., 1993; Fanning et al., 1988; Verdugo-Ihl et al., 2019; Wade et al., 2012). OD and smaller IOCG deposits within the Olympic Cu-Au province are generally hosted within Hiltaba Suite granitoid plutons and are characterised by a large magnetic anomaly (Hayward & Skirrow, 2010; Johnson & Cross, 1995). Deposits in the Olympic Cu-Au Province all occur close to deep and long

NW–ENE trending structures which have been interpreted as the conduit to fluid flow for Cu-Au mineralisation (L. Courtney-Davies et al., 2019; Hayward & Skirrow, 2010).

The Olympic Dam Breccia Complex (ODBC) within the Roxby Downs Granite hosts the orebody of the OD deposit (Reeve et al., 1990; Verdugo-Ihl et al., 2019). OD is defined by a subsurface breccia around a dense Fe-rich core with lateral and vertical sulphide zonation relative to the Fe-rich core (Hitzman, 2000; Reeve et al., 1990; Verdugo-Ihl et al., 2019). The main Fe-oxide within the deposit is hematite, regardless of economic mineralisation, with magnetite present and more dominant at depth and towards the deposit margins (Ciobanu et al., 2015; Ehrig et al., 2013; Verdugo-Ihl et al., 2017).

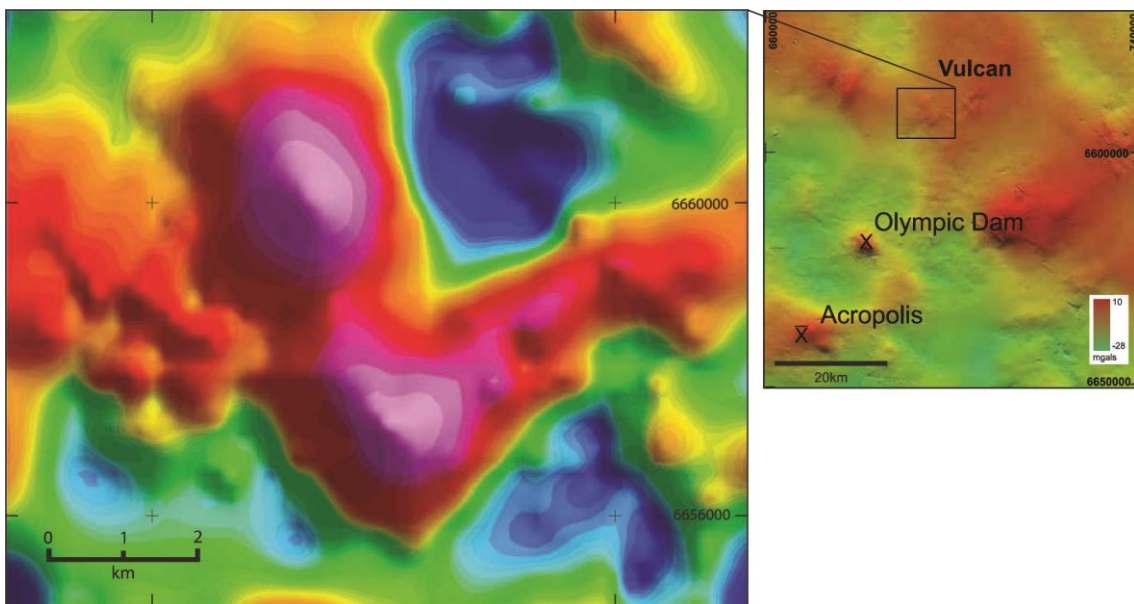


Figure 2: Residual gravity image over the Vulcan prospect showing the distance of Vulcan from other Eastern Gawler Craton deposits. Modified from (Reid et al., 2013).

The Vulcan prospect is similar to OD in that it is a subsurface breccia defined by a Fe-oxide-rich core, implying that there is a possible continuation of the hematite breccia

over the entire anomaly (Figure 2; Reid et al., 2013). The prospect is considered to have two endmembers of mineralisation (Reid et al., 2013):

1. Magnetite \pm Hematite with Chlorite and Sericite
2. Hematite with Sericite, Chalcopyrite, Bornite, Pyrite, Chlorite, Quartz and Molybdenum

The high grade zones of mineralisation at Vulcan occur within the hematite-dominant endmember, with magnetite endmembers being far less common. This endmember comprises a hematite breccia which encompasses a fine grained hematite-sericite-chlorite-rich matrix that surrounds clasts of quartz, carbonates and sulphides (Reid et al., 2013).

Previous research has given a molybdenite Re-Os date of 1586 ± 8 Ma for the timing of Cu-Au mineralization and the related hematite brecciation at Vulcan. This result indicates that the formation was part of the same early Mesoproterozoic magmatic event in which many deposits within the Olympic Cu-Au province were also formed (Reid et al., 2013). The granitic protolith at Vulcan has been constrained to 1743 ± 7 Ma which was thought to be the Moonta Porphyry or the Burkitt Granite (C. M. Fanning et al., 2007; Fraser & Neumann, 2010; Reid et al., 2013). However, there has been no study into either the magnetite dominant endmembers, or the fluid sources for the Vulcan prospect.

3. METHODS

3.1 Sampling Procedure

Sampling from the Vulcan prospect was completed at Fortescue Metals Group core library during March and April of 2020. Samples for REE mineral analysis were

selected based on analysis of downhole geochemical core assays that highlighted areas with high concentrations of REEs. Samples were collected from host lithologies, alteration zones, breccia zones and dyke structures (Sample descriptions available in Appendix A). 43 core samples were taken from six different drillholes (VUD001, VUD003, VUD007, VUD009, VUD016 and VUD017), representing a comprehensive array of samples that highlight the textural and mineralogical variation in the deposit. The textural variety in the samples range from hematite-rich to magnetite-rich breccias. 41 samples taken were cut into thin section blocks and sent to Adelaide Petrographics to be made into 30 μm polished thin sections.

3.2 Petrography

Samples were characterised using an Olympus BX51 System Microscope which allows for both reflected light and transmitted light analyses. An attached DP21 Microscope digital camera was used to take photomicrographs of different minerals and textures in order to determine the grains to be analysed. Thin sections used for analysis in this study are described in Table 3. Complete petrographic descriptions of each sample are available in Appendix B.

3.3 Scanning Electron Microscope (SEM)

Samples were imaged using a FEI Quanta 600 SEM-MLA. Images were primarily used to identify hematite, magnetite and apatite textures as well as REE-bearing phases within the selected thin sections. Electron backscatter maps and MLA map images were produced using specifications overviewed in Table 1.

Method	Mineral Liberation Analysis Session 1	Mineral Liberation Analysis Session 2
Samples	VUD009: 801, 852, 973, 994	VUD007: 1084, 1183 VUD016: 1488 VUD017: 1210
Spot Size	7	7.1
Beam Energy	24.92kV	24.88kV
Working Distance	10	10.1
Minimum Grain Size	1µm	1µm

Table 1: Parameters used for SEM sessions that were completed during this study

3.4 Laser Ablation Coupled Plasma Mass Spectrometry (LA-ICP-MS)

Two LA-ICP-MS sessions were used to determine elemental composition of REE-bearing minerals (apatite and florencite), hematite and zircon. Simultaneous geochronological measurements of apatite, zircon and hematite were made during these analyses. A separate laser session was used to create elemental maps of euhedral hematite and apatite grains. The details for the LA-ICP-MS specifications is outlined in Table 2.

APATITE

Methods adapted from Chew et al. (2014) and S. Krneta et al. (2017) were used for LA-ICP-MS work with adjustments made for the equipment that is available at Adelaide Microscopy (Table 2). Apatite was ablated for elemental composition by spot analyses of euhedral grains as well as simultaneous geochronological measurements of ^{201}Hg , ^{204}Pb , ^{206}Pb , ^{207}Pb , ^{232}Th and ^{238}U isotopes. Elemental maps of apatite were also conducted on several samples. Mapping was completed by ablating sets of parallel lines in a grid across the target area and/or grain.

HEMATITE

Methods adapted from Liam Courtney-Davies et al. (2019) and Verdugo-Ihl et al. (2019) were used for LA-ICP-MS work with adjustments made according to the specifications of the equipment at Adelaide Microscopy (Table 2). Hematite was analysed firstly for geochronology using ^{201}Hg , ^{204}Pb , ^{206}Pb , ^{207}Pb , ^{232}Th and ^{238}U isotopes. Elemental maps of various euhedral hematite grains were conducted on a subsequent laser ablation session due to the requirement of a change to the configuration of the laser. Mapping was completed by ablating sets of parallel lines in a grid across the target area and/or grain.

FLORENCITE

Florencite was ablated for elemental analysis according to methods adapted from Schmandt et al. (2019), adjusted for a more comprehensive analysis. A smaller spot size (13 μm) was used for florencite compared to apatite (Table 2).

ZIRCON

Methods from Paton et al. (2010) were used for LA-ICP-MS analysis. Zircon was ablated for simultaneous measurements of elemental composition as well as isotopes for geochronology (^{201}Hg , ^{204}Pb , ^{206}Pb , ^{207}Pb , ^{232}Th and ^{238}U). Details for zircon analyses are documented further in Table 2.

LA-ICP-MS Parameters				
Mineral	Apatite and Florencite	Zircon	Hematite	Elemental Maps
Laser Wavelength	193 nm	193 nm	193 nm	193 nm
Pulse Duration	20 ns	20 ns	20 ns	20 ns
Spot Size	30 μm 13μm	20 μm	30 μm	17 μm or 11 μm
Laser Energy	195 mJ	110 mJ	110 mJ	195 mJ
Repetition Rate	5 Hz	5 Hz	5 Hz	10 Hz
Fluence	3.5 J/cm ²	2 J/cm ²	3.5 J/cm ²	3.5 J/cm ²
Background Collection	30 s	30 s	30 s	30 s
Ablation Time	30 s	30 s	30 s	Variable
Scanned Masses	29, 31, 43, 51, 55, 57, 88, 89, 90, 139, 140, 141, 146, 147, 153, 157, 159, 163, 165, 166, 169, 172, 175, 178, 201, 204, 206, 207, 208, 232, 238	27, 29, 49, 57, 89, 91, 139, 140, 141, 146, 147, 153, 157, 159, 163, 165, 166, 169, 172, 175, 178, 202, 204, 206, 207, 208, 232, 238	24, 27, 29, 31, 43, 49, 51, 55, 57, 59, 60, 65, 66, 75, 88, 89, 90, 93, 95, 118, 137, 139, 140, 141, 146, 147, 153, 157, 159, 163, 165, 166, 169, 172, 175, 178, 181, 182, 204, 206, 207, 208, 232, 238	24, 27, 29, 31, 43, 45, 49, 51, 55, 57, 59, 60, 66, 69, 75, 88, 89, 90, 93, 95, 118, 137, 139, 140, 141, 146, 147, 153, 157, 159, 163, 165, 166, 169, 172, 175, 178, 181, 182, 206, 208, 232, 238
Standards	NIST610 , 401, Madagascar , McClure Mountain, NIST610	GJ , Pleovice, 91500, NIST610	GJ , GSD , HFO (Liam Courtney-Davies et al., 2019)	GSD was used for Hematite and Magnetite Maps NIST612 was used for Apatite Maps

Table 2: Parameters used during the LA-ICP-MS sessions for Apatite, Hematite, Florencite, Zircon and elemental maps. Parameters in red were used for Florencite trace element analysis spots. Standards in bold were used as the primary standards.

3.5 Data Reduction

GEOCHRONOLOGY

LA-ICP-MS data was processed using Laser Ablation Data Reduction (LADR) software (Norris Scientific) (Norris & Danyushevsky, 2018). Isoplot (Ludwig, 2003) was used for both hematite and apatite to create Tera-Wasserburg plots and calculate the weighted mean age for apatite and hematite.

Geochronology methods within this study follow procedures that Chew et al. (2014) have outlined. The unanchored intercept of this line with the y-axis of the concordia

represents the assumed initial common Pb within the system ($^{207}\text{Pb}/^{206}\text{Pb}$ ratio). Where the line intercepts with the x-axis, this estimates the U-Pb formation age of the population (Chew et al., 2014). Isoplot was used to create Tera-Wasserburg plots for apatite (Ludwig, 2003).

For apatite U-Pb geochronology, Madagascar apatite (U-Pb TIMS 473.5 ± 0.7 Ma; (Chew et al., 2014)) was utilised as the primary standard and two secondary apatite standards 401 apatite (524.7 ± 7.8) and McClure Mountain apatite (U-Pb TIMS 523.51 ± 1.47 Ma; (Schoene et al., 2006)) were used to perform accuracy checks. The NIST610 standard was used as a primary standard within the apatite LA-ICP-MS run to calculate the trace element data. Data that was not within concordia space or contained less than 0.5ppm Ca or ^{238}U was not used for age calculation.

Hematite geochronology methods were adapted from Liam Courtney-Davies et al. (2019). The primary standards are the Hydrated Ferric Oxide (HFO) that was developed by Liam Courtney-Davies et al. (2019) and the GJ-1 zircon (Jackson et al., 2004). The secondary reference standard used was GSD-1G basalt glass (Jochum et al., 2005). Zircon geochronology was completed using the GJ-1 zircon (Jackson et al., 2004) as the primary reference material, while 91500 (Wiedenbeck et al., 1995) and Plešovice (Sláma et al., 2008) were analysed as secondary reference materials.

TRACE ELEMENTS

Trace element maps of apatite, hematite and magnetite were produced using the Iolite software package (Paton et al., 2011). The composition of these grains was calculated using the internal Iolite function *Trace Element_IS DRS* system (Paton et al., 2011), using a standard value of 39.36 wt% Ca in apatite, 69.94 wt% Fe in hematite and 72.36 wt% Fe in magnetite.

4. OBSERVATIONS AND RESULTS

4.1 Vulcan Sample Petrography

The Vulcan prospect cores examined are defined by subsurface hematite-rich and magnetite-rich breccias with abundant sericite, chlorite and potassium feldspar (potassic) alteration. The dominant lithologies are:

HEMATITE-RICH BRECCIAS

These breccias can range from massive 60–80% hematite (Figure 3a) overprinting previous host material, to 20–30% hematite with clasts of quartz and albite-rich material. Hematite grains range in size from 2–3 cm grains to 10–20 μm disseminations. Hematite has a tendency to form classic bladed structures, especially noticeable on the edges or toward the edges of grains. The sulphides, chalcopyrite and pyrite are common as small 10 μm crystals within the matrix. Overall, these lithologies are dominated by hematite, apatite, albite, quartz, barite, florencite and minor blebby sulphides (Figure 3b). Sericite alteration is the most common alteration style but potassic alteration is also seen.

MAGNETITE-RICH BRECCIAS

Magnetite breccias are defined by 20–100 μm magnetite crystals often with hematite rims around grains within a dolomite-rich and chlorite-rich matrix. These breccias are in general coarser-grained than hematite-only lithologies and contain 1–2 cm clasts composed of metamorphic minerals (albite, chlorite, apatite and dolomite) (Figure 3d, 3e). These lithologies are always dominated by widespread chlorite alteration of any remaining host material and often are altered by potassic alteration (Figure 3c, 3d). The

sulphides chalcopyrite and pyrite are far more common than in lithologies with hematite only and form large 50–100 μm crystals within the breccia matrix. Sulphides are commonly veined through these sections, forming massive mineralisation (Figure 3f). Magnetite, hematite, chlorite, dolomite, quartz, sulphides and apatite are the most common minerals within this breccia.

GNEISSIC/MYLONITIC CLASTS

Gneissic metamorphic material is common throughout the core. These metamorphic clasts are strongly foliated and often contain porphyroblasts of apatite. This lithology is often extremely fine grained up to mylonitic in texture and is dominated by albite, chlorite and quartz (Figure 3e). Often sections will contain very little to no Fe-oxides but will still record minor potassic alteration. The main alteration style is chlorite-sericite.

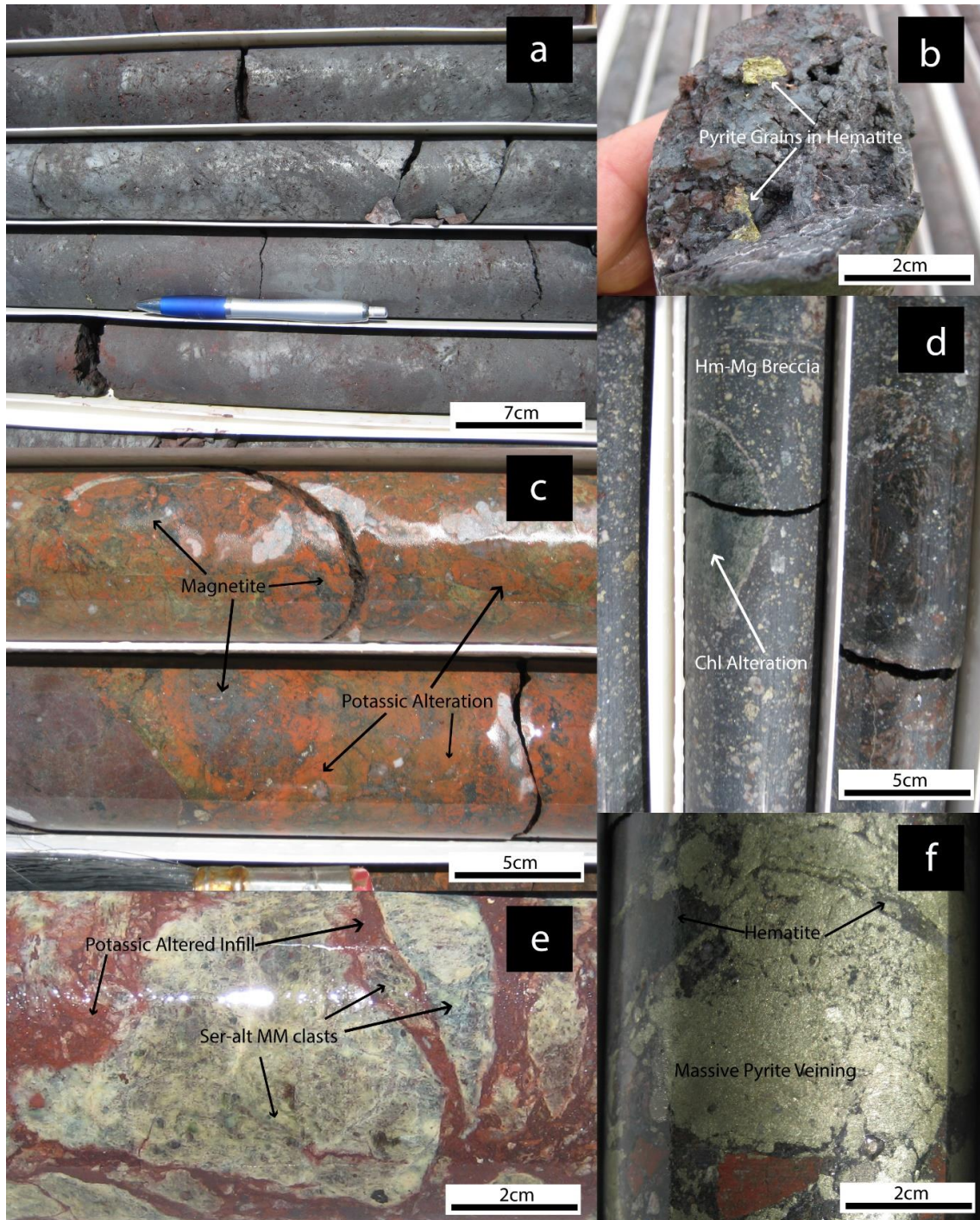


Figure 3: Core photos from the Vulcan prospect highlighting various textures in the prospect. a) Massive hematite breccias in VUD009. **b)** Blebby sulphides within a hematite-rich core from VUD009. **c)** Potassic alteration of host in a magnetite-rich section of core from VUD007. **d)** A chlorite altered clast as well as suspended metamorphic clasts within a magnetite-rich section of core from VUD007. **e)** Clasts of sericite-altered metamorphic material within potassic altered hematite in VUD009. **f)** Massive sulphides, chalcopyrite and pyrite, from VUD003. Abbreviations: Ser: sericite, MM: metamorphic, chl: chlorite, Hm: Hematite, Mg: Magnetite

Representative samples were taken for analysis from both hematite-rich and magnetite-rich endmembers. Table 3 presents the thin sections used for analysis within this project and the mineralogy and alteration assemblage of each.

Hole	Sample	Mineralogy	Alteration Assemblage	Used for
VUD009	801	Hematite, Florencite, Albite, Apatite, Quartz, Sulphides, Zircon	Sericite Alteration	Apatite U-Pb Geochronology/Trace Elements, Apatite Mapping, Florencite Trace Elements, Zircon U-Pb Geochronology
VUD009	852	Hematite, Florencite, Barite, Apatite, Quartz, Sulphides	Sericite Alteration	Apatite U-Pb Geochronology/Trace Elements, Hematite U-Pb Geochronology/Trace Elements, Hematite Mapping, Florencite Trace Elements
VUD009	973	Hematite, Florencite, Albite, Apatite, Quartz, Sulphides, Zircon	Sericite Alteration	Apatite U-Pb Geochronology/Trace Elements, Hematite U-Pb Geochronology/Trace Elements, Hematite Mapping, Florencite Trace Elements, Zircon U-Pb Geochronology
VUD009	994	Hematite, Florencite, Albite, Apatite, Quartz, Sulphides	Sericite Alteration	Hematite Mapping
VUD007	1084	Magnetite ± Hematite, Chlorite, Dolomite, Albite, Apatite, Quartz, Sulphides	Chlorite Alteration, Potassic Alteration	Apatite U-Pb Geochronology/Trace Elements
VUD007	1183	Magnetite ± Hematite, Chlorite, Dolomite, Albite, Apatite, Quartz, Sulphides	Chlorite Alteration, Potassic Alteration	Apatite U-Pb Geochronology/Trace Elements
VUD016	1488	Hematite, Florencite, Albite, Apatite, Quartz, Sulphides	Sericite Alteration	Apatite U-Pb Geochronology/Trace Elements
VUD017	1210	Magnetite ± Hematite, Chlorite, Dolomite, Albite, Apatite, Quartz, Sulphides	Chlorite Alteration, Potassic Alteration	Apatite U-Pb Geochronology/Trace Elements

Table 3: Vulcan Prospect samples used for SEM and LA-ICP-MS analysis within this project and the mineralogy and alteration assemblage of each.

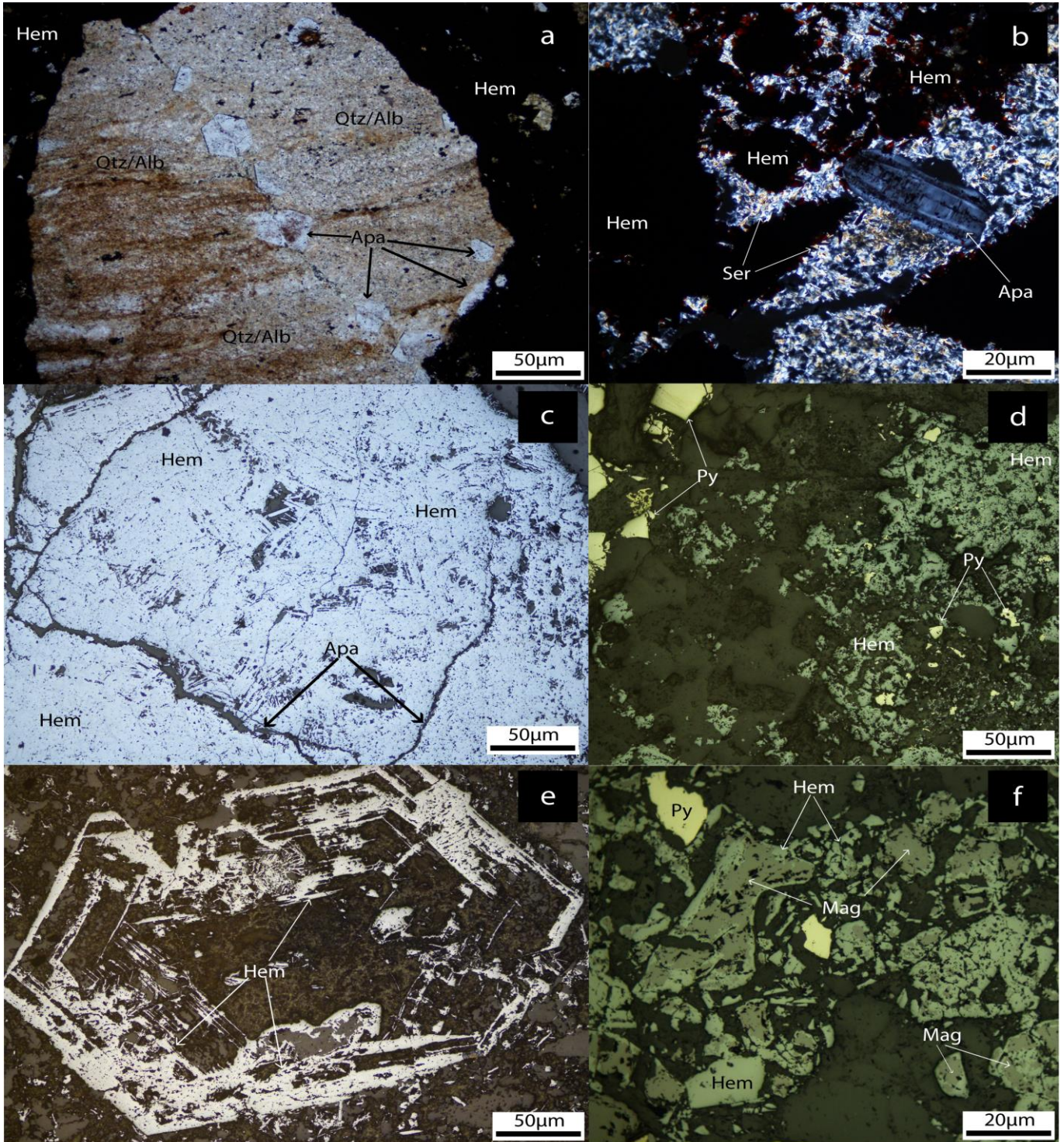


Figure 4: Reflected light (RL) and transmitted light (TL) images of hematite and apatite textures.
 a) VUD009 – Sample 801: TL image of apatite grains within a metamorphic clast surrounded by massive hematite. b) VUD009 – Sample 1020: TL image of apatite grain with zoned inclusions surrounded by a sericite mush but bounded by bladed hematite. c) VUD009 – Sample 852: RL image of apatite veins within massive hematite displaying classic bladed textures. d) VUD003 – Sample 894: RL image of granular hematite with small pyrite crystals. e) VUD016 – Sample 1091: RL image of late hematite-rich fluids overprinting grains of the host apatite. f) VUD007 – Sample 1192: RL image of magnetite-rich cores with hematite rims suggesting overprinting.
 Abbreviations: Qtz: quartz, Hem: hematite, Mag: magnetite, Py: pyrite, Apa: Apatite, Alb: albite, Ser: sericite

4.2 Standards

All standard results for LA-ICP-MS analysis can be found in Appendix C.

4.3 Apatite

Apatite grains within this study were distinguished as apatite 1 through 3 based on their crystallisation/growth habits and associated mineralogy. Their petrography, trace element analyses, and geochronology, where collected, is summarised below. Full petrographic descriptions can be found in Appendix B. Apatite trace element data can be found in Appendix D. Apatite U-Pb geochronology can be found in Appendix E.

APATITE 1

Petrography

Apatite 1 forms coarse (mm scale) euhedral hexagonal crystals within unbrecciated fragments of host rock in VUD009 sample 801 (Figure 4a). From the analysed thin sections, Apatite 1 grains are found within VUD009 sample 801, VUD009 sample 973 and VUD016 sample 1488 (Table 3). Apatite 1 is common alongside hematite breccias and is very rare to absent in magnetite-rich thin sections. These crystals are almost always associated with either quartz, albite and/or sericite within hematite-rich sections. Apatite 1 grains are much larger than apatite 2 or 3 grains, possibly due to multiple stages of growth. Within these large grains there are often inclusions of very fine material (possibly hematite) which are preferentially zoned toward the centre of these grains (Figure 4b). Apatite grains are still present within the breccia but are extremely small (1 μm). These are possibly broken grains of apatite 1 from the metamorphic clasts due to relationship to metamorphic minerals.

Trace Elements

Chondrite normalised REE plots for apatite highlights that apatite 1 REE trends are very similar across samples. Samples 801 and 1488 (Figure 5) are strongly depleted in LREEs before returning to a typical apatite decreasing REE trend. Sample 973 (Figure 5) is slightly more enriched in LREE but still returns to a typical apatite decreasing REE trend through MREE and HREE.

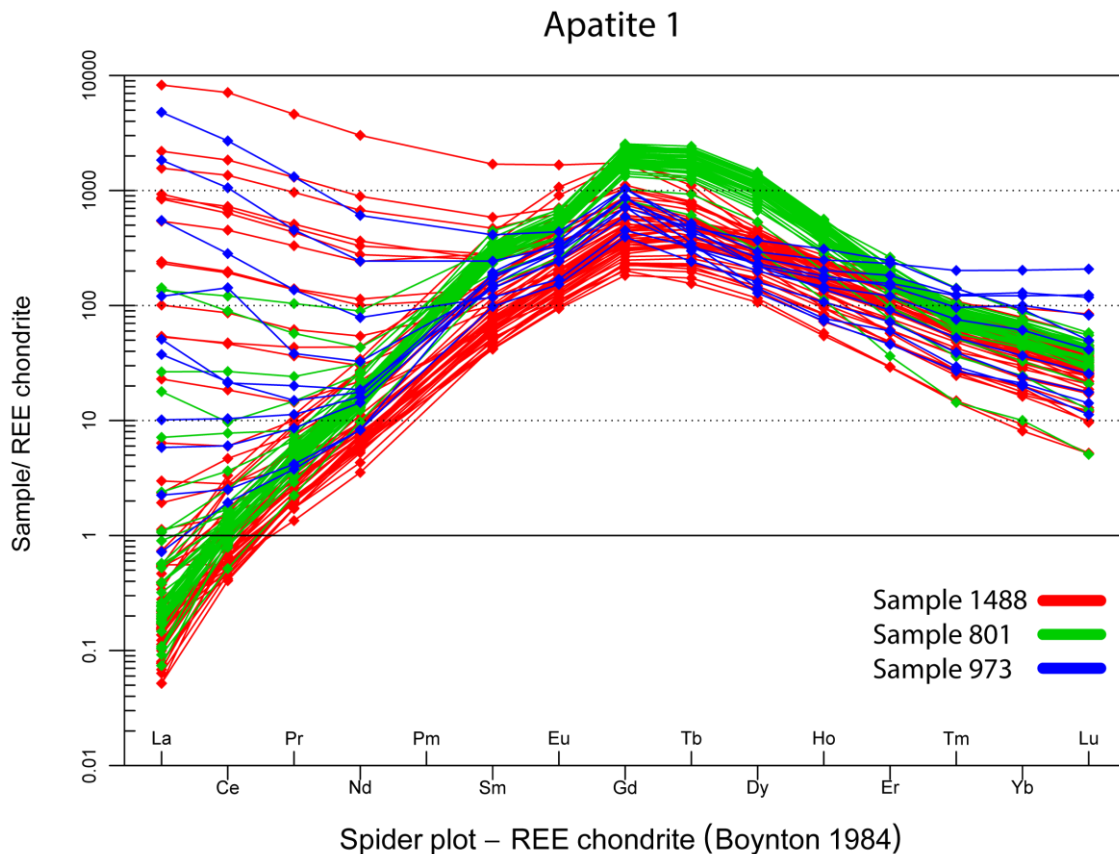


Figure 5: Chondrite-normalised REE plots for apatite 1 samples from laser ablation for a) 1488 samples (red). b) 801 samples (green). c) 973 samples (blue). Chondrite values are from (Boynton, 1984).

U-Pb Geochronology

Hole VUD009:

801: Forty-one analyses of 801 apatite results in a ^{207}Pb corrected $^{206}\text{Pb}/^{238}\text{U}$ weighted mean age of 461 ± 9 Ma with a MSWD value of 2.3 and $^{207}\text{Pb}/^{206}\text{Pb}$ ratio of 0.528 ± 0.029 (Figure 6a). This age has high precision due to the high number of analyses and large apatite grains with few inclusions.

973: Nine analyses of 973 apatite results in a ^{207}Pb corrected $^{206}\text{Pb}/^{238}\text{U}$ weighted mean age of 544 ± 46 Ma with a MSWD value of 6.4 and $^{207}\text{Pb}/^{206}\text{Pb}$ ratio of 0.408 ± 0.026 (Figure 6c). These apatites had a small sample size and large errors within the Tera-Wasserburg plot which led to a large age error.

Hole VUD016:

1488: Fifty-five analyses of 1488 apatite results in a ^{207}Pb corrected $^{206}\text{Pb}/^{238}\text{U}$ weighted mean age of 510 ± 8 Ma with a MSWD value of 7.4 and $^{207}\text{Pb}/^{206}\text{Pb}$ ratio of 0.725 ± 0.0134 (Figure 6b). The large number of samples coupled with large inclusion free apatite led to a well resolved U-Pb age and common Pb line.

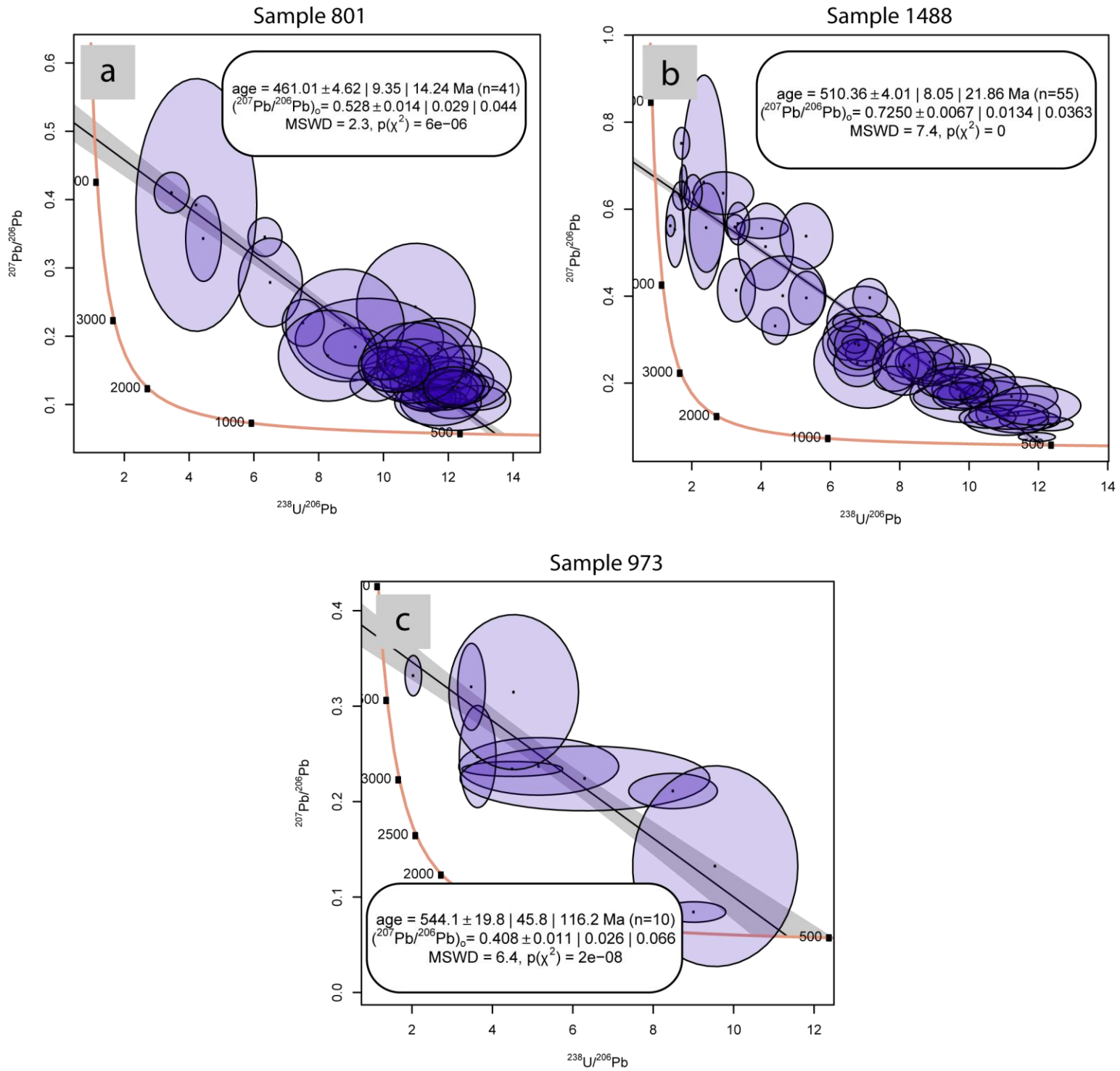
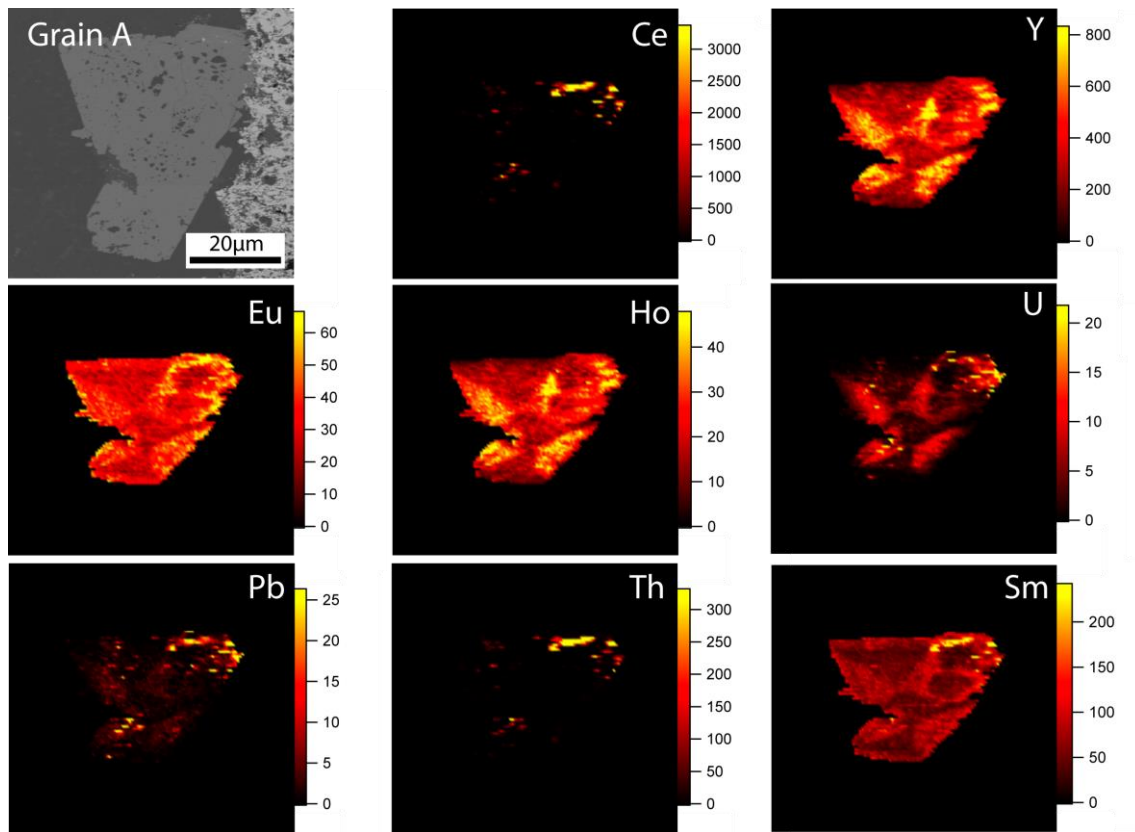


Figure 6: Tera-Wasserburg plots and corresponding ages of apatite 1 samples from laser ablation session. Apatite samples are as follows: a) 801. b) 1488. c) 973. The line represents the line of best fit used to calculate the common lead line. The sample population for each plot is represented by the corresponding n=.

Maps

All apatite grains with elemental mapping data are from sample 801 and are of apatite 1 grains. These grains are zoned in Y, Mn, Sm, Eu, Gd, Tb, Dy, Ho, Er, Tm, Yb, Lu and U. Apatite 1 displays a depleted core with enrichments on the rim of HREEs, Y, Sr, Mn, ^{206}Pb , Th and ^{238}U . Apatite veining within the metamorphic clasts is also depleted in Pb, Th and ^{238}U but still displays similar zonation with HREEs, Y, Sr and Mn. All maps produced by the LA-ICP-MS during this study can be found in Appendix F.



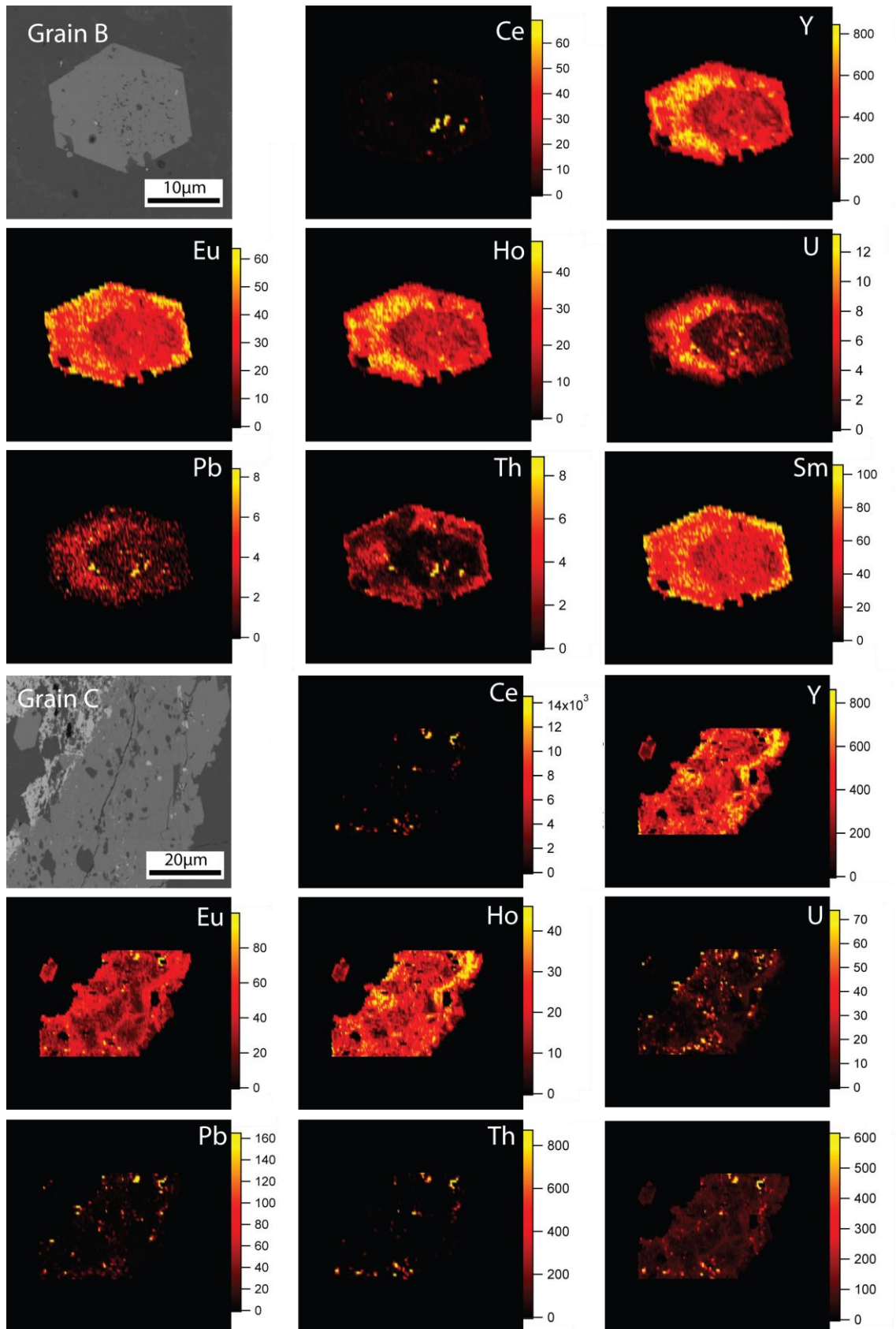


Figure 7: Elemental maps of apatite highlighting the distribution of trace elements within apatite grains from sample 801. All three apatite grains are hosted within a clast of metamorphic material, mainly quartz and albite. Maps of grain A) and B) depict euhedral apatite grains within these clasts whereas grain C) depicts apatite that is forming a vein structure within the clast. All values are in ppm unless otherwise specified.

APATITE 2

Petrography

Apatite 2 grains are found in VUD009 sample 852 and VUD009 sample 973 (Table 3).

Apatite 2 is defined by vein structures between grains of either host metamorphosed material or hematite grains. In sample 852 which is composed almost entirely of massive bladed hematite, apatite 2 is found within fractures between coarse hematite grains. This apatite is very fine grained (10-40 μm) and is often associated with barite, florencite and albite as can be seen in VUD009 sample 852 (Figure 4c).

These grains have been separated from apatite 3 grains due to host lithology differences.

Trace Elements

Apatite 2 records two similar REE trends. These are both strongly LREE-enriched compared to the apatite 1 REE trends. The first trend has a relative depletion in LREE increasing in abundance through MREE where it returns to a decreasing HREE trend. This trend is seen in Sample 973 (Figure 8). The second trend is a decreasing REE trend through from the light to the HREE's, HREE with a negative Eu anomaly and a positive Ce anomaly. This trend is shown by Sample 852 (Figure 8).

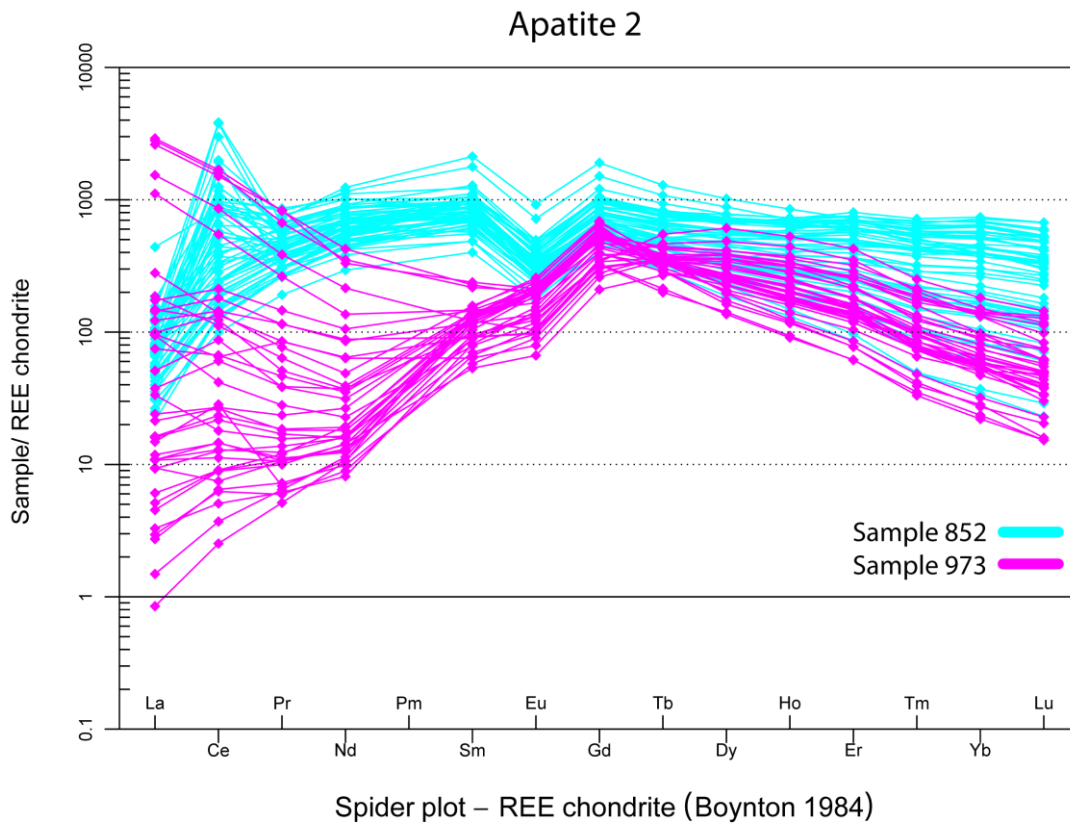


Figure 8: Chondrite-normalised REE plot for apatite 2 samples from laser ablation for a) 852 samples (light blue). b) 973 samples (pink). Chondrite values are from (Boynton, 1984).

U-Pb Geochronology

Hole VUD009:

852: Fifty-five analyses of 852 apatite results in a ^{207}Pb corrected $^{206}\text{Pb}/^{238}\text{U}$ weighted mean age of 1095.04 ± 10 Ma with a MSWD value of 4.5 and $^{207}\text{Pb}/^{206}\text{Pb}$ ratio of 0.890 ± 0.082 (Figure 9a). This apatite is relatively free of inclusions and has a large sample size producing a very precise U-Pb age.

973: Thirty-seven analyses of 973 apatite results in a ^{207}Pb corrected $^{206}\text{Pb}/^{238}\text{U}$ weighted mean age of 986 ± 18 Ma with a MSWD value of 5.1 and $^{207}\text{Pb}/^{206}\text{Pb}$ ratio of

0.277 ± 0.015 (Figure 9b). 1000 Ma apatite has large errors within the Tera-Wasserburg plot which possibly affected the common Pb line producing a larger age error.

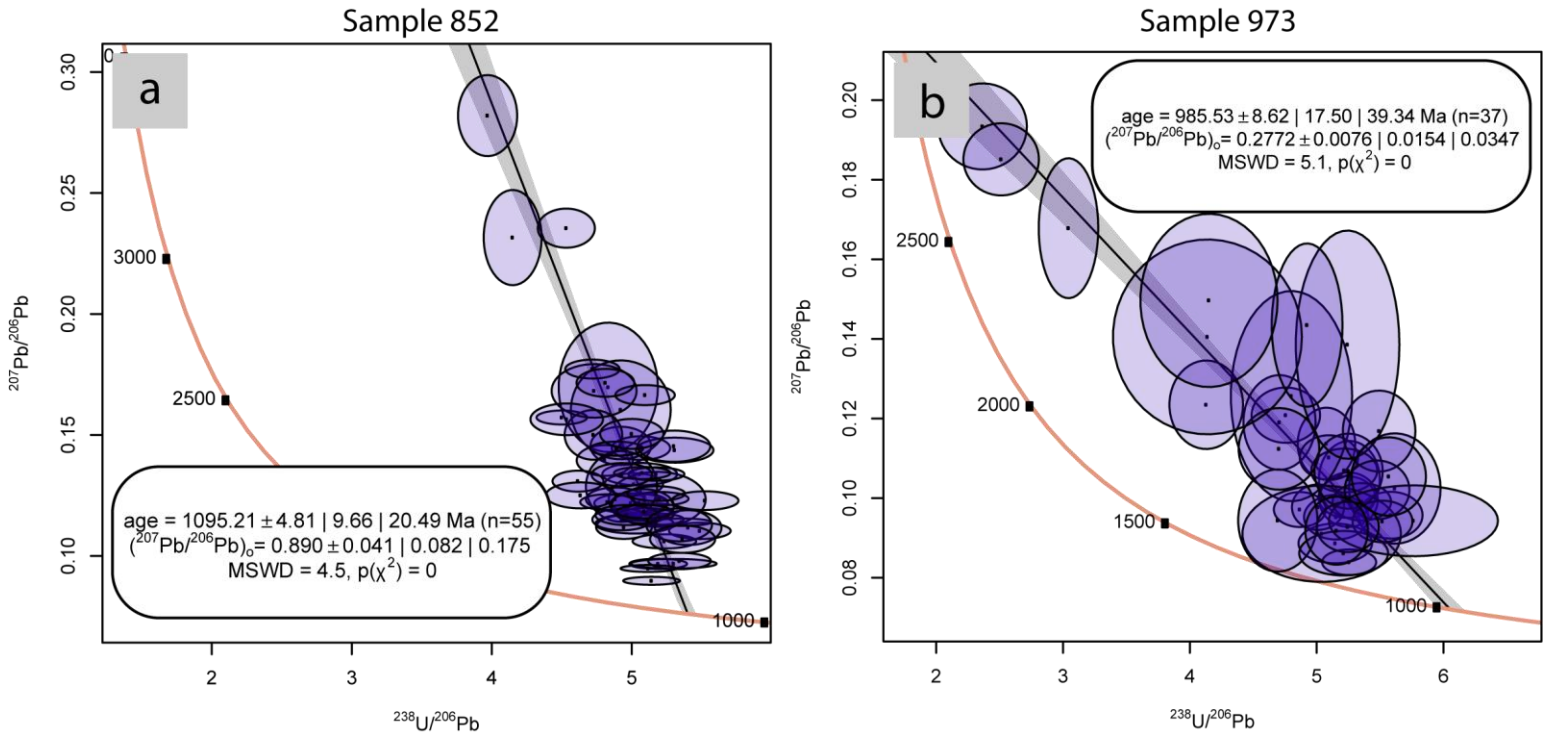


Figure 9: Tera-Wasserburg plots and corresponding ages of apatite 2 samples from laser ablation. Apatite samples are as follows: a) 852. b) 973. The line represents the line of best fit used to calculate the common lead line. The sample population for each plot is represented by the corresponding n=.

APATITE 3

Petrography

In samples where magnetite is the dominant Fe-oxide, apatite is found as small subhedral grains or as veins between dolomite crystals. Apatite 3 is defined by veining between metamorphic clasts and small growths within fractures. Large euhedral crystals of apatite are not commonly found in these lithologies. From the samples analysed this texture can be observed in VUD007 sample 1084, VUD007 sample 1183 and VUD017 sample 1210 (Table 3).

Trace Elements

Apatite 3 samples are relatively abundant in LREE compared to both apatite 1 and apatite 2 and decreasing abundance of REE through LREE, MREE and HREE. Samples that display this continuous decreasing REE trend pattern are 1084, 1183 and 1210 (Figure 10). These samples display similar REE trends to that of apatite 2, sample 852 (Figure 8). Sample 852 is more strongly depleted in all LREE than these samples and is more enriched in HREE than these samples. Apatite 2 and apatite 3 share similarities through the MREE especially the large Eu anomaly, however the trace element patterns differ in HREE where apatite 3 samples are slightly enriched.

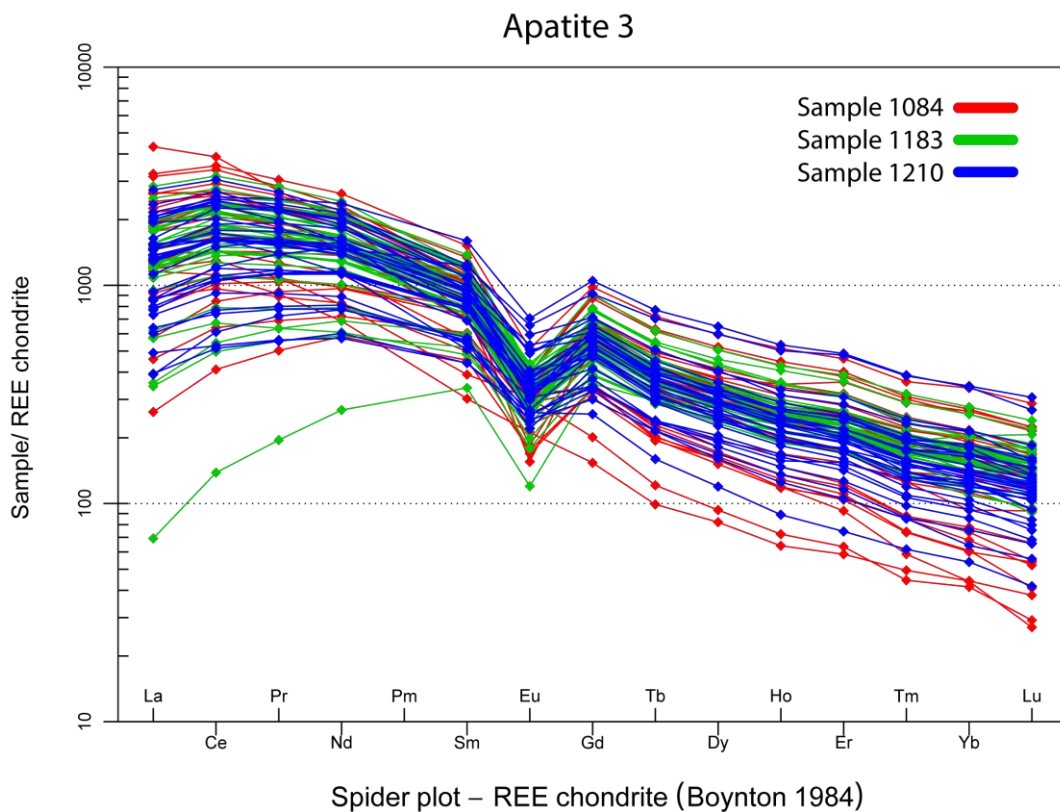


Figure 10: Chondrite-normalised REE plot for apatite 3 samples from laser ablation session for a) 1084 samples (red). b) 1183 samples (green). c) 1210 samples (dark blue). Chondrite values are from (Boynton, 1984).

U-Pb Geochronology

Hole VUD007:

1084: Twenty-eight analyses of 1084 apatite results in a ^{207}Pb corrected $^{206}\text{Pb}/^{238}\text{U}$ weighted mean age of 1543 ± 25 Ma with a MSWD value of 2.4 and $^{207}\text{Pb}/^{206}\text{Pb}$ ratio of 0.447 ± 0.048 (Figure 11a). Sample 1084 apatite included samples with high error within the Tera-Wasserburg plot which may have led to the variability in the U-Pb age data.

1183: Thirty-three analyses of 1183 apatite results in a ^{207}Pb corrected $^{206}\text{Pb}/^{238}\text{U}$ weighted mean age of 1611 ± 24 Ma with a MSWD value of 4.2 and $^{207}\text{Pb}/^{206}\text{Pb}$ ratio of 0.479 ± 0.059 (Figure 11b). Apatite in sample 1183 contained apatite with large error on the Tera-Wasserburg plot which led to some variability within the U-Pb age as consistent with the error.

Hole VUD017:

1210: Thirty-two analyses of 1210 apatite results in a ^{207}Pb corrected $^{206}\text{Pb}/^{238}\text{U}$ weighted mean age of 1522 ± 42 Ma with a MSWD value of 3.3 and $^{207}\text{Pb}/^{206}\text{Pb}$ ratio of 0.286 ± 0.025 (Figure 11c). Sample 1210 is relatively well resolved, although some apatite grains have a large error which has led to a high error in the U-Pb age.

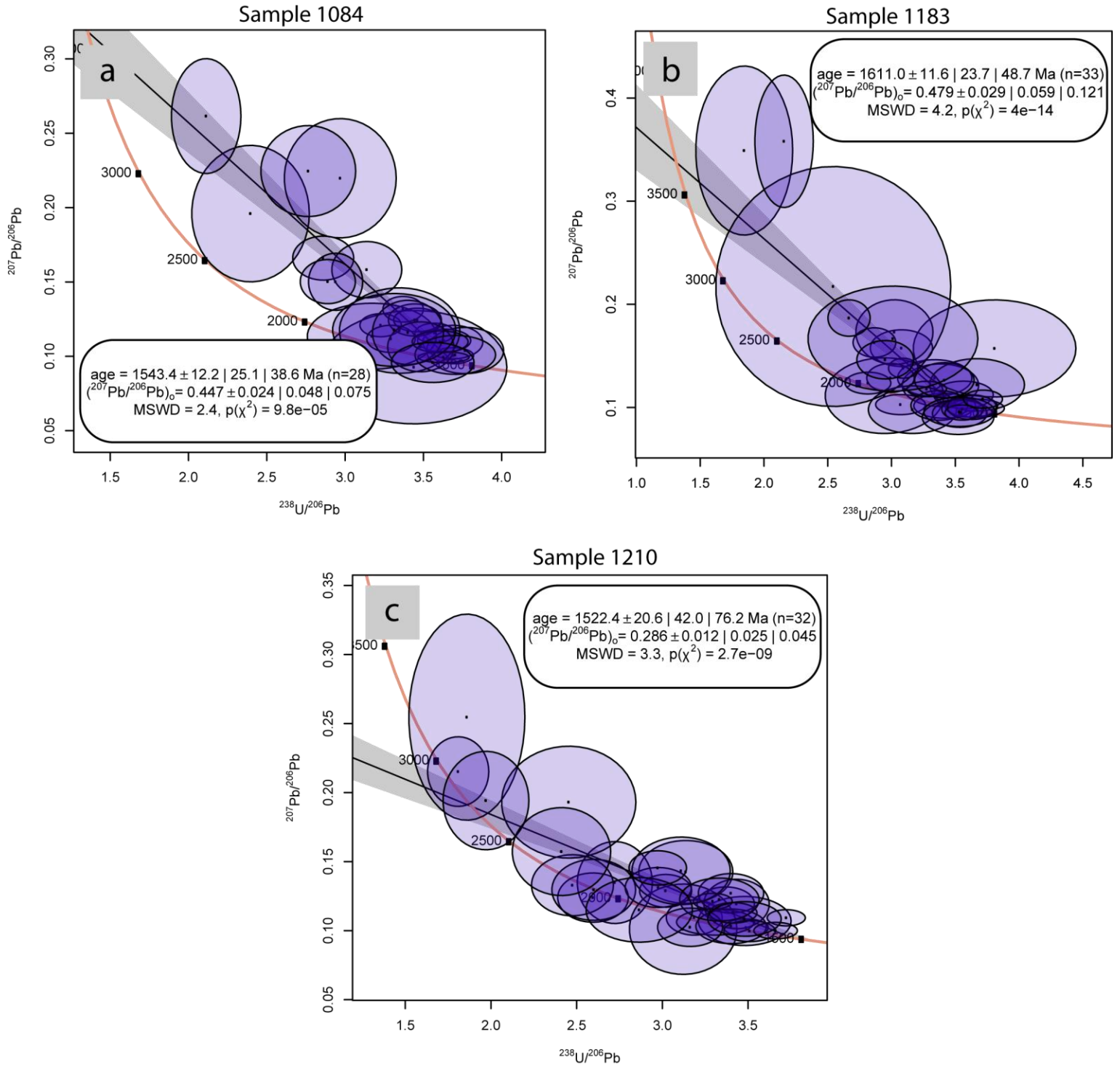


Figure 11: Tera-Wasserburg plots and corresponding ages of apatite 3 samples from laser ablation. Apatite samples are as follows: a) 1084. b) 1183. c) 1210. The line represents the line of best fit used to calculate the common lead line. The sample population for each plot is represented by the corresponding n=.

4.4 Hematite

PETROGRAPHY

Hematite is the most dominant iron-oxide at the Vulcan prospect and can be observed as a paragenetically late stage with replacement textures observed of the host rock (Figure 4e). Hematite is present in every thin section within this study. It ranges from massive to granular to veined. Hematite is observed as infill with alteration products such as sericite, which is common around hematite stringer veins. Hematite can be completely dominant and often overprints the host (Figure 3a). Bladed hematite textures are the most common texture observed as throughout the sample suite (Figure 4c). Hematite often contains rare small euhedral crystals of sulphides, pyrite and chalcopyrite. Often there is evidence for mineralisation of sulphides with timing similar to the hematite (Figure 4d).

TRACE ELEMENTS

Trace element analysis of hematite grains was attempted but due to abundant micro-inclusions of likely apatite grains there was contamination of the trace element trend. Hematite trace element data can be found in Appendix G.

U-PB GEOCHRONOLOGY

Hematite LA-ICP-MS data for U-Pb geochronology can be found in Appendix H. Methods from L. Courtney-Davies et al. (2019) were adapted in this study. Hematite ablation spots with less than 50 ppm ^{238}U and/or hematite ablation spots with $^{206}\text{Pb} > ^{238}\text{U}$ were omitted from analysis. Due to the samples collected having micro inclusions and the main mineral within these samples other than hematite being apatite, any

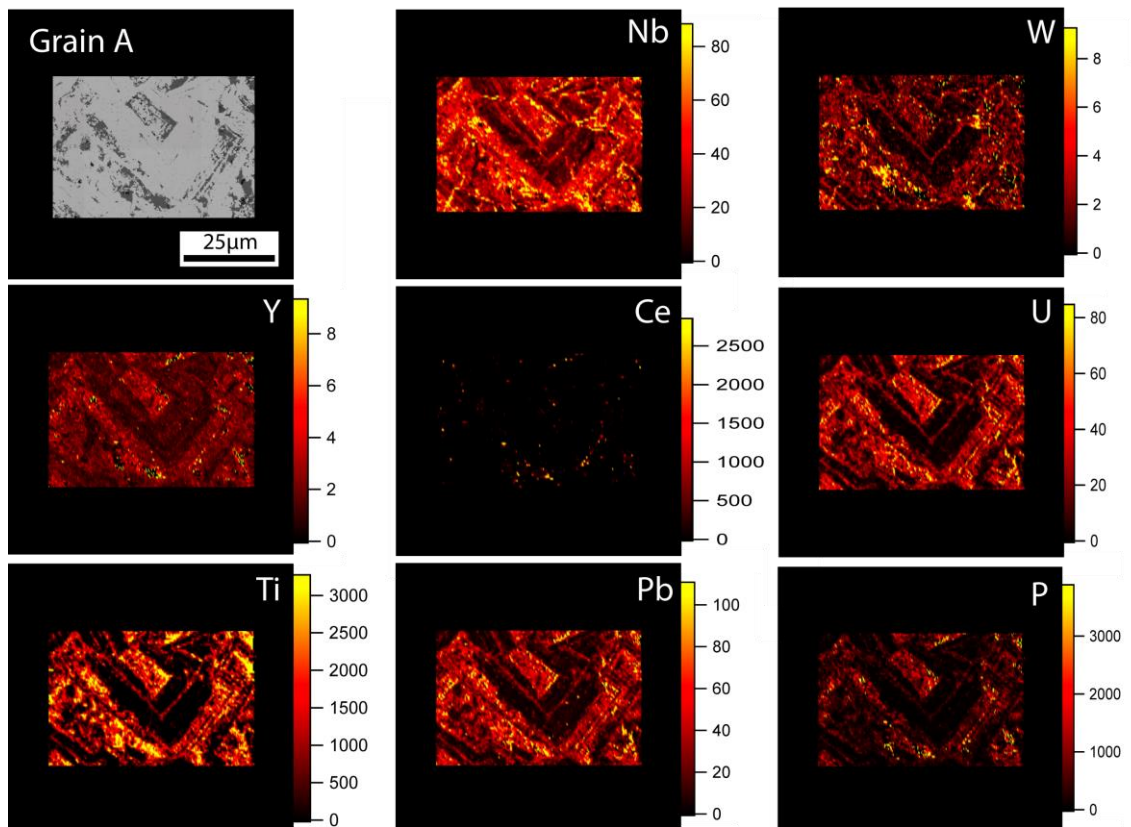
samples with greater than 50 ppm Ca or P were also omitted. Also, as the REE and Y (REY) concentrations within the prospect are mainly hosted in apatite and florencite, any points with greater than 10 ppm Σ REY were also omitted. After these conditions, not enough points were left on concordia for a robust age for hematite data. Hematite U-Pb geochronology can be found in Appendix H.

MAPS

Hematite is zoned in Nb, W, Y, U, Ti, Pb, P and Sc from multiple growths (Figure 12).

There is very little evidence to suggest zonation for REE, as REEs are either homogeneously low, or as unidentifiable inclusions within hematite grains (Figure 12).

Hematite trace element enrichment differs between grains found within metamorphic mineral-rich breccias and zones where hematite is completely dominating the thin section.



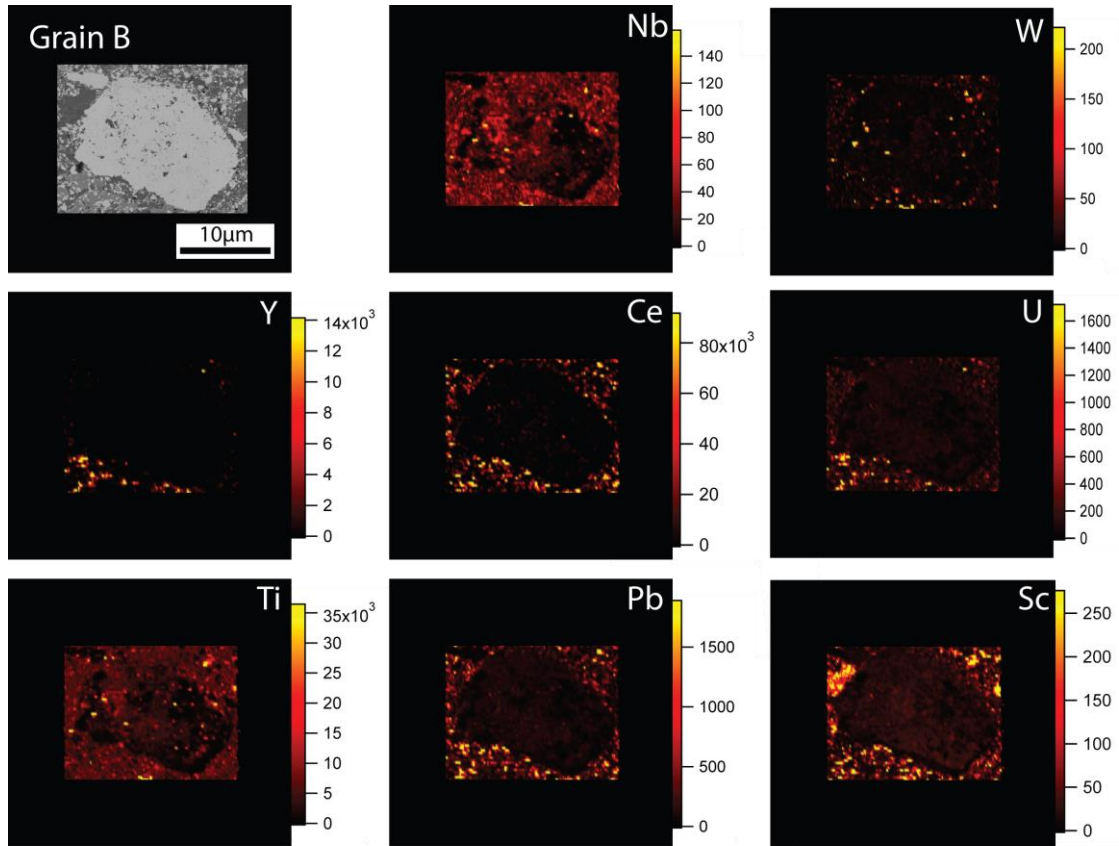


Figure 12: Elemental maps of hematite highlighting the distribution of trace elements within hematite grains from sample 994 and 973. Grain A depicts hematite from sample 994 and is defined by multiple stages of growth intergrown with metamorphic material. Grain B depicts a hematite grain from Sample 973 that has formed within a hematite, albite, quartz, apatite breccia. All values are in ppm unless otherwise specified.

4.5 Magnetite

PETROGRAPHY

Commonly magnetite is associated with hematite although is far less abundant throughout the sample suite, only appearing in a relatively small number of samples. In the samples analysed, magnetite is present in VUD007 sample 1084, VUD007 sample 1183 and VUD017 1210. Often hematite can be seen with hematite rims and there is no evidence for thin sections of magnetite without hematite present (Figure 3f). Within thin sections where magnetite is present in typical feathery magnetite structures as well as creating granular textures. Magnetite is often associated with dolomite, albite and quartz

as well as abundant chlorite alteration throughout these sections. Sulphides (pyrite, chalcopyrite) are more abundant within sections that contain magnetite as the dominant Fe-oxide as compared to when hematite is more abundant (Figure 3f).

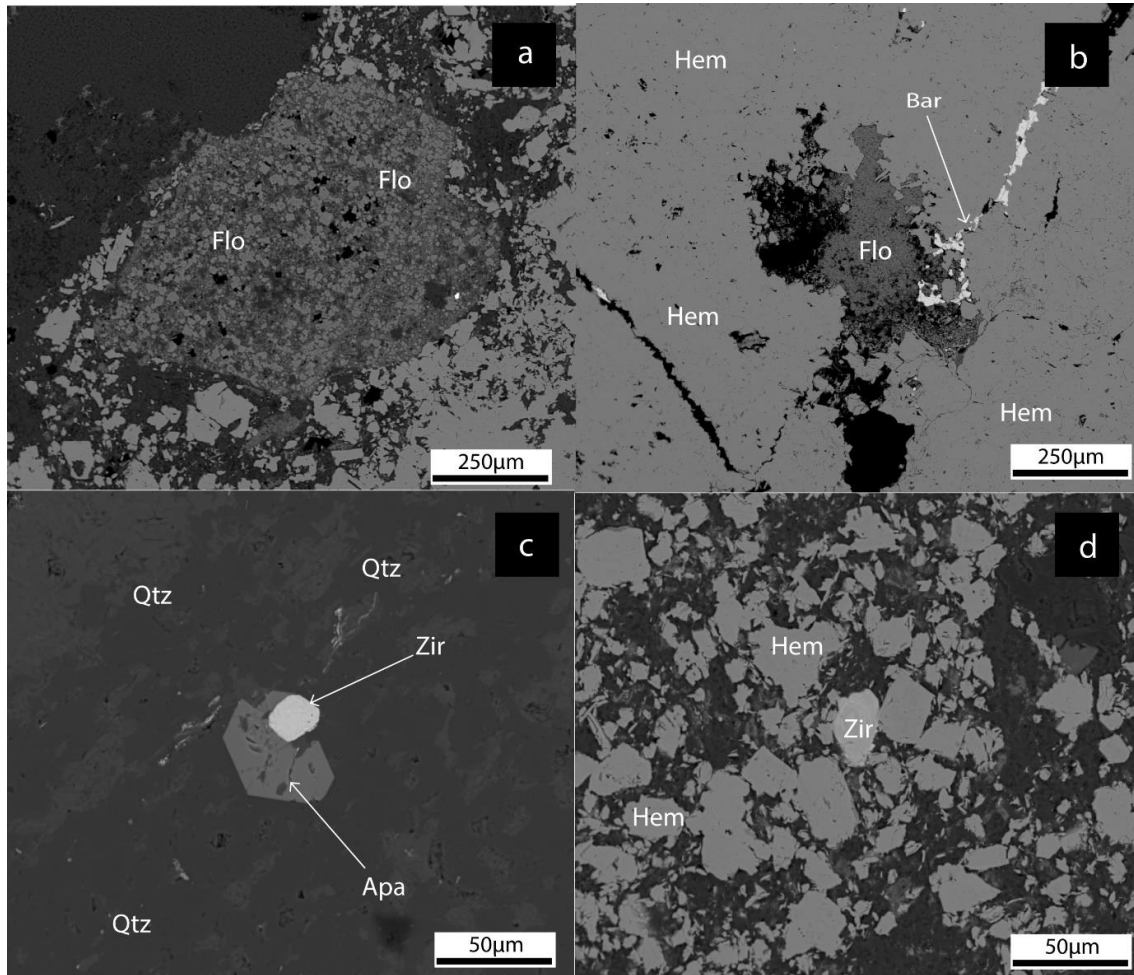


Figure 13: BSE images of florencite and zircon grains from SEM analyses. a) intergrown florencite and quartz grains from sample 801. b) Florencite infill of a fracture within massive hematite associated with barite from sample 852. c) A zircon grain that has crystallised inside a metamorphic fragment of quartz with an apatite grain from sample 801. d) A zircon grain within a hematite-rich breccia from sample 973.

Abbreviations: Flo: florencite, Bar: barite, Zir: zircon, Hem: hematite, Apa: apatite.

4.6 Zircon

PETROGRAPHY

Small ca. 20 µm zircon grains are found throughout the sample suite. Zircons analysed within this study were from VUD009 sample 801 and VUD009 973 (Table 3). Within

sample 801, zircon grains were hosted by grains of pyrite or apatite (Figure 13c). In sample 973 zircons were hosted either within clasts of metamorphic material dominated by albite, quartz and apatite or within the hematite breccia (Figure 13d).

GEOCHRONOLOGY

Zircon LA-ICP-MS data for U-Pb geochronology can be found in Appendix I.

Zircon analysis within this study was unsuccessful due to three main reasons. Many of the zircon grains within the sample were too small for an ablation target which led to an insufficient sample size for a robust age estimate for these zircons. Secondly, of the zircons ablated during this study all had undergone lead loss. This led to none of the zircons plotting on concordia which generated an age of 6.847 ± 0.104 with a MSWD of 1600. Thirdly, some zircons fractured during ablation generating a very short signal, which wasn't robust enough for confidence in the analysis.

4.7 Florencite

PETROGRAPHY

Florencite is an LREE-enriched mineral that is common throughout the Vulcan prospect within thin sections that contained apatite 2 or apatite 3 grains. These sections were, VUD 009 sample 801, VUD 009 sample 852, VUD 009 sample 973, VUD 009 sample 994 and VUD 017 sample 1488 (Table 3). Florencite occurs in two forms. Mainly florencite occurs as $>20 \mu\text{m}$ fine grained disseminations within the breccia matrix (Figure 13a), or florencite grains form angular aggregates as infill or outline select shapes indicating replacement of previous mineral textures (Figure 3b). Florencite is extremely vuggy and often varies in shape from irregular to angular. Florencite within

the Vulcan prospect is almost always as infill between hematite grains in a breccia (Figure 13a). However florencite does also occur in veins and can be seen in sample 852 (Figure 13b).

Trace Elements

All florencite samples display similar chondrite-normalised REE trends with substantial LREE enrichments and decreasing concentrations across MREE and HREE (Figure 14). All florencite samples display a slightly negative Eu anomaly. Sample 852 is slightly enriched in LREEs compared to 801 and 973 (Figure 14) but there is significant variation within the sample populations of 801 and 973. Florencite trace element data can be found in Appendix J.

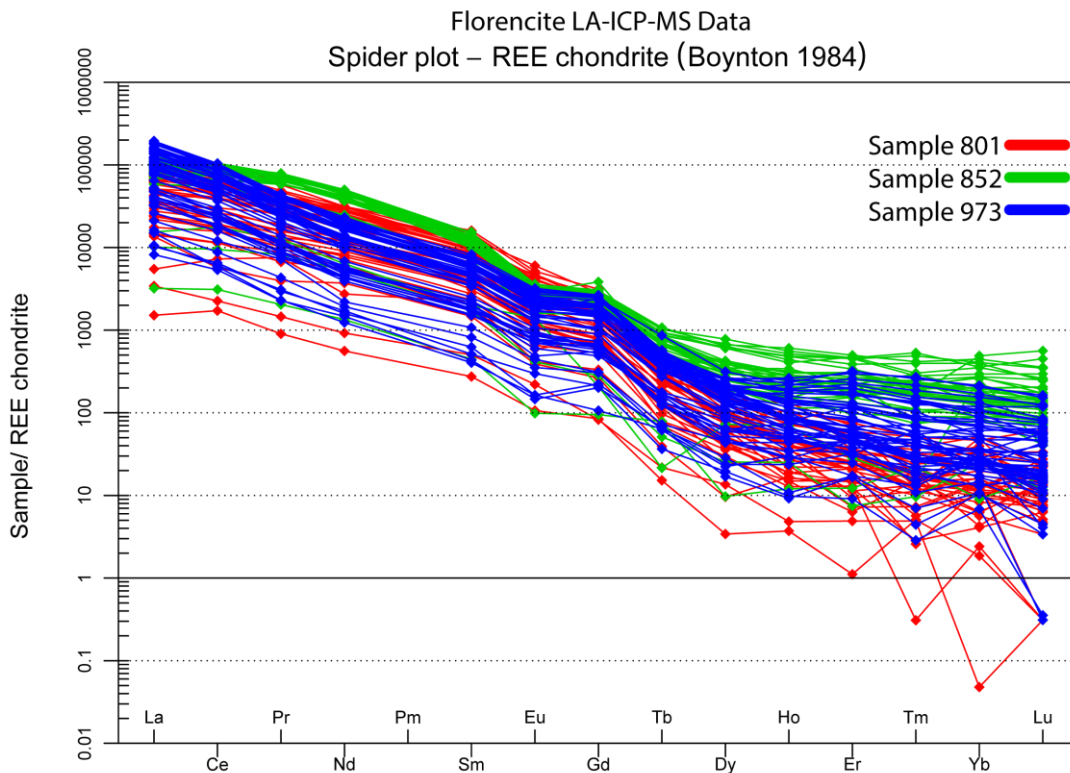


Figure 14: Chondrite-normalised REE plots for florencite samples from laser ablation for a) 801 samples (red). b) 852 samples (green). c) 973 samples (blue). Chondrite values are from (Boynton, 1984).

5. DISCUSSION

5.1 Apatite 1 – Metamorphic Clast-hosted Apatite

These apatite crystals are metamorphic apatite grains and have been classified as such for two reasons:

1. Apatite crystals are hosted as porphyroblasts within foliated clasts of metamorphic material.
2. The $^{207}\text{Pb}/^{206}\text{Pb}$ ratio is very low on average, which would indicate Pb derivation from an evolved source, possibly metamorphic source (Kirkland et al., 2017).

TRACE ELEMENT SIGNATURE

Apatite 1 (Figure 5) has a significant depletion in LREE when compared to other apatite populations. This preferential depletion from apatite has been noted from other IOCG and IOA deposits such as Kiruna, OD and Acropolis. Krneta (2017) determined that decreases in pH, temperature, and fluid salinity, along with a rise in oxygen fugacity allow LREE to occur as chloride complexes. This effectively causes partitioning of LREE away from apatite due to inhibition of apatite to intake these complexes (S. Krneta et al., 2017; Migdisov et al., 2016). At OD LREE depletion in apatite is observed with high grade bornite ores (S. Krneta et al., 2017). This apatite commonly contains inclusions of the overprinting assemblage (hematite, sericite) (S. Krneta et al., 2017). While apatite 1 from Vulcan displays LREE depletions in the trace element signature, it is not associated with high grades of Cu. Both the hematite-sericite

overprinting assemblage and inclusions as observed by (S. Krneta et al., 2017), are observed in all apatite grains within this study with depletions in LREE. At the Acropolis deposit early LREE depleted apatite is attributed to low salinity, low pH fluids altering the original grain (Sasha Krneta et al., 2017). This alteration caused monazite precipitation as inclusions within the apatite grains (Sasha Krneta et al., 2017). This is a textural relationship which is not seen at Vulcan, even with florencite. Thus, it is more likely that there was growth of apatite 1 in an environment where florencite was more likely to precipitate and take up these LREE-chloride complexes. An alternate hypothesis is that by the time apatite 1 had grown, florencite had partitioned all of the LREE within the fluid and thus apatite 1 was growing in an LREE-depleted fluid.

ELEMENTAL MAPPING

Mapping of apatite 1 grains within this study highlights that there were at least two stages of growth. Apatite 1 from Vulcan shows a depleted core, with a second growth showing enrichments in HREE, U, Y and a rim with enrichment in MREE and Th (Figure 7). LREE is completely depleted across all grains, the only LREE enrichments are within small inclusions within the grain. These are similar enrichment patterns to apatite grains at OD. S. Krneta et al. (2017) mapped an apatite grain from a section of the Roxby Downs Granite (RDG) which had been hematite-sericite altered and this also showed a depleted core with enrichments in Y, MREE, HREE, U and Th on the rim. This zoning was interpreted to be hydrothermal alteration as it was also commonly seen along fractures within the grain. This would explain the rim zonation that is seen at Vulcan also as petrography indicates that late hydrothermal fluids brecciated the host rock after the two stages of apatite 1 growth.

TIMING OF APATITE GROWTH

Apatite 1 samples (Figure 6) produced ages of 461 ± 9 Ma, 510 ± 8 Ma and 544 ± 46 Ma respectively. These ages likely represent growth during the Delamarian Orogeny which lasted ~24 Ma from 514 Ma to 490 Ma (Foden et al., 2006). Whilst sample 1488 is younger than this range, it is within error of published ages of Delamarian samples (Foden et al., 2006).

Apatite grains of a similar age have been identified at OD. These are U-Pb dating of authigenic apatite and U-Pb dating of hydrothermal apatite and monazite, both at 440-480Ma (Kamenetsky et al., 2015). These ages are within error of apatite 1 from Vulcan. The authigenic apatite was dated from a bedded sedimentary package and the hydrothermal apatite was dated from a basaltic dyke, unrelated to mineralisation at OD (Kamenetsky et al., 2015). This contrasts with the metamorphic apatite grains dated at Vulcan which were all taken from hematite breccias. From elemental mapping it is clear that there were two stages of growth for these apatites (Figure 7). This implies that the date for Vulcan apatite 1 grains either correspond to the earliest formation of apatite within the hematite breccias or the second growth of these grains as the mineral cooled below ~ 350°C (Chew et al., 2014). It is unlikely that the second growth, if at a different time, didn't reset the full grain as the dates produced for each sample are robust. An age difference between core and rim would show as variability within the concordia plot due to the amount of sample spots used, however this was not the case (Figure 6).

5.2 Apatite 2 – Hematite-hosted Hydrothermal Apatite

Apatite 2 grains are likely hydrothermal apatite because apatite grains are either hosted within vein structures cross-cutting hematite grains, or are veining between grains of the host rock (albite, quartz). These grains are generally smaller than apatite 1 suggesting nucleation was prevalent over growth. Apatite 2 grains are not seen to be hosted within a metamorphic fragment.

TRACE ELEMENT SIGNATURE

Samples 852 and 973 (Figure 8) are vein hosted apatite that have depleted REE signatures, but are more enriched than apatite 1 samples. Sample 852 (Figure 8) displays a well constrained signature, whereas sample 973 shows a range in values for REE values. At OD, REY-CI-depleted zones show similar patterns to sample 852 (S. Krneta et al., 2017). The OD trace element signature however doesn't have a negative La anomaly as can be seen in sample 852. An LREE depleted pattern with enriched MREE and HREE is observed within the Roxby Downs Granite at OD similar to what is seen for sample 973 (S. Krneta et al., 2017). This signature is only observed at OD in zones with abundant hematite-sericite alteration throughout the sample (S. Krneta et al., 2017). The variance in La/LREE abundance across sample 852 and 973 likely represents the beginning of florencite crystallisation and therefore LREE remobilisation across the prospect. Sample 852 is ~100 Ma older than sample 973, which might indicate that La was the first LREE to remobilise. At ~980 Ma remobilisation and crystallisation of florencite was already well established and other LREE were mobilising into florencite also which would explain relative depletions in 973.

TIMING OF APATITE GROWTH

Apatite 2 samples (Figure 9) produced ages of 985 ± 18 Ma and 1095 ± 10 Ma respectively. This represents ages of the waning stages of the Musgravian orogeny and this is consistent with xenotime ages from OD (Cherry et al., 2017). In the Gawler Craton these ages have also been recorded by Reid et al. (2017) with Ar/Ar dates for adularia veins ~70km NW of Vulcan. This implies that the late Musgravian orogeny had a thermal effect on the eastern Gawler Craton.

5.3 Apatite 3 – Magnetite-hosted Hydrothermal Apatite

Apatite 3 grains are likely hydrothermal because grains were veining pervasively through the host or hematite \pm magnetite-rich material. Also, large growths of apatite are very rare. Small grains may imply nucleation was more common than growth.

TRACE ELEMENT SIGNATURE

Apatite 3 samples (Figure 10) display LREE enrichment with decreasing enrichment across MREE and HREE with a slight negative Eu anomaly. This flat LREE enriched signature is typical of early hydrothermal apatite in the Olympic Cu-Au Province (Ismail et al., 2014; Kontonikas-Charos et al., 2014; Krneta, 2017; S. Krneta et al., 2017; Sasha Krneta et al., 2017). Most commonly this apatite signature is seen with magnetite-chlorite-carbonate with minor hematite-sericite alteration which is the case for these three samples from the Vulcan prospect. This pattern is also seen at OD in apatite grains from REE and chlorine depleted samples from the deep and distal mineralisation within the deposit (S. Krneta et al., 2017). These samples were often associated with minor hematite-sericite alteration of a magnetite-chlorite host which is similar at Vulcan.

TIMING OF APATITE GROWTH

Apatite 3 samples (Figure 11) produced ages of 1522 ± 42 Ma, 1543 ± 25 Ma and 1611 ± 24 Ma respectively. These ages are consistent (with MSWD corrected error) with apatite dates recorded at OD, which has tied apatite within chalcopyrite-pyrite-rich zones to ~ 1.6 Ga (S. Krneta et al., 2017). Therefore these apatite ages are likely related to cooling following the ~ 1590 - 1580 Hiltaba Suite Event (Hall et al., 2018) which are temporally associated with significant alteration and Cu-Au-U-REE mineralisation (Hand et al., 2007). These apatite ages are also within error of the Re-Os Molybdenum dates as studied by Reid et al. (2013) which indicates that these apatites are the same age as Vulcan Cu-Au mineralisation.

5.4 Florencite

TRACE ELEMENT SIGNATURE

Florencite within the Vulcan prospect has a decreasing REE trend with LREE > MREE > HREE. This trend is ubiquitous for florencite and is also seen at OD (Schmandt et al., 2019). However, compared to OD, only one REE bearing mineral and no fluocarbonates were identified within the prospect. This feature may explain the enrichments in MREE and HREE as these are preferentially consumed by bastnasite and sychysite at OD (Schmandt et al., 2019).

At Vulcan, florencite is only present within holes with apatite ages 1100 Ma or later. In samples where apatite was dated at 1100 Ma and 900 Ma, florencite is significantly less abundant than in samples with apatite 1. This lack of florencite may indicate that the volume of mineralisation increases with time. This implies that florencite was a late mineralisation phase and was just beginning to form during thermal events around

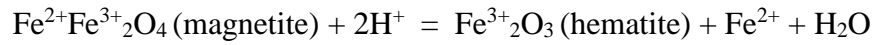
1100Ma. Therefore florencite crystallisation has a likely association with the Musgravian Orogeny as there was formation beginning during the waning phases of this event. At OD florencite represents the latest mineralisation within the REE-phosphate group (Schmandt et al., 2019). Florencite at OD is evidence for an evolution toward lower temperature conditions, where apatite shows patterns of MREE and HREE enrichment and LREE depletion as mineralisation progresses. Florencite shows the opposite trend (Schmandt et al., 2019). Leaching of LREE from early hydrothermal apatite and feldspars was likely taken up by florencite at OD further substantiating the hypothesis that florencite is a late stage mineralisation (Kontonikas-Charos, Ciobanu, Cook, Ehrig, Ismail, et al., 2018; Kontonikas-Charos et al., 2017; Kontonikas-Charos, Ciobanu, Cook, Ehrig, Krneta, et al., 2018; Schmandt et al., 2019). As the same results have been reached from this study, this can be extended to the Vulcan Prospect. At OD florencite likely formed at a lower pH and lower temperatures during a late stage of deposit evolution (Schmandt et al., 2019). At Vulcan, apatite already shows LREE depleted patterns which indicates that conditions were moved to lower temperature and a lower pH during these younger thermal events.

5.5 Hematite and Magnetite

PETROGRAPHY

Hematite is the most dominant Fe-oxide in the Vulcan prospect, with magnetite being localised in deeper sections of the prospect. In thin sections with magnetite, hematite is pseudomorphing the rims of the magnetite grains. This implies that over the history of the prospect there has been a change in pH that produced an acidic environment (Mücke

& Cabral, 2005; Ohmoto, 2003). This change in pH facilitated the conversion of magnetite to hematite by the leaching of Fe²⁺ (Mücke & Cabral, 2005; Ohmoto, 2003).



This equation for hematite pseudomorphic replacement of magnetite suggested by Ohmoto (2003) produces H₂O as an endmember within the reaction. This increase in fluid might allow for REE remobilisation, and especially the LREE, which are more readily transported (Migdisov et al., 2016).

In thin sections where ca. 1590 Ma apatite is dated there is magnetite present. This supports the hypothesis that magnetite is an early mineralisation stage that crystallised during a higher pH environment. Over time it may be that a gradual shift to lower temperature and lower pH conditions led to pseudomorphing of grains into hematite. (S. Krneta et al., 2017; Mücke & Cabral, 2005; Ohmoto, 2003; Schmandt et al., 2019). This implies that the Vulcan prospect has undergone significant post-deposition processes.

TRACE ELEMENT SIGNATURE

There is a lot of variation within the data due to inclusions within the hematite that have been ablated. The trace element signature is similar to that of 1590Ma hydrothermal apatite. This is likely because the results have been skewed by inclusions within the hematite.

ELEMENTAL MAPPING

Magnetite elemental mapping was outside of the scope of this study and therefore only hematite grains were mapped during laser ablation.

Hematite grains within this study that were mapped show distinct zoning patterns for Nb, Y, Ti, Pb, W and U. LREE is depleted (0 – 5ppm) for hematite grains mapped within this study while around the grain there are peaks in LREE, likely in florencite crystallisation. At OD hematite samples are enriched in LREE compared to the Vulcan prospect with (1 – 30 ppm) being recorded at the deposit (Verdugo-Ihl et al., 2019; Verdugo-Ihl et al., 2017). These abundances are also recorded in hematite from Wirrda Well but Acropolis hematite samples are much more depleted in LREE, similar to what is seen at Vulcan (L. Courtney-Davies et al., 2019). This could support the hypothesis that there has been a LREE remobilisation event at Vulcan during the later stages of prospect genesis as recorded remobilisation of REE has been recorded from other deposits within the Olympic Cu-Au Province (Ciobanu et al., 2013; S. Krneta et al., 2017; Sasha Krneta et al., 2017; Schmandt et al., 2019; Verdugo-Ihl et al., 2017).

The simplest way to explain this change to lower temperatures, pressures and pH is an uplift event, which would lead to hematite pseudomorphing, florencite crystallisation and LREE remobilisation (S. Krneta et al., 2017; Mücke & Cabral, 2005; Ohmoto, 2003; Schmandt et al., 2019).

Ma, 520.39 ± 12.89 Ma (this study), Late Mesoproterozoic apatite had ages of 1087.04 ± 12.61 Ma, 981.10 ± 31.30 Ma (this study), and Middle Mesoproterozoic apatite recorded ages of 1546.10 ± 39.20 Ma, 1627.50 ± 36.30 Ma, 1546.40 ± 59.90 Ma (this study). Re-Os dating of molybdenite showed an age of ~ 1586 from (Reid et al., 2013). SHRIMP U-Pb analysis of zircon grains from across the Vulcan prospect recorded ages of ~ 1820 Ma, ~ 1920 Ma, ~ 1980 Ma, ~ 2190 Ma (Jagodzinski, 2005). Olympic Dam: Fluoroapatite, ~ 1.59 Ga (Apukhtina et al., 2017), ~ 0.82 Ga (Apukhtina et al., 2016; Huang et al., 2015), $\sim 0.44-0.48$ Ga (Kamenetsky et al., 2015). Chalcopyrite dated at ~ 1.26 Ga by Re-Os (McInnes et al., 2008). Hematite U-Pb at $\sim 1.59-1.58$ Ga (Apukhtina et al., 2017; Ciobanu et al., 2013; L. Courtney-Davies et al., 2019). U-Pb dating of magnetite revealed ~ 1.76 Ga (Courtney-Davies et al., 2020; L. Courtney-Davies et al., 2019); ~ 1.59 Ga magmatic hematite inferred from dating of surrounding minerals (Apukhtina et al., 2017). Vein hosted xenotime at ~ 1.08 Ga (Cherry et al., 2017). Hydrothermal monazite dated at $\sim 0.44-0.48$ Ga (Kamenetsky et al., 2015). U-Pb dating of zircon revealed hydrothermal and magmatic zircon at ~ 1.59 Ga; hydrothermal zircon at ~ 1.14 Ga and other zircon grains at 0.49 Ga (Jagodzinski, 2014). Uraninite at OD is dated at ~ 1.59 Ga (Apukhtina et al., 2017), $\sim 1.4-1.3$ Ga, ~ 1.22 Ga, ~ 0.83 Ga and ~ 0.57 Ga (Johnson, 1993). Acropolis: Monazite U-Pb dating reveals two ages at acropolis at $\sim 0.43-0.53$ Ga and $\sim 1.37-1.44$ Ga (Cherry et al., 2018). U-Pb dating of hematite produced a date of ~ 1.59 Ga (L. Courtney-Davies et al., 2019). U-Pb dating of apatite at Acropolis dates apatite at ~ 1.59 Ga (Cherry et al., 2018). Xenotime dated at ~ 1.38 Ga (Cherry et al., 2018). TIMS zircon dating shows dates of ~ 1.59 Ga for Acropolis (McPhie et al., 2020). Wirrda Well: Hematite U-Pb dating gains an age of ~ 1.62 Ga (L. Courtney-Davies et al., 2019). Caption modified from (Maas et al., 2020).

MINERALISATION TIMING WITHIN THE OLYMPIC CU-AU PROVINCE

There is little published evidence for multiple episodes of Cu-Au-(U) mineralisation within the Olympic Cu-Au province, but geochronological evidence has shown superimposed events have impacted these deposits (Apukhtina et al., 2016; L. Courtney-Davies et al., 2019; Huang et al., 2015).

At OD, Sm-Nd carbonate based chronology uncovered that there were likely three formation ages at ca. $1.60-1.55$ Ga, 0.82 Ga and 0.5 Ga (Maas et al., 2020) (Figure x). Figure 15 represents the geochronology work done in this study and its relationship to other deposits within the eastern Gawler Craton. This chronology is consistent with ages for other minerals (gangue and ore) from both OD and other deposits within Olympic Cu-Au Province (Figure 15). Mineral ages both at OD and Vulcan are consistent with timing of tectonic events (Maas et al., 2020). This implies a multi-stage evolution of carbonate formation rather than periodic resetting due to a thermal anomaly. This is likely due to changes in local fluids brought on by regional responses to large scale

tectonic events (Maas et al., 2020). This multi-stage evolution is supported by the textural, mineralogical and compositional diversity of the carbonate populations (Maas et al., 2020).

This suggests that apatite mineralisation can be used as an indicator at the Vulcan prospect in order to determine the type of Cu-Fe-REE mineralisation at the core scale. This coupled with apatite geochronology, petrography and LA-ICP-MS analysis can provide accurate timing and locality on mineralisation, and post-ore events on the deposit scale.

5 CONCLUSIONS AND OUTLOOK

- Metamorphic-clast hosted apatite grains produced ages of 461 ± 9 Ma, 510 ± 8 Ma and 544 ± 46 Ma consistent with the Delamarian Orogeny.
- When hematite is the dominant Fe-Oxide, hydrothermal apatite grains record ages of 985 ± 18 Ma and 1095 ± 10 Ma corresponding with the waning phases of the Musgravian Orogeny. Florencite crystallisation commencement is ubiquitous with these apatite grains and therefore late stage alteration and REE remobilisation. This implies the Musgravian Orogeny has a thermal effect on the Vulcan prospect.
- When magnetite is the dominant Fe-Oxide, hydrothermal apatite grains record ages of 1522 ± 42 Ma, 1543 ± 25 Ma and 1611 ± 24 Ma within error of the Hiltaba Suite magmatic/hydrothermal event. These apatites are within error of the mineralisation age of Cu-Au given by Reid et al. (2013) therefore apatite 3 textures have an association with mineralisation at the Vulcan prospect.

- The Vulcan prospect has undergone a post depositional event which has facilitated a change to lower fluid pH and lower temperature. This has been interpreted as an uplift event.
- Apatite REE patterns and geochronology can be used as an indicator into mineralisation style at IOCG deposits within the Olympic Cu-Au province.

Vulcan geochronology is supported by other deposits within the Olympic Cu-Au province. Large scale structural and thermal controls due to regional tectonic events are the main cause for changes in fluid chemistry and therefore mineralisation at Vulcan and within the Olympic Cu-Au province.

ACKNOWLEDGMENTS

Firstly, I would like to sincerely thank Karin Barovich for all of the help throughout the year. I would not have been able to complete this project without all of the advice and encouragement. I would also like to thank Martin Hand for all the help with sample preparation and thin section analysis. A special thanks goes out to Aoife McFadden and Sarah Gilbert for all of their help with the SEM and LA-ICP-MS. Thanks also to Brad Cave for all of the support and guidance throughout the year, I really appreciate it. To the honours cohort, thanks for the fun year and for the supportive work environment of the honours room. Finally, a special thanks to Greg Swain, Maria Dmitrijeva, Jon Berthiaume and the team from FMG for their experience and for funding such an interesting and exciting project.

REFERENCES

- Allen, S. R., McPhie, J., Ferris, G., & Simpson, C. (2008). Evolution and architecture of a large felsic Igneous Province in western Laurentia: The 1.6 Ga Gawler Range Volcanics, South Australia. *Journal of Volcanology and Geothermal Research*, 172(1-2), 132-147. <https://doi.org/https://doi.org/10.1016/j.jvolgeores.2005.09.027>
- Allen, S. R., Simpson, C., McPhie, J., & Daly, S. J. (2003). Stratigraphy, distribution and geochemistry of widespread felsic volcanic units in the Mesoproterozoic Gawler Range Volcanics, South Australia. *Australian Journal of Earth Sciences*, 50, 97-112. <https://doi.org/10.1046/j.1440-0952.2003.00980.x>
- Apukhtina, O. B., Kamenetsky, V. S., Ehrig, K., Kamenetsky, M. B., Maas, R., Thompson, J., McPhie, J., Ciobanu, C. L., & Cook, N. J. (2017). Early, deep magnetite-fluorapatite mineralization at the Olympic Dam Cu-U-Au-Ag deposit, South Australia. *Economic Geology*, 112(6), 1531-1542.
- Apukhtina, O. B., Kamenetsky, V. S., Ehrig, K., Kamenetsky, M. B., McPhie, J., Maas, R., Meffre, S., Goemann, K., Rodemann, T., & Cook, N. J. (2016). Postmagmatic magnetite–apatite assemblage in mafic

- intrusions: a case study of dolerite at Olympic Dam, South Australia. *Contributions to Mineralogy and Petrology*, 171(1), 2.
- Barton, M. D. (2014). Iron Oxide(-Cu-Au-REE-P-Ag-U-Co) Systems. *Treatise on Geochemistry: Second Edition*, 13, 515-541. <https://doi.org/10.1016/B978-0-08-095975-7.01123-2>
- Barton, M. D., & Johnson, D. A. (1996). Evaporitic-Source Model for Igneous-Related Fe oxide-(REE-Cu-Au-U) Mineralization. *Geology*, 24(3), 259-262. [https://doi.org/10.1130/0091-7613\(1996\)024<0259:ESMFIR>2.3.CO;2](https://doi.org/10.1130/0091-7613(1996)024<0259:ESMFIR>2.3.CO;2)
- Barton, M. D., & Johnson, D. A. (2000). Alternative Brine Sources for Fe-Oxide(-Cu-Au) Systems: Implications for Hydrothermal Alteration and Metals.
- Blissett, A. H., Creaser, R. A., Daly, S. J., Flint, R., & Parker, A. J. (1993). *Gawler Range Volcanics* (Vol. 1). South Australia Geological Survey, Bulletin 54.
- Boynton, W. V. (1984). Cosmochemistry of the rare earth elements: meteorite studies. In *Developments in geochemistry* (Vol. 2, pp. 63-114). Elsevier.
- Cherry, A., Kamenetsky, V., McPhie, J., Kamenetsky, M., Ehrig, K., & Keeling, J. (2017). Post-1590 Ma modification of the supergiant Olympic Dam deposit: links with regional tectonothermal events. Proceedings, 14th SGA Biennial Meeting 'Mineral Resources to Discover', Québec City, QC, Canada.
- Cherry, A., Kamenetsky, V., McPhie, J., Thompson, J., Ehrig, K., Meffre, S., Kamenetsky, M., & Krneta, S. (2018). Tectonothermal events in the Olympic IOCG Province constrained by apatite and REE-phosphate geochronology. *Australian Journal of Earth Sciences*, 65(5), 643-659.
- Chew, D., Petrus, J., & Kamber, B. (2014). U-Pb LA-ICPMS dating using accessory mineral standards with variable common Pb. *Chemical Geology*(363), 185-199.
- Chew, D. M., & Spikings, R. A. (2015). Geochronology and thermochronology using apatite: time and temperature, lower crust to surface. *Elements*, 11(3), 189-194.
- Ciobanu, C. L., Ehrig, K., Cook, N. J., & Wade, B. (2015). Trace Element Signatures in Iron Oxides from the Olympic Dam IOCG Deposit, South Australia.
- Ciobanu, C. L., Wade, B. P., Cook, N. J., Mumm, A. S., & Giles, D. (2013). Uranium-bearing hematite from the Olympic Dam Cu-U-Au deposit, South Australia: A geochemical tracer and reconnaissance Pb-Pb geochronometer. *Precambrian Research*, 238, 129-147.
- Cochrane, R., Spikings, R. A., Chew, D., Wotzlaw, J.-F., Chiaradia, M., Tyrrell, S., Schaltegger, U., & Van der Lelij, R. (2014). High temperature (> 350 C) thermochronology and mechanisms of Pb loss in apatite. *Geochimica et Cosmochimica Acta*, 127, 39-56.
- Cook, N., Ciobanu, C. L., George, L., Zhu, Z.-Y., Wade, B., & Ehrig, K. (2016). Trace element analysis of minerals in magmatic-hydrothermal ores by laser ablation inductively-coupled plasma mass spectrometry: Approaches and opportunities. *Minerals*, 6(4), 111.
- Corfu, F., & Stone, D. (1998). The significance of titanite and apatite U-Pb ages: constraints for the post-magmatic thermal-hydrothermal evolution of a batholithic complex, Berens River area, northwestern Superior Province, Canada. *Geochimica et Cosmochimica Acta*, 62(17), 2979-2995.
- Courtney-Davies, L., Ciobanu, C. L., Tapster, S. R., Cook, N. J., Ehrig, K., Crowley, J. L., Verdugo-Ihl, M. R., Wade, B. P., & Condon, D. J. (2020). Opening the magmatic-hydrothermal window: High-precision U-Pb geochronology of the Mesoproterozoic Olympic Dam Cu-U-Au-Ag deposit, South Australia. *Economic Geology*.
- Courtney-Davies, L., Ciobanu, C. L., Verdugo-Ihl, M. R., Dmitrijeva, M., Cook, N. J., Ehrig, K., & Wade, B. (2019). Hematite geochemistry and geochronology resolve genetic and temporal links among iron-oxide copper gold systems, Olympic Dam district, South Australia. *Precambrian Research*, 335. <https://doi.org/10.1016/j.precamres.2019.105480>
- Courtney-Davies, L., Tapster, S., Ciobanu, C., Cook, N., Verdugo Ihl, M., Ehrig, K., Kennedy, A., Gilbert, S., Condon, D., & Wade, B. (2019). A multi-technique evaluation of hydrothermal hematite U-Pb isotope systematics: Implications for ore deposit geochronology. *Chemical Geology*. <https://doi.org/10.1016/j.chemgeo.2019.03.005>
- Courtney-Davies, L., Zhu, Z., Ciobanu, C. L., Wade, B. P., Cook, N. J., Ehrig, K., Cabral, A. R., & Kennedy, A. (2016). Matrix-matched iron-oxide laser ablation ICP-MS U-Pb geochronology using mixed solution standards. *Minerals*, 6(3), 85.
- Creaser, R. A. (1995). Neodymium isotopic constraints for the origin of Mesoproterozoic felsic magmatism, Gawler Craton, South Australia. *Canadian Journal of Earth Sciences*, 32(4), 460-471.
- Daly, S. J. (1998). Tectonic evolution and exploration potential of the Gawler Craton, South Australia. *AGSO J. Aust. Geol. Geophys.*, 17, 145-168. <https://ci.nii.ac.jp/naid/10025313206/en/>

- Ehrig, K., McPhie, J., & Kamenetsky, V. (2013). Geology and Mineralogical Zonation of the Olympic Dam Iron Oxide Cu-U-Au-Ag Deposit, South Australia. *16*, 237-268.
<https://doi.org/https://doi.org/10.5382/SP.16.11>
- Fairclough, M., Schwarz, M., & Ferris, G. (2003). *Interpreted Crystalline Basement Geology of the Gawler Craton*. South Australia, South Australian Geological Survey.
- Fanning, C., Teale, G., & Reid, A. (2007). *A geochronological framework for the Gawler Craton, South Australia*. Primary Industries and Resources SA.
- Fanning, C. M., Flint, R., Parker, A. J., Ludwig, K. R., & Blissett, A. H. (1988). Refined Proterozoic evolution of the Gawler Craton, South Australia, through U-Pb zircon geochronology. *Precambrian Research*, 40-41, 363-386. [https://doi.org/https://doi.org/10.1016/0301-9268\(88\)90076-9](https://doi.org/https://doi.org/10.1016/0301-9268(88)90076-9)
- Fanning, C. M., Reid, A. J., & Teale, G. S. (2007). A geochronological framework for the Gawler Craton, South Australia. *South Australia Geological Survey Bulletin*, 55(258).
- Ferris, G., Schwarz, M., & Heithersay, P. (2002). Hydrothermal iron oxide copper-gold and related deposits: A global perspective.
- Ferris, G. M. (2001). *The geology and geochemistry of granitoids in the Childara region, West Gawler craton, South Australia: implications for the Proterozoic tectonic history of the Western Gawler craton, and development of lode-style gold mineralisation at Tunkilla University of Tasmania*].
- Fleet, M. E., & Pan, Y. (1997). Site preference of rare earth elements in fluorapatite: Binary (LREE+HREE)-substituted crystals. *American Mineralogist*, 82(9-10), 870-877.
- Foden, J., Elburg, M. A., Dougherty-Page, J., & Burt, A. (2006). The timing and duration of the Delamerian Orogeny: correlation with the Ross Orogen and implications for Gondwana assembly. *The Journal of Geology*, 114(2), 189-210.
- Fraser, G. L., & Neumann, N. (2010). *New SHRIMP U-Pb zircon ages from the Gawler Craton and Curnamona Province, South Australia, 2008-2010*. Geoscience Australia.
- Gawęda, A., Szopa, K., & Chew, D. (2014). LA-ICP-MS U-Pb dating and REE patterns of apatite from the Tatra Mountains, Poland as a monitor of the regional tectonomagmatic activity. *Geochronometria*, 41(4), 306-314.
- Groves, D. I., Bierlein, F. P., Meinert, L. D., & Hitzman, M. W. (2010). Iron oxide copper-gold (IOCG) deposits through Earth history: Implications for origin, lithospheric setting, and distinction from other epigenetic iron oxide deposits. *Economic Geology*, 105(3), 641-654.
<https://doi.org/https://doi.org/10.2113/gsecongeo.105.3.641>
- Hall, J. W., Glorie, S., Reid, A. J., Boone, S. C., Collins, A. S., & Gleadow, A. (2018). An apatite U-Pb thermal history map for the northern Gawler Craton, South Australia. *Geoscience Frontiers*, 9(5), 1293-1308.
- Hand, M., Reid, A., & Jagodzinski, E. (2007). Tectonic Framework and Evolution of the Gawler Craton, Southern Australia. *Economic Geology*, 102(8), 1377-1395.
<https://doi.org/10.2113/gsecongeo.102.8.1377>
- Hayward, N., & Skirrow, R. G. (2010). Geodynamic setting and controls on iron oxide Cu-Au (\pm U) ore in the Gawler Craton, South Australia. In T. M. Porter (Ed.), *Hydrothermal Iron Oxide Copper-Gold & Related Deposits: A Global Perspective* (Vol. 3, pp. 9-31). PGC Publishing.
- Hitzman, M. W. (2000). Iron oxide-Cu-Au deposits: What, where, when, and why. *Hydrothermal iron oxide copper-gold and related deposits: A global perspective*, 1, 9-25.
- Howard, K. E. (2006). *Provenance of Palaeoproterozoic metasedimentary rocks in the eastern Gawler Craton, Southern Australia: Implications for reconstruction models of Proterozoic Australia*
- Huang, Q., Kamenetsky, V. S., McPhie, J., Ehrig, K., Meffre, S., Maas, R., Thompson, J., Kamenetsky, M., Chambefort, I., & Apukhtina, O. (2015). Neoproterozoic (ca. 820–830 Ma) mafic dykes at Olympic Dam, South Australia: links with the gairdner large igneous province. *Precambrian Research*, 271, 160-172.
- Ismail, R., Ciobanu, C. L., Cook, N. J., Teale, G. S., Giles, D., Mumm, A. S., & Wade, B. (2014). Rare earths and other trace elements in minerals from skarn assemblages, Hillside iron oxide-copper-gold deposit, Yorke Peninsula, South Australia. *Lithos*, 184, 456-477.
- Jackson, S. E., Pearson, N. J., Griffin, W. L., & Belousova, E. A. (2004). The application of laser ablation-inductively coupled plasma-mass spectrometry to in situ U-Pb zircon geochronology. *Chemical Geology*, 211(1), 47-69. <https://doi.org/https://doi.org/10.1016/j.chemgeo.2004.06.017>
- Jagodzinski, E. (2005). Compilation of SHRIMP U-Pb geochronological data, Olympic Domain, Gawler Craton, South Australia, 2001-2003. *Geoscience Australia Record*, 20, 197.
- Jagodzinski, E. (2014). The age of magmatic and hydrothermal zircon at Olympic Dam. Australian Earth Sciences Convention (AESCon), Sustainable Australia,

- Jochum, K. P., Willbold, M., Raczek, I., Stoll, B., & Herwig, K. (2005). Chemical Characterisation of the USGS Reference Glasses GSA-1G, GSC-1G, GSD-1G, GSE-1G, BCR-2G, BHVO-2G and BIR-1G Using EPMA, ID-TIMS, ID-ICP-MS and LA-ICP-MS. *Geostandards and Geoanalytical Research*, 29(3), 285-302. <https://doi.org/10.1111/j.1751-908X.2005.tb00901.x>
- Johnson, J. P. (1993). The geochronology and radiogenic isotope systematics of the Olympic Dam copper-uranium-gold-silver deposit, South Australia.
- Johnson, J. P., & Cross, K. C. (1995). U-Pb geochronological constraints on the genesis of the Olympic Dam Cu-U-Au-Ag deposit, South Australia. *Economic Geology*, 90(5), 1046-1063.
- Kamenetsky, V. S., Ehrig, K., Maas, R., Meffre, S., Kamenetsky, M., McPhie, J., Apukhtina, O., Huang, Q., Thompson, J., & Ciobanu, C. L. (2015). The supergiant Olympic Dam Cu-U-Au-Ag ore deposit: Toward a new genetic model. *Society of Economic Geologists, SEG*.
- Kirkland, C., Hollis, J., Danišik, M., Petersen, J., Evans, N., & McDonald, B. (2017). Apatite and titanite from the Karrat Group, Greenland; implications for charting the thermal evolution of crust from the U-Pb geochronology of common Pb bearing phases. *Precambrian Research*, 300, 107-120.
- Kirkland, C., Yakymchuk, C., Szilas, K., Evans, N., Hollis, J., McDonald, B., & Gardiner, N. (2018). Apatite: a U-Pb thermochronometer or geochronometer? *Lithos*, 318, 143-157.
- Kontonikas-Charos, A., Ciobanu, C. L., & Cook, N. J. (2014). Albitization and redistribution of REE and Y in IOCG systems: insights from Moonta-Wallaroo, Yorke Peninsula, South Australia. *Lithos*, 208, 178-201.
- Kontonikas-Charos, A., Ciobanu, C. L., Cook, N. J., Ehrig, K., Ismail, R., Krneta, S., & Basak, A. (2018). Feldspar mineralogy and rare-earth element (re) mobilization in iron-oxide copper gold systems from South Australia: a nanoscale study. *ALKIS KONTONIKAS-CHAROS ET AL. FELDSPARS IN IOCG SYSTEMS. Mineralogical Magazine*, 82(S1), S173-S197.
- Kontonikas-Charos, A., Ciobanu, C. L., Cook, N. J., Ehrig, K., Krneta, S., & Kamenetsky, V. S. (2017). Feldspar evolution in the Roxby Downs Granite, host to Fe-oxide Cu-Au(U) mineralisation at Olympic Dam, South Australia. *Ore Geology Reviews*, 80, 838-859.
- Kontonikas-Charos, A., Ciobanu, C. L., Cook, N. J., Ehrig, K., Krneta, S., & Kamenetsky, V. S. (2018). Rare earth element geochemistry of feldspars: examples from Fe-oxide Cu-Au systems in the Olympic Cu-Au Province, South Australia. *Mineralogy and Petrology*, 112(2), 145-172.
- Krneta, S. (2017). *The evolution of apatite in iron-oxide-copper-gold mineralization of the Olympic Cu-Au Province: unraveling magmatic and hydrothermal histories through changes in morphology and trace element chemistry*
- Krneta, S., Ciobanu, C., Cook, N., Ehrig, K., & Kontonikas-Charos, A. (2017). Rare Earth Element Behaviour in Apatite from the Olympic Dam Cu-U-Au-Ag Deposit, South Australia. *Minerals*, 7, 135.
- Krneta, S., Cook, N. J., Ciobanu, C. L., Ehrig, K., & Kontonikas-Charos, A. (2017). The Wirrda Well and Acropolis prospects, Gawler Craton, South Australia: Insights into evolving fluid conditions through apatite chemistry. *Journal of Geochemical Exploration*, 181, 276-291.
- Ludwig, K. R. (2003). *User's Manual for Isoplot 3.00: A Geochronological Toolkit for Microsoft Excel*. Kenneth R. Ludwig. <https://books.google.com.au/books?id=OutNAQAIAAJ>
- Maas, R., Apukhtina, O. B., Kamenetsky, V. S., Ehrig, K., Sprung, P., & Münker, C. (2020). Carbonates at the supergiant Olympic Dam Cu-U-Au-Ag deposit, South Australia part 2: Sm-Nd, Lu-Hf and Sr-Pb isotope constraints on the chronology of carbonate deposition. *Ore Geology Reviews*, 103745.
- Mao, M., Rukhlov, A. S., Rowins, S. M., Spence, J., & Coogan, L. A. (2016). Apatite trace element compositions: a robust new tool for mineral exploration. *Economic Geology*, 111(5), 1187-1222.
- Mark, C., Cogné, N., & Chew, D. (2016). Tracking exhumation and drainage divide migration of the Western Alps: A test of the apatite U-Pb thermochronometer as a detrital provenance tool. *Bulletin*, 128(9-10), 1439-1460.
- McFarlane, C. (2006). Palaeoproterozoic evolution of the Challenger Au deposit, South Australia, from monazite geochronology. *Journal of Metamorphic Geology*, 24(1), 75-87.
- McInnes, B., Keays, R. R., Lambert, D. D., Hellstrom, J., & Allwood, J. (2008). Re-Os geochronology and isotope systematics of the Tanami, Tennant Creek and Olympic Dam Cu-Au deposits. *Australian Journal of Earth Sciences*, 55(6-7), 967-981.
- McPhie, J., Ehrig, K., Kamenetsky, M., Crowley, J., & Kamenetsky, V. (2020). Geology of the Acropolis prospect, South Australia, constrained by high-precision CA-TIMS ages. *Australian Journal of Earth Sciences*, 67(5), 699-716.
- Migdisov, A., Williams-Jones, A., Brugger, J., & Caporuscio, F. A. (2016). Hydrothermal transport, deposition, and fractionation of the REE: Experimental data and thermodynamic calculations. *Chemical Geology*, 439, 13-42.

- Mücke, A., & Cabral, A. R. (2005). Redox and nonredox reactions of magnetite and hematite in rocks. *Geochemistry*, 65(3), 271-278.
- Mumin, H., Corriveau, L., Somarin, A. K., & Ootes, L. (2007). Iron oxide copper-gold-type polymetallic mineralization in the Contact Lake belt, Great Bear magmatic zone, Northwest Territories, Canada. *Exploration and Mining Geology*, 16, 187-208. <https://doi.org/https://doi.org/10.2113/gsemg.16.3-4.187>
- Norris, A., & Danyushevsky, L. (2018, 12/8). Towards Estimating the Complete Uncertainty Budget of Quantified Results Measured by LA-ICP-MS. Goldschmidt, Boston.
- Ohmoto, H. (2003). Nonredox transformations of magnetite-hematite in hydrothermal systems. *Economic Geology*, 98(1), 157-161.
- Parak, T. (1975). Kiruna iron ores are not "intrusive-magmatic ores of the Kiruna type". *Economic Geology*, 70(7), 1242-1258. <https://doi.org/https://doi.org/10.2113/gsecongeo.70.7.1242>
- Paton, C., Hellstrom, J., Paul, B., Woodhead, J., & Hergt, J. (2011). Iolite: Freeware for the Visualisation and Processing of Mass Spectrometric Data. *Journal of Analytical Atomic Spectrometry*, 26(12), 2508-2518. <https://doi.org/10.1039/C1JA10172B>
- Paton, C., Woodhead, J. D., Hellstrom, J. C., Hergt, J. M., Greig, A., & Maas, R. (2010). Improved laser ablation U-Pb zircon geochronology through robust downhole fractionation correction. *Geochemistry, Geophysics, Geosystems*, 11(3). <https://doi.org/10.1029/2009gc002618>
- Payne, J., Barovich, K., & Hand, M. (2006). On the tectonic setting of the magmatic suite previously known as the 'Arc-like Tunkillia/Ifould.'. Geological Society of Australia Abstracts,
- Payne, J. L., Barovich, K. M., & Hand, M. (2006). Provenance of metasedimentary rocks in the northern Gawler Craton, Australia: implications for Palaeoproterozoic reconstructions. *Precambrian Research*, 148(3-4), 275-291.
- Payne, J. L., Hand, M., Barovich, K. M., & Wade, B. P. (2008). Temporal constraints on the timing of high-grade metamorphism in the northern Gawler Craton: implications for assembly of the Australian Proterozoic. *Australian Journal of Earth Sciences*, 55(5), 623-640. <https://doi.org/10.1080/08120090801982595>
- Piccoli, P. M., & Candela, P. A. (2002). Apatite in igneous systems. *Reviews in Mineralogy and Geochemistry*, 48(1), 255-292.
- Reeve, J. S., Cross, K. C., Smith, R. N., & Oreskes, N. (1990). The Olympic Dam Cu-U-Au-Ag deposit, South Australia. In *Geology of the Mineral Deposits of Australia and Papua New Guinea* (Vol. 14, pp. 1009-1035). Australian Institute of Mining and Metallurgy Monograph.
- Reid, A., Hand, M., Jagodzinski, E., Kelsey, D., & Pearson, N. (2006). Paleoproterozoic orogenesis in the southeastern Gawler Craton, South Australia. *Australian Journal of Earth Sciences*, 55(4), 449-471.
- Reid, A., Jourdan, F., & Jagodzinski, E. (2017). Mesoproterozoic fluid events affecting Archean crust in the northern Olympic Cu-Au Province, Gawler Craton: insights from 40Ar/39Ar thermochronology. *Australian Journal of Earth Sciences*, 64(1), 103-119.
- Reid, A., Smith, R. N., Baker, T., Jagodzinski, E., Selby, D., Gregory, C. J., & Skirrow, R. G. (2013). Re-Os DATING OF MOLYBDENITE WITHIN HEMATITE BRECCIAS FROM THE VULCAN Cu-Au PROSPECT, OLYMPIC Cu-Au PROVINCE, SOUTH AUSTRALIA. *Economic Geology*, 108, 883-894. <https://doi.org/https://doi.org/10.2113/econgeo.108.4.883>
- Ruiz, C. F., & Ericksen, G. E. (1962). Metallogenic provinces of Chile, S.A. *Economic Geology*, 57, 91-106. <https://doi.org/https://doi.org/10.2113/gsecongeo.57.1.91>
- Schmandt, D. S., Cook, N. J., Ciobanu, C. L., Ehrig, K., Wade, B. P., Gilbert, S., & Kamenetsky, V. S. (2019). Rare Earth Element Phosphate Minerals from the Olympic Dam Cu-U-Au-Ag Deposit, South Australia: Recognizing Temporal-Spatial Controls On Re Mineralogy in an Evolved IOCG System. *The Canadian Mineralogist*, 57(1), 3-24. <https://doi.org/10.3749/canmin.1800043>
- Schoene, B., & Bowring, S. A. (2007). Determining accurate temperature-time paths from U-Pb thermochronology: An example from the Kaapvaal craton, southern Africa. *Geochimica et Cosmochimica Acta*, 71(1), 165-185.
- Schoene, B., Crowley, J., Condon, D., Schmitz, M., & Bowring, S. (2006). Reassessing the uranium decay constants for geochronology using ID-TIMS U-Pb data. *Geochimica et Cosmochimica Acta*, 70, 426-445. <https://doi.org/10.1016/j.gca.2005.09.007>
- Sillitoe, R. (2003). Iron oxide-copper-gold deposits: An Andean view. *Mineralium Deposita*, 38(7), 787-812. <https://doi.org/10.1007/s00126-003-0379-7>
- Simon, A. C., Knipping, J., Reich, M., Barra, F., Deditius, A. P., Bilenker, L., & Childress, T. (2018). Kiruna-Type Iron Oxide-Apatite (IOA) and Iron Oxide Copper-Gold (IOCG) Deposits Form by a Combination of Igneous and Magmatic-Hydrothermal Processes: Evidence from the Chilean Iron Belt. In

- A. M. Arribas R & J. L. Mauk (Eds.), *Metals, Minerals, and Society* (Vol. 21, pp. 0). Society of Economic Geologists (SEG). <https://doi.org/10.5382/sp.21.06>
- Skirrow, R. G., Bastrakov, E., Barovich, K., Fraser, G. L., Creaser, R. A., Fanning, C. M., Raymond, O. L., & Davidson, G. J. (2007). Timing of iron oxide Cu-Au-(U) hydrothermal activity and Nd isotope constraints on metal sources in the Gawler craton, South Australia: . *Economic Geology*, 102(8), 1441-1470. <https://doi.org/https://doi.org/10.2113/gsecongeo.102.8.1441>
- Skirrow, R. G., Bastrakov, E., Davidson, G. J., Raymond, O. L., & Heithersay, P. (2002). The geological framework, distribution and controls of Fe-oxide Cu-Au mineralisation in the Gawler Craton, South Australia. Part II. Alteration and mineralisation. In *Hydrothermal Iron Oxide Copper-Gold & Related Deposits: A Global Perspective* (Vol. 2, pp. 33-47).
- Sláma, J., Košler, J., Condon, D. J., Crowley, J. L., Gerdes, A., Hanchar, J. M., Horstwood, M. S. A., Morris, G. A., Nasdala, L., Norberg, N., Schaltegger, U., Schoene, B., Tubrett, M. N., & Whitehouse, M. J. (2008). Plešovice zircon — A new natural reference material for U–Pb and Hf isotopic microanalysis. *Chemical Geology*, 249(1), 1-35. <https://doi.org/https://doi.org/10.1016/j.chemgeo.2007.11.005>
- Swain, G., Hand, M., Teasdale, J., Rutherford, L., & Clark, C. (2005). Age constraints on terrane-scale shear zones in the Gawler Craton, southern Australia. *Precambrian Research*, 139(3-4), 164-180.
- Swain, G., Woodhouse, A., Hand, M., Barovich, K., Schwarz, M., & Fanning, C. (2005). Provenance and tectonic development of the late Archaean Gawler Craton, Australia; U–Pb zircon, geochemical and Sm–Nd isotopic implications. *Precambrian Research*, 141(3-4), 106-136.
- Vassallo, J., & Wilson, C. (2001). Structural repetition of the Hutchison Group metasediments, Eyre Peninsula, South Australia. *Australian Journal of Earth Sciences*, 48(2), 331-345.
- Vassallo, J., & Wilson, C. (2002). Palaeoproterozoic regional-scale non-coaxial deformation: an example from eastern Eyre Peninsula, South Australia. *Journal of Structural Geology*, 24(1), 1-24.
- Verdugo-Ihl, M. R., Ciobanu, C. L., Cook, N. J., Ehrig, K., & Courtney-Davies, L. (2019). Defining early stages of IOCG systems: evidence from iron oxides in the outer shell of the Olympic Dam deposit, South Australia. *Mineralium Deposita*, 55, 429-452. <https://doi.org/10.1007/s00126-019-00896-2>
- Verdugo-Ihl, M. R., Ciobanu, C. L., Cook, N. J., Ehrig, K., Courtney-Davies, L., & Gilbert, S. (2017). Textures and U-W-Sn-Mo signatures in hematite from the Olympic Dam Cu-U-Au-Ag deposit, South Australia: Defining the archetype for IOCG deposits. *Ore Geology Reviews*, 91, 173-195. <https://doi.org/http://dx.doi.org/10.1016/j.oregeorev.2017.10.007>
- Wade, C., Reid, A., Wingate, M. T. D., Jagodzinski, E., & Barovich, K. (2012). Geochemistry and geochronology of the c. 1585 Ma Benagerie Volcanic Suite, southern Australia: Relationship to the Gawler Range Volcanics and implications for the petrogenesis of a Mesoproterozoic silicic large igneous province. *Precambrian Research*, 206-207, 17-35. <https://doi.org/https://doi.org/10.1016/j.precamres.2012.02.020>
- Wiedenbeck, M., Allé, P., Corfu, F., Griffin, W., Meier, M., Oberli, F., Von Quadt, A., Roddick, J. C., & Spiegel, W. (1995). Three natural zircon standards for U - Th - Pb, Lu - Hf, trace element and REE analyses. *Geostandards Newsletter*, 19, 1-23. <https://doi.org/10.1111/j.1751-908X.1995.tb00147.x>
- Williams, P. J., Barton, M. D., Johnson, D. A., Fontboté, L., de Haller, A., Mark, G., Oliver, N. H. S., & Marschik, R. (2005). Iron Oxide Copper-Gold Deposits: Geology, Space-Time Distribution, and Possible Modes of Origin. *Economic Geology 100th Anniversary Volume*, 371-405. <https://doi.org/https://doi.org/10.5382/AV100.13>

APPENDIX A: SAMPLE DESCRIPTIONS

Depth	Hole	Description	Reason For Sample Collection	Thin section
801.45 - 801.55	VUD009	Mafic Intrusion? Trace Element enriched. Angular clasts in a finer matrix	Dating REE elements in possible mafic intrusion, may give age of intrusion and therefore relative age constraint of host and/or Hematite	Y
852.00 - 852.10	VUD009	Massive Hematite ± Magnetite with barite crystals present, other gangue minerals also present, slightly magnetic	Attempting to date the Hematite endmember of the Vulcan deposit and determine the possible protolith, gangue minerals provide copious information about fluid and its source and origin	Y
866.10 - 866.20	VUD009	Massive Hematite ± Magnetite with texture being more crystalline	Attempting to date the Hematite endmember of the Vulcan deposit and determine the possible protolith	Y
876.60 - 876.70	VUD009	Mafic Intrusion? Trace Element enriched. Angular clasts in a finer matrix	Dating REE elements in possible mafic intrusion, may give age of intrusion and therefore relative age constraint of host and/or Hematite	N
904.00 - 904.10	VUD009	Massive Hematite ± Magnetite, slightly brecciated, Hematite disseminated throughout, finer grained and easily fracturing	Attempting to date the Hematite endmember of the Vulcan deposit and determine the possible protolith	Y
952.80 - 952.90	VUD009	Massive Hematite, disseminated and easily fracturing	Attempting to date the Hematite endmember of the Vulcan deposit and determine the possible protolith	Y
962.50 - 962.60	VUD009	Large clasts of Hematite stranded in Hematite rich matrix, heavily brecciated, maybe indicative of secondary fluid pathway?	Secondary fluid flow could provide trace element enrichment and mineralisation enrichment Cu-Au which could be useful for mine planning and dating of fluid types	Y
973.50 - 973.60	VUD009	Heavily Brecciated Massive Hematite, possibly indicative of a secondary or tertiary fluid flow	Secondary fluid flow could provide trace element enrichment and mineralisation enrichment Cu-Au which could be useful for mine planning and dating of fluid types	Y
994.00 - 994.10	VUD009	Heavily Brecciated Massive Hematite, Heavily Enriched in REE	Enrichment in REE could provide new dating method for these samples	Y

1020.60 - 1020.70	VUD009	Brecciated Massive Hematite with infill, infill being very soft (soapy) texture and pale discoloured (white) colour	Attempting to date the Hematite endmember of the Vulcan deposit and determine the possible protolith	Y
1070.20 - 1070.30	VUD009	Brecciated Hematite, heavily enriched in Nd	Enrichment in Nd could provide new dating method for these samples	Y
885.90 - 885.95	VUD016	Hematite Dominated Breccia (massive style hematite with small clasts) Strong sericitic alteration	High Zr values	Y
1001.15 - 1001.20	VUD016	Ser, chl, hematite schist with varying levels of schistosity. Hematite generally in veinlets.	High Zr values, elevated REE with some Hematite	Y
1091.90 - 1092.00	VUD016	Strong red hematite alteration of host, slightly brecciated, similar to mafic? Units in VUD009	High Zr, High La, slight increase to background sulphide content	Y
1123.00 - 1123.05	VUD016	Brecciated Massive Hematite with infill, infill being very soft (soapy) texture and pale discoloured (white) colour	Massive hematite, some increase in REE	Y
1151.10 - 1151.20	VUD016	Massive Hm	Steely grey hematite might have some elevated La and P	Y
1172.40 - 1172.50	VUD016	Hematite Dominated Breccia (massive style hematite with small clasts) Strong sericitic alteration	High Zr values	Y
1375.60 - 1375.70	VUD016	Heavy Hematite alteration, similar to mafic? Units in VUD009	High Zr and Hf, maybe potential Monazite	Y
1437.55 - 1437.65	VUD016	Blebby sulphides in a brecciated hematite matrix with heavy sericite alteration	High Zr and Hf, maybe potential Monazite with Cu sulphides	Y
1488.05 - 1488.15	VUD016	Blebby sulphides in a brecciated hematite matrix with heavy sericite alteration	High Zr and Hf, maybe potential Monazite with Cu sulphides	Y
938.00 - 938.20	VUD001	Host? Altered red rock with veining and disseminated sulphides, mainly py, cpy with rare bornite and Hematite	High copper with Hematite	Y
968.35 - 968.50	VUD001	Clasts of the Host? Red rock altered? Heavily brecciated, with veining and disseminated py, cpy, ser	High Zr and Hf, maybe potential Zircons with Cu sulphides	Y

1058.85 - 1059.00	VUD001	Large magnetite? Crystals with brecciated matrix, trace sulphides, mainly py, cpy. Seralt present	Magnetite with py endmember	Y
1064.55 - 1064.65	VUD001	Host? Altered red rock with veining deformed magnetite? With Hematite nad rare py, cpy	Magnetite with py endmember	Y
878.75 - 878.95	VUD003	Massive Hematite with py,cpy ± Magnetite. Sericite alteration with high Hf, Zr correlation	High Zr and Hf, maybe potential Zircons with Cu sulphides	Y
894.00 - 894.15	VUD003	Hematite Dominated Breccia with host? Red rock alteration and strong py,cpy mineralisation ± Bornite	High Zr and Hf, maybe potential Zircons with Cu sulphides, Hematite with sulphides endmember	Y
930.20 - 930.38	VUD003	Massive disseminated brecciated sulphides. Bornite common. Highest copper interval for VUD cores	Massive Sulphides	Y
1017.65 - 1017.75	VUD003	Host? Red rock altration with sericite, Hematite and pyrite	Host, with some sulphides, maybe dating host compared to hematite endmember?	Y
1025.30 - 1025.45	VUD003	Disseminated sulphides with py, cpy, bn in a Hematite rich matrix with host? Red rock alteration with sericite	Host? With hematite and sulphides, may be able to ascertain a textural relationship	N
1126.70 - 1126.85	VUD017	Granitic Host/Intrusion? With hematite ± magnetite and blebby sulphides increasing in grade up to bornite	High Zr and Hf correlation and blebby sulphides with a granitic? Host?	Y
1140.70 - 1141.00	VUD017	Granitic Host/Intrusion? With hematite ± magnetite as slightly magnetic, maybe pyrrohtite. Heavily brecciated, sericite alteration common	High Cu with a granitic? Host?	Y
1174.58 - 1174.75	VUD017	Brecciated Hm with Magnetite and some gangue. Py,cpy common with some rare bornite. Sample is slightly magnetic	High Zr and Hf correlation and blebby sulphides with a granitic? Host?	Y
1210.13 - 1210.25	VUD017	Massive Magnetite grain with brecciated sulphides, Hematite, Gangue and sericite alteration	Sampling Magnetite with Host?	Y

1221.55 - 1221.80	VUD017	Brecciated sample with magnetite and Hematite. Includes blebby sulphides. Py, cpy, Bn and granitic origin of host? Ser alteration also present	Sampling Magnetite with Host?	Y
1259.80 - 1259.95	VUD017	Massive Magnetite endmember. Some chl alteration with gangue and small blebby sulphides ± hematite	Sampling Massive Magnetite Endmember	Y
1268.00 - 1268.35	VUD017	Massive Magnetite endmember. Some Sericite alteration with gangue and small blebby sulphides ± hematite	Sampling Massive Magnetite Endmember	Y
1062.35 - 1062.50	VUD007	Mafic Intrusion? Trace Element enriched. Angular clasts in a finer matrix	UTAS sampled and elevated REEs	Y
1084.50 - 1084.70	VUD007	Stringer gangue veining with sericite and chlorite alteration. Pyrite, Chalcopyrite and rare Bornite. Possible granitic intrusion? Host? In some sections	Sampling hematite endmember with high Zr and Hf correlations for zircons. UTAS sampled nearby	Y
1100.15 - 1100.30	VUD007	Host? Sericite alteration with gangue and elevated Zr.	High Zr and Hf, correlation, possibility of some zircons with 'red rock' host	Y
1144.20 - 1144.35	VUD007	Massive Magnetite ± hematite with blebby sulphides and gangue stringer veins	Sampling Magnetite Endmember	Y
1155.20 - 1155.40	VUD007	Heavily brecciated Magnetite ± hematite with high sulphides and gangue. Sericite and chlorite alteration present and some evidence for possible granitic intrusion?	Sampling Magnetite Endmember	Y
1183.00 - 1183.20	VUD007	Massive Magnetite ± hematite with blebby sulphides	Sampling Magnetite Endmember	Y
1192.05 - 1192.20	VUD007	Brecciated Magnetite ± hematite with blebby sulphides and gangue minerals, chlorite alteration present	Sampling Magnetite Endmember	Y

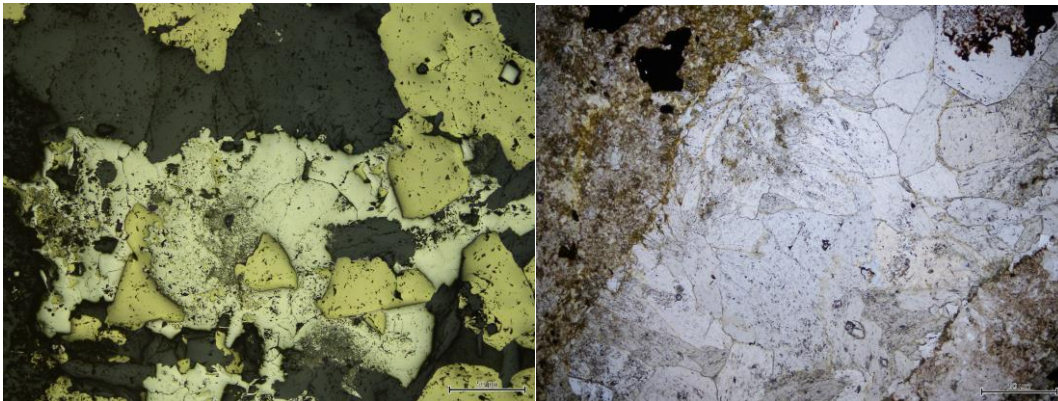
APPENDIX B: PETROGRAPHY

VUD001

938 – 938.20

Description:

This sample depicts macroscopic chalcopyrite clusters within large quartz/albite fragments. The sample is dominated by a sericite-albite-dolomite ‘mash’ of crystals in a granoblastic texture. There is abundant sericitic and chloritic alteration throughout the sample overprinting albite and other potential feldspars. Metamorphic fragments contain large apatite crystals with red inclusions in the centre (possibly hematite).

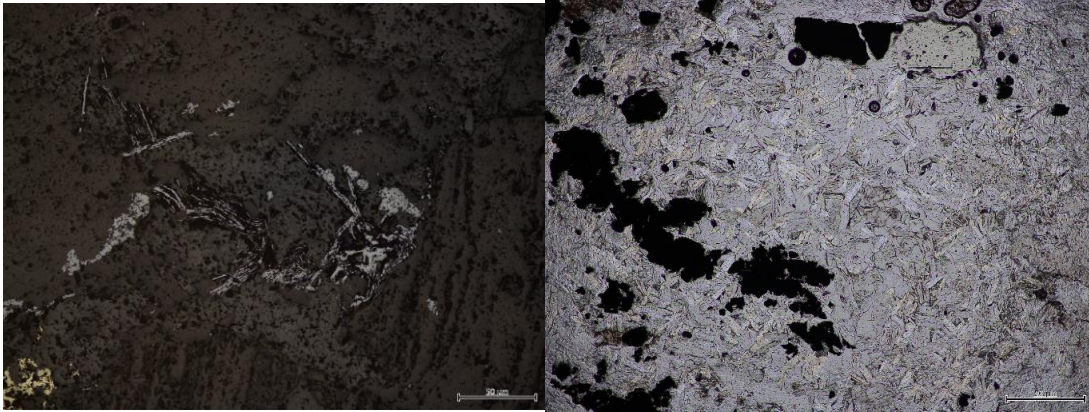


968.35 – 968.50

Description:

This sample is defined by metamorphic foliation, albite and quartz are the two most dominant minerals within this section. Quartz and albite within this section are very small and have a granular texture and commonly quartz is crosscutting in vein structures. Zircon grains are common within the foliation and porphyroblasts within the foliation display evidence of deformation. Pyrite clasts are also present within the section but only appear with veins and are heavily fractured. Hydrothermal hematite is

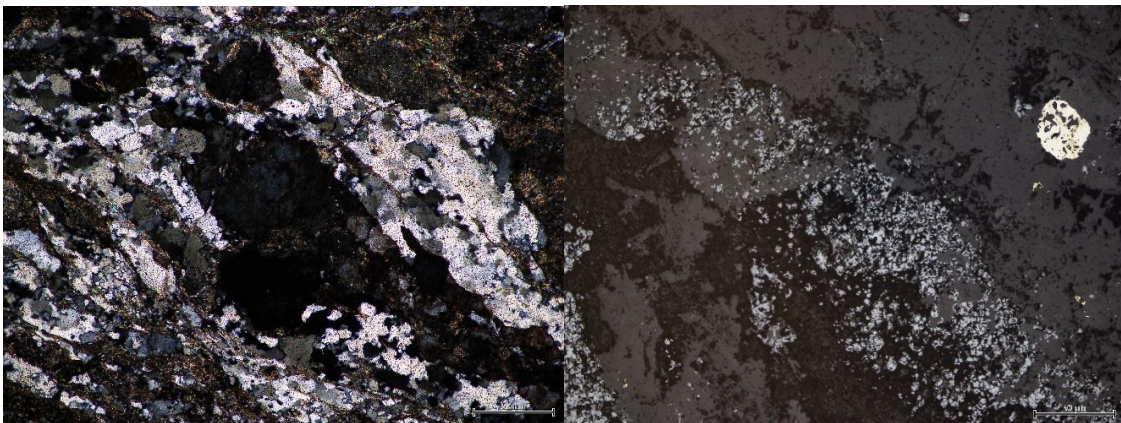
present within the section in veins with sulphides. Red rock alteration is the most common alteration style present within the section.



1058.85 – 1059.00

Description:

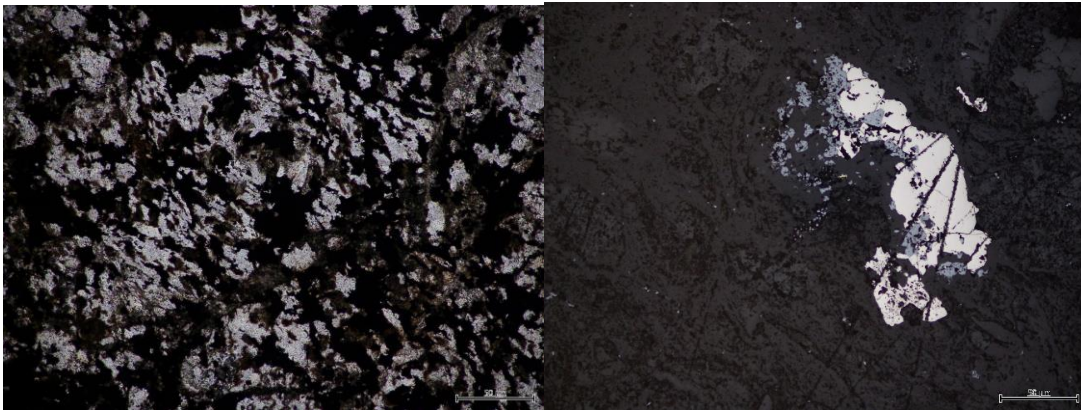
This sample is a mylonite which is defined by its metamorphic foliation. The host rock has been almost completely overprinted by red rock alteration and some minor chlorite alteration is present. The section is dominated by quartz and albite rich foliation which vein around large porphyroblasts of apatite which have experienced some deformation. This sample other than the apatite porphyroblasts is extremely fine grained and has a granular texture of grains. Some sulphides are also present, mainly pyrite which is always within veins with hematite.



1064.55 – 1064.65

Description:

This sample is dominated by two massive magnetite grains which have been slightly overprinted by hematite. There is some evidence that these grains have undergone plastic deformation. The host in this sample is extremely altered both by red rock and chlorite with minor sericite alteration also present. Alteration is most pronounced on the edges of Fe-Oxides. However, the host that hasn't been altered is defined by foliation and is mainly quartz and albite dominated. Sulphides are also present within this sample as pyrite, which is generally as small clusters near or around veins of hematite/magnetite.



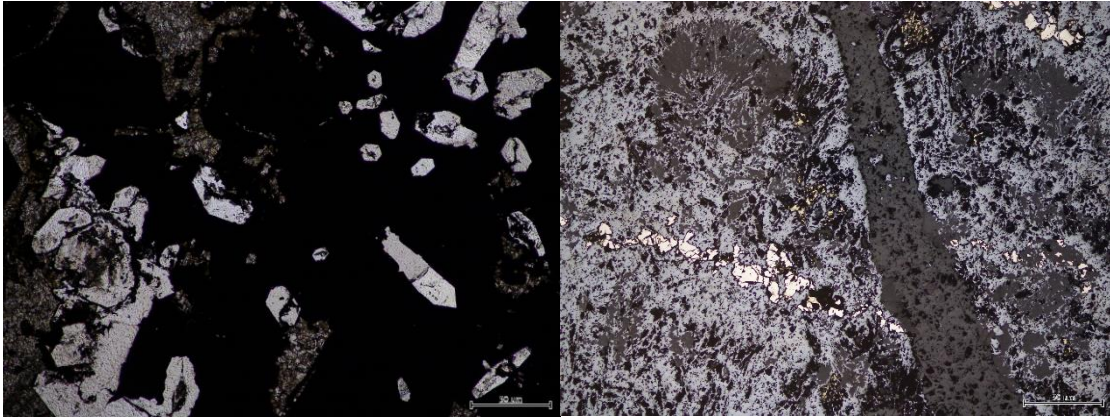
VUD003

878.75 – 878.95

Description:

This sample is defined by plastically deformed hematite structures and veining sulphides. Pyrite and chalcopyrite are both common within this section, however

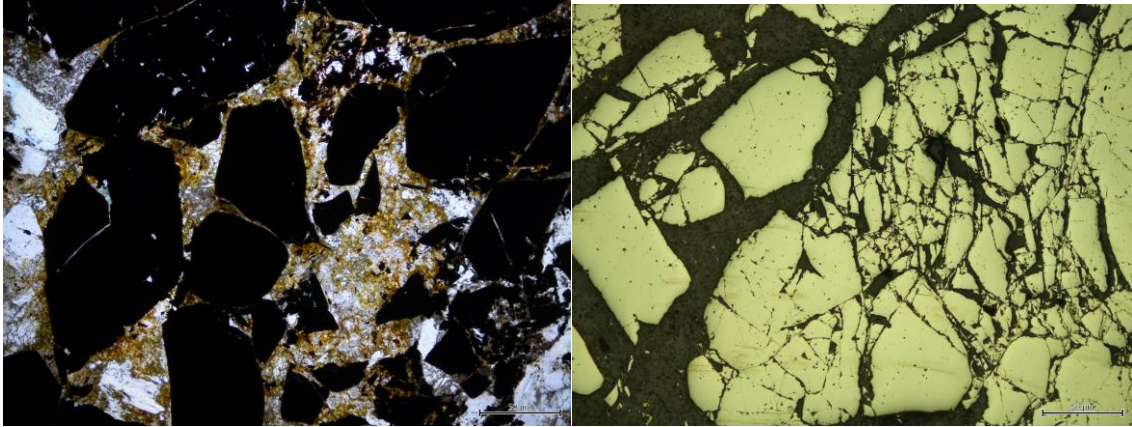
chalcopyrite is the dominant sulphide. Hematite is forming feathery and fan like structures which likely implies that there was some overprinting of magnetite by late hematite fluids within this section. There are large apatite grains within the massive sulphides however these are not common within the magnetite/hematite. The host rock however has been heavily altered by red rock and chlorite alteration.



894 – 894.15

Description:

This sample is dominated by a massive sulphide vein which is mainly comprised of heavily fractured pyrite and blebby chalcopyrite. This has altered the surrounding host rock and therefore is likely to be an infill and alteration style veinlet. The host is comprised of albite, sericite and quartz with rare dolomite crystals and apatite near the chalcopyrite. Texturally the host is a ‘mash’ texture with veining quartz and pyrite, there are small fragments of disseminated hematite within the mash as well as pyrite. Discoloured ‘red rock stained’ fragments of quartz and albite host larger albites than within the surrounding rock.



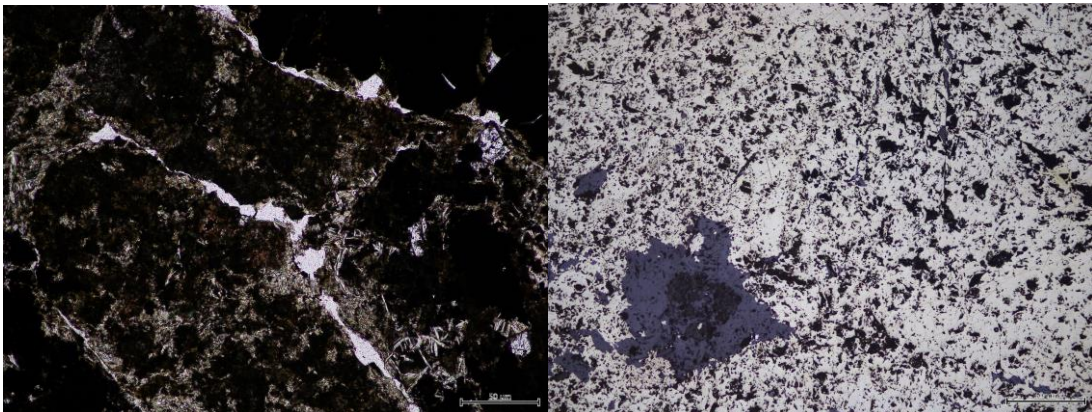
930.20 – 930.38

Description:

This sample is a massive sulphide vein which is dominated by pyrite and chalcopyrite.

There is almost no Fe-Oxides within this sample with only some very small grains of hematite present. Two clasts of metamorphic material remain in this section which are dominated by albite and quartz but also contain some small apatites and muscovite

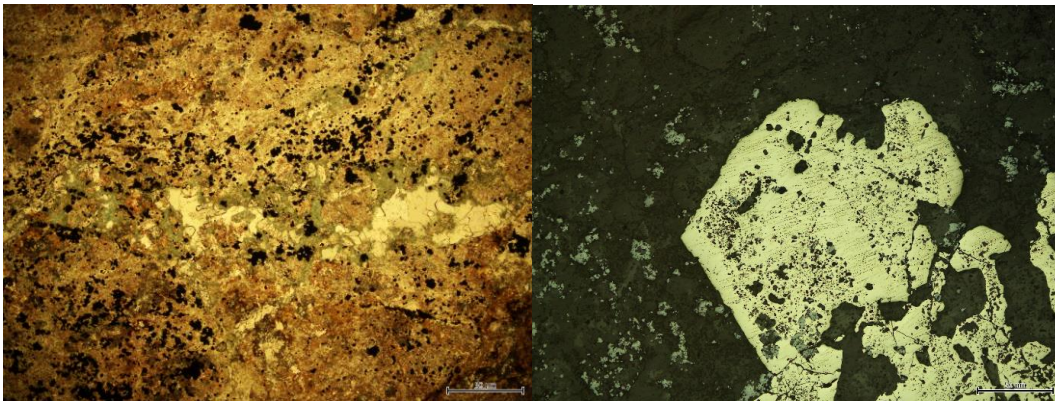
crystals. Other than these clasts most of the host has been altered and is hard to identify.



1017.65 – 1017.75

Description:

This sample depicts large metamorphic fragments mainly composed of albite, quartz and dolomite but is dominated by a sericite-chlorite altered mash of albite and quartz. There are some quartz veins that cross cut the host rock and evidence of apatite crystals. This sample also contains magnetite and hematite, of which is forming typical feathery (magnetite) structures, however both hematite and magnetite are intergrown with the hematite being more abundant. The hematite is also disseminated throughout the sample as small grains generally forming on the edges of host grains or veining through fractures within the sample. Pyrite is also present within the sample and it is inclusion rich and sometimes contains hematite/magnetite inclusions which likely implies co-crystallisation with the oxides. There is more evidence for sericite alteration with and around oxides.

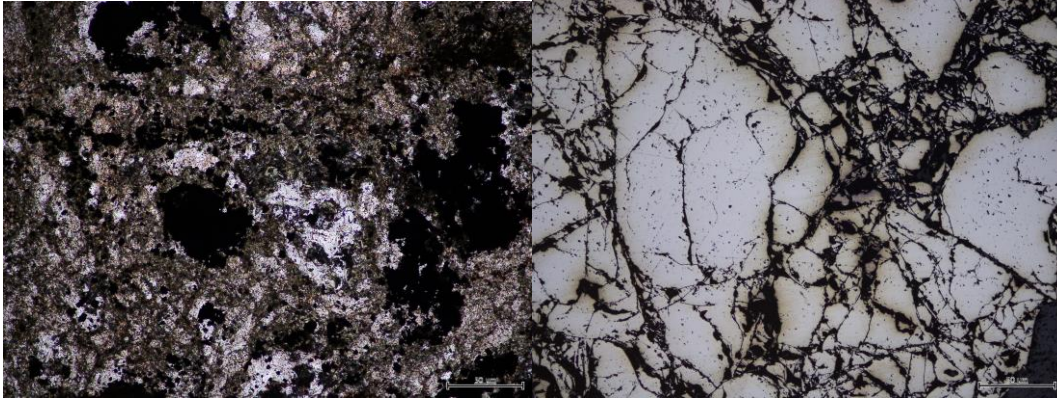


1025.30 – 1025.45

Description:

This sample has almost been completely altered by red rock alteration and seems to define a vein of hematite and sulphide material between two altered sections. There is still some host remaining which is dominated by granoblastic textured quartz and albite, this has been slightly altered by chlorite. Pyrite is the dominant sulphide within this thin

section and there is an obvious association in timing between the hematite and the pyrite. Hematite is bladed in texture and is disseminated throughout the vein.

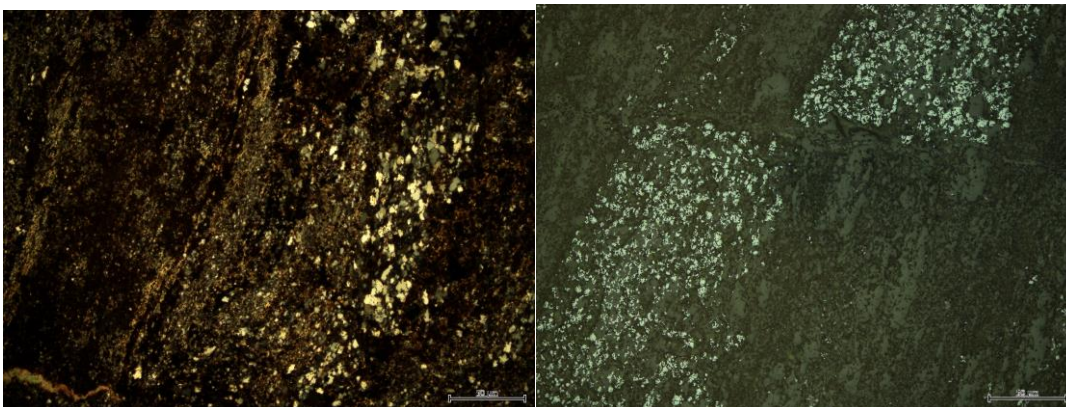


VUD007

1062.35 – 1062.50

Description:

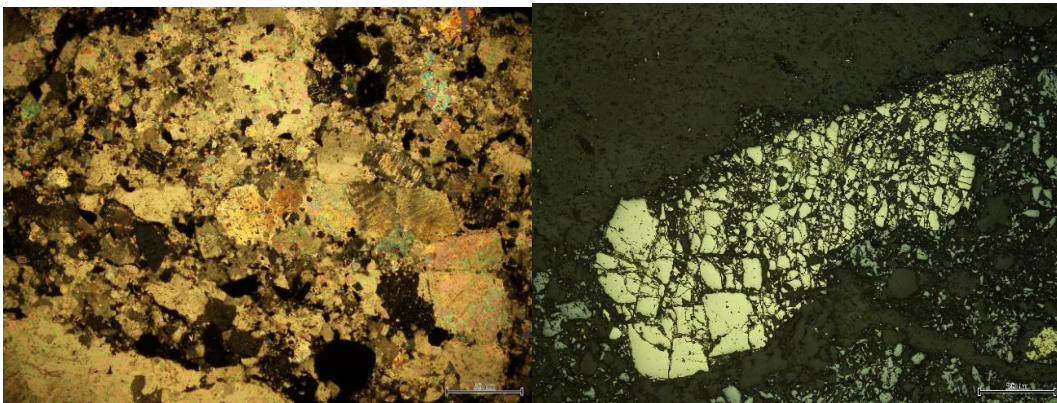
Metamorphic minerals define macroscopic foliation within this sample which shows structural events such as faulting. The metamorphic mash of chlorite-sericite-albite is faulted and interbedded with quartz and hematite veining.



1084.50 – 1084.70

Description:

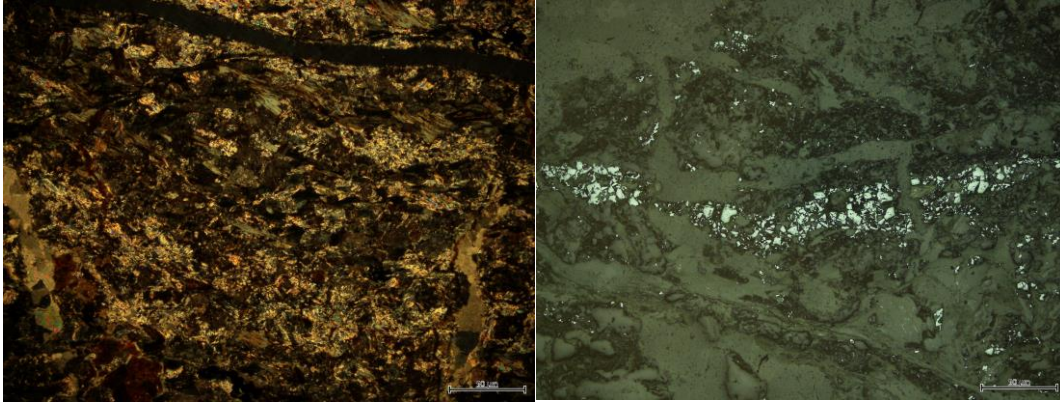
This sample is dominated by massive hematite with a bladed texture which has a relationship with pyrite and chalcopyrite. There are many instances of hematite replacing the host rock creating replacement textures of host grain shapes. Areas with hematite have had the host heavily brecciated however there are still some metamorphic fragments which are made up of quartz-albite-sericite-dolomite with common apatite crystals.



1100.15 – 1100.30

Description:

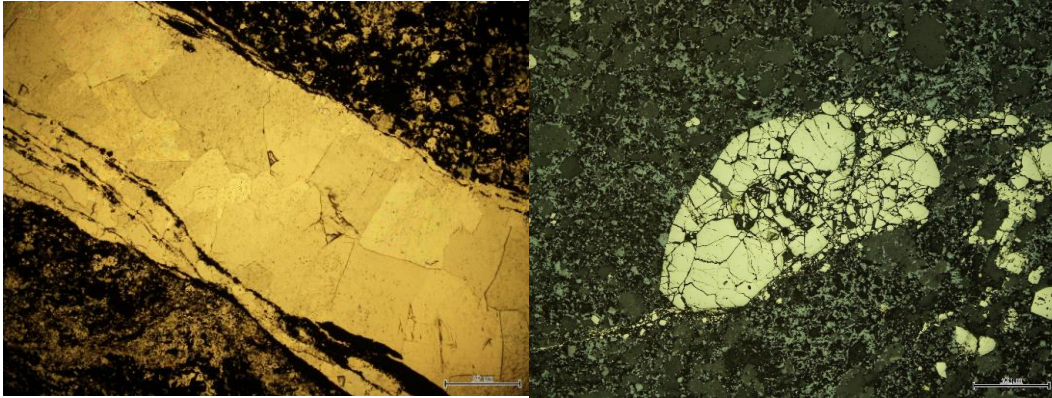
This sample is almost all altered metamorphic rock, chlorite and dolomite define this sample with albite. There are multiple quartz veins and hematite veins which display granoblastic textures and crosscut the host. Alteration defines this sample with 'red rock', sericitic and chlorite alteration all present.



1144.20 – 1144.35

Description:

Magnetite and hematite are disseminated throughout this sample and have come in the same fluid event as there are no grains that don't contain both hematite and magnetite. This is generally as disseminated grains however there are rare feathery magnetite structures within the sample. Sulphides (py-cpy) have grown around magnetite and hematite crystals and these are heavily fractured. Hematite replacement structures of host grains are also common. There are metamorphic fragments of the host rock within the massive oxides however these have been strongly altered by ser-chl-hem. These are likely veins that have come through late and are generally made up of albite-dolomite-chlorite and have not been brecciated like the rest of the host.

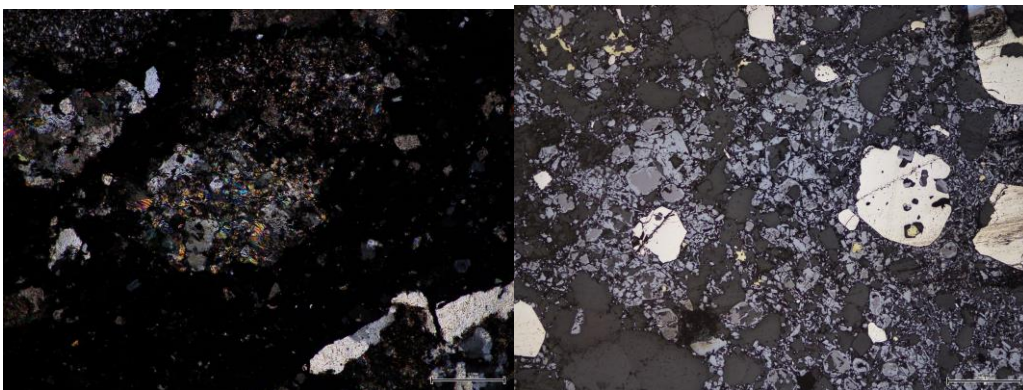


1155.20 – 1155.40

Description:

This sample depicts extreme brecciation of the host rock with clasts present within disseminated magnetite \pm hematite. There is obvious overprinting of the magnetite by late hematite. The texture of the Fe-Oxides is granular, however in some sections it is displaying classic bladed hematite textures. Blebby sulphides are present throughout the sample and are likely associated with the magnetite endmember of Fe-Oxides.

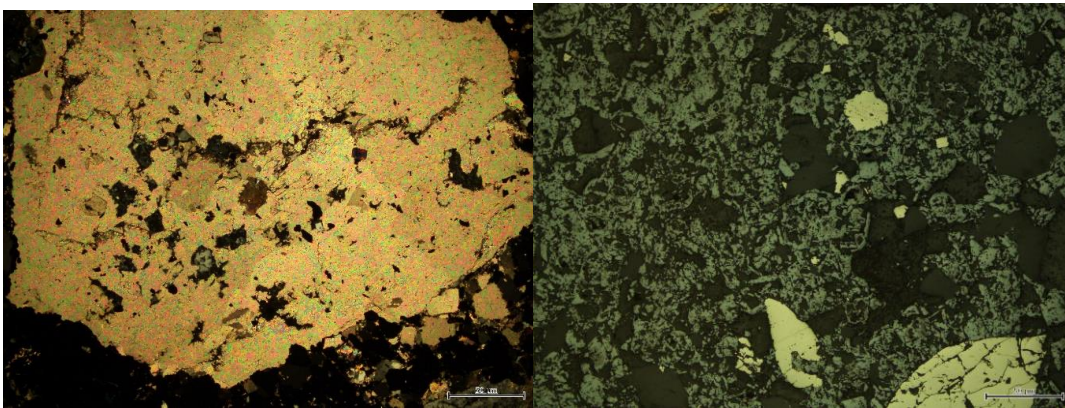
Metamorphic fragments within the hematite breccia are dominated by quartz, albite and dolomite with rare grains of muscovite. Apatite grains are within some of the fragments but are very small.



1183.00 – 1183.20

Description:

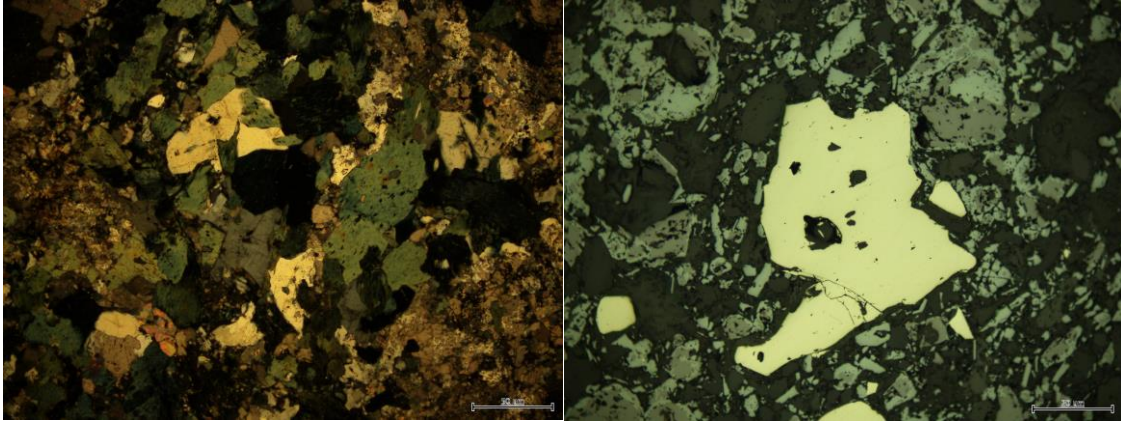
This sample is defined by magnetite and hematite structures however magnetite is the dominant oxide. Pyrite and chalcopyrite are common throughout the sample with hematite and magnetite and this implies a co-crystallisation or similar fluid event. Some feathery magnetite structures are also present within the sample. Fragments of the host are within the section that haven't been brecciated by the oxides, these are quartz-dolomite-chlorite rich and sericite alteration is common within these fragments. There are rare apatite crystals within the sample and is dominated by chlorite and sericite alteration.



1192.05 – 1192.20

Description:

This sample is dolomite and chlorite dominated with chlorite and sericite alteration being the most prominent feature of the sample. These dominate the fragments of host that haven't been brecciated by the abundant Fe-Oxides within the sample (magnetite and hematite) and have a 'mash' texture. There are two styles of iron oxides within the sample, the first is veined and this crosscuts the host rock, and the second is disseminated and in replacement structures. Pyrite and chalcopyrite are present mainly with magnetite but can be also with hematite albeit at smaller quantities.



VUD009

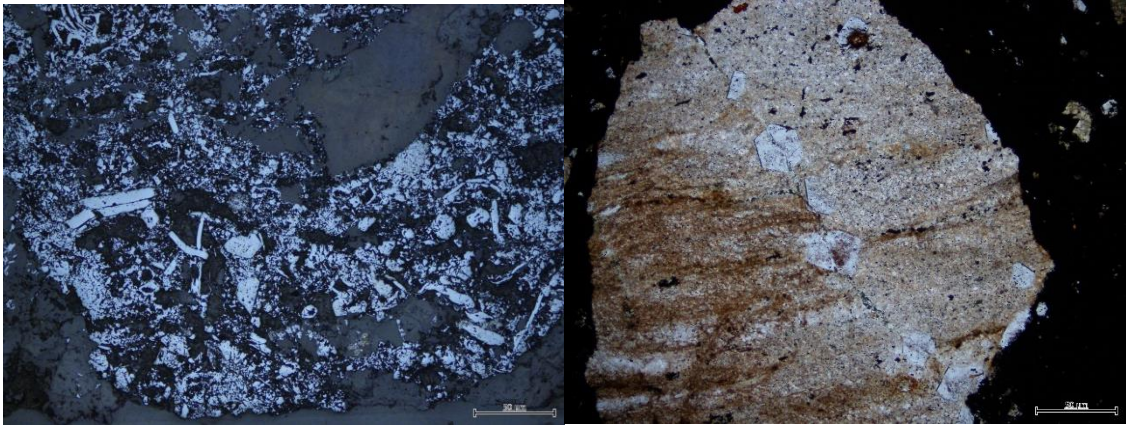
801.45 – 801.55

Description:

This sample depicts massive hematite that has a granular ‘fluid’ texture and is macroscopically banded. There are several metamorphic fragments within the massive hematite, which likely predate any hematite mineralisation. Metamorphic fragments contain albite, quartz, apatite, hornblende/chlorite, sill/muscovite and sericite. Albite is generally as larger tabular crystals sometimes containing inclusions. Apatite is common within this sample forming distinctive hexagonal crystals with a zonal arrangement of inclusions toward the core. Quartz is generally with or around albite crystals and is showing distinctive strained extinction. Sericite is common within the sample and is alteration of albite. Hornblende/chlorite and sill/muscovite are occurring with sericite, possibly late metamorphism after apatite crystallisation? Pyrite and chalcopyrite inclusions are common within, quartz/albite, granular hematite and are very small.

Crystallisation Sequence:

Sulphide → Inclusions within Apatite → Apatite → MM Fragments → Sulphide → Hematite



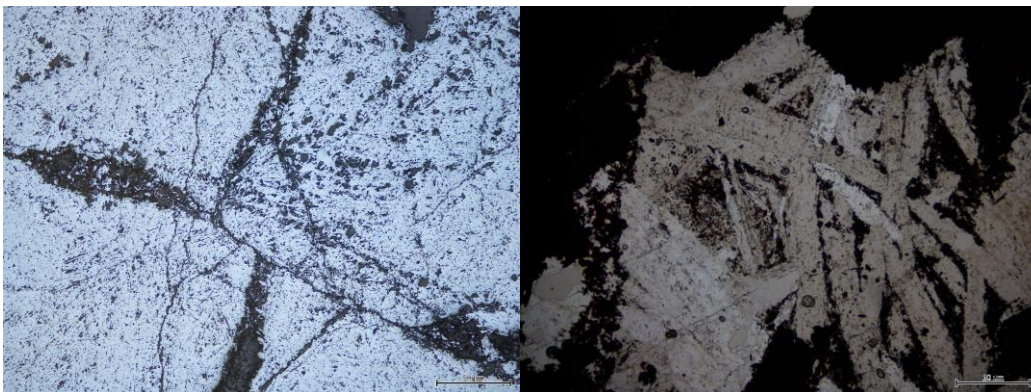
852.00 – 852.10

Description:

Massive hematite with clasts of very coarse albite, hematite is generally forming bladed textures close to and around albite crystals. Albite occurs in bladed, elongate structures, with distinctive twinning very common. There is a possibility that the hematite has been infilled and brecciated by an albite rich member, in which large crystals had a chance to form. Rare small pyrite and chalcopyrite grains within the massive hematite, generally occurring with each other or in euhedral crystals, but no presence of sulphides within the albite member.

Crystallisation Sequence:

Sulphide → Hematite → Albite



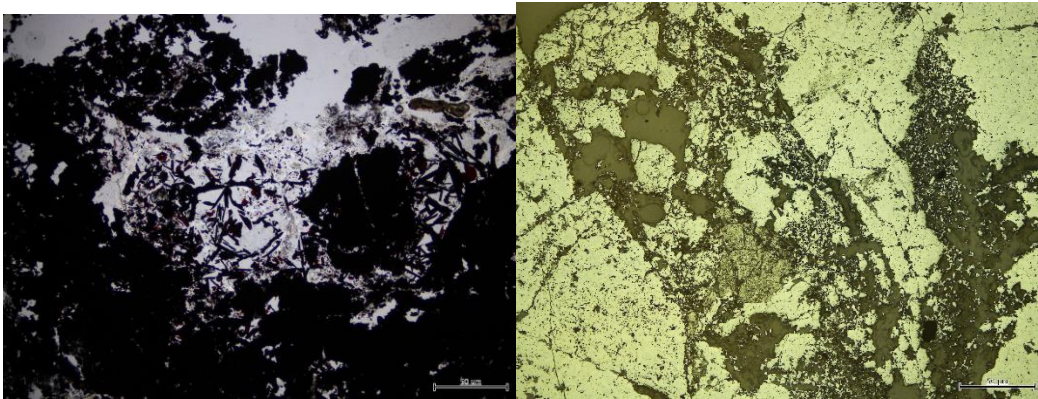
866.10 – 866.20

Description:

Massive hematite that has been brecciated likely by an albite endmember that has infilled the massive hematite crystals. Hematite is nodular but is bladed in texture on edges, especially bladed within places where there is more brecciation of the hematite. Sericite alteration of the albite protolith is common where hematite is bladed. Unaltered albite crystals are very rare, with sericite alteration being very common. Small grains of py and cpy are common within the hematite with large grains being less frequent, there is no evidence of any py, cpy within the albite member.

Crystallisation Sequence:

Sulphide → Hematite → Albite



904.00 – 904.10

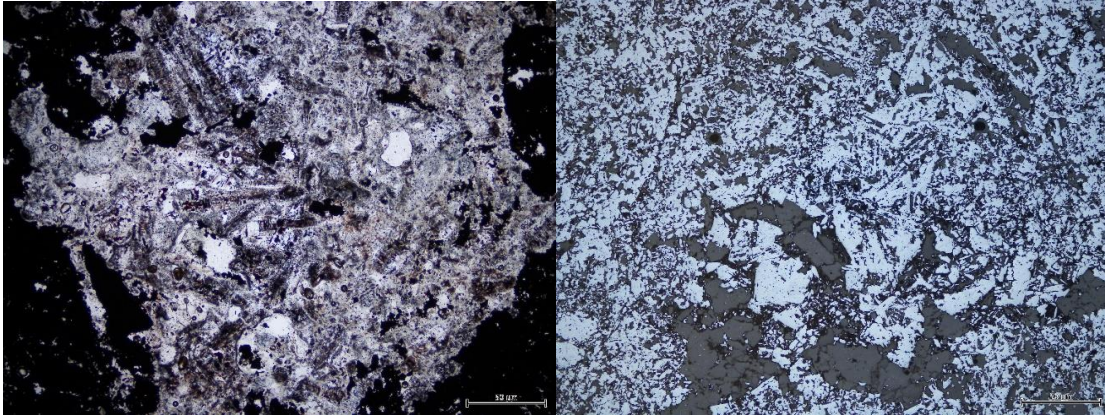
Description:

Massive hematite with a granular texture that has been brecciated by very coarse albite crystals. These albite crystals are forming as elongate euhedral crystals with distinctive twinning common in the grains. Sericite alteration of albite grains throughout the sample, generally on smaller grains. Albite crystals contain inclusions of fine hematite within the centre of the grain, implying a crystallisation of hematite before albite.

Chalcopyrite and pyrite crystals can be found within both the albite and the hematite implying a possibility of two generations of sulphides. Often when the pyrite and chalcopyrite is within albite there is a tendency for the edges to be sericitically altered.

Crystallisation Sequence:

Sulphide → Hematite → Sulphide? → Albite



952.80 – 952.90

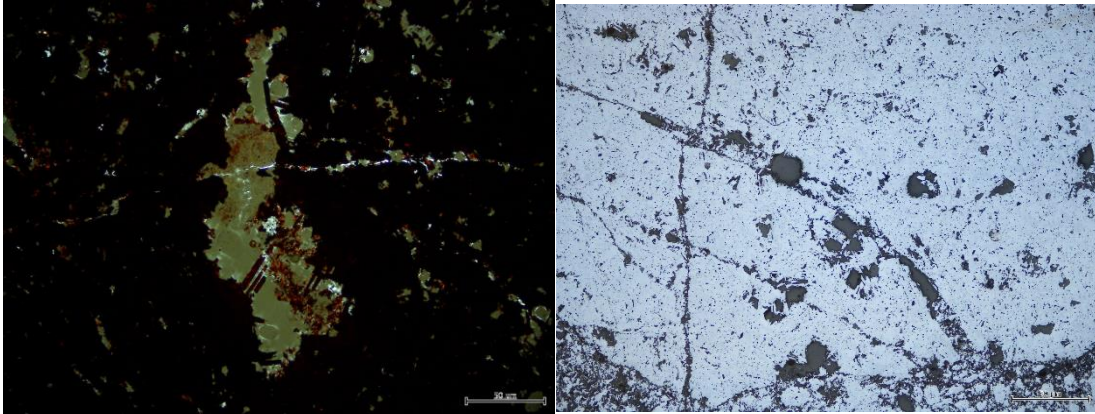
Description:

Massive hematite with a granular texture that has been heavily fractured, generally there is a tendency for the hematite to become more bladed around these fracture zones.

Euhedral albite crystals are very rare, however, it is common to sericitic alteration of the albite protolith. Pyrite and chalcopyrite can be found within the hematite however only as extremely small crystals.

Crystallisation Sequence:

Sulphide → Hematite → Albite



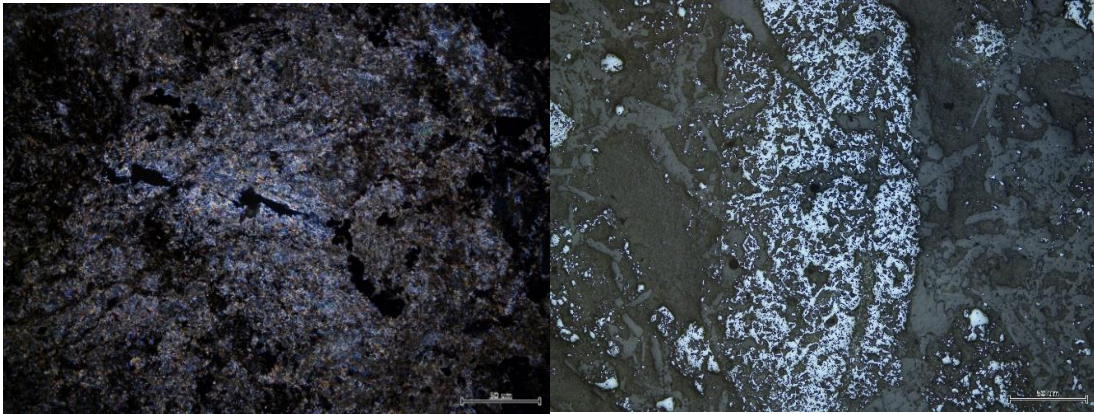
962.50 – 962.60

Description:

Massive hematite with a granular texture that isn't showing any bladed textures at a macroscopic scale, however, within veinlets hematite is extremely bladed at high magnifications. Albite within the sample is very coarse and is forming long euhedral elongate crystals that are distinctively twinned. Often the albite crystals contain hematite inclusions with zoning of the growth of the albite around these crystals i.e. there are no inclusions within edges however, central of these crystals there are often inclusions. Hematite is broken up and contains a lot of 'pores' which commonly contain albite? Possible two stages of hematite growth or cogenetic growth? Pyrite and chalcopyrite are present both within the massive hematite and often within albite veinlets crosscutting the hematite crystals, therefore likely that the cpy and py predate the hematite and albite.

Crystallisation Sequence:

Sulphide → Hematite → Albite → Hematite?



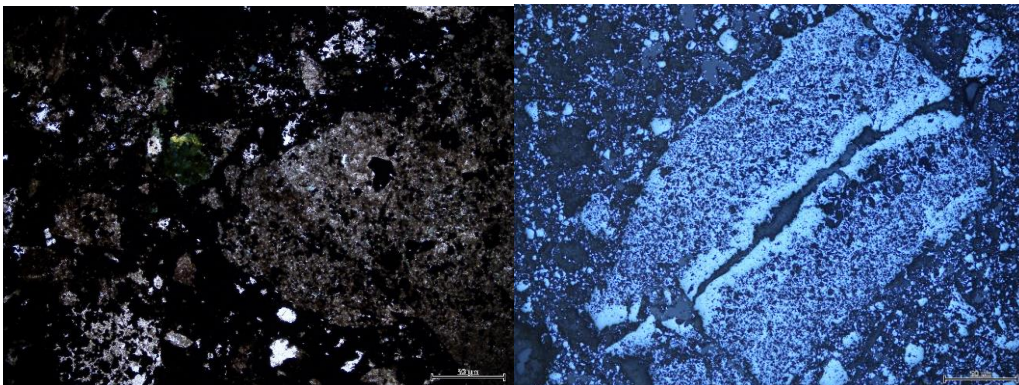
973.50 – 973.60

Description:

Massive hematite with a granular texture, however, this texture changes within veins where it is more disseminated and often on edges of grains there is a distinctive bladed texture. Albite within the sample is generally quite small and granular with a large amount of sericitic overprint, however there are a few larger grains that form euhedral elongate crystals that are distinctively twinned. This sample has ‘red rock’ alteration (Fe staining) and hornblende/chlorite present often within sericite grains. Pyrite and chalcopyrite are present often as tiny euhedral grains within the hematite, likely predating.

Crystallisation Sequence:

Sulphide → Hematite → Hornblende? → Albite → Sericite



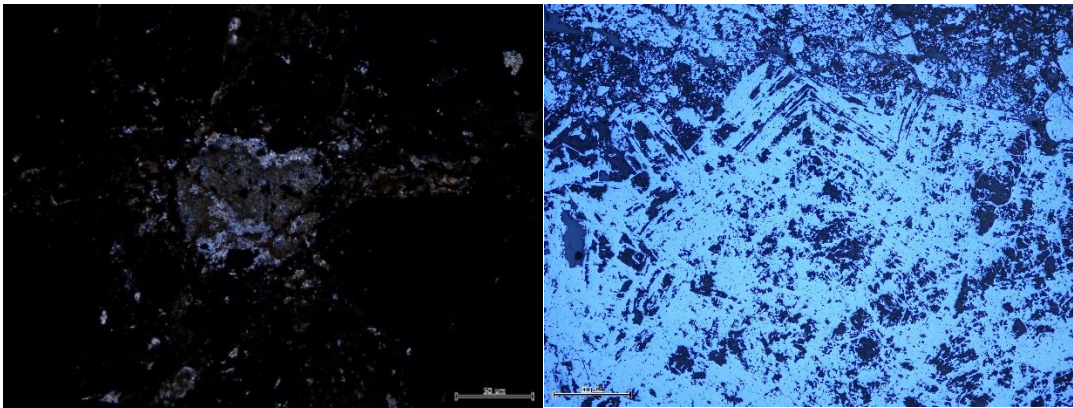
994.00 – 994.10

Description:

Massive hematite with a cockscombe texture dominates this sample. Forming triangular and hexagonal 'banding' structures with sericite interbands, this implies a likely cogeneration of 2nd stage hematite and albite. Matrix between the hematite grains is almost entirely composed of albite and sericitic alteration of albite. Albite within this sample is almost completely overprinted by sericite, albite crystals are very rare. Grains of hornblende/chlorite are rare within the matrix probably predating the albite. Very small inclusions pyrite and chalcopyrite are present within the hematite however are not found in any other minerals.

Crystallisation Sequence:

Sulphide → Hematite → Hematite/Albite → Alteration Products/Hornblende



1020.60 – 1020.70

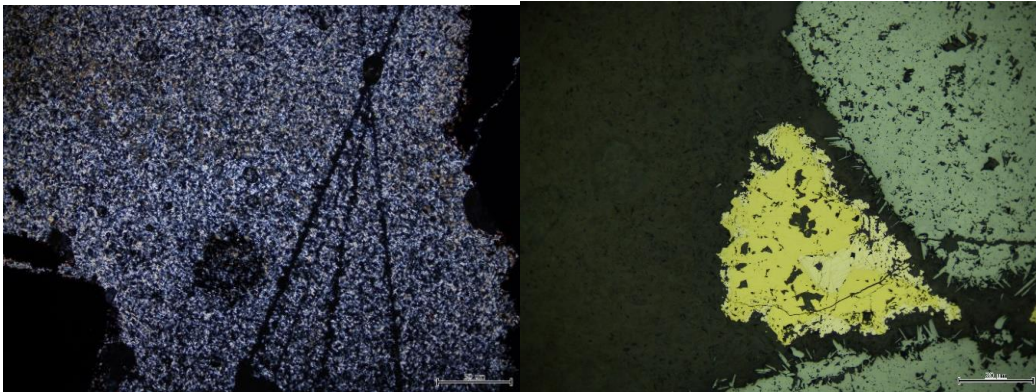
Description:

This sample depicts massive hematite which is often bladed on the edges and also shows this texture within veinlets and brecciation zones. Large grains of hematite within this sample are extremely homogenous and depict very rare inclusions of sericitic albite.

This sample contains rare elongate albite grains which depict distinctive twinning and hematite inclusions, implying hematite predating the albite. These inclusions are zoned toward the core of the albite grains. Albite is more common toward the edges of hematite grains whereas the infill is dominated by sericitic alteration of a likely albite protolith. Pyrite and chalcopyrite inclusions are common within this sample at high magnification. There are likely two stages of sulphides within this sample, as there are larger grains of sulphides 'moated' by the albite/sericite and smaller inclusions in the hematite. Chalcopyrite grains within the hematite are likely rimmed by bornite?

Crystallisation Sequence:

Sulphide → Hematite → Sulphide → Albite → Sericite



1070.20 – 1070.30

Description:

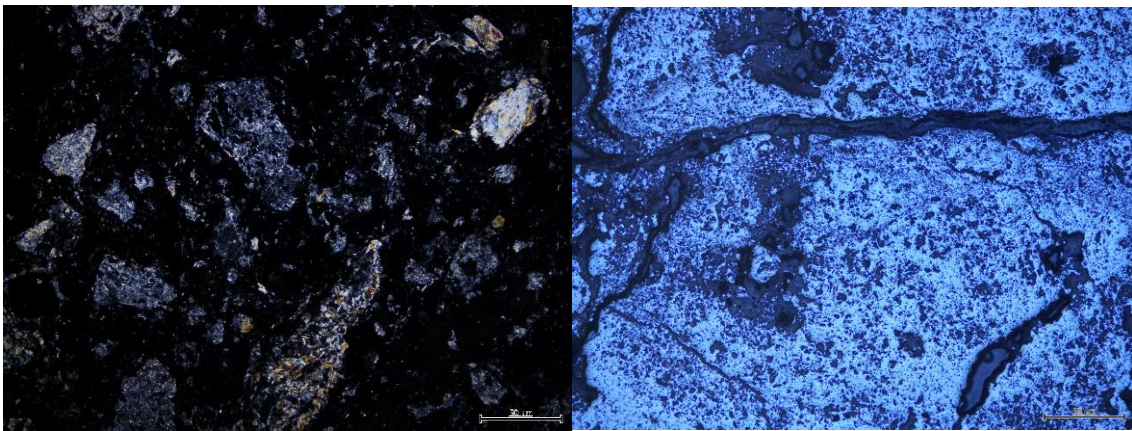
Massive hematite dominates this samples with a granular texture, but it has been heavily fractured. Where the hematite has been fractured and brecciated it is showing a bladed texture compared to the homogenous granular grains. Within the hematite grains there are commonly inclusions of albite and sericite. Albite is generally forming long elongate crystals however many of these have been overprinted by sericitic alteration. Albite crystals often have inclusions of hematite implying hematite predates the albite and therefore the alteration. Hornblende/chlorite and sillimanite crystals are common

within the sericite matrix possibly implying a metamorphic fluid injection before alteration. Also within this sample there are very rare zircon? Grains within the sericite alteration. Pyrite and chalcopyrite grains are common within the hematite however these are very small, these are not seen within any of the other minerals.

Crystallisation Sequence:

Sulphide → Hematite → Hornblende/chlorite, Sillimanite → Albite → Sericitic

Alteration



VUD016

885.90 – 885.95

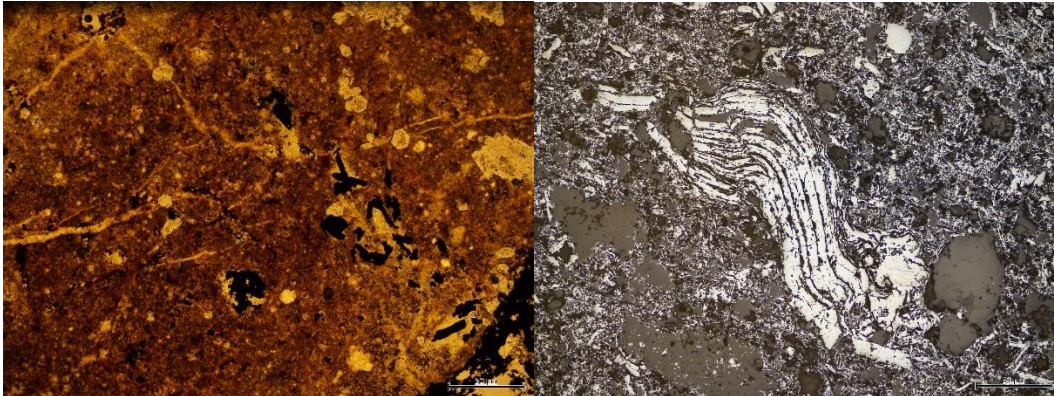
Description:

This sample depicts massive hematite that has a granular ‘fluid’ texture and is occasionally as large bladed fragments. Two stages of hematite growth might be recorded due to large hematite fragments recording plastic deformation and others show no deformation. There are several metamorphic fragments within the massive hematite, which predate any hematite mineralisation. Metamorphic fragments contain albite, quartz, apatite, chlorite and muscovite. Sericite is almost completely overprinting sample near hematite. Apatite is common within this sample forming distinctive

hexagonal crystals. Quartz is generally with or around albite crystals and is showing distinctive strained extinction. Pyrite and chalcopyrite inclusions are rare within the hematite, only as small euhedral grains.

Crystallisation Sequence:

MM Fragments → Hematite → Deformation → Hematite with Sulphides



1001.15 – 1001.20

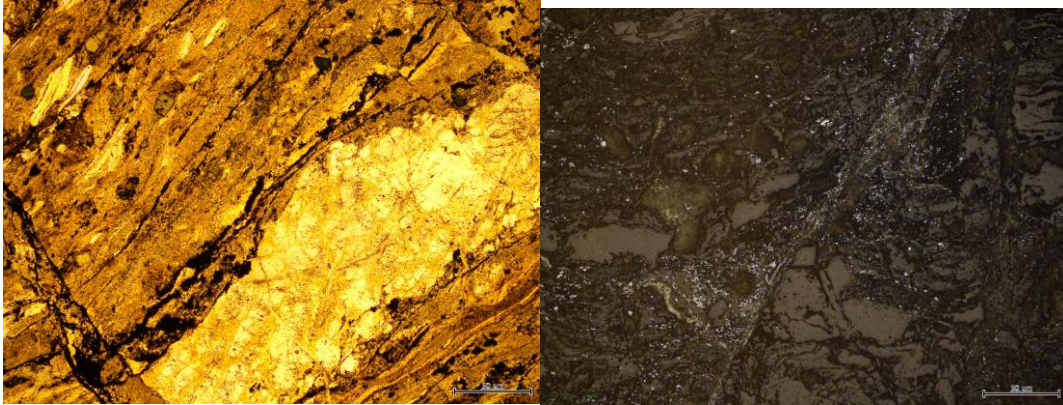
Description:

This sample shows macroscopic foliation of a metamorphosed host. Albite and quartz dominate the sample with rare chlorite on fracture zones within the albite crystals.

Muscovite also appears as euhedral crystals within larger fragments of albite. Large quartz veins crosscut albite within the sample. Late granular hematite has altered this sample, with sericite alteration widespread and intense. Delta/sigma clasts of granular hematite are common within the sample, indicating there was deformation after hematite infill. Hematite is generally most often within fractures between albite crystals.

Crystallisation Sequence:

Albite/Quartz → Chlorite → Hematite



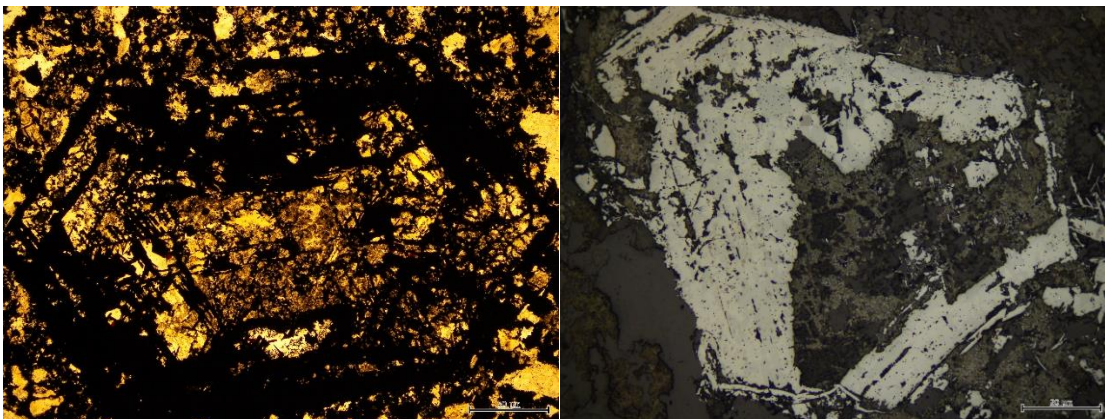
1091.90 – 1092.00

Description:

Metamorphosed fragments of the host rock overprinted by late massive hematite forming elongate bladed structures. Replacement textures of the hematite are large and have both infilled and brecciated the host rock. Host fragments are dominated by albite and quartz with sericitic alteration common where there is hematite. No sulphides or apatite is present within this sample.

Crystallisation Sequence:

Albite/Quartz → Hematite



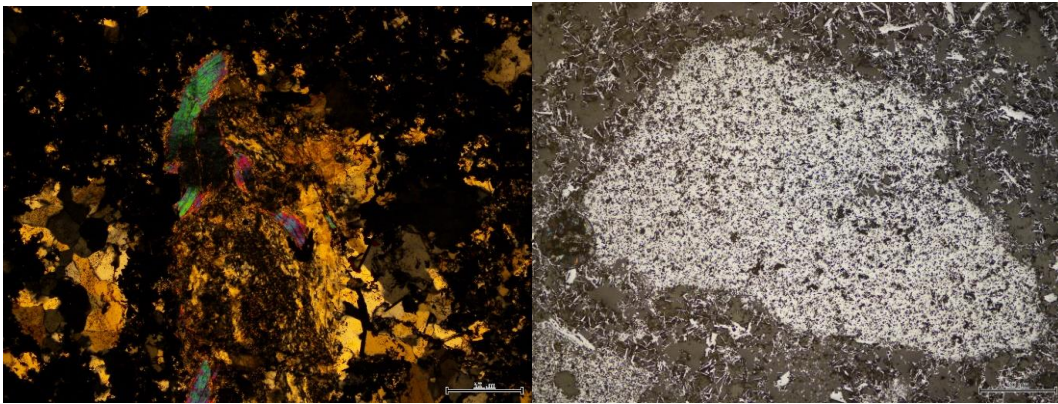
1123.00 – 1123.05

Description:

Heavily bladed massive hematite dominates this sample. The hematite crosscuts the host with thin bladelike structures indicating a late growth. Replacement structures are also present within the sample. The host is dominated by albite, with some small crystals of quartz within the matrix. Sulphides are present as small grains within the albite that has been brecciated by the hematite.

Crystallisation Sequence:

Albite/Quartz → Hematite with Sulphides



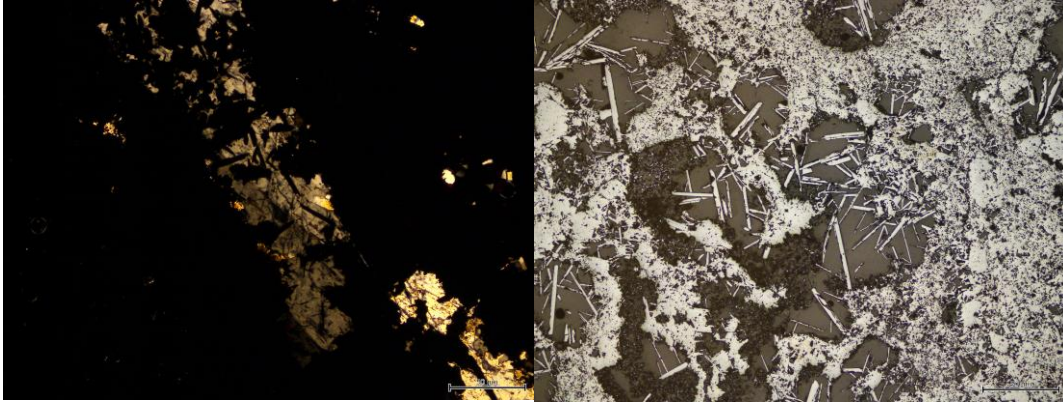
1151.10 – 1151.20

Description:

Massive hematite with a bladed texture that has almost completely overprinted the host rock with rare small albite grains. Sericite alteration is barely present, possibly completely overprinted by the hematite.

Crystallisation Sequence:

Albite → Hematite



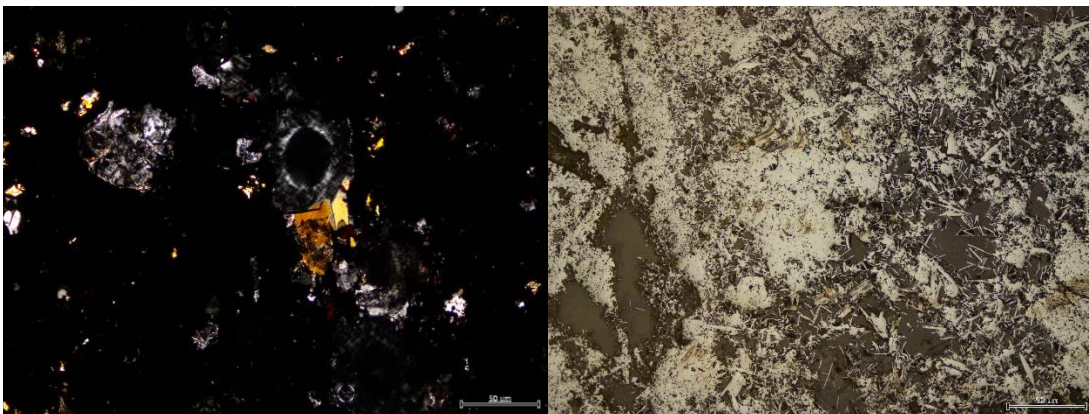
1172.40 – 1172.50

Description:

Massive hematite with a bladed texture that has almost completely overprinted the host rock with rare small albite grains. In this sample albite grains are completely overprinted by sericitic alteration and there is evidence for veinlets of hematite within these grains. Rare pyrite and chalcopyrite are present within the albite, but on fracture zones and near or with hematite.

Crystallisation Sequence:

Albite → Hematite → Sulphide



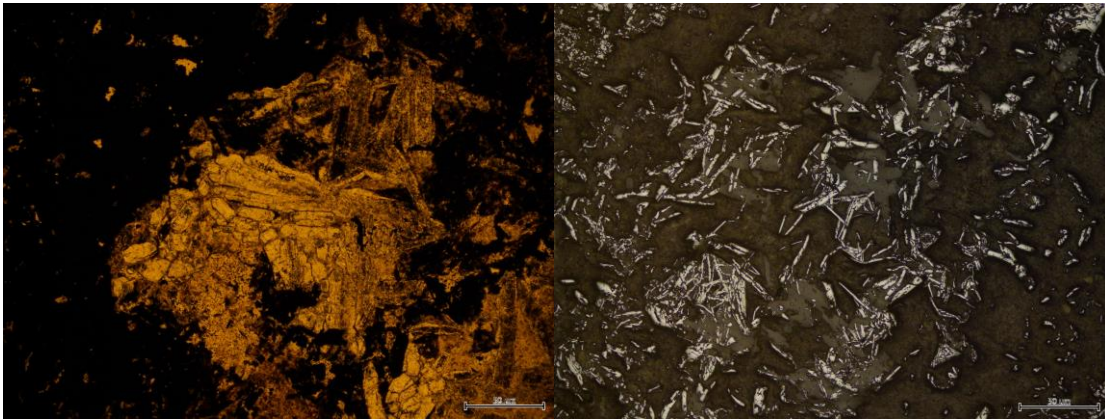
1375.60 – 1375.70

Description:

Massive hematite dominates this sample with a granular texture and blading toward the edges of some grains. It is likely that the hematite in this sample records two crystallisation stages as some hematite is showing evidence of plastic deformation and some isn't. However, the hematite is later stage than the host within this sample which is dominated by elongate albite crystals within metamorphic fragments which have been highly altered by sericite. No sulphides are present within this sample.

Crystallisation Sequence:

Albite → Hematite → Deformation → Hematite



1437.55 – 1437.65

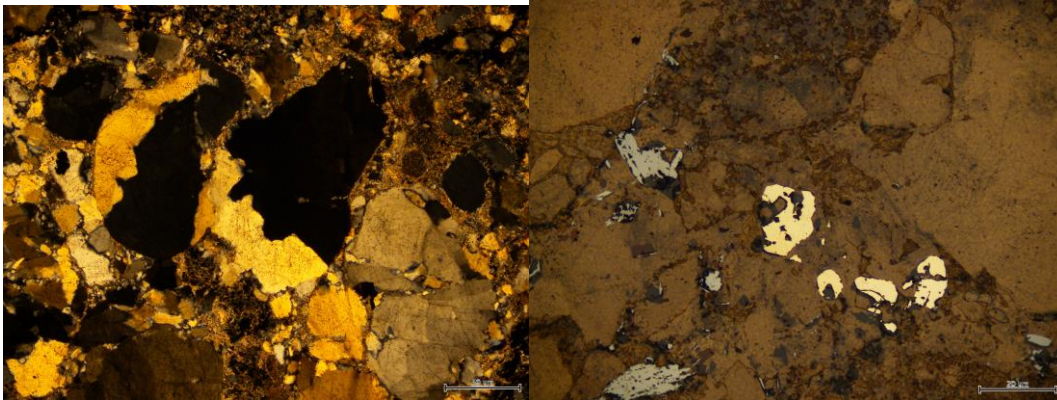
Description:

This sample is dominated by large euhedral albite crystals with distinctive twinning and there is some presence of quartz. These albites contain inclusions and are heavily altered toward edges and especially near hematite. Hematite within this sample is occurring as small bladed fragments dominating infill on albite crystal boundaries and fracture zones. Sulphides are within the albite however always occur with or around hematite.

Implies that there is a single hematite sulphide event.

Crystallisation Sequence:

Albite → Hematite with Sulphide → Alteration



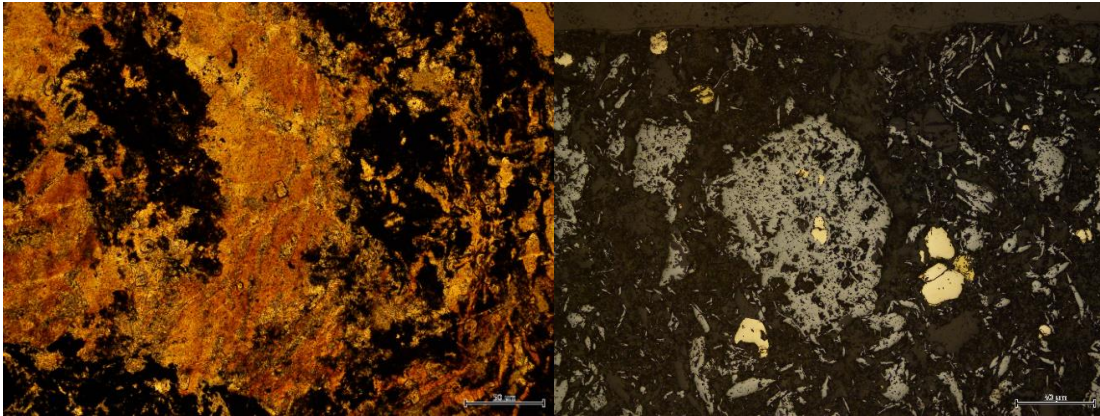
1488.05 – 1488.15

Description:

This sample depicts massive hematite that has a granular ‘hydrothermal fluid’ texture and is occasionally as large bladed fragments which have been deformed. Two stages of hematite growth might be recorded due to large hematite fragments recording plastic deformation and others show no deformation. There are several metamorphic fragments within the massive hematite, which predate any hematite mineralisation. Metamorphic fragments contain albite, quartz and euhedral small apatite crystals. Sericite alteration is heavy where there is hematite around a host grain, with intense alteration where veinlets of hematite have intruded albite. Apatite is common within this sample forming distinctive hexagonal crystals. Sulphides are abundant within this sample in the albite however these always occur with or around hematite. Implies that there is a single hematite sulphide event

Crystallisation Sequence:

Albite → Hematite with Sulphides → Alteration and Deformation → Hematite with Sulphides

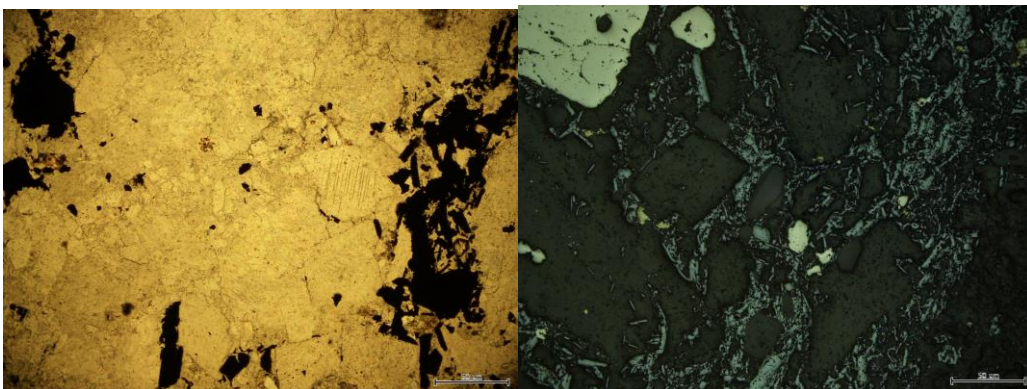


VUD017

1126.70 – 1126.85

Description:

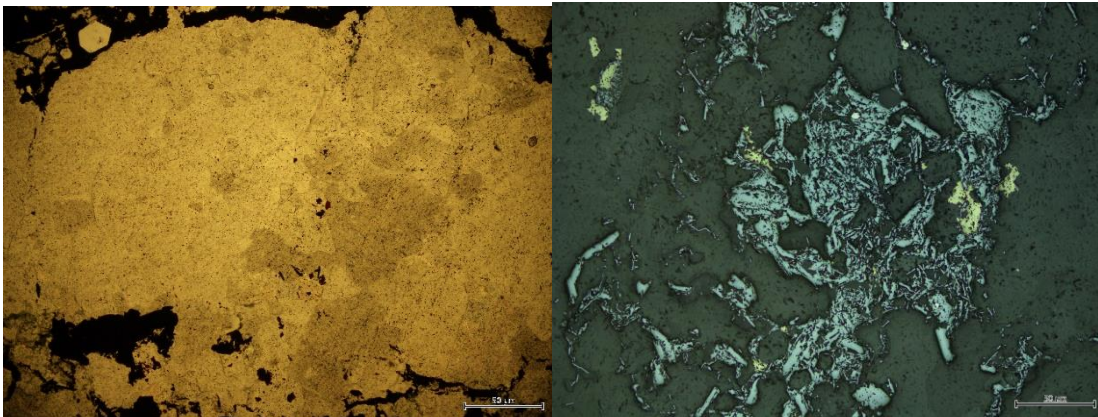
This sample is dominated by dolomite but also contains quartz, albite and apatite and is generally forming as a granoblastic texture. This has been slightly altered by sericite and chlorite and there is evidence for ‘red rock’ staining. This sample is very magnetite rich and shows distinctive feathery magnetite structures which is general don’t intrude the host but rim around the grains. Sulphides are present within the sample with the oxides implying a similar fluid event. Pyrite is forming much larger crystals than the chalcopyrite and tends to be less fractures. Fe-Oxides and sulphides are concentrated within stringer veins between host grains.



1140.70 – 1141.00

Description:

This sample is dominated by a granoblastic texture of host rock which is dominated by dolomite but also contains quartz, albite and apatite. This has been slightly altered by sericite and chlorite and there is evidence for ‘red rock’ staining. Magnetite dominates the Fe-Oxides within this sample and is generally forming feathery veinlet structures however bladed hematite is also present. Magnetite and Hematite are generally as veinlets and as such aren’t brecciated the surrounding rock but forming around the original grains. Sulphides are present within the sample with the oxides implying a similar fluid event. Pyrite is forming much larger crystals than the chalcopyrite and tends to be less fractures. There is evidence for some apatites within chalcopyrite crystals.

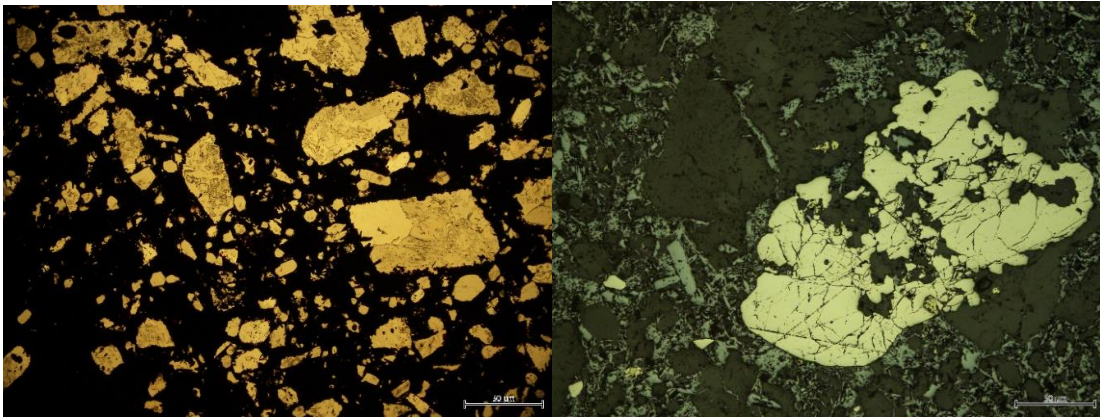


1174.58 – 1174.75

Description:

This sample depicts massive hematite and magnetite which have come into the rock as a fluid and brecciated the host rock, within the sample there are only small fragments of the host rock remaining that haven’t been brecciated. These fragments are dominated by dolomite, quartz and chlorite and form a ‘mash’ texture of grains, these are almost

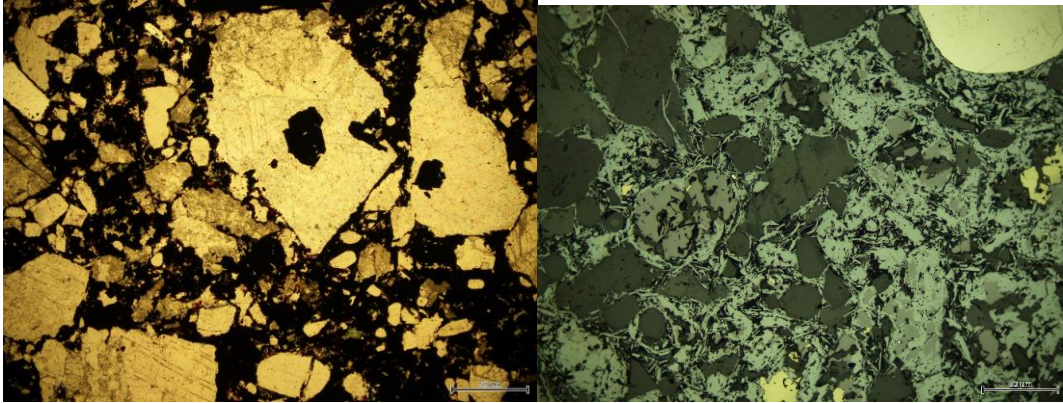
always associated with ‘red rock’ alteration. The iron oxides are sometimes forming both replacement and feathery structures and are associated with pyrite and chalcopyrite.



1210.13 – 1210.25

Description:

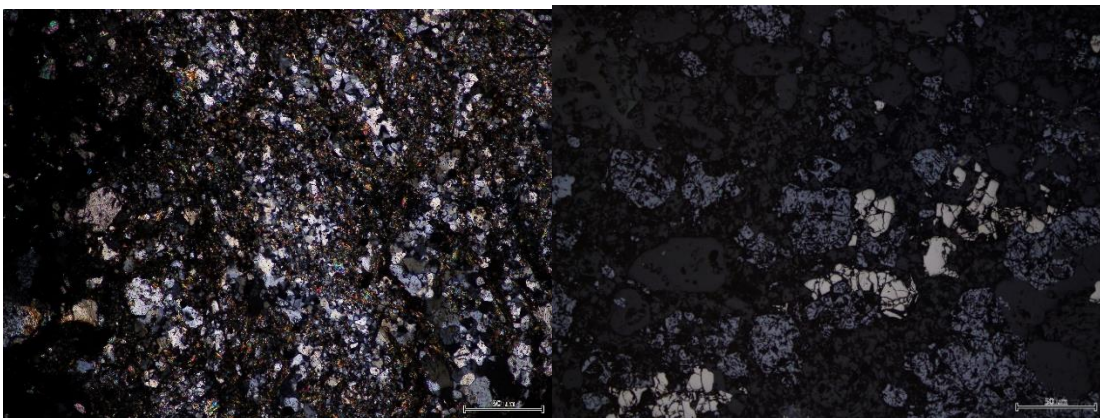
This sample is massive hematite and magnetite which has infilled and brecciated the sample, there is evidence of both feathery and bladed structures. Sulphides are almost always associated with the Fe-Oxides however there are also large pyrite veins throughout the sample which may be a different event. There are fragments of the host that haven't been brecciated within the sample that are dominated by dolomite, quartz and albite in a granoblastic texture. Chlorite is also present within this sample that has slightly altered the host.



1221.55 – 1221.80

Description:

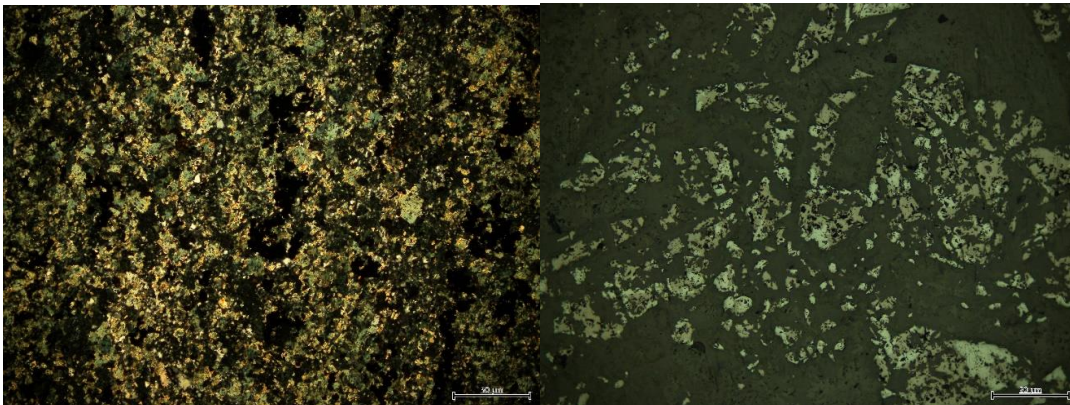
A massive magnetite-hematite rich breccia defines this thin section with clasts of metamorphic material still present within breccia clasts. Magnetite within this sample is being pseudomorphed and replaced by hematite with bladed structures being progressively more common. Sulphides are granular and associated with the timing of the hematite pseudomorphs. There is evidence for brittle plastically deforming ore. The clasts of metamorphic material are dominated by albite, quartz and dolomite with small crystals of titanate, rutile and apatite present.



1259.80 – 1259.95

Description:

Massive Fe-oxide sample which displays magnetite and hematite in bladed and replacement textures throughout the sample. There are two distinct members within this sample, the first being a chlorite rich host which has a granoblastic texture and has mineralogy of albite-chlorite-sericite-quartz. This host has been brecciated by the Fe-Oxides throughout the sample and stringer veins of oxides are common pervasively through these fragments. The second is a magnetite rich member which has overgrown and replaces the host which is heavily bladed and contains relationships to sulphides. This member contains many different styles of Fe-oxide textures and generally rims host grains that haven't been brecciated.

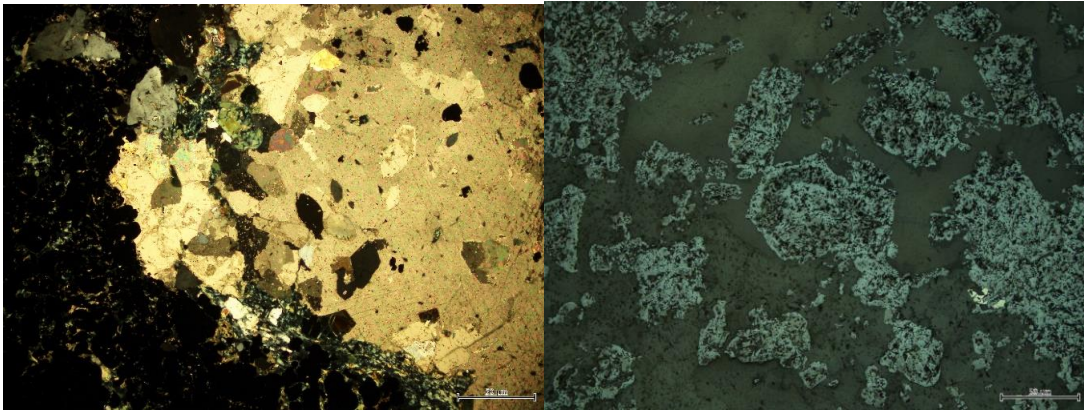


1268.00 – 1268.35

Description:

This sample is an example of a massive Fe-oxide endmember thin section with intergrown hematite and magnetite that display clast like structures. The Fe-Oxides are associated with sulphides and there is no evidence for sulphides within the host unless there is a stringer vein of oxide pervasive through the host. The fluid that has grown the Fe-Oxides has completely overprinted the host, there are some small fragments of the

host still remaining but they have been altered and broken. The host fragments are dominated by dolomite and quartz with rare small apatites.



APPENDIX C: STANDARDS FOR U-PB GEOCHRONOLOGY

Apatite

Laser Session 1:

The Madagascar apatite standard produced an age of 473.35 ± 1.53 Ma, the McClure Mountain standard produced a mean age of 544.12 ± 16.50 Ma and the 401 apatite standard produced an age of 527.08 ± 7.43 Ma. The Madagascar standard agrees with the published age of Madagascar apatite (U-Pb TIMS 473.5 ± 0.7 Ma; (Chew et al., 2014)) and the 401 apatite standard also agrees with the published age (524.7 ± 7.8) within error. The McClure Mountain standard produced an age (with error) 3 Ma older than published (U-Pb TIMS 523.51 ± 1.47 Ma; (Schoene et al., 2006)). This age is still within the range of published ages for this standard, therefore high accuracy of the U-Pb data is still expected.

Laser Session 2:

The Madagascar Apatite standard produced an age of 473.64 ± 0.70 Ma, the McClure Mountain Standard produced a mean age of 522.75 ± 12.07 Ma and the 401 apatite standard produced an age of 532.42 ± 3.60 Ma. All three standards agree with the published age (within error), Madagascar apatite (U-Pb TIMS 473.5 ± 0.7 Ma; (Chew et al., 2014)), 401 apatite (524.7 ± 7.8), McClure Mountain (U-Pb TIMS 523.51 ± 1.47 Ma; (Schoene et al., 2006)). This suggests high accuracy of the U-Pb results gained by the LA-ICP-MS.

Hematite Geochronology:

Standards and Accuracy:

The primary standard the GJ-1 zircon produced a concordant age of 582.47 ± 9.09 Ma which is slightly lower than the TIMS U-Pb published age of 608.5 ± 0.4 Ma (Jackson et al., 2004) however, it is within error of other published ages of this zircon and within error of published ages for this zircon for the original Jackson et al. (2004) paper. The HFO standard was also used however there are no published ages for this standard developed by Liam Courtney-Davies et al. (2019).

Zircon

The GJ-1 zircon produced a concordant age of 601.80 ± 4.10 Ma which is within published age of TIMS analysis from Jackson et al. (2004). 91500 zircon standard produced a concordant age of 1058.26 ± 20.54 Ma which is consistent with the published age of 91500 at 1058.10 ± 2.8 Ma (Wiedenbeck et al., 1995). Plešovice was the last standard used for zircon analyses which was dated at 336.71 ± 2.28 which is within error of the published date of 337.13 ± 0.37 Ma (Sláma et al., 2008).

APPENDIX D: APATITE TRACE ELEMENT DATA

Apatite 1														
Sample	La	Ce	Pr	Nd	Sm	Eu	Gd	Tb	Dy	Ho	Er	Tm	Yb	Lu
801_apatite - 10	0.06	0.87	0.56	9.67	61.20	41.91	570.9 2	102.2 0	414.0 9	37.23	42.23	3.05	14.43	1.46
801_apatite - 11	8.22	21.57	2.94	18.81	68.03	43.91	563.9 4	100.0 9	404.5 7	36.37	41.05	2.91	12.76	1.34
801_apatite - 12	44.20	72.29	6.98	25.90	36.91	22.06	266.2 5	43.90	171.7 0	14.35	16.05	1.17	5.14	0.40
801_apatite - 13	0.07	0.97	0.45	9.44	51.91	38.99	481.5 5	83.83	331.6 2	30.00	31.62	2.07	10.29	0.95
801_apatite - 14	0.33	2.04	0.90	15.84	60.01	34.45	451.5 8	77.91	316.8 3	27.94	32.10	2.34	10.33	0.91
801_apatite - 15	0.10	0.69	0.35	7.33	50.56	36.50	475.6 0	82.74	338.6 8	29.93	32.64	2.16	9.55	1.06
801_apatite - 16	0.10	1.08	0.69	12.59	79.96	48.92	577.8 9	84.15	300.6 8	25.85	27.14	1.87	8.17	0.77
801_apatite - 17	0.06	0.84	0.56	8.23	45.15	28.48	363.2 3	60.45	229.2 8	20.03	20.45	1.67	6.86	0.67
801_apatite - 18	0.06	0.74	0.41	8.18	56.82	38.42	533.6 4	96.62	387.7 8	35.08	40.80	3.00	13.73	1.55
801_apatite - 19	0.34	1.37	0.50	7.70	52.75	33.84	440.3 4	74.27	294.7 0	25.74	29.63	2.15	9.65	0.96
801_apatite - 2	0.07	0.89	0.56	8.32	64.10	43.81	584.7 0	103.0 8	425.4 7	37.09	39.59	2.69	11.41	1.24
801_apatite - 20	0.12	1.08	0.52	10.75	57.15	36.34	443.6 7	77.06	303.2 6	26.23	30.39	2.30	9.69	0.97

801_apatite - 21	0.06	0.98	0.61	10.52	65.73	44.84	554.45	91.84	361.50	31.44	34.74	2.43	10.56	1.11
801_apatite - 23	0.74	2.94	0.82	10.77	56.52	35.21	447.09	76.48	299.33	26.63	31.49	2.50	11.40	1.07
801_apatite - 24	2.21	6.27	1.00	12.00	52.14	29.04	343.42	57.38	215.75	21.10	30.57	2.73	11.95	1.21
801_apatite - 25	0.03	0.42	0.27	5.86	29.98	18.96	212.90	28.93	98.08	8.05	7.63	0.47	2.09	0.16
801_apatite - 26	5.53	7.83	1.80	15.24	67.03	35.34	474.35	79.21	300.01	28.58	40.71	3.46	15.95	1.78
801_apatite - 27	41.97	97.69	12.69	53.76	61.36	37.50	481.48	83.39	329.71	29.25	32.31	2.36	10.39	1.03
801_apatite - 28	0.16	1.13	0.59	9.92	68.20	43.98	611.14	109.89	443.92	39.63	46.75	2.98	13.90	1.44
801_apatite - 3	0.17	1.04	0.56	8.08	57.04	39.00	518.05	91.35	363.87	31.98	38.05	2.86	11.99	1.30
801_apatite - 30	0.08	1.09	0.62	11.98	62.44	36.75	491.10	81.32	310.76	28.57	36.79	2.88	13.05	1.28
801_apatite - 31	0.06	0.83	0.52	9.54	68.99	47.97	658.32	114.91	463.06	40.42	45.52	3.10	12.61	1.29
801_apatite - 32	0.06	0.85	0.51	9.73	67.67	45.02	603.73	107.16	440.35	39.45	46.49	3.14	13.92	1.45
801_apatite - 33	0.06	1.07	0.73	13.66	86.77	49.68	650.55	106.18	404.94	38.40	55.27	4.59	18.32	1.87
801_apatite - 34	0.28	1.26	0.48	8.62	55.31	39.15	511.33	91.50	365.12	32.56	36.12	2.37	10.73	1.04
801_apatite - 35	0.08	0.99	0.62	11.57	68.31	39.88	555.71	93.14	356.19	31.81	39.82	3.00	13.35	1.27
801_apatite - 36	0.06	0.98	0.67	10.83	67.91	40.44	548.64	95.75	381.03	33.91	41.08	3.01	14.00	1.38

801_apatite - 37	0.03	0.94	0.53	10.08	63.28	39.35	547.6 1	95.29	377.6 6	33.55	39.10	2.89	12.91	1.36
801_apatite - 38	0.03	0.64	0.46	7.38	53.98	37.78	501.8 2	87.27	351.7 8	31.18	36.40	2.56	10.81	1.08
801_apatite - 4	0.08	1.17	0.71	11.11	61.10	35.25	451.7 6	72.57	275.3 7	26.23	36.41	3.09	14.61	1.38
801_apatite - 42	0.18	1.56	0.77	11.14	57.70	40.19	504.9 3	85.78	340.7 2	29.54	31.96	2.23	9.83	0.98
801_apatite - 43	0.07	1.32	0.75	11.51	60.85	33.46	406.7 2	66.76	255.3 7	25.09	36.22	3.24	14.94	1.55
801_apatite - 44	0.12	1.01	0.65	10.61	75.97	50.78	633.9 0	105.5 9	407.5 1	35.33	37.42	2.49	10.40	1.14
801_apatite - 47	0.02	0.76	0.48	9.29	57.07	39.01	510.1 0	87.56	364.4 2	33.26	38.13	2.79	11.18	1.32
801_apatite - 48	0.12	0.88	0.54	7.91	48.65	35.86	460.2 5	77.87	311.0 3	27.62	32.15	2.07	9.33	0.88
801_apatite - 5	0.06	1.08	0.63	10.61	62.85	34.73	427.5 3	68.50	262.3 3	24.67	34.78	2.91	13.07	1.36
801_apatite - 50	0.03	0.90	0.50	8.42	47.73	29.36	379.8 1	62.77	244.0 2	21.92	25.13	1.99	9.36	0.99
801_apatite - 51	0.05	0.81	0.47	8.88	57.41	39.23	534.1 5	93.37	378.5 3	33.28	37.74	2.59	12.12	1.26
801_apatite - 52	77.97	170.70	18.10	63.77	63.74	37.72	475.3 0	84.21	336.2 9	30.06	35.58	2.70	10.70	1.11
801_apatite - 53	0.34	1.55	0.63	9.13	58.63	33.30	401.8 8	63.10	238.0 4	21.01	28.65	2.51	11.12	1.03
801_apatite - 54	0.05	0.85	0.58	8.33	48.71	33.23	414.1 1	69.64	277.9 9	24.16	27.44	1.85	8.94	0.91
801_apatite - 55	0.07	1.02	0.50	9.94	57.53	39.73	520.8 0	91.59	378.2 8	36.68	48.97	4.76	28.32	3.91

801_apatite - 6	0.06	1.34	0.69	11.36	63.29	33.07	412.47	66.86	257.19	25.18	37.26	3.33	15.20	1.56
801_apatite - 7	0.05	0.67	0.40	8.04	47.24	33.67	424.84	73.15	292.81	26.18	31.01	2.04	9.95	0.93
801_apatite - 9	0.06	0.85	0.59	9.33	65.17	43.80	594.21	104.16	423.91	38.01	41.62	2.91	13.15	1.37
973_apatite - 1	10.40	14.56	1.91	9.82	24.38	15.60	149.20	16.39	78.42	12.74	27.49	2.79	11.18	1.08
973_apatite - 10	170.48	228.41	16.69	47.16	23.00	12.45	116.65	15.31	74.39	13.01	30.93	3.11	20.95	2.65
973_apatite - 11	44.52	146.09	14.01	52.97	17.84	7.16	88.21	26.01	196.65	37.89	89.59	8.13	37.97	4.65
973_apatite - 12	1.02	4.10	0.75	4.87	15.80	10.57	112.04	15.50	87.28	14.57	31.94	3.08	12.63	1.41
973_apatite - 13	6.63	21.42	2.22	10.85	20.28	13.91	135.86	16.17	78.61	13.05	28.36	2.45	11.22	1.29
973_apatite - 14	1.81	4.87	1.05	8.61	29.64	21.83	223.99	20.77	83.62	14.55	38.38	4.02	27.01	3.79
973_apatite - 15	1485.09	2184.22	160.60	364.28	80.40	32.20	268.77	24.60	94.39	17.91	48.68	6.53	42.41	6.69
973_apatite - 16	3.36	11.82	1.30	7.83	13.65	7.15	79.76	16.28	104.82	18.26	38.04	3.15	13.34	1.56
973_apatite - 17	0.92	5.05	0.72	5.37	12.93	7.81	91.95	22.05	156.80	31.64	73.56	6.58	27.56	2.68
973_apatite - 18	15.84	70.44	4.70	18.79	23.10	14.75	142.43	16.67	82.71	14.23	30.83	2.75	12.12	1.49
973_apatite - 19	3047.22	4284.19	307.40	691.35	101.75	28.27	196.50	18.27	68.24	9.99	22.48	1.98	9.72	0.98
973_apatite - 2	901.45	1360.25	100.52	255.28	44.35	14.19	115.37	16.76	97.43	17.55	37.45	3.38	15.42	1.86

973_apatite-20	45.97	99.82	6.24	22.19	26.39	16.13	148.60	17.56	85.02	14.43	33.00	3.30	14.25	1.63
973_apatite-21	29.31	33.81	3.43	13.65	15.40	8.64	88.12	17.31	116.04	22.62	55.68	6.11	28.57	3.64
973_apatite-23	3.35	9.09	1.29	8.49	22.92	14.56	145.10	20.12	125.29	24.26	53.89	5.18	20.46	1.99
973_apatite-24	23.18	54.06	5.67	21.15	25.08	13.44	131.42	18.48	100.82	17.82	38.25	3.58	16.88	2.02
973_apatite -25	37.34	115.29	4.67	19.55	27.51	18.25	184.08	22.56	118.62	22.26	51.71	4.56	19.36	1.60
973_apatite-27	1.88	7.30	1.31	7.66	26.61	14.37	144.98	16.46	81.15	12.85	29.68	2.51	12.21	1.31
973_apatite-28	7.44	21.78	2.88	15.95	25.69	14.43	135.14	15.89	81.04	13.39	29.03	2.50	11.37	1.24
973_apatite -29	569.81	853.82	55.44	145.92	47.54	24.02	227.08	16.41	45.66	5.54	12.65	0.95	4.18	0.36
973_apatite-3	6.70	19.42	2.47	10.39	29.16	18.98	181.33	19.52	83.04	14.08	34.48	3.54	20.39	3.05
973_apatite-30	53.74	171.50	17.79	63.40	28.40	12.22	102.64	13.58	72.29	12.01	26.07	2.73	13.45	1.56
973_apatite-31	4.60	22.98	0.84	6.42	17.48	11.34	121.25	20.55	133.09	26.87	67.33	6.91	31.48	3.80
973_apatite-32	3.67	11.73	1.36	7.40	18.55	9.79	84.56	10.10	43.93	6.52	12.98	1.08	4.61	0.49
973_apatite-33	37.91	116.66	14.09	51.36	22.87	9.98	100.08	18.27	124.07	23.86	53.54	5.44	29.06	4.09
973_apatite-35	57.82	90.25	7.79	23.56	27.25	15.04	148.28	16.97	88.55	15.60	33.64	3.17	12.27	1.60
973_apatite-36	11.64	48.97	4.73	22.37	18.78	9.09	83.73	9.47	45.64	6.74	12.90	1.14	4.93	0.49

973_apatite-37	0.18	1.21	0.36	6.13	43.36	27.43	242.75	17.30	50.17	6.70	10.29	1.06	4.10	0.33
973_apatite-38	63.47	100.85	8.17	26.03	36.44	22.99	213.70	16.10	46.26	6.45	11.31	0.91	3.93	0.37
973_apatite -39	15.76	17.13	2.45	11.14	27.71	17.80	153.19	15.18	64.21	10.50	25.34	2.45	12.77	1.33
973_apatite-4	1.40	7.20	1.22	8.62	10.41	4.90	54.34	12.77	89.48	16.22	31.86	2.58	11.93	1.07
973_apatite-40	2.92	6.04	1.29	7.80	21.90	14.56	156.15	16.56	72.80	12.41	29.83	3.31	15.67	1.77
973_apatite-41	1.59	7.33	1.46	11.66	24.09	15.03	138.31	15.81	73.33	12.47	26.56	2.37	9.86	1.10
973_apatite -42	0.22	1.56	0.46	4.99	19.10	11.24	102.28	11.43	51.48	7.70	15.13	1.27	4.99	0.57
973_apatite-43	3.40	10.44	1.51	9.70	24.63	15.64	146.73	13.95	55.90	8.65	16.25	1.35	5.69	0.66
973_apatite-44	4.95	17.52	2.07	9.51	17.35	9.71	100.19	15.24	89.60	16.09	33.94	3.02	13.60	1.59
973_apatite-45	0.26	2.04	0.63	6.31	30.19	18.89	178.44	16.86	63.09	8.90	17.98	1.56	6.68	0.73
973_apatite -46	3.14	8.39	1.38	9.66	33.74	23.19	227.08	19.53	70.67	12.17	32.74	3.94	25.39	3.98
973_apatite-47	30.83	108.82	10.41	38.09	12.41	5.83	67.36	16.70	116.07	20.10	45.14	4.34	20.42	2.42
973_apatite-48	476.26	694.40	47.02	129.16	23.63	7.61	80.62	16.72	109.77	20.72	44.84	4.15	18.43	2.38
973_apatite -49	11.65	17.55	1.83	10.58	35.90	21.36	186.83	14.15	41.36	5.28	9.63	0.87	4.41	0.46
973_apatite-5	86.72	112.12	9.37	29.26	30.85	18.09	167.33	13.81	52.23	8.39	16.31	1.27	5.92	0.51

973_apatite-50	868.97	1299.12	81.80	211.46	42.45	15.02	137.87	21.04	133.78	25.94	60.34	5.80	27.83	3.17
973_apatite-51	5.05	18.95	2.26	11.44	25.95	16.65	159.14	15.87	64.37	10.07	21.89	2.12	10.61	1.56
973_apatite -52	0.70	2.03	0.51	4.95	37.90	26.94	268.24	22.32	70.93	9.95	19.16	1.70	7.65	0.82
973_apatite-53	810.50	1218.03	101.62	198.79	46.43	15.66	126.06	15.45	82.66	14.69	31.16	2.36	10.86	0.97
973_apatite-55	0.85	5.23	0.88	5.95	11.24	6.64	72.50	17.47	122.66	22.82	46.79	3.96	19.16	1.97
973_apatite-56	15.36	28.91	2.58	13.84	32.23	18.69	182.90	16.11	65.89	11.07	23.52	2.02	10.11	0.90
973_apatite-57	29.80	52.43	10.34	38.64	17.88	7.27	78.38	16.94	114.02	22.30	53.24	5.86	29.79	4.28
973_apatite-58	8.96	16.96	1.80	10.71	28.52	20.88	211.26	18.36	75.11	11.58	24.88	2.41	12.08	1.38
973_apatite-59	125.42	190.07	12.81	34.82	43.26	27.16	264.24	21.62	71.58	10.00	18.99	1.59	5.47	0.62
973_apatite-6	0.46	2.99	0.79	6.82	26.00	17.64	174.11	17.49	72.66	12.36	27.70	2.53	11.52	1.23
973_apatite-60	1236.07	1828.26	117.18	295.59	53.51	15.37	134.60	27.43	183.75	36.90	80.78	7.31	29.33	3.45
973_apatite-7	2.88	10.24	1.68	9.53	23.12	14.88	153.68	17.03	81.15	13.14	29.59	2.51	11.76	1.08
973_apatite-8	344.73	442.64	32.18	81.82	28.62	15.99	141.02	14.56	66.93	11.48	24.77	2.41	11.24	1.21
1488 - 1	2563.18	5745.06	562.85	1811.39	330.71	122.66	451.63	45.00	150.37	17.33	33.99	3.34	19.79	2.72
1488 - 10	0.05	0.67	0.46	5.81	22.90	19.66	155.59	26.09	103.17	11.37	21.35	2.17	7.97	0.89

1488 - 11	0.17	1.21	0.58	7.85	32.68	30.66	202.9 0	26.17	87.58	9.31	14.93	1.38	5.84	0.67
1488 - 12	267.89	587.02	62.23	218.38	48.42	25.02	150.7 1	22.96	94.79	11.70	21.18	1.94	8.62	0.90
1488 - 13	0.23	2.27	1.12	15.41	65.80	66.61	448.3 1	58.43	169.6 5	15.03	21.94	1.87	7.78	0.70
1488 - 14	0.03	0.70	0.34	5.13	18.55	17.87	131.1 0	23.15	97.05	11.63	21.21	2.08	9.27	0.88
1488 - 15	61.81	166.20	17.71	67.97	81.25	72.90	496.4 4	60.29	170.3 9	14.41	20.60	1.80	7.00	0.72
1488 - 16	16.53	38.21	5.29	26.15	47.66	45.33	288.5 9	38.01	122.5 6	11.77	20.34	1.62	8.01	0.77
1488 - 17	0.05	0.47	0.25	3.58	12.86	10.81	86.48	18.05	94.32	12.97	24.09	2.06	10.63	1.04
1488 - 18	0.17	2.69	1.36	20.49	84.58	78.60	479.1 0	52.45	127.6 5	9.31	12.09	0.89	4.02	0.31
1488 - 19	0.92	2.27	0.48	4.49	10.18	7.55	58.55	10.70	54.12	6.82	12.74	1.19	4.84	0.55
1488 - 2	0.17	0.45	0.16	2.12	8.50	9.01	73.17	15.57	74.94	9.96	19.04	1.90	7.42	0.84
1488 - 20	71.77	155.25	16.80	60.25	22.73	14.70	100.7 4	16.95	84.82	10.63	19.69	1.68	8.36	0.96
1488 - 21	0.02	0.41	0.27	3.37	8.13	6.91	47.39	8.21	37.23	4.13	6.17	0.48	1.93	0.17
1488 - 22	0.07	0.54	0.25	3.60	8.65	8.06	52.06	7.35	34.32	3.91	6.11	0.47	1.70	0.17
1488 - 23	0.02	0.40	0.25	4.03	14.46	13.71	120.8 2	24.97	124.7 8	16.65	31.73	2.77	13.07	1.37
1488 - 24	167.63	365.44	40.37	145.13	55.04	36.24	208.2 8	27.54	107.1 8	12.75	22.65	1.78	7.64	0.83
1488 - 27	0.05	0.57	0.35	4.78	9.92	7.57	60.58	10.93	55.84	7.44	12.89	1.20	5.07	0.57
1488 - 28	0.07	0.41	0.26	3.63	12.66	11.44	93.32	18.65	93.87	12.78	23.87	2.36	11.15	1.03
1488 - 29	0.02	0.33	0.21	3.14	11.52	10.10	80.07	16.56	81.35	10.73	20.41	1.81	8.56	0.82

1488 - 3	0.14	2.08	1.06	16.46	35.69	26.58	155.7 4	25.49	134.7 3	17.96	32.75	2.73	11.18	1.18
1488 - 30	0.02	0.53	0.35	5.23	15.54	13.30	116.0 1	24.79	135.1 0	19.68	38.04	3.55	16.47	1.78
1488 - 31	0.03	0.58	0.41	5.61	16.69	12.81	91.16	17.22	88.11	12.18	22.44	1.98	9.51	0.94
1488 - 32	0.02	0.37	0.25	3.85	14.65	13.25	115.7 2	23.89	116.8 0	15.48	29.92	2.69	12.90	1.29
1488 - 33	7.12	14.91	1.76	13.21	24.54	18.70	125.9 0	21.13	108.5 1	15.18	28.18	2.46	11.02	1.21
1488 - 34	0.05	0.41	0.25	3.75	8.27	7.13	53.74	9.30	43.57	5.18	9.86	0.80	3.50	0.39
1488 - 35	0.04	0.58	0.29	4.38	14.21	12.82	101.3 5	22.20	111.4 1	14.94	28.67	2.69	13.09	1.34
1488 - 36	0.08	0.36	0.21	2.58	9.84	8.11	57.82	10.42	44.45	6.02	10.13	0.85	4.19	0.41
1488 - 37	0.04	0.58	0.29	4.49	13.71	12.80	104.7 1	22.29	115.7 7	14.60	28.78	2.65	13.08	1.21
1488 - 38	0.02	0.67	0.31	4.25	17.33	16.40	130.2 7	24.25	104.8 4	13.20	23.61	2.28	9.60	1.03
1488 - 4	0.06	1.77	1.15	18.73	72.37	62.63	334.0 4	33.12	71.78	4.93	6.00	0.48	1.34	0.10
1488 - 40	484.59	1096.23	117.59	404.34	91.70	46.37	269.6 7	37.16	136.4 4	15.84	26.15	2.53	10.97	1.09
1488 - 41	0.02	0.58	0.23	4.30	14.21	12.93	95.42	17.04	77.14	10.25	18.73	1.72	8.18	0.80
1488 - 42	6.80	18.55	2.82	22.23	71.86	63.63	373.3 9	39.08	95.05	6.63	8.55	0.67	3.11	0.25
1488 - 43	0.73	3.78	0.92	9.27	12.60	9.20	64.18	12.17	62.04	7.71	15.69	1.28	6.27	0.60
1488 - 44	0.04	0.78	0.38	4.63	13.51	10.91	92.97	18.67	97.87	12.74	24.94	2.24	11.29	1.11
1488 - 45	0.12	1.37	0.72	8.16	33.20	32.28	226.7 0	36.36	134.0 8	15.21	28.60	2.48	12.52	1.13
1488 - 46	0.60	2.16	0.64	8.51	30.60	29.87	194.4 3	24.68	74.34	6.85	9.91	0.91	3.70	0.38

1488 - 47	0.06	0.86	0.43	6.72	18.28	15.13	124.56	23.69	124.39	16.89	32.48	2.99	12.81	1.42
1488 - 48	134.47	219.40	18.81	64.58	17.91	12.67	72.38	12.75	67.20	8.61	15.84	1.44	6.75	0.60
1488 - 49	16.76	37.54	4.45	18.05	18.16	14.84	122.04	24.88	123.50	16.53	32.41	3.06	13.42	1.43
1488 - 5	0.09	0.78	0.56	5.71	15.20	11.92	82.83	15.52	77.11	10.34	19.06	1.65	6.90	0.70
1488 - 51	0.17	0.86	0.39	4.66	12.42	9.64	80.63	15.98	83.25	11.04	21.54	1.85	9.24	0.84
1488 - 52	0.11	2.02	0.91	10.00	12.72	8.14	58.61	9.88	47.56	6.09	10.21	0.84	3.39	0.32
1488 - 53	680.46	1487.19	159.16	534.18	114.04	51.87	264.97	34.54	143.34	16.39	31.25	2.49	11.41	1.11
1488 - 54	0.05	0.78	0.32	5.43	14.68	13.40	99.18	19.06	86.08	11.24	20.99	2.03	9.17	0.86
1488 - 55	261.46	513.05	52.82	166.29	48.78	32.62	218.78	32.28	114.49	12.31	21.41	1.86	8.59	0.84
1488 - 56	0.12	0.83	0.38	4.10	19.92	18.35	145.29	26.44	111.21	13.79	24.45	2.33	10.18	1.02
1488 - 57	0.35	1.18	0.35	4.28	13.53	11.97	106.07	22.17	107.09	15.00	27.89	2.61	12.95	1.22
1488 - 6	288.62	552.67	57.33	197.68	54.50	26.50	134.74	19.10	92.13	11.72	21.44	1.85	7.98	0.79
1488 - 63	0.04	1.15	0.61	8.99	36.29	33.07	219.00	27.96	92.56	8.73	14.01	1.27	5.41	0.67
1488 - 64	0.04	1.38	0.62	12.71	48.32	49.05	341.08	44.13	126.54	11.05	15.97	1.28	5.95	0.57
1488 - 65	0.05	0.52	0.25	3.86	10.98	9.22	77.44	15.47	75.82	9.75	18.48	1.66	7.26	0.84
1488 - 66	0.06	0.46	0.25	3.45	11.76	10.81	80.02	15.83	76.60	10.04	18.12	1.73	7.86	0.81
1488 - 67	0.15	2.25	1.43	23.81	83.26	72.22	389.00	35.14	75.01	4.81	5.00	0.38	1.33	0.12
1488 - 68	1.98	4.84	1.22	16.25	48.23	31.35	181.23	24.81	125.60	17.12	30.79	2.50	11.77	1.16

1488 - 69	0.05	1.25	0.79	9.58	35.21	26.10	157.38	25.74	132.89	17.55	35.60	3.14	12.59	1.44
1488 - 7	0.08	1.65	0.91	13.12	60.84	57.06	359.83	40.53	90.87	6.29	9.69	0.76	2.89	0.28
1488 - 70	0.04	0.84	0.33	6.08	15.10	12.29	88.06	14.92	78.30	10.34	18.52	1.70	6.57	0.78
1488 - 71	196.73	299.29	27.14	76.24	16.99	10.03	64.97	12.30	60.10	7.93	14.29	1.31	5.84	0.63
1488 - 72	74.83	159.80	17.06	68.22	27.65	19.54	144.47	23.91	103.59	12.50	23.61	2.09	9.10	0.92
1488 - 73	31.27	69.74	7.53	32.55	19.35	14.51	115.75	21.61	111.26	14.48	29.24	2.75	12.74	1.27
1488 - 74	0.03	0.47	0.33	4.93	20.15	19.21	140.45	18.54	56.96	5.11	9.08	0.72	2.41	0.33
1488 - 8	0.05	0.34	0.21	3.69	12.21	11.77	114.80	24.90	121.96	15.65	31.02	2.81	12.65	1.46
1488 - 9	0.07	0.44	0.24	3.27	9.49	8.66	69.02	12.93	65.87	8.69	16.15	1.56	6.55	0.71
Apatite 2														
852_apatite - 1	23.80	197.79	56.45	420.43	183.03	24.39	164.91	16.84	72.30	10.69	20.29	1.60	7.76	0.93
852_apatite - 10	29.48	251.56	61.44	420.52	160.86	22.52	162.67	19.97	111.02	21.35	56.14	6.98	42.45	5.30
852_apatite - 11	24.11	326.37	60.45	401.01	150.16	22.12	174.71	25.08	143.60	27.43	76.41	9.38	54.93	7.26
852_apatite - 12	24.45	190.84	48.07	331.44	136.46	21.86	158.31	22.09	126.48	23.79	62.26	7.23	40.48	4.88
852_apatite - 13	20.31	196.57	52.23	361.40	134.33	21.27	165.84	24.53	144.34	27.43	76.05	8.62	46.79	5.85
852_apatite - 14	38.29	781.33	105.04	615.87	168.57	23.22	180.96	27.14	173.33	37.75	120.67	17.59	120.71	16.57
852_apatite - 15	42.47	363.44	71.67	466.37	165.81	24.80	211.30	30.31	189.61	40.07	118.44	15.21	91.57	12.33

852_apatite - 16	13.17	120.85	31.70	229.52	95.08	15.60	125.03	17.79	105.61	20.29	52.26	6.21	34.80	4.25
852_apatite - 17	31.61	698.01	89.38	695.24	346.51	52.96	390.57	51.22	284.27	51.20	132.01	15.25	83.71	9.65
852_apatite - 18	24.65	517.52	74.18	482.25	167.82	23.44	173.60	22.41	125.78	24.60	70.10	9.28	58.20	7.80
852_apatite - 19	33.31	271.31	65.33	453.84	172.97	24.04	174.64	22.25	124.53	22.20	58.41	6.62	37.23	4.81
852_apatite - 2	31.06	759.52	88.41	743.63	414.03	67.55	493.02	61.14	328.31	61.07	150.79	16.59	82.47	9.88
852_apatite - 20	9.54	80.15	23.35	176.33	78.20	12.91	117.07	18.33	115.79	21.02	52.29	6.04	31.43	4.20
852_apatite - 21	7.74	107.49	32.41	273.09	125.11	18.41	130.20	15.23	73.41	12.42	28.41	3.33	16.90	2.41
852_apatite - 22	22.21	467.85	54.30	374.34	161.27	26.14	211.94	30.59	187.20	37.13	105.67	13.51	82.27	10.83
852_apatite - 23	44.01	307.25	76.05	515.59	188.97	24.72	157.29	16.67	75.66	11.94	26.31	2.44	13.25	1.57
852_apatite - 24	38.96	143.22	54.59	368.93	137.99	19.50	130.41	14.45	63.68	10.42	23.14	2.39	13.17	1.65
852_apatite - 25	8.24	100.22	32.26	263.80	127.51	17.72	132.70	13.80	60.31	9.48	18.08	1.58	7.14	0.74
852_apatite - 26	16.84	194.46	46.11	324.99	147.75	27.03	209.43	31.65	184.60	37.61	114.11	14.30	89.60	11.88
852_apatite - 27	22.05	268.16	52.85	364.37	155.98	26.91	205.08	29.52	178.76	36.35	100.77	13.23	78.21	10.44
852_apatite - 28	6.64	104.13	33.00	271.86	138.06	20.82	145.23	17.27	81.98	12.91	28.24	2.93	16.87	1.95
852_apatite - 3	36.38	684.23	80.36	524.26	179.80	26.24	223.56	33.04	219.93	51.73	168.59	23.28	154.65	21.70

852_apatite - 30	136.22	683.15	69.55	361.27	111.05	18.90	140.24	18.12	116.14	28.42	93.58	13.87	96.30	14.03
852_apatite - 31	138.60	1201.34	78.29	421.34	161.17	27.94	230.90	34.95	223.93	48.03	151.43	21.76	136.67	17.85
852_apatite - 32	21.09	300.64	42.35	291.07	116.16	19.77	158.37	23.50	157.19	38.01	125.03	18.12	118.24	16.98
852_apatite - 33	31.23	174.39	45.93	289.83	107.68	17.19	152.20	24.49	175.92	42.39	146.96	21.44	150.00	21.60
852_apatite - 34	33.49	3047.03	61.15	419.72	167.45	25.90	226.05	33.68	216.62	48.33	145.83	19.48	129.86	16.69
852_apatite - 36	14.07	1559.94	36.83	285.91	150.11	25.97	229.76	36.81	231.60	49.53	149.45	20.36	135.91	17.32
852_apatite - 37	13.24	125.06	33.38	256.63	120.29	19.19	133.20	15.42	79.80	13.37	31.87	3.44	17.48	2.02
852_apatite - 38	21.74	438.31	50.85	357.66	157.09	25.06	191.35	27.53	162.51	32.40	90.88	12.07	71.43	8.95
852_apatite - 39	16.98	761.68	42.75	315.88	143.79	22.83	181.40	24.98	153.09	32.96	97.62	13.47	81.72	10.46
852_apatite - 4	24.14	416.69	61.59	407.59	139.75	21.05	165.92	24.95	148.73	29.52	82.94	10.43	63.64	8.06
852_apatite - 40	21.92	739.95	58.93	424.86	169.71	25.89	205.01	27.81	165.79	35.78	105.22	13.93	83.44	11.06
852_apatite - 43	30.22	2421.42	59.42	432.53	195.76	29.13	246.60	35.46	222.44	48.96	142.31	19.68	133.83	16.75
852_apatite - 44	15.44	162.14	43.07	346.32	137.81	20.64	155.62	18.39	104.41	19.36	51.09	5.59	33.91	4.07
852_apatite - 45	20.92	1011.54	68.99	514.53	216.85	31.59	267.19	36.16	217.48	48.27	137.92	17.83	111.18	13.26
852_apatite - 46	11.01	124.14	37.73	293.65	125.03	18.01	130.27	16.36	79.34	14.63	34.60	4.33	21.90	2.65

852_apatite - 47	25.77	129.75	37.16	252.80	94.58	13.53	103.70	14.09	87.24	15.55	38.06	3.93	20.97	2.28
852_apatite - 49	55.06	841.16	100.27	663.98	239.60	33.36	263.61	35.71	210.04	50.54	156.84	22.39	141.49	18.83
852_apatite - 5	43.85	3106.88	81.74	528.47	191.87	29.48	252.48	36.21	229.54	47.18	143.23	18.70	120.49	15.77
852_apatite - 50	30.80	1317.42	76.01	553.00	249.95	36.45	313.17	44.40	251.37	52.38	158.15	21.07	132.51	16.93
852_apatite - 51	18.23	198.37	45.12	318.16	138.67	25.07	191.89	26.32	170.43	35.42	102.52	12.86	76.84	10.27
852_apatite - 52	39.08	762.61	75.17	443.54	136.26	19.34	160.33	21.32	131.04	27.19	76.26	10.28	62.95	8.64
852_apatite - 53	25.19	1305.52	73.34	482.46	189.28	30.37	248.54	38.68	248.22	52.62	158.63	22.01	144.62	19.44
852_apatite - 54	27.58	625.36	82.69	547.44	205.54	32.10	244.88	35.10	213.19	44.45	130.38	16.99	105.40	13.97
852_apatite - 55	17.46	626.26	45.73	364.59	210.00	35.62	268.72	37.65	223.65	45.74	126.40	15.98	93.35	11.70
852_apatite - 56	48.79	1608.50	93.38	605.12	200.84	28.06	228.32	32.18	190.64	41.54	125.90	17.47	109.12	15.39
852_apatite - 57	12.41	116.74	36.84	314.12	187.84	33.68	268.64	39.48	236.43	49.45	145.81	18.89	114.97	15.43
852_apatite - 58	32.20	1020.07	66.10	422.18	136.68	20.67	171.12	23.43	140.03	30.62	89.18	12.58	81.42	11.04
852_apatite - 59	16.62	198.45	54.21	405.10	170.34	24.74	170.60	20.53	103.55	19.25	47.49	5.68	30.04	3.72
852_apatite - 6	24.56	228.42	57.21	393.39	145.85	18.55	148.98	17.91	102.18	18.22	44.87	4.95	28.43	3.56
852_apatite - 60	23.71	358.39	48.08	329.12	142.67	25.17	199.44	28.44	179.11	36.89	102.18	13.44	83.04	10.69

852_apatite - 61	9.80	537.99	37.08	324.20	199.24	34.02	274.98	38.27	233.34	47.62	129.66	15.84	94.17	11.34
852_apatite - 62	14.74	147.35	38.18	300.96	132.83	19.48	152.74	19.83	102.29	20.17	50.62	6.14	35.48	4.44
852_apatite - 63	18.10	940.86	49.54	400.68	191.36	29.99	255.60	35.84	224.19	46.19	130.68	16.81	108.96	13.41
852_apatite - 7	38.96	199.16	60.66	405.80	157.76	23.33	167.20	21.41	116.48	21.24	53.16	5.91	32.16	4.01
852_apatite - 8	14.67	158.09	43.86	364.41	176.16	26.41	190.54	23.71	120.81	21.34	55.58	6.47	34.37	4.41
852_apatite - 9	12.29	150.38	42.96	338.66	143.37	21.20	143.72	18.00	94.62	16.83	42.30	4.80	27.14	3.39
973_apatite - 1	10.40	14.56	1.91	9.82	24.38	15.60	149.20	16.39	78.42	12.74	27.49	2.79	11.18	1.08
973_apatite - 10	170.48	228.41	16.69	47.16	23.00	12.45	116.65	15.31	74.39	13.01	30.93	3.11	20.95	2.65
973_apatite - 11	44.52	146.09	14.01	52.97	17.84	7.16	88.21	26.01	196.65	37.89	89.59	8.13	37.97	4.65
973_apatite - 12	1.02	4.10	0.75	4.87	15.80	10.57	112.04	15.50	87.28	14.57	31.94	3.08	12.63	1.41
973_apatite - 13	6.63	21.42	2.22	10.85	20.28	13.91	135.86	16.17	78.61	13.05	28.36	2.45	11.22	1.29
973_apatite - 14	1.81	4.87	1.05	8.61	29.64	21.83	223.99	20.77	83.62	14.55	38.38	4.02	27.01	3.79
973_apatite - 15	1485.09	2184.22	160.60	364.28	80.40	32.20	268.77	24.60	94.39	17.91	48.68	6.53	42.41	6.69
973_apatite - 16	3.36	11.82	1.30	7.83	13.65	7.15	79.76	16.28	104.82	18.26	38.04	3.15	13.34	1.56
973_apatite - 17	0.92	5.05	0.72	5.37	12.93	7.81	91.95	22.05	156.80	31.64	73.56	6.58	27.56	2.68

973_apatite - 18	15.84	70.44	4.70	18.79	23.10	14.75	142.43	16.67	82.71	14.23	30.83	2.75	12.12	1.49
973_apatite - 19	3047.22	4284.19	307.40	691.35	101.75	28.27	196.50	18.27	68.24	9.99	22.48	1.98	9.72	0.98
973_apatite - 2	901.45	1360.25	100.52	255.28	44.35	14.19	115.37	16.76	97.43	17.55	37.45	3.38	15.42	1.86
973_apatite - 20	45.97	99.82	6.24	22.19	26.39	16.13	148.60	17.56	85.02	14.43	33.00	3.30	14.25	1.63
973_apatite - 21	29.31	33.81	3.43	13.65	15.40	8.64	88.12	17.31	116.01	22.62	55.68	6.11	28.57	3.64
973_apatite - 23	3.35	9.09	1.29	8.49	22.92	14.56	145.10	20.12	125.29	24.26	53.89	5.18	20.46	1.99
973_apatite - 24	23.18	54.06	5.67	21.15	25.08	13.44	131.42	18.48	100.82	17.82	38.25	3.58	16.88	2.02
973_apatite - 25	37.34	115.29	4.67	19.55	27.51	18.25	184.08	22.56	118.62	22.26	51.71	4.56	19.36	1.60
973_apatite - 27	1.88	7.30	1.31	7.66	26.61	14.37	144.98	16.46	81.15	12.85	29.68	2.51	12.21	1.31
973_apatite - 28	7.44	21.78	2.88	15.95	25.69	14.43	135.11	15.89	81.04	13.39	29.03	2.50	11.37	1.24
973_apatite - 29	569.81	853.82	55.44	145.92	47.54	24.02	227.08	16.41	45.66	5.54	12.65	0.95	4.18	0.36
973_apatite - 3	6.70	19.42	2.47	10.39	29.16	18.98	181.33	19.52	83.04	14.08	34.48	3.54	20.39	3.05
973_apatite - 30	53.74	171.50	17.79	63.40	28.40	12.22	102.61	13.58	72.29	12.01	26.07	2.73	13.45	1.56
973_apatite - 31	4.60	22.98	0.84	6.42	17.48	11.34	121.25	20.55	133.09	26.87	67.33	6.91	31.48	3.80
973_apatite - 32	3.67	11.73	1.36	7.40	18.55	9.79	84.56	10.10	43.93	6.52	12.98	1.08	4.61	0.49

973_apatite - 33	37.91	116.66	14.09	51.36	22.87	9.98	100.08	18.27	124.07	23.86	53.54	5.44	29.06	4.09
973_apatite - 35	57.82	90.25	7.79	23.56	27.25	15.04	148.28	16.97	88.55	15.60	33.64	3.17	12.27	1.60
973_apatite - 36	11.64	48.97	4.73	22.37	18.78	9.09	83.73	9.47	45.64	6.74	12.90	1.14	4.93	0.49
973_apatite - 37	0.18	1.21	0.36	6.13	43.36	27.43	242.75	17.30	50.17	6.70	10.29	1.06	4.10	0.33
973_apatite - 38	63.47	100.85	8.17	26.03	36.44	22.99	213.70	16.10	46.26	6.45	11.31	0.91	3.93	0.37
973_apatite - 39	15.76	17.13	2.45	11.14	27.71	17.80	153.19	15.18	64.21	10.50	25.34	2.45	12.77	1.33
973_apatite - 4	1.40	7.20	1.22	8.62	10.41	4.90	54.34	12.77	89.48	16.22	31.86	2.58	11.93	1.07
973_apatite - 40	2.92	6.04	1.29	7.80	21.90	14.56	156.15	16.56	72.80	12.41	29.83	3.31	15.67	1.77
973_apatite - 41	1.59	7.33	1.46	11.66	24.09	15.03	138.31	15.81	73.33	12.47	26.56	2.37	9.86	1.10
973_apatite - 42	0.22	1.56	0.46	4.99	19.10	11.24	102.28	11.43	51.48	7.70	15.13	1.27	4.99	0.57
973_apatite - 43	3.40	10.44	1.51	9.70	24.63	15.64	146.73	13.95	55.90	8.65	16.25	1.35	5.69	0.66
973_apatite - 44	4.95	17.52	2.07	9.51	17.35	9.71	100.19	15.24	89.60	16.09	33.94	3.02	13.60	1.59
973_apatite - 45	0.26	2.04	0.63	6.31	30.19	18.89	178.44	16.86	63.09	8.90	17.98	1.56	6.68	0.73
973_apatite - 46	3.14	8.39	1.38	9.66	33.74	23.19	227.08	19.53	70.67	12.17	32.74	3.94	25.39	3.98
973_apatite - 47	30.83	108.82	10.41	38.09	12.41	5.83	67.36	16.70	116.07	20.10	45.14	4.34	20.42	2.42

973_apatite - 48	476.26	694.40	47.02	129.16	23.63	7.61	80.62	16.72	109.77	20.72	44.84	4.15	18.43	2.38
973_apatite - 49	11.65	17.55	1.83	10.58	35.90	21.36	186.83	14.15	41.36	5.28	9.63	0.87	4.41	0.46
973_apatite - 5	86.72	112.12	9.37	29.26	30.85	18.09	167.33	13.81	52.23	8.39	16.31	1.27	5.92	0.51
973_apatite - 50	868.97	1299.12	81.80	211.46	42.45	15.02	137.87	21.04	133.78	25.94	60.34	5.80	27.83	3.17
973_apatite - 51	5.05	18.95	2.26	11.44	25.95	16.65	159.14	15.87	64.37	10.07	21.89	2.12	10.61	1.56
973_apatite - 52	0.70	2.03	0.51	4.95	37.90	26.94	268.24	22.32	70.93	9.95	19.16	1.70	7.65	0.82
973_apatite - 53	810.50	1218.03	101.62	198.79	46.43	15.66	126.06	15.45	82.66	14.69	31.16	2.36	10.86	0.97
973_apatite - 55	0.85	5.23	0.88	5.95	11.24	6.64	72.50	17.47	122.66	22.82	46.79	3.96	19.16	1.97
973_apatite - 56	15.36	28.91	2.58	13.84	32.23	18.69	182.90	16.11	65.89	11.07	23.52	2.02	10.11	0.90
973_apatite - 57	29.80	52.43	10.34	38.64	17.88	7.27	78.38	16.94	114.02	22.30	53.24	5.86	29.79	4.28
973_apatite - 58	8.96	16.96	1.80	10.71	28.52	20.88	211.26	18.36	75.11	11.58	24.88	2.41	12.08	1.38
973_apatite - 59	125.42	190.07	12.81	34.82	43.26	27.16	264.24	21.62	71.58	10.00	18.99	1.59	5.47	0.62
973_apatite - 6	0.46	2.99	0.79	6.82	26.00	17.64	174.11	17.49	72.66	12.36	27.70	2.53	11.52	1.23
973_apatite - 60	1236.07	1828.26	117.18	295.59	53.51	15.37	134.60	27.43	183.75	36.90	80.78	7.31	29.33	3.45
973_apatite - 7	2.88	10.24	1.68	9.53	23.12	14.88	153.68	17.03	81.15	13.14	29.59	2.51	11.76	1.08

973_apatite - 8	344.73	442.64	32.18	81.82	28.62	15.99	141.0 2	14.56	66.93	11.48	24.77	2.41	11.24	1.21
Apatite 3														
1084 - 1	81.48	332.41	61.35	349.03	88.58	12.88	87.11	11.11	62.44	12.13	32.38	4.06	19.48	2.98
1084 - 10	210.47	519.90	78.45	357.05	97.92	15.29	99.67	13.42	74.84	13.19	33.21	4.14	20.92	2.49
1084 - 11	5661.2 4	10816.2 5	1050.2 9	3673.3 8	437.28	76.86	323.0 9	36.70	177.7 0	30.04	70.53	7.38	42.61	5.06
1084 - 12	235.40	712.51	113.67	558.07	147.87	29.28	159.1 6	19.80	103.5 2	18.26	40.91	4.00	23.05	2.96
1084 - 13	1006.1 9	2854.75	371.71	1579.3 8	296.22	37.66	254.1 5	34.21	191.7 5	36.87	96.86	11.73	70.68	9.26
1084 - 15	1338.9 3	3136.25	329.81	1164.8 4	144.98	23.16	88.57	9.31	48.82	8.46	22.34	2.76	14.17	1.68
1084 - 16	450.34	1344.97	189.66	828.15	169.89	19.32	146.9 6	17.96	100.9 9	18.20	47.76	5.63	32.14	4.24
1084 - 17	241.70	820.99	126.82	605.67	153.42	20.42	151.7 7	19.94	113.0 7	21.01	53.62	6.57	36.17	4.74
1084 - 18	750.68	2075.80	276.45	1186.8 3	241.47	29.26	225.5 7	29.16	163.1 2	30.84	80.24	9.76	53.58	6.93
1084 - 19	142.27	516.85	84.13	432.70	117.95	19.44	119.5 2	15.12	82.05	14.31	36.12	4.05	23.44	3.05
1084 - 2	699.02	2172.11	302.34	1328.1 2	261.39	29.34	232.6 9	29.86	167.9 3	32.10	84.38	10.01	56.59	7.22
1084 - 21	590.15	1728.09	247.04	1135.8 4	251.67	42.57	245.9 2	30.57	163.0 5	31.13	75.67	8.43	45.58	5.71
1084 - 22	547.48	1667.64	234.09	1006.2 8	182.92	25.99	138.6 2	16.26	83.32	14.32	36.83	4.52	27.58	3.44
1084 - 23	381.92	729.48	70.93	214.94	29.55	26.85	17.66	2.02	10.37	1.74	3.94	0.39	2.89	0.38
1084 - 25	601.71	1908.78	267.37	1147.9 1	195.04	23.58	150.1 4	17.52	96.98	18.37	50.20	6.29	35.74	4.64

1084-26	499.49	1469.95	202.61	872.98	178.33	25.93	165.0 2	21.96	131.8 4	24.93	72.61	9.34	53.61	8.36
1084 - 27	826.83	2097.23	265.67	1110.6 9	202.51	18.93	170.7 1	21.81	119.2 2	22.49	59.20	7.25	40.04	5.01
1084 - 28	284.78	895.34	131.38	587.05	146.59	22.71	139.9 0	19.72	111.5 6	20.89	54.93	6.43	38.29	4.60
1084 - 29	359.43	902.07	111.26	411.91	58.96	15.56	39.80	4.70	26.44	4.59	12.30	1.60	9.23	1.22
1084 - 3	272.45	778.92	108.19	497.34	97.09	16.91	79.44	9.20	51.35	8.56	19.44	1.90	9.18	0.87
1084-30	109.74	386.42	63.23	316.53	80.49	15.47	75.58	10.31	53.35	9.77	22.45	2.65	14.33	1.32
1084-31	160.80	512.54	72.01	302.24	47.37	14.47	26.55	2.52	10.43	1.29	2.33	0.16	0.76	0.07
1084 - 33	977.75	2737.73	347.03	1387.1 7	223.49	28.19	172.8 6	21.41	121.9 1	25.26	75.65	9.38	55.34	7.24
1084 - 34	606.90	1745.28	225.33	894.28	136.57	21.19	86.68	9.53	52.78	9.27	23.19	2.41	12.73	1.32
1084-35	555.33	1614.02	222.08	985.18	200.90	26.74	190.6 2	26.23	157.1 9	30.94	90.39	11.69	66.89	9.77
1084-36	958.56	2770.38	372.07	1572.2 7	305.46	41.64	261.3 7	34.51	184.0 2	34.41	88.28	10.02	58.31	7.20
1084 - 37	814.45	2369.38	314.85	1272.7 5	217.80	25.79	163.3 2	19.91	109.4 6	20.02	52.92	6.54	37.77	5.20
1084 - 38	455.03	1519.74	211.44	849.52	134.95	19.03	88.57	10.83	58.54	10.58	25.98	2.84	15.47	1.76
1084 - 39	178.68	682.64	114.17	580.00	141.25	13.59	131.7 5	17.73	100.3 6	18.99	52.18	6.23	32.82	4.63
1084-4	473.50	1385.61	191.47	862.05	181.95	26.15	171.0 2	20.20	108.1 5	19.68	49.14	5.64	30.36	4.23
1084-40	1074.6 4	2893.31	388.85	1768.2 1	365.70	72.26	340.6 6	42.69	223.3 5	37.53	84.99	8.57	40.77	5.02
1084-41	569.39	1876.17	306.57	1561.8 2	420.47	96.11	440.7 4	50.64	242.8 0	38.96	79.62	6.52	26.90	2.67
1084-42	241.75	817.26	125.03	592.06	135.16	22.28	128.1 4	15.17	78.27	14.17	36.75	4.42	24.85	3.16

1084-44	368.83	1220.93	204.79	1042.4 8	266.84	56.41	264.5 0	34.79	181.3 8	31.79	73.06	6.83	31.68	3.95
1084 - 46	368.73	1047.28	131.38	488.98	76.03	22.36	52.16	5.75	30.07	5.20	13.32	1.44	8.67	0.94
1084-47	363.20	1351.97	248.83	1307.7 7	346.19	53.32	322.4 1	42.52	235.3 7	41.32	99.72	10.51	51.48	5.15
1084-48	365.25	1250.69	195.08	915.71	185.64	26.11	161.7 5	19.47	101.9 8	18.35	50.87	5.90	32.91	4.74
1084-49	421.91	1246.46	184.53	852.71	179.42	27.39	156.8 9	19.01	99.11	18.22	44.85	5.49	29.66	3.97
1084 - 5	595.76	1744.31	234.19	1011.9 0	201.85	25.10	179.7 0	23.41	133.5 4	25.45	67.00	8.06	45.36	5.70
1084-50	579.72	1903.83	318.11	1668.0 8	436.74	101.9 7	471.3 7	59.93	312.5 4	51.43	107.2 0	9.03	33.97	3.20
1084-51	97.99	390.09	69.14	383.67	89.62	12.84	83.82	9.82	52.70	9.60	25.06	2.79	12.54	1.77
1084 - 53	580.76	1903.08	279.85	1245.3 4	214.28	25.72	167.0 1	20.49	109.9 1	20.07	54.46	7.02	41.24	5.40
1084 - 54	385.84	1338.90	201.94	915.14	201.59	23.19	175.2 9	22.71	128.7 5	24.49	65.17	7.54	43.19	5.43
1084 - 55	817.84	2172.11	274.63	1142.6 4	185.89	21.10	141.5 6	16.97	92.62	16.86	43.82	5.20	28.89	3.80
1084 - 56	376.92	1158.15	173.31	822.22	167.86	21.78	143.9 7	17.80	96.41	18.28	48.25	6.04	33.70	4.48
1084 - 57	668.57	1893.26	239.28	918.53	137.11	18.63	91.38	10.52	55.51	9.76	25.21	2.83	16.27	2.12
1084 - 58	410.16	1291.78	188.48	888.11	173.22	11.42	152.3 2	18.51	104.0 2	18.38	50.80	5.79	31.55	3.94
1084 - 59	430.27	1154.89	154.34	673.11	110.99	12.46	86.00	9.63	51.05	8.56	21.85	2.39	12.55	1.74
1084-6	1129.0 9	2611.27	297.45	1168.8 3	209.93	27.43	163.3 8	20.27	103.5 0	18.85	46.22	5.52	30.27	3.94
1084-60	779.93	1971.34	257.61	1060.6 1	180.47	26.14	141.5 6	16.34	82.16	14.49	33.35	3.87	21.64	2.63

1084-7	144.39	377.04	60.39	321.78	95.81	14.49	102.1 9	14.24	76.16	12.76	28.27	2.78	11.61	1.05
1084-8	291.91	1212.10	202.80	997.36	191.42	16.83	151.1 7	17.46	94.92	17.28	44.31	4.96	28.05	3.10
1084-9	802.09	2210.33	298.59	1317.9 7	270.57	40.95	238.2 4	31.35	173.1 6	32.32	86.64	10.58	59.95	8.22
1183 - 1	335.36	1025.22	150.84	712.05	144.76	19.00	125.2 2	15.35	84.28	15.17	40.28	4.88	25.84	3.32
1183-10	28.63	120.67	25.21	159.09	64.74	10.68	87.81	12.87	74.56	13.93	38.17	4.43	23.15	3.20
1183 - 11	378.62	1310.74	202.90	959.54	216.21	32.17	198.0 3	25.33	140.6 0	25.78	64.89	7.67	42.15	5.65
1183 - 12	548.99	1527.93	205.01	876.76	163.93	23.33	139.1 3	17.09	94.06	18.16	48.23	5.93	35.96	4.91
1183 - 13	568.95	1720.11	236.25	1016.8 9	180.48	22.36	142.3 7	17.55	95.02	17.35	46.31	5.62	32.58	4.32
1183 - 14	777.55	2241.31	302.40	1282.0 2	237.46	26.90	181.7 1	21.92	115.8 0	21.51	56.01	6.58	39.02	5.55
1183 - 15	191.70	638.19	95.15	473.82	113.86	14.62	109.7 2	13.54	78.27	15.33	42.03	5.10	29.92	4.27
1183 - 16	607.90	1909.68	276.20	1228.5 3	236.74	29.21	203.2 8	25.46	137.8 4	25.16	66.26	7.98	44.72	6.06
1183 - 17	294.23	892.67	129.58	603.80	144.99	20.24	148.0 5	19.00	107.7 7	19.05	48.66	5.82	29.29	4.02
1183-18	264.21	727.29	105.57	489.58	109.60	19.48	101.6 8	12.34	65.63	10.44	25.67	2.79	14.66	2.00
1183-19	425.00	1221.95	170.00	740.51	142.73	25.05	123.5 5	16.26	84.88	15.08	33.38	3.62	18.18	2.21
1183 - 2	399.54	1145.77	165.10	781.06	168.14	19.51	148.4 5	18.09	96.67	17.43	45.26	5.31	29.98	3.70
1183 - 20	177.58	543.12	77.51	365.57	93.73	16.32	99.89	13.83	83.67	16.39	44.29	5.48	31.87	4.18

1183 - 24	346.94	1104.79	169.94	839.05	181.62	20.37	159.7 4	20.16	100.4 0	19.62	51.68	6.46	37.11	4.99
1183 - 26	110.76	440.93	77.37	412.67	116.47	17.16	117.1 8	15.89	88.58	16.32	42.75	5.36	29.78	3.67
1183 - 27	368.62	1149.23	167.87	767.04	152.07	20.84	129.3 9	16.45	89.76	17.16	46.40	5.76	34.78	4.89
1183 - 28	630.02	1871.64	261.96	1154.9 5	210.86	26.73	179.9 5	21.20	119.7 3	22.20	59.86	7.37	43.08	5.96
1183 - 29	416.94	1293.13	190.85	888.29	169.37	26.52	144.5 1	16.98	85.93	15.22	37.94	4.51	24.13	3.39
1183 - 3	403.64	1328.73	190.03	821.26	150.78	19.62	118.1 8	13.93	75.16	13.59	36.34	4.31	22.83	3.09
1183 - 30	369.97	1247.89	193.30	918.76	185.55	27.50	155.3 8	19.30	101.3 0	18.69	47.33	5.87	32.64	4.55
1183 - 31	213.80	816.31	141.62	742.09	182.91	18.45	166.1 2	21.54	121.5 7	22.08	58.41	6.88	37.88	5.08
1183 - 32	484.39	1526.36	221.89	1005.4 4	197.13	25.68	156.9 2	18.88	102.6 5	18.55	48.21	5.83	31.17	4.46
1183 - 33	455.18	1471.61	212.34	943.28	178.89	24.60	141.0 5	16.88	91.26	16.98	45.38	5.51	34.64	4.62
1183 - 34	288.58	960.52	152.23	766.80	177.66	25.86	166.3 7	21.25	113.4 8	20.17	48.39	5.76	32.05	3.85
1183 - 35	610.35	1909.01	263.02	1101.9 7	192.96	27.99	143.1 4	17.62	93.24	16.64	43.38	5.45	31.29	4.14
1183 - 36	471.22	1380.73	198.37	897.70	171.23	22.75	140.3 6	17.42	94.42	17.75	45.59	5.62	32.27	4.37
1183 - 37	561.28	1841.30	270.76	1190.1 9	215.23	24.75	163.6 9	18.83	100.6 8	17.62	47.58	5.69	33.15	4.37
1183 - 38	18.95	87.21	19.85	133.58	64.49	11.37	81.15	10.34	50.29	7.82	15.88	1.42	7.18	0.75

1183 - 4	451.76	1401.18	201.57	923.06	209.84	29.92	200.2 2	26.06	147.4 7	29.26	76.27	9.43	53.59	7.08
1183 - 40	548.84	1862.47	274.90	1267.4 7	228.20	27.94	176.3 7	21.59	112.6 0	20.27	51.03	6.08	36.45	4.72
1183 - 42	11.03	20.10	1.82	7.55	1.26	0.94	0.33	0.15	1.23	0.29	1.12	0.12	1.42	0.29
1183 - 43	634.54	2063.45	296.78	1339.0 7	269.26	30.76	235.5 2	29.39	162.7 1	30.64	81.52	10.31	57.95	7.73
1183 - 44	40.54	158.67	27.93	151.61	47.22	9.70	60.80	9.06	54.16	10.00	25.29	2.70	13.74	1.41
1183 - 46	619.35	1854.54	252.08	1068.2 1	177.46	19.97	127.2 9	14.91	78.26	13.69	35.72	4.48	24.93	3.57
1183 - 47	257.00	848.11	144.54	755.81	182.97	24.46	160.1 8	19.99	102.8 9	17.77	43.49	5.14	28.02	3.90
1183 - 49	483.87	1642.35	247.36	1123.4 3	212.38	24.09	165.0 7	19.64	106.8 9	19.36	50.02	6.08	36.50	4.90
1183 - 5	371.78	1205.98	180.98	870.47	184.17	18.04	160.1 0	19.83	109.3 0	19.97	54.02	6.76	37.77	5.01
1183 - 52	278.30	722.98	103.60	473.79	116.30	16.49	113.4 0	15.89	92.91	16.78	43.46	5.12	28.29	3.59
1183 - 53	222.30	672.09	101.97	497.61	130.19	18.85	137.3 7	16.96	89.34	15.02	34.85	3.59	17.99	1.76
1183 - 54	570.76	1743.25	248.53	1135.9 9	214.28	27.41	169.6 7	20.50	112.7 8	20.85	55.42	7.14	42.03	5.79
1183 - 55	547.09	1622.98	226.01	997.29	179.86	23.80	138.8 8	16.40	87.62	15.85	39.39	4.82	27.15	3.45
1183 - 56	882.04	2559.86	344.06	1455.1 4	238.01	30.30	168.4 3	19.48	104.7 2	19.27	51.34	6.57	38.77	5.21
1183 - 58	25.55	94.60	16.53	99.32	38.18	8.15	56.81	7.80	43.93	6.97	15.15	1.37	5.49	0.50
1183 - 59	21.44	111.95	23.84	160.99	66.08	8.82	91.82	14.00	88.20	18.49	52.65	6.56	37.78	5.06
1183 - 6	441.32	1264.25	181.53	830.94	166.83	25.10	147.8 7	18.55	96.74	17.11	42.14	4.85	27.22	3.79

1183 - 61	390.59	1164.67	168.51	778.97	156.22	23.72	132.1 8	16.90	95.86	18.09	50.30	6.26	42.69	6.66
1183 - 64	106.89	401.00	67.81	352.33	101.38	13.15	101.1 2	14.18	80.36	14.68	37.20	4.37	24.58	2.93
1183 - 65	96.53	362.17	65.30	377.84	114.24	16.18	120.6 0	15.03	84.07	13.76	33.05	3.55	17.12	1.97
1183 - 67	485.07	1374.06	191.56	829.52	147.96	24.83	118.0 9	13.73	74.20	13.46	34.61	3.86	20.30	2.53
1183 - 68	458.96	1480.08	214.72	951.66	189.64	25.25	151.2 0	19.72	105.7 5	19.20	52.32	6.40	37.76	5.17
1183 - 7	330.97	1043.16	158.60	749.76	156.43	23.72	138.0 3	16.96	86.32	15.25	36.07	4.08	21.74	2.74
1183 - 71	879.37	1976.96	254.61	1093.5 8	211.87	34.66	184.2 8	21.72	114.9 0	20.04	49.86	5.75	33.38	4.89
1183 - 9	595.15	1774.94	238.37	1006.8 0	187.01	27.69	151.3 7	19.53	104.1 8	18.97	49.89	6.23	37.21	5.31
1210 - 10	473.05	1406.92	194.32	855.24	161.02	23.75	124.4 1	15.87	87.38	15.30	39.89	4.96	27.62	3.70
1210 - 12	644.76	1895.48	242.29	949.56	134.33	18.84	89.13	11.14	61.70	11.28	32.35	4.17	24.85	3.54
1210 - 13	638.69	1978.04	266.57	1098.8 4	187.31	23.29	140.8 5	17.38	93.68	17.21	46.18	5.76	35.30	4.70
1210 - 14	621.35	1956.47	273.47	1215.1 5	232.68	35.94	182.8 1	24.02	129.5 2	23.92	64.67	7.87	45.17	5.94
1210 - 16	849.11	2464.05	325.32	1319.9 9	209.54	21.89	154.6 4	18.74	103.0 1	19.60	51.97	6.36	38.93	5.19
1210 - 17	225.08	770.60	126.03	615.44	112.55	23.99	76.37	8.64	41.91	6.91	16.23	1.76	9.54	1.04
1210 - 18	398.15	1293.69	188.17	834.39	160.39	19.72	124.3 3	14.79	79.29	14.00	37.18	4.28	25.81	3.48
1210 - 2	152.03	427.34	68.57	343.27	85.93	18.89	87.97	11.36	66.00	12.05	31.25	3.54	20.63	2.43
1210 - 20	480.40	1310.26	171.53	685.04	99.06	19.22	66.54	7.58	38.52	6.38	15.64	2.00	11.28	1.35

1210 - 21	601.81	1629.26	220.83	955.04	182.74	37.17	149.0 4	18.53	102.1 2	17.80	45.96	5.71	34.19	4.07
1210 - 23	117.78	404.44	62.47	308.63	69.64	13.60	68.30	8.32	44.53	7.95	18.99	2.04	10.56	1.18
1210 - 24	151.80	457.14	73.99	382.14	95.63	19.84	94.28	12.60	68.57	11.89	29.39	3.16	17.47	1.97
1210 - 25	156.97	548.15	90.24	449.66	104.04	20.30	91.64	11.94	65.01	11.47	28.42	3.11	16.79	2.18
1210 - 26	226.95	744.65	112.01	532.79	106.28	22.54	89.09	11.40	63.43	11.74	29.81	3.45	19.56	2.57
1210 - 28	404.20	1309.62	194.05	904.79	180.94	27.26	148.6 9	18.12	95.54	16.93	41.73	4.51	26.22	3.01
1210 - 3	122.05	415.21	67.68	361.12	85.83	17.79	77.73	10.19	51.62	8.99	22.08	2.76	13.42	1.80
1210 - 33	460.14	1053.17	139.78	586.73	98.14	19.96	68.60	7.91	38.01	6.89	15.93	1.77	9.71	1.13
1210 - 36	100.65	285.21	30.61	121.04	18.37	4.40	9.01	1.20	8.21	1.55	4.78	0.70	4.17	0.72
1210 - 38	728.04	2173.00	274.45	1146.0 9	184.06	29.92	120.8 3	14.46	82.96	13.88	37.70	4.29	26.70	3.02
1210 - 39	448.67	1442.93	215.32	987.34	194.74	29.51	154.3 9	19.05	108.5 7	19.45	52.31	6.18	34.95	4.68
1210 - 42	267.93	906.33	144.24	715.15	163.02	20.78	152.9 8	19.43	109.6 6	20.26	54.12	6.39	34.49	4.20
1210 - 45	435.38	1244.33	182.42	845.87	162.84	24.85	129.8 7	16.14	90.78	15.07	42.75	4.83	30.79	3.48
1210 - 46	290.93	727.63	106.56	504.27	109.35	18.74	95.48	12.60	71.86	13.44	32.94	3.64	17.38	2.26
1210 - 47	265.19	858.21	137.15	675.26	150.89	24.63	123.6 7	14.90	80.08	14.63	37.01	4.51	25.24	3.32
1210 - 48	425.09	1298.32	190.78	885.35	174.28	27.92	148.0 0	17.63	95.53	17.74	43.49	5.13	28.30	3.75
1210 - 5	638.43	2054.89	303.30	1424.0 3	311.65	51.87	271.7 9	36.53	208.5 3	38.29	102.2 5	12.57	71.33	8.64
1210 - 52	264.34	891.98	143.16	683.14	150.77	22.95	125.9 3	15.00	79.52	13.93	35.73	4.20	23.81	3.39

1210 - 54	348.61	1212.61	194.03	933.08	195.82	39.19	157.8 5	20.24	103.9 3	19.07	50.11	6.34	35.11	4.31
1210 - 58	764.68	2536.13	362.34	1542.0 1	247.70	32.53	172.0 7	20.65	106.3 9	19.64	50.34	6.02	37.61	5.15
1210 - 59	411.85	1327.49	199.24	904.08	166.72	25.17	128.6 2	15.62	84.21	15.53	40.28	4.73	29.83	4.04
1210 - 6	290.20	965.21	143.36	678.55	134.68	24.78	107.5 4	13.74	73.08	13.22	33.62	3.87	21.75	2.71
1210 - 60	268.47	983.02	169.58	895.29	238.27	48.18	236.7 3	33.39	192.8 6	36.06	100.5 5	12.46	72.16	9.88
1210 - 61	120.88	493.72	88.29	463.72	112.30	16.20	107.1 9	13.98	77.12	14.10	37.25	4.88	26.90	3.61
1210 - 62	671.00	2011.81	287.07	1282.2 4	243.06	43.62	184.8 7	23.85	131.0 7	22.54	59.86	7.53	44.62	5.06
1210 - 65	422.39	1298.02	193.47	903.83	185.21	26.86	156.8 7	18.81	100.1 8	18.04	46.14	5.62	31.14	4.17
1210 - 66	197.93	598.49	94.80	467.36	105.69	17.55	85.11	10.23	54.39	9.73	24.32	2.78	15.82	2.11
1210 - 67	458.47	1540.98	235.61	1091.3 2	214.08	35.85	169.9 3	21.35	115.7 9	20.81	53.80	6.66	37.58	4.37
1210 - 68	406.14	1194.52	180.35	868.09	187.66	29.75	161.8 2	20.16	108.6 5	19.13	48.77	5.66	32.73	4.20
1210 - 69	110.19	363.69	60.62	319.42	80.80	17.59	79.91	9.72	49.19	8.49	21.21	2.40	12.41	1.51
1210 - 7	121.29	388.30	63.77	346.27	87.32	16.25	83.00	9.89	50.99	9.05	21.38	2.32	12.19	1.39
1210 - 70	508.20	1826.85	269.18	1195.4 8	210.63	22.52	163.5 6	19.86	106.8 1	19.38	52.67	6.41	38.83	5.00
1210 - 71	248.00	846.19	137.99	686.17	153.88	26.17	136.1 1	16.61	91.34	16.36	40.92	5.09	29.30	3.96
1210 - 72	186.73	621.73	97.72	486.97	108.99	18.62	96.69	11.37	58.52	10.57	26.61	3.17	17.89	2.19
1210 - 73	238.84	858.86	139.21	696.39	154.83	26.43	134.5 0	16.64	91.90	16.53	44.04	5.16	29.61	3.88

1210 - 74	458.22	1317.12	185.16	829.50	164.00	22.30	136.9 6	16.64	92.35	16.59	42.46	5.12	28.57	3.85
1210 - 75	183.60	381.30	53.37	255.08	56.77	10.99	49.28	5.91	30.37	4.55	11.35	1.25	6.59	0.77
1210 - 76	436.63	1357.77	199.00	872.69	161.25	24.20	129.6 2	16.29	86.42	15.76	40.43	4.85	28.61	3.53
1210 - 8	260.47	677.12	108.30	567.86	141.74	29.68	134.3 4	17.54	94.24	16.41	41.10	4.86	26.40	3.23
1210 - 9	144.65	427.15	69.73	358.68	88.52	18.36	83.10	10.28	53.20	8.70	22.41	2.56	13.26	1.58
Standards Run 1														
401 - 1	3462.4 3	7839.97	825.89	2880.4 9	427.34	42.38	357.1 3	44.03	245.5 2	47.85	127.2 2	15.44	83.89	10.22
401 - 10	3654.4 2	8233.30	867.10	2993.9 6	438.52	43.97	368.8 6	45.71	258.0 1	49.45	135.0 1	15.68	87.89	10.36
401 - 11	3530.1 7	7964.67	839.44	2912.4 0	429.83	42.59	359.0 8	44.08	250.1 5	47.70	130.7 8	15.58	85.40	10.49
401 - 12	3518.9 1	7990.52	835.03	2916.7 0	432.09	42.66	363.2 3	44.18	250.1 6	47.41	131.6 5	15.50	83.91	10.25
401 - 13	3440.0 0	7817.39	824.37	2864.2 3	423.17	42.78	354.3 1	43.70	247.4 8	47.33	128.5 8	15.16	85.08	10.25
401 - 14	3392.4 5	7673.89	806.47	2817.0 4	412.23	41.98	349.5 9	43.22	241.4 7	47.03	126.4 6	15.10	83.07	10.22
401 - 15	3439.1 8	7817.74	821.56	2858.8 4	419.39	41.95	351.5 6	43.69	243.6 1	46.40	126.1 8	15.16	83.12	10.05
401 - 16	3530.1 4	7974.71	840.59	2922.2 3	426.47	42.67	358.7 3	44.09	248.8 4	47.84	129.4 0	15.43	84.65	10.12
401 - 17	3560.7 0	8000.25	834.90	2910.7 3	428.10	42.70	357.9 6	44.28	247.7 8	47.93	128.8 9	15.30	83.95	10.26
401 - 18	3548.8 5	7988.74	840.97	2916.8 5	423.86	42.60	361.2 8	44.44	249.3 6	47.91	128.7 6	15.23	84.63	10.52

401 - 19	3574.5 1	8029.04	841.98	2929.3 2	431.63	43.26	362.9 1	44.23	248.8 4	48.23	129.7 2	15.61	86.18	10.14
401 - 2	3450.5 2	7751.37	820.11	2854.7 2	422.36	42.28	353.0 1	44.01	246.1 8	47.40	127.8 1	15.34	84.15	10.28
401 - 20	3537.8 5	7978.39	832.45	2908.1 0	425.34	42.93	359.9 6	44.15	249.4 9	48.21	128.1 0	15.17	83.83	10.36
401 - 3	3430.0 7	7719.94	823.90	2868.2 0	421.45	42.19	354.9 9	43.47	245.0 2	47.34	127.8 1	15.30	85.00	10.01
401 - 4	3529.7 8	7840.38	842.85	2919.6 6	429.20	42.46	366.9 7	44.91	251.4 6	48.07	130.5 9	15.25	84.45	10.29
401 - 5	3467.5 3	7852.79	821.34	2853.1 5	423.65	42.49	355.1 1	43.99	244.1 5	47.22	129.2 6	15.34	86.48	10.13
401 - 6	3467.8 3	7871.56	822.78	2878.3 9	421.92	42.23	355.8 8	43.91	242.1 2	47.32	127.7 7	15.46	85.44	10.29
401 - 7	3493.0 0	7885.44	836.62	2887.5 6	427.09	41.75	357.8 3	43.91	248.3 8	47.95	129.6 1	15.34	85.90	10.23
401 - 8	3498.8 8	7833.16	834.09	2895.4 9	428.72	43.10	359.5 9	44.04	249.1 0	47.54	129.7 7	15.20	85.20	10.26
401 - 9	3573.6 8	8067.26	846.26	2954.5 5	435.43	44.13	365.3 7	44.74	252.2 1	48.66	130.8 7	15.93	87.07	10.74
MAD - 1.csv	2101.8 9	4185.36	436.10	1514.9 3	196.93	28.48	120.3 9	12.45	59.28	9.99	24.19	2.92	16.42	2.22
MAD - 10.csv	2080.2 2	4122.65	432.95	1511.1 3	194.50	28.51	119.9 9	12.42	59.95	10.08	25.05	2.91	16.25	2.18
MAD - 11.csv	2088.2 9	4170.54	439.42	1513.1 0	197.29	28.56	120.4 2	12.10	60.48	9.92	24.74	2.79	16.37	2.22
MAD - 12.csv	2122.0 0	4240.93	446.88	1553.3 5	200.88	29.04	122.2 7	12.33	60.51	10.09	25.31	2.87	15.78	2.22
MAD - 13.csv	2088.5 0	4180.34	439.66	1530.2 6	200.37	28.43	122.0 7	12.63	58.86	10.21	24.76	2.89	16.95	2.22

MAD - 14.csv	2102.3 4	4204.98	442.01	1532.9 7	200.35	28.60	122.4 1	12.58	60.47	9.99	24.56	2.94	16.39	2.23
MAD - 15.csv	2082.8 1	4151.17	432.51	1509.0 3	199.10	28.81	120.0 0	12.35	59.65	10.01	23.98	2.77	16.36	2.19
MAD - 16.csv	2098.2 3	4185.71	441.27	1537.4 8	200.86	28.15	122.3 8	12.19	59.95	10.08	24.75	2.94	16.30	2.26
MAD - 17.csv	2055.2 0	4077.81	428.34	1480.3 8	191.32	28.27	119.6 1	11.95	58.12	9.92	24.73	2.82	16.15	2.13
MAD - 18.csv	2046.7 9	4070.82	426.93	1486.2 7	194.87	27.90	117.6 1	12.01	58.83	9.71	24.64	2.79	15.75	2.21
MAD - 19.csv	2108.3 8	4213.08	439.20	1539.7 2	198.67	29.40	122.1 9	12.31	59.39	10.24	24.65	2.96	15.90	2.18
MAD - 2.csv	2106.0 4	4179.17	435.34	1524.3 6	200.31	28.56	118.5 9	12.39	59.94	10.10	24.98	2.96	16.22	2.26
MAD - 20.csv	2096.5 1	4179.47	437.08	1519.0 8	199.82	28.65	119.9 6	12.46	59.89	10.28	23.87	2.96	16.37	2.21
MAD - 3.csv	2106.0 7	4124.55	436.39	1528.7 8	198.51	28.91	119.3 8	12.60	61.13	10.23	24.86	2.85	16.35	2.25
MAD - 4.csv	2113.7 7	4142.62	442.89	1538.2 1	202.49	28.91	120.7 4	12.39	60.13	10.17	24.87	2.93	16.17	2.13
MAD - 5.csv	2095.2 9	4174.59	439.06	1520.0 8	198.22	28.56	119.9 8	12.34	60.23	9.92	24.79	2.81	16.57	2.13
MAD - 6.csv	2108.7 1	4188.20	438.62	1520.1 2	200.23	28.45	121.2 9	12.40	59.43	10.14	25.25	2.86	16.06	2.21
MAD - 7.csv	2151.9 4	4256.39	447.47	1559.0 1	204.03	29.09	124.7 5	12.79	62.26	10.22	25.12	2.89	16.91	2.18
MAD - 8.csv	2141.6 0	4219.44	446.82	1542.5 4	203.69	29.21	123.4 9	12.51	61.97	10.22	25.16	2.91	16.23	2.26
MAD - 9.csv	2118.5 2	4249.76	445.24	1543.4 0	199.26	29.03	122.7 8	12.88	61.21	10.12	25.36	2.99	16.97	2.23

McClure - 1.csv	1174.7 9	1886.53	176.11	583.54	69.38	24.53	47.44	5.21	25.97	4.70	12.11	1.57	9.49	1.30
McClure - 10.csv	1643.8 4	2546.67	234.04	774.32	91.45	31.92	63.63	6.91	34.95	6.52	17.23	2.11	13.18	1.91
McClure - 11.csv	1914.0 0	2942.42	256.11	802.55	89.07	45.32	59.49	6.56	34.93	6.88	17.99	2.31	15.06	2.24
McClure - 12.csv	1325.7 5	2070.08	183.80	646.52	73.66	20.04	42.64	5.38	23.73	4.74	10.21	2.52	10.01	2.06
McClure - 13.csv	1596.0 4	2462.18	218.48	700.82	77.61	32.57	53.54	5.45	27.91	5.37	13.93	1.80	10.88	1.67
McClure - 14.csv	1678.3 9	2645.06	239.74	777.64	87.11	36.06	59.53	6.50	32.99	6.13	16.60	2.08	11.99	1.80
McClure - 15.csv	-179.84	-29.72	39.25	188.96	194.73	- 456.8 7	741.9 6	58.13	- 170.3 1	32.73	-84.86	-13.98	- 100.0 3	52.55
McClure - 16.csv	1225.8 5	2156.05	217.15	765.89	97.70	28.20	67.03	7.04	36.20	6.14	15.68	1.71	10.02	1.42
McClure - 17.csv	1727.4 7	2730.35	246.75	803.28	92.93	49.28	67.35	7.41	38.91	7.11	19.66	2.50	15.41	2.33
McClure - 18.csv	-24.57	-383.16	-46.28	-830.41	44.69	-10.55	14.72	13.48	19.59	7.54	-29.86	-25.48	64.74	-6.40
McClure - 19.csv	1950.3 2	3227.02	300.08	990.99	114.48	46.83	81.52	8.75	46.18	8.67	22.41	2.90	17.46	2.39
McClure - 2.csv	1669.0 0	2548.28	225.75	742.03	82.92	34.73	58.37	6.13	33.26	6.35	16.80	2.16	13.55	2.04
McClure - 20.csv	1466.4 2	2297.69	211.18	704.25	83.33	33.79	59.62	6.41	33.17	6.38	16.98	2.13	14.19	2.33
McClure - 3.csv	1417.9 8	2219.01	203.34	664.24	74.38	33.19	54.26	5.24	27.00	4.93	12.61	1.44	8.19	1.17
McClure - 4.csv	1954.5 2	2996.58	268.36	840.02	91.00	45.88	61.18	6.62	35.51	6.43	18.09	2.34	14.76	2.15

McClure - 5.csv	1668.49	2758.05	258.17	884.22	105.35	34.78	74.63	8.04	42.02	7.68	20.01	2.37	14.93	2.16
McClure - 6.csv	1621.10	2642.60	241.63	786.65	90.26	44.74	60.64	6.49	33.14	6.12	16.55	1.94	11.78	1.60
McClure - 7.csv	1171.96	1918.93	184.79	638.25	79.13	24.96	57.74	5.80	28.97	5.06	12.43	1.49	7.98	1.16
McClure - 8.csv	1507.37	2382.01	221.43	719.70	86.45	35.78	58.92	6.33	31.64	6.03	16.38	1.96	12.48	1.82
McClure - 9.csv	1348.80	2593.45	278.38	1032.91	143.26	34.89	102.48	11.56	57.21	9.98	24.86	2.75	15.05	1.86
NIST610 - 1.csv	435.08	448.63	444.09	426.12	448.63	443.71	444.52	432.04	433.48	444.00	451.46	430.11	446.49	435.56
NIST610 - 10.csv	440.88	453.65	447.51	429.70	453.40	447.77	450.05	436.33	436.00	447.78	454.41	435.29	448.96	437.87
NIST610 - 11.csv	443.00	456.95	450.60	433.92	454.95	450.72	453.61	440.83	439.16	451.63	458.17	438.74	454.77	442.57
NIST610 - 12.csv	437.05	450.02	445.47	426.07	451.29	444.74	444.43	433.15	434.93	446.43	451.87	431.26	445.23	435.49
NIST610 - 13.csv	435.74	448.81	443.71	426.38	444.92	441.27	443.55	434.01	432.57	444.98	450.94	431.46	445.36	433.95
NIST610 - 14.csv	444.43	456.09	452.54	433.75	461.35	450.27	454.67	440.21	441.64	453.23	459.29	438.75	454.91	444.28
NIST610 - 15.csv	439.38	452.72	445.46	430.03	453.50	443.63	448.34	433.96	435.41	447.19	452.61	432.74	447.25	437.95
NIST610 - 16.csv	440.49	455.13	450.48	429.78	452.29	451.48	449.53	440.03	438.46	450.65	457.27	437.17	452.63	439.93
NIST610 - 17.csv	444.05	457.40	452.15	435.03	458.28	452.04	453.14	440.38	442.22	455.23	460.57	439.90	455.95	443.52
NIST610 - 18.csv	435.86	447.31	443.75	424.89	447.50	441.90	444.63	433.50	431.55	442.54	449.32	429.98	443.91	434.36

NIST610 - 19.csv	438.39	450.28	446.76	427.31	454.06	444.33	451.47	437.19	438.56	449.46	452.74	433.57	447.92	437.92
NIST610 - 2.csv	445.14	458.71	452.09	434.08	457.61	450.76	453.68	442.22	440.75	454.22	458.68	440.12	453.71	442.65
NIST610 - 20.csv	441.70	456.00	449.34	432.77	452.16	449.59	446.76	436.93	435.68	448.77	457.37	436.55	452.21	440.20
NIST610 - 3.csv	439.03	448.16	447.21	428.55	451.09	445.18	448.32	435.08	434.50	448.18	454.88	433.93	448.33	437.08
NIST610 - 4.csv	441.00	452.98	448.85	431.58	455.11	447.10	449.70	439.03	439.63	449.86	455.08	436.12	451.80	441.02
NIST610 - 5.csv	439.91	456.47	446.91	427.85	449.44	447.93	448.87	435.82	435.73	448.66	455.83	434.49	448.02	438.08
NIST610 - 6.csv	440.06	456.78	449.14	432.25	456.61	449.71	449.08	438.20	438.29	449.31	454.19	435.47	452.00	439.95
NIST610 - 7.csv	441.16	451.06	448.22	429.60	455.64	446.33	450.57	437.80	438.00	450.29	453.93	436.76	451.85	439.28
NIST610 - 8.csv	438.82	450.50	447.75	430.40	450.28	443.05	447.42	436.14	435.93	447.62	456.09	433.19	448.04	438.66
NIST610 - 9.csv	439.04	452.34	448.38	430.14	452.55	448.50	447.82	437.51	437.89	450.08	455.46	434.58	450.83	439.96
Standards Run 2														
401 - 1.csv	0.47	3708.36	8553.59	848.33	2986.74	439.04	43.28	365.03	44.86	253.21	48.86	132.26	15.71	86.22
401 - 10.csv	0.53	3392.22	7965.80	795.65	2766.09	409.56	41.35	345.76	42.65	238.67	45.78	122.28	14.77	81.76
401 - 11.csv	0.50	3613.21	8294.51	829.18	2898.29	422.18	42.68	356.46	44.23	249.20	47.42	128.41	15.50	84.68
401 - 12.csv	0.43	3710.95	8519.22	848.80	2961.68	434.50	43.04	364.28	45.09	253.73	49.13	133.03	15.58	85.32

401 - 13.csv	0.37	3594.78	8374.2 5	829.87	2911.0 3	421.9 4	42.45	356.3 3	44.38	247.1 1	47.84	127.9 7	15.59	85.57
401 - 14.csv	0.52	3503.42	8171.4 7	809.21	2843.2 6	417.2 9	42.55	348.2 1	42.99	243.7 3	46.83	126.6 0	15.28	83.73
401 - 15.csv	0.52	3366.07	7918.3 1	793.38	2756.9 2	412.1 5	40.69	343.6 6	42.06	237.6 4	45.68	124.8 6	15.03	81.12
401 - 16.csv	0.46	3523.85	8241.7 1	821.45	2846.6 8	419.2 4	42.74	356.0 0	43.69	242.3 4	47.13	127.6 5	15.23	84.66
401 - 17.csv	0.51	3493.62	8136.3 7	805.43	2815.3 0	416.8 2	42.06	352.7 0	43.34	247.2 0	47.02	126.8 2	15.05	83.51
401 - 18.csv	0.43	3537.23	8214.3 1	818.68	2875.7 0	427.4 5	42.24	356.9 3	43.51	247.8 4	48.11	128.2 2	15.53	84.38
401 - 19.csv	0.56	3600.04	8348.2 0	836.11	2896.0 4	427.4 4	42.75	357.6 7	44.34	249.4 9	48.51	129.7 6	15.23	86.48
401 - 2.csv	0.56	3775.72	8595.6 5	858.67	2983.1 3	440.2 8	43.34	364.3 4	44.95	257.6 8	49.62	133.1 1	15.82	87.94
401 - 20.csv	0.54	3608.77	8405.7 8	839.43	2888.1 6	423.6 4	42.47	361.8 9	44.40	248.3 3	48.52	130.0 8	15.52	84.35
401 - 21.csv	0.51	3591.69	8292.5 5	834.96	2903.3 6	427.0 4	42.34	362.3 3	43.49	248.4 7	47.64	129.3 5	15.38	84.78
401 - 22.csv	0.50	3599.20	8324.7 9	831.71	2894.3 2	425.6 5	42.21	361.9 5	44.14	248.5 2	47.28	129.7 4	15.31	85.31
401 - 23.csv	0.41	3559.45	8303.2 1	828.99	2869.7 9	425.6 4	42.42	358.0 9	43.49	244.5 0	47.57	128.7 4	15.74	85.19
401 - 24.csv	0.40	3634.04	8419.8 8	840.57	2890.4 6	428.4 4	42.93	359.8 7	44.06	247.1 3	47.77	130.4 9	15.68	85.10
401 - 25.csv	0.44	3495.42	8148.9 8	810.17	2833.2 3	415.0 5	41.44	346.9 1	43.20	242.4 1	47.95	128.2 6	15.06	84.98
401 - 26.csv	0.53	3609.46	8406.5 3	829.29	2890.3 6	421.3 2	42.77	358.9 7	43.61	249.7 3	47.95	129.3 4	15.63	84.03

401 - 27.csv	0.41	3726.80	8546.6 8	853.62	2958.1 4	441.2 4	43.61	365.8 8	45.26	254.1 0	48.71	131.4 2	15.77	89.33
401 - 28.csv	0.48	3656.97	8451.1 0	839.99	2930.4 3	429.3 8	42.85	360.8 3	44.02	249.5 7	48.04	128.2 7	15.29	86.20
401 - 29.csv	0.48	3692.30	8467.7 5	854.28	2958.0 0	430.5 7	43.13	370.5 8	44.46	252.2 3	48.48	132.3 9	16.07	86.71
401 - 3.csv	0.42	3492.99	8116.8 3	821.53	2844.7 7	417.9 8	42.21	353.9 8	43.26	242.8 7	47.01	127.7 4	15.18	81.83
401 - 30.csv	0.52	3688.27	8544.9 9	852.04	2944.5 8	432.4 5	43.07	364.9 0	45.05	251.7 7	48.41	130.8 2	15.59	86.10
401 - 4.csv	0.39	3488.99	8115.1 3	817.41	2837.1 5	420.3 8	42.42	352.4 8	43.93	242.9 4	46.98	127.5 4	15.27	82.91
401 - 5.csv	0.49	3473.34	8144.8 8	813.23	2820.9 5	412.9 9	41.80	351.4 3	42.92	241.4 7	46.70	127.9 9	15.23	83.72
401 - 6.csv	0.54	3586.40	8373.4 1	837.03	2891.6 0	426.9 5	42.00	364.8 0	43.95	248.8 2	47.69	129.8 6	15.43	85.48
401 - 7.csv	0.55	3739.54	8663.5 7	861.84	2984.3 3	437.1 6	43.95	367.3 0	45.38	257.6 7	49.42	133.8 0	15.82	88.25
401 - 8.csv	0.49	3615.38	8465.9 4	842.81	2917.5 2	419.3 2	42.88	362.7 7	44.34	250.7 1	48.16	131.1 1	15.85	85.41
401 - 9.csv	0.47	3477.87	8083.5 1	809.03	2844.0 4	417.3 0	40.95	350.1 4	42.53	241.7 8	46.73	126.5 6	15.15	83.50
MAD - 1.csv	17.66	2119.24	4429.7 4	445.78	1553.2 2	201.9 6	29.02	126.4 9	12.65	60.32	10.26	25.14	2.83	17.21
MAD - 2.csv	18.20	2131.73	4415.9 2	443.07	1548.9 2	206.6 0	29.37	124.9 2	12.40	62.53	10.21	25.59	2.95	16.74
MAD - 3.csv	17.77	2111.36	4391.3 5	440.63	1538.4 9	202.0 2	28.82	123.2 0	12.41	59.37	10.13	25.03	2.89	15.69
MAD - 4.csv	18.22	2132.80	4432.6 6	443.40	1557.0 8	200.2 8	29.10	122.9 1	12.28	60.89	10.33	25.72	2.87	16.80

MAD - 5.csv	17.97	2106.11	4388.4 3	440.42	1516.1 4	195.9 0	28.88	121.6 6	12.28	59.54	10.15	25.32	2.94	16.00
MAD - 6.csv	18.00	2107.01	4390.6 5	440.25	1527.8 1	199.9 5	29.08	122.2 0	12.53	60.49	10.02	25.71	2.92	16.79
MAD - 7.csv	18.09	2103.30	4455.4 9	443.59	1544.9 6	197.8 6	29.19	121.0 7	12.44	60.91	10.25	25.35	2.87	16.85
MAD - 8.csv	17.68	2104.47	4365.0 4	437.93	1532.2 4	199.9 2	28.50	119.7 9	12.40	59.47	10.04	24.67	2.92	16.41
MAD - 9.csv	17.78	2090.81	4365.7 8	439.04	1526.8 8	197.2 1	28.55	120.6 3	12.36	59.94	10.01	24.06	2.82	15.89
MAD - 10.csv	17.91	2092.44	4398.3 6	440.34	1528.0 0	199.5 6	28.29	120.8 4	12.49	59.89	10.09	25.04	2.88	16.55
MAD - 11.csv	17.72	2083.55	4373.0 9	432.51	1521.9 1	197.4 0	28.40	119.3 0	12.35	59.93	9.92	24.65	2.95	16.10
MAD - 12.csv	18.06	2101.53	4383.9 3	438.26	1516.5 5	197.1 1	28.67	119.3 3	12.36	59.38	10.12	24.97	2.86	16.59
MAD - 13.csv	18.46	2122.42	4470.0 6	443.42	1557.6 8	201.6 0	29.08	123.0 8	12.70	60.04	10.19	25.30	2.90	17.17
MAD - 14.csv	17.39	2097.43	4384.8 1	434.17	1515.7 6	200.2 9	28.09	121.0 4	12.50	59.99	10.24	24.48	2.88	16.82
MAD - 15.csv	18.02	2089.86	4373.3 3	437.88	1520.7 8	198.1 0	28.31	121.2 4	12.22	60.18	10.09	24.29	2.85	16.42
MAD - 16.csv	17.46	2058.17	4321.8 7	431.07	1501.5 0	195.8 5	28.23	122.2 0	12.31	59.69	10.01	23.98	2.86	16.28
MAD - 17.csv	17.45	2090.35	4397.2 7	436.77	1527.6 1	197.7 7	28.12	121.5 9	12.52	60.56	10.23	24.87	2.81	16.65
MAD - 18.csv	17.90	2082.29	4344.8 3	437.14	1518.4 2	197.1 8	27.38	119.5 0	12.09	60.51	9.85	25.02	2.81	16.69
MAD - 19.csv	17.36	2090.54	4361.3 9	438.00	1520.5 4	197.3 6	28.19	122.0 2	12.41	59.95	9.97	24.65	2.93	15.77

MAD - 20.csv	17.32	2090.71	4369.8 6	439.23	1526.3 5	196.9 7	28.43	121.3 5	12.25	59.55	10.06	24.91	2.76	16.34
MAD - 21.csv	18.33	2078.60	4364.9 0	434.50	1512.9 8	196.0 0	28.29	119.5 4	12.30	59.58	10.16	24.96	2.98	16.85
MAD - 22.csv	17.20	2078.40	4347.9 5	435.97	1503.8 3	195.6 0	28.36	120.9 0	12.48	58.72	9.95	24.33	2.96	16.30
MAD - 23.csv	17.37	2091.88	4381.5 4	437.49	1515.1 6	199.7 7	28.91	121.3 0	12.45	59.28	10.34	24.32	2.90	17.11
MAD - 24.csv	17.97	2096.59	4380.9 6	441.37	1519.7 6	200.3 4	28.00	119.9 5	12.63	60.17	9.93	25.64	2.92	15.43
MAD - 25.csv	17.41	2100.52	4432.2 3	439.55	1532.7 2	200.8 0	28.95	122.3 0	12.36	60.14	10.22	24.95	2.92	16.50
MAD - 26.csv	17.07	2083.24	4335.7 9	432.08	1510.9 8	195.9 3	28.42	120.7 7	12.33	60.59	10.33	24.57	2.90	16.15
MAD - 27.csv	18.18	2098.08	4406.9 8	442.16	1530.4 8	200.8 6	28.65	119.6 1	12.42	60.48	9.86	24.93	2.93	16.29
MAD - 28.csv	17.11	2083.87	4372.3 9	439.09	1516.9 4	198.0 3	28.50	120.6 5	12.39	60.61	10.07	24.25	3.02	16.56
MAD - 29.csv	17.50	2088.96	4375.4 3	438.33	1534.7 3	200.4 2	28.43	121.1 5	12.31	59.67	10.25	25.07	2.94	15.96
MAD - 30.csv	17.28	2073.59	4377.5 1	439.87	1531.7 5	197.4 6	28.69	122.3 4	12.60	59.06	9.97	24.65	2.91	16.15
McClure - 1.csv	2.26	1334.32	2087.2 9	192.32	647.44	79.25	25.13	55.13	6.05	31.70	5.78	16.05	2.09	12.12
McClure - 10.csv	3.78	2286.28	3330.2 0	263.98	792.71	91.00	34.16	73.27	8.64	51.98	11.43	35.50	4.96	34.55
McClure - 11.csv	1.89	1268.28	2115.3 6	207.10	736.77	92.04	25.58	69.28	7.46	38.64	6.92	18.32	2.17	12.88
McClure - 12.csv	2.26	1474.62	2451.7 3	237.99	847.36	107.9 9	29.98	79.25	8.69	44.59	8.27	21.74	2.60	15.21

McClure - 13.csv	3.71	1744.60	2793.63	252.82	825.83	94.02	41.31	65.74	7.07	38.29	7.14	18.98	2.31	14.81
McClure - 14.csv	3.48	1492.99	2398.49	219.67	721.47	84.29	35.02	57.15	6.20	32.56	6.09	16.34	1.96	12.27
McClure - 15.csv	5.65	1480.36	2646.31	267.05	919.77	116.10	35.62	81.65	8.86	45.63	8.19	20.66	2.41	13.87
McClure - 16.csv	7.18	1621.78	2988.50	292.90	1018.37	128.25	38.99	89.78	9.80	51.77	9.03	23.07	2.63	14.54
McClure - 17.csv	2.02	1243.57	2242.85	228.67	807.73	101.60	27.57	73.56	7.74	40.30	7.02	17.01	2.18	11.29
McClure - 18.csv	2.53	1283.43	2338.30	237.47	843.84	108.54	30.52	76.89	8.24	43.27	7.46	18.71	2.28	11.79
McClure - 19.csv	3.82	1990.77	3053.33	277.75	911.11	106.58	55.57	74.83	8.04	44.45	8.11	22.60	2.83	18.73
McClure - 2.csv	3.45	1347.12	2272.05	224.19	791.89	99.65	27.80	69.58	7.51	37.44	6.87	16.99	2.10	11.97
McClure - 20.csv	3.73	1888.37	2959.56	262.45	866.50	101.97	54.92	71.79	7.69	40.68	7.71	20.74	2.76	17.53
McClure - 21.csv	2.13	1269.43	1949.87	178.11	588.57	67.86	25.09	47.61	4.94	24.14	4.37	11.56	1.16	7.36
McClure - 22.csv	1.62	1234.79	1878.22	167.82	534.73	59.56	23.62	43.00	4.25	21.19	3.85	9.98	1.20	7.13
McClure - 23.csv	4.61	1657.28	2729.09	251.93	836.52	96.54	36.53	69.14	7.39	37.93	7.02	19.26	2.35	14.77
McClure - 24.csv	3.52	1611.90	2664.62	248.48	823.35	95.74	36.16	67.20	7.28	38.01	7.00	19.03	2.37	13.73
McClure - 25.csv	0.59	1684.46	2578.53	227.92	741.19	80.62	38.47	55.06	5.77	29.93	5.40	14.13	1.62	10.27
McClure - 26.csv	5.30	1961.63	3373.46	304.58	1014.51	120.03	47.52	82.40	8.79	45.13	8.23	21.76	2.62	15.59

McClure - 27.csv	2.07	1458.79	2153.20	194.36	642.40	73.56	26.06	50.32	5.20	26.40	4.85	12.35	1.40	8.15
McClure - 28.csv	6.13	1866.63	2956.73	266.55	878.29	100.44	35.37	71.04	7.38	38.77	6.99	17.76	2.12	12.21
McClure - 29.csv	2.71	1432.43	2340.80	221.41	744.93	89.24	33.98	61.55	6.90	34.56	6.56	17.92	2.31	14.26
McClure - 3.csv	3.37	1452.42	2406.81	230.05	793.92	98.93	29.65	70.25	7.34	38.99	6.91	17.57	2.14	12.86
McClure - 30.csv	3.97	1611.88	2671.18	249.01	841.61	97.82	38.35	69.85	7.64	41.26	7.40	20.21	2.48	16.56
McClure - 4.csv	3.52	1198.32	2065.01	205.26	726.69	91.64	25.93	64.86	6.92	33.53	6.17	15.85	1.80	10.06
McClure - 5.csv	5.31	1982.83	3377.17	305.41	1004.58	119.03	49.00	83.55	9.06	47.36	8.83	23.17	2.98	17.94
McClure - 6.csv	5.53	2034.41	3489.11	316.10	1036.93	124.47	51.60	85.10	9.43	48.70	8.94	24.06	3.02	18.51
McClure - 7.csv	6.46	1624.73	2449.07	213.22	686.06	77.37	34.09	53.97	5.49	26.74	5.03	13.34	1.65	9.84
McClure - 8.csv	3.75	1334.46	1901.53	160.21	504.66	54.00	25.48	39.59	3.58	18.24	3.50	9.51	1.17	7.36
McClure - 9.csv	4.19	2300.06	3387.19	268.41	810.72	93.22	34.31	74.29	9.17	54.57	11.59	36.93	5.22	35.75
NIST610 - 1.csv	450.91	442.78	454.13	449.01	432.76	456.07	449.38	447.39	439.51	439.69	450.72	454.14	438.21	450.69
NIST610 - 2.csv	444.36	436.99	451.75	442.95	427.05	449.23	444.54	449.36	434.23	434.16	447.12	452.62	431.31	449.19
NIST610 - 3.csv	447.03	442.17	454.60	451.51	431.26	455.23	448.00	450.52	438.70	437.39	450.66	459.84	439.09	452.08
NIST610 - 4.csv	446.97	437.84	451.44	448.09	428.84	452.67	447.35	450.06	435.67	436.78	447.44	452.83	432.13	447.97

NIST610 - 5.csv	447.05	437.58	450.59	446.74	426.40	446.69	443.07	448.17	434.20	432.80	445.14	453.39	431.39	447.00
NIST610 - 6.csv	456.06	442.63	455.59	451.20	433.87	458.07	447.26	448.49	439.85	441.49	453.14	457.69	436.92	453.14
NIST610 - 7.csv	443.91	437.44	450.94	446.10	427.02	449.07	446.63	447.85	435.43	434.31	445.92	452.80	433.14	449.49
NIST610 - 8.csv	448.24	442.64	455.11	451.04	433.08	455.62	449.48	450.32	438.19	439.78	452.19	459.15	438.34	450.50
NIST610 - 9.csv	451.07	440.58	453.84	450.90	430.52	456.85	448.52	448.71	438.42	437.40	449.40	458.03	437.13	450.95
NIST610 - 10.csv	447.52	439.43	452.13	447.58	429.43	452.64	446.45	448.62	436.39	436.53	448.57	453.63	433.08	448.97
NIST610 - 11.csv	447.84	439.22	453.13	446.95	430.50	452.13	447.76	450.53	435.89	438.21	449.21	456.09	433.70	451.14
NIST610 - 12.csv	448.36	440.83	452.89	447.24	429.50	450.23	448.16	450.62	437.29	435.69	448.77	454.06	435.22	448.91
NIST610 - 13.csv	444.02	439.65	452.52	445.68	429.73	452.46	445.69	449.51	437.00	438.28	449.49	452.23	434.22	447.84
NIST610 - 14.csv	445.91	440.42	453.55	444.29	430.34	453.13	444.55	445.78	435.45	435.69	448.53	450.86	434.07	452.32
NIST610 - 15.csv	445.09	438.42	451.64	445.80	428.45	454.79	446.41	448.17	437.71	436.42	448.03	454.96	437.40	448.00
NIST610 - 16.csv	451.85	441.70	454.50	451.63	431.71	456.68	450.72	449.71	440.82	437.75	450.10	458.54	437.60	452.16
NIST610 - 17.csv	443.78	438.84	451.15	441.84	427.92	450.99	441.46	443.24	432.46	433.90	447.15	446.85	430.78	448.29
NIST610 - 18.csv	448.03	441.21	454.89	449.85	432.15	451.86	447.30	451.18	438.38	440.25	450.88	455.95	435.17	451.76
NIST610 - 19.csv	449.81	439.99	453.66	451.29	430.23	451.48	448.88	451.53	437.61	436.37	450.04	458.02	436.56	450.47

NIST610 - 20.csv	448.86	440.03	452.37	447.72	429.77	452.2 2	447.9 2	447.0 3	435.6 6	437.6 9	447.9 8	455.7 5	434.7 8	449.5 3
NIST610 - 21.csv	449.35	439.47	451.57	448.11	429.77	453.5 7	447.1 1	450.9 5	436.5 8	436.1 3	447.6 1	453.9 0	432.5 8	449.5 6
NIST610 - 22.csv	450.38	440.59	454.54	450.38	430.30	452.7 2	447.5 7	451.7 9	438.3 7	437.9 5	450.5 2	457.3 3	436.0 3	450.4 8
NIST610 - 23.csv	449.06	439.03	451.72	448.86	428.28	452.9 7	446.7 6	448.7 1	437.3 4	435.7 6	447.2 1	454.7 9	435.5 1	449.4 7
NIST610 - 24.csv	450.56	440.96	454.28	450.74	431.80	457.5 4	449.3 5	453.2 1	438.4 1	438.2 7	450.8 4	459.4 1	437.4 2	450.4 6
NIST610 - 25.csv	448.97	441.32	454.48	448.09	429.97	451.1 2	446.7 7	449.5 1	435.7 9	437.5 5	449.7 5	457.4 2	434.8 2	452.2 6
NIST610 - 26.csv	443.68	438.64	451.54	444.72	430.06	450.8 2	444.0 1	443.0 4	435.5 0	436.4 4	448.2 1	451.7 0	432.3 1	447.6 5
NIST610 - 27.csv	448.48	439.68	451.00	446.53	429.20	453.8 2	447.0 5	447.9 2	437.4 4	436.7 9	449.1 6	453.8 1	435.5 2	450.1 7
NIST610 - 28.csv	447.97	440.44	455.15	449.69	430.93	453.5 5	447.8 2	448.3 2	438.0 5	437.3 0	448.8 9	454.3 3	435.9 2	449.9 2
NIST610 - 29.csv	444.34	436.59	450.62	443.95	426.81	449.9 7	444.4 8	446.1 4	433.8 9	434.4 5	447.1 8	452.1 8	431.6 6	447.2 0
NIST610 - 30.csv	450.54	443.41	455.38	451.48	433.19	455.8 2	449.5 6	453.6 1	439.7 7	439.5 5	450.8 2	457.7 1	438.0 0	452.8 0

APPENDIX E: APATITE U-PB GEOCHRONOLOGY DATA

Apatite 1				
Sample	238U/206Pb	238U/206Pb	207Pb/206Pb	207Pb/206Pb
801_apatite - 10	11.3837	0.7137	0.1251	0.0187
801_apatite - 11	6.3440	0.4284	0.3452	0.0232
801_apatite - 12	6.5094	0.8060	0.2787	0.0530
801_apatite - 13	10.9971	1.4938	0.2428	0.0762
801_apatite - 14	12.2172	1.3922	0.1052	0.0352
801_apatite - 15	11.4559	1.0209	0.1324	0.0319
801_apatite - 16	13.4233	1.6021	0.2154	0.0520
801_apatite - 17	9.5637	1.8691	0.1956	0.0490
801_apatite - 18	12.0728	0.8208	0.1265	0.0201
801_apatite - 19	11.7373	0.8458	0.1520	0.0323
801_apatite - 2	9.1394	0.8092	0.1843	0.0228
801_apatite - 20	7.5228	0.5296	0.2195	0.0280
801_apatite - 21	12.1306	1.0394	0.1350	0.0279
801_apatite - 23	10.6634	0.5959	0.1343	0.0236
801_apatite - 24	4.4437	0.4488	0.3429	0.0512
801_apatite - 25	4.2226	1.5252	0.3921	0.1512
801_apatite - 26	8.8110	1.4936	0.2159	0.0673
801_apatite - 27	3.4650	0.4425	0.4101	0.0244
801_apatite - 28	12.1381	0.6296	0.0945	0.0122
801_apatite - 3	9.7265	0.6191	0.1296	0.0203
801_apatite - 30	12.0612	0.8796	0.1302	0.0271
801_apatite - 31	12.8889	0.7205	0.1098	0.0146
801_apatite - 32	11.9035	0.8272	0.1234	0.0229
801_apatite - 33	11.3132	0.6454	0.1095	0.0148
801_apatite - 34	10.2769	0.7171	0.1518	0.0231
801_apatite - 35	10.1531	0.5218	0.1388	0.0156
801_apatite - 36	11.6506	0.6044	0.1106	0.0128
801_apatite - 37	11.8302	0.6050	0.1070	0.0123
801_apatite - 38	11.3935	0.6859	0.1099	0.0165
801_apatite - 4	10.5286	0.5781	0.1624	0.0181
801_apatite - 42	11.6999	1.0859	0.1814	0.0367
801_apatite - 43	11.0317	0.8013	0.1646	0.0259
801_apatite - 44	12.5546	1.1310	0.1402	0.0377
801_apatite - 47	11.6821	1.0905	0.1031	0.0277
801_apatite - 48	8.2875	1.2535	0.1714	0.0543
801_apatite - 5	10.7026	0.7398	0.1460	0.0220
801_apatite - 50	11.3195	1.2206	0.1730	0.0406
801_apatite - 51	12.3106	0.7783	0.1243	0.0206

801_apatite-52	5.5255	0.5159	0.2409	0.0253
801_apatite-53	6.3801	0.5048	0.1994	0.0286
801_apatite - 54	10.9077	1.2997	0.1610	0.0482
801_apatite-55	14.5279	0.5977	0.0688	0.0067
801_apatite - 6	10.0557	0.5979	0.1603	0.0195
801_apatite - 7	10.3379	0.9052	0.1561	0.0312
801_apatite - 9	12.1531	0.7570	0.1254	0.0243
973_apatite-1	4.0314	0.6129	0.5559	0.0192
973_apatite - 10	9.8975	1.3105	0.1739	0.0525
973_apatite-11	6.7993	0.8347	0.2953	0.0646
973_apatite-12	1.6948	0.2030	0.6310	0.0268
973_apatite-13	3.2865	0.4452	0.4136	0.0594
973_apatite - 14	8.8267	0.6248	0.2330	0.0318
973_apatite-15	1.1870	0.1322	0.5598	0.0506
973_apatite-16	4.1360	0.6543	0.5138	0.0815
973_apatite-17	9.8685	0.6473	0.1725	0.0247
973_apatite-18	2.3556	0.5276	0.6621	0.2013
973_apatite-19	5.3131	0.4220	0.3959	0.0499
973_apatite-2	8.9977	0.8410	0.2542	0.0410
973_apatite-20	3.2485	0.2301	0.5589	0.0233
973_apatite-21	2.4245	0.4098	0.5574	0.0837
973_apatite-23	1.5191	0.2198	0.5532	0.0708
973_apatite-24	9.6617	0.5987	0.1858	0.0282
973_apatite - 25	1.7581	0.0868	0.6633	0.0312
973_apatite-27	8.8763	0.8147	0.2487	0.0408
973_apatite-28	10.7179	0.7929	0.1705	0.0286
973_apatite - 29	10.4654	0.7067	0.2059	0.0312
973_apatite-3	6.9949	0.4569	0.2697	0.0251
973_apatite-30	11.9551	0.4349	0.0762	0.0084
973_apatite-31	9.7937	0.6828	0.2511	0.0323
973_apatite-32	12.3435	0.5349	0.1064	0.0130
973_apatite-33	6.5061	0.4785	0.2918	0.0319
973_apatite-35	6.9549	0.8633	0.3367	0.0702
973_apatite-36	11.7438	0.7151	0.1147	0.0179
973_apatite-37	7.0340	1.2329	0.2485	0.0868
973_apatite-38	11.4201	0.9977	0.1308	0.0371
973_apatite - 39	8.4175	0.9172	0.2664	0.0453
973_apatite-4	1.4562	0.7242	0.6600	0.2601
973_apatite-40	1.7068	0.1880	0.7514	0.0298
973_apatite-41	8.2832	0.5576	0.2409	0.0365
973_apatite - 42	0.7059	0.2260	0.7484	0.0948
973_apatite-43	4.4141	0.3241	0.3314	0.0347
973_apatite-44	10.1248	0.5642	0.1841	0.0246

973_apatite-45	11.2303	1.0864	0.1695	0.0368
973_apatite - 46	4.6324	1.0082	0.4009	0.0750
973_apatite-47	6.7185	0.3150	0.2909	0.0178
973_apatite-48	0.1306	0.0288	0.8846	0.0098
973_apatite - 49	5.3060	0.6217	0.5379	0.0619
973_apatite-5	6.7852	0.5628	0.2464	0.0445
973_apatite-50	9.1344	0.6041	0.1679	0.0223
973_apatite-51	6.8235	0.5775	0.2877	0.0463
973_apatite - 52	2.9138	0.7122	0.6367	0.0400
973_apatite-53	11.0809	0.9867	0.1149	0.0284
973_apatite-55	2.0387	0.2125	0.6385	0.0334
973_apatite-56	9.6361	0.9070	0.1969	0.0296
973_apatite-57	9.7526	0.6555	0.1694	0.0256
973_apatite-58	1.3876	0.1052	0.5618	0.0200
973_apatite-59	2.6395	0.3592	0.3602	0.0410
973_apatite-6	1.8279	0.2700	0.4079	0.0751
973_apatite-60	7.8112	0.4572	0.2100	0.0235
973_apatite-7	10.5311	0.6685	0.1212	0.0201
973_apatite-8	0.5783	0.2219	0.4560	0.1110
1488 - 1	6.4573	0.3192	0.3390	0.0167
1488 - 10	11.1412	0.9437	0.1276	0.0273
1488 - 11	1.5849	0.4040	0.4853	0.1177
1488 - 12	9.5369	0.7220	0.2035	0.0346
1488 - 13	6.5632	1.5121	0.5095	0.0618
1488 - 14	3.3370	0.2663	0.5668	0.0399
1488-15	7.1434	0.4057	0.3965	0.0358
1488 - 16	1.3067	0.3113	0.5382	0.1064
1488 - 17	11.9071	1.0748	0.1485	0.0370
1488 - 18	8.1300	0.7483	0.2401	0.0553
1488 - 19	5.1468	0.2373	0.0886	0.0041
1488 - 2	5.1533	1.6265	0.2368	0.0246
1488 - 20	5.5833	0.2055	0.0957	0.0048
1488 - 21	5.2378	0.1825	0.1003	0.0043
1488 - 22	5.2578	0.1962	0.1047	0.0079
1488 - 23	9.0076	0.6524	0.0843	0.0088
1488 - 24	4.4970	1.0232	0.2342	0.0064
1488 - 27	5.2517	0.1886	0.0996	0.0056
1488 - 28	5.0773	0.1854	0.1137	0.0074
1488 - 29	5.1537	0.2072	0.0952	0.0046
1488 - 3	1.3085	0.1072	0.2447	0.0059
1488 - 30	2.3654	0.2859	0.1934	0.0088
1488 - 31	4.7570	0.2207	0.1208	0.0057
1488 - 32	4.8674	0.1674	0.0971	0.0036

1488 - 33	4.7070	0.2328	0.1190	0.0097
1488 - 34	5.0972	0.1881	0.1102	0.0046
1488 - 35	3.6326	0.3738	0.2472	0.0438
1488 - 36	5.6163	0.2946	0.1024	0.0113
1488 - 37	5.2176	0.2128	0.1069	0.0045
1488 - 38	2.0326	0.1684	0.3319	0.0173
1488 - 4	6.7295	0.8593	0.1275	0.0169
1488 - 40	5.0106	0.1678	0.0977	0.0047
1488 - 41	5.3561	0.1887	0.0991	0.0039
1488 - 42	4.8013	0.3908	0.1256	0.0216
1488 - 43	5.2561	0.1743	0.0839	0.0026
1488 - 44	5.0396	0.5107	0.0910	0.0099
1488 - 45	4.6938	0.2554	0.0944	0.0105
1488 - 46	2.5586	2.1320	0.8300	0.5059
1488 - 47	3.1719	0.2368	0.2058	0.0234
1488 - 48	6.2999	2.5387	0.2242	0.0277
1488 - 49	4.7028	0.2600	0.1124	0.0084
1488 - 5	5.2129	0.2866	0.0862	0.0046
1488 - 51	5.2515	0.2202	0.1068	0.0077
1488 - 52	3.4797	0.2813	0.3202	0.0372
1488 - 53	5.4925	0.2339	0.1168	0.0083
1488 - 54	5.4765	0.2086	0.1021	0.0060
1488 - 55	5.2438	0.3338	0.1386	0.0234
1488 - 56	8.4939	0.9011	0.2111	0.0151
1488 - 57	5.5191	0.1931	0.0941	0.0043
1488 - 6	4.1293	0.2371	0.1235	0.0091
1488 - 63	4.5308	1.3183	0.3147	0.0664
1488 - 64	4.1387	0.6088	0.1405	0.0200
1488 - 65	2.5124	0.2432	0.1851	0.0074
1488 - 66	5.7628	0.5449	0.0943	0.0073
1488 - 67	9.5418	1.6790	0.1324	0.0860
1488 - 68	3.0431	0.1918	0.1678	0.0144
1488 - 69	5.5690	0.2392	0.1054	0.0081
1488 - 7	3.8418	0.1727	0.1073	0.0089
1488 - 70	5.2457	0.1999	0.0928	0.0052
1488 - 71	5.7818	0.7446	0.1334	0.0145
1488 - 72	0.8239	0.1505	0.3720	0.0448
1488 - 73	4.9245	0.2280	0.1435	0.0168
1488 - 74	3.2454	0.1954	0.1338	0.0032
1488 - 8	5.1574	0.2020	0.0918	0.0070
1488 - 9	4.1510	0.4420	0.1497	0.0178
Apatite 2				
852_apatite - 1	4.8320	0.2896	0.1697	0.0218

852_apatite - 10	4.9932	0.2137	0.1218	0.0034
852_apatite - 11	5.0142	0.1707	0.1296	0.0038
852_apatite - 12	5.0565	0.2183	0.1338	0.0038
852_apatite - 13	4.9213	0.1768	0.1455	0.0065
852_apatite - 14	5.1407	0.1690	0.1193	0.0020
852_apatite - 15	5.0547	0.1669	0.1219	0.0033
852_apatite - 16	5.0655	0.1706	0.1446	0.0040
852_apatite - 17	4.8837	0.1728	0.1234	0.0040
852_apatite - 18	4.8071	0.1641	0.1395	0.0052
852_apatite - 19	5.4860	0.1801	0.1104	0.0028
852_apatite - 2	4.9215	0.2915	0.1604	0.0167
852_apatite - 20	5.3063	0.2263	0.1437	0.0042
852_apatite - 21	4.7259	0.1682	0.1500	0.0084
852_apatite - 22	5.1674	0.1669	0.1152	0.0019
852_apatite - 23	4.1489	0.1691	0.2316	0.0161
852_apatite - 24	5.7071	0.2092	0.1982	0.0064
852_apatite - 25	5.1816	0.2830	0.1234	0.0093
852_apatite - 26	5.2326	0.1856	0.1060	0.0024
852_apatite - 27	5.0196	0.2286	0.1133	0.0033
852_apatite - 28	4.9268	0.2081	0.1287	0.0120
852_apatite - 3	5.1887	0.1686	0.0967	0.0017
852_apatite - 30	4.9444	0.1630	0.1119	0.0040
852_apatite - 31	6.1645	0.4548	0.1141	0.0032
852_apatite - 32	5.1412	0.1656	0.0897	0.0013
852_apatite - 33	5.2995	0.2502	0.0968	0.0016
852_apatite - 34	4.8913	0.1549	0.1444	0.0024
852_apatite - 36	4.9292	0.1729	0.1150	0.0036
852_apatite - 37	3.9699	0.1729	0.2820	0.0137
852_apatite - 38	5.1022	0.1643	0.1172	0.0021
852_apatite - 39	4.8262	0.1593	0.1223	0.0027
852_apatite - 4	5.2013	0.1670	0.1237	0.0023
852_apatite - 40	5.1754	0.1635	0.1339	0.0023
852_apatite - 43	4.5002	0.1475	0.1572	0.0024
852_apatite - 44	4.7308	0.2482	0.1682	0.0091
852_apatite - 45	5.0782	0.1822	0.1205	0.0058
852_apatite - 46	5.3010	0.2124	0.1454	0.0053
852_apatite - 47	4.5323	0.1668	0.2355	0.0066
852_apatite - 49	5.3411	0.1832	0.0979	0.0028
852_apatite - 5	4.7191	0.1588	0.1772	0.0032
852_apatite - 50	4.9637	0.1831	0.1169	0.0034
852_apatite - 51	5.8035	0.2405	0.1038	0.0029
852_apatite - 52	5.0948	0.1737	0.1665	0.0034
852_apatite - 53	5.3569	0.1732	0.1140	0.0012

852_apatite - 54	5.1754	0.1678	0.1258	0.0025
852_apatite - 55	5.0747	0.1651	0.1343	0.0020
852_apatite - 56	4.8117	0.1688	0.1716	0.0047
852_apatite - 57	5.1178	0.1619	0.0948	0.0012
852_apatite - 58	4.5352	0.2121	0.1565	0.0054
852_apatite - 59	4.9288	0.1768	0.1336	0.0039
852_apatite - 6	5.4030	0.1941	0.1117	0.0059
852_apatite - 60	4.6159	0.1489	0.1309	0.0035
852_apatite - 61	5.0895	0.1626	0.1183	0.0023
852_apatite - 62	5.3377	0.1921	0.1129	0.0056
852_apatite - 63	4.6344	0.2029	0.1250	0.0044
852_apatite - 7	5.5231	0.1952	0.1229	0.0032
852_apatite - 8	5.3628	0.1903	0.1069	0.0046
852_apatite - 9	4.9998	0.1848	0.1505	0.0051
973_apatite - 1	5.1468	0.2373	0.0886	0.0041
973_apatite - 10	5.1533	1.6265	0.2368	0.0246
973_apatite - 11	5.5833	0.2056	0.0957	0.0048
973_apatite - 12	5.2378	0.1825	0.1003	0.0043
973_apatite - 13	5.2578	0.1962	0.1047	0.0079
973_apatite - 14	9.0076	0.6524	0.0843	0.0088
973_apatite - 15	4.4970	1.0232	0.2342	0.0064
973_apatite - 16	5.2517	0.1886	0.0996	0.0056
973_apatite - 17	5.0773	0.1854	0.1137	0.0074
973_apatite - 18	5.1537	0.2072	0.0952	0.0046
973_apatite - 19	1.3085	0.1072	0.2447	0.0059
973_apatite - 2	2.3654	0.2859	0.1934	0.0088
973_apatite - 20	4.7570	0.2207	0.1208	0.0057
973_apatite - 21	4.8674	0.1674	0.0971	0.0036
973_apatite - 23	4.7070	0.2328	0.1190	0.0097
973_apatite - 24	5.0972	0.1881	0.1102	0.0046
973_apatite - 25	3.6326	0.3738	0.2472	0.0438
973_apatite - 27	5.6163	0.2946	0.1024	0.0113
973_apatite - 28	5.2176	0.2128	0.1069	0.0045
973_apatite - 29	2.0326	0.1684	0.3319	0.0173
973_apatite - 3	6.7295	0.8593	0.1275	0.0169
973_apatite - 30	5.0106	0.1678	0.0977	0.0047
973_apatite - 31	5.3561	0.1887	0.0991	0.0039
973_apatite - 32	4.8013	0.3908	0.1256	0.0216
973_apatite - 33	5.2561	0.1743	0.0839	0.0026
973_apatite - 35	5.0396	0.5107	0.0910	0.0099
973_apatite - 36	4.6938	0.2554	0.0944	0.0105
973_apatite - 37	2.5586	2.1320	0.8300	0.5059
973_apatite - 38	3.1719	0.2368	0.2058	0.0234

973_apatite - 39	6.2999	2.5387	0.2242	0.0277
973_apatite - 4	4.7028	0.2600	0.1124	0.0084
973_apatite - 40	5.2129	0.2866	0.0862	0.0046
973_apatite - 41	5.2515	0.2202	0.1068	0.0077
973_apatite - 42	3.4797	0.2813	0.3202	0.0372
973_apatite - 43	5.4925	0.2339	0.1168	0.0083
973_apatite - 44	5.4765	0.2086	0.1021	0.0060
973_apatite - 45	5.2438	0.3338	0.1386	0.0234
973_apatite - 46	8.4939	0.9011	0.2111	0.0151
973_apatite - 47	5.5191	0.1931	0.0941	0.0043
973_apatite - 48	4.1293	0.2371	0.1235	0.0091
973_apatite - 49	4.5308	1.3183	0.3147	0.0664
973_apatite - 5	4.1387	0.6088	0.1405	0.0200
973_apatite - 50	2.5124	0.2432	0.1851	0.0074
973_apatite - 51	5.7628	0.5449	0.0943	0.0073
973_apatite - 52	9.5418	1.6790	0.1324	0.0860
973_apatite - 53	3.0431	0.1918	0.1678	0.0144
973_apatite - 55	5.5690	0.2392	0.1054	0.0081
973_apatite - 56	3.8418	0.1727	0.1073	0.0089
973_apatite - 57	5.2457	0.1999	0.0928	0.0052
973_apatite - 58	5.7818	0.7446	0.1334	0.0145
973_apatite - 59	0.8239	0.1505	0.3720	0.0448
973_apatite - 6	4.9245	0.2280	0.1435	0.0168
973_apatite - 60	3.2454	0.1954	0.1338	0.0032
973_apatite - 7	5.1574	0.2020	0.0918	0.0070
973_apatite - 8	4.1510	0.4420	0.1497	0.0178
Apatite 3				
1084 - 1	2.3961	0.3067	0.1960	0.0375
1084 - 10	0.5483	0.1036	0.1907	0.0159
1084 - 11	1.0345	0.0934	0.1984	0.0059
1084 - 12	0.3726	0.0598	0.1748	0.0228
1084 - 13	2.8601	0.1593	0.1660	0.0121
1084 - 15	3.6902	0.1065	0.1004	0.0044
1084 - 16	3.6880	0.1564	0.1096	0.0092
1084 - 17	2.9692	0.2919	0.2197	0.0328
1084 - 18	3.6323	0.1390	0.1106	0.0063
1084 - 19	3.4395	0.4849	0.0927	0.0311
1084 - 2	3.1385	0.1825	0.1583	0.0155
1084 - 21	1.8413	0.0997	0.1154	0.0099
1084 - 22	3.7666	0.2008	0.1039	0.0127
1084 - 23	2.8542	0.1319	0.1192	0.0116
1084 - 25	3.5715	0.1028	0.1157	0.0054
1084 - 26	1.4492	0.1332	0.2050	0.0237

1084 - 27	3.2272	0.1083	0.1209	0.0063
1084 - 28	3.1709	0.3370	0.1135	0.0181
1084 - 29	2.9393	0.1413	0.1501	0.0157
1084 - 3	3.2931	0.1267	0.1118	0.0075
1084 - 30	0.4484	0.0991	0.3159	0.0389
1084 - 31	3.0552	0.5426	0.1789	0.0544
1084 - 33	3.3706	0.1057	0.1317	0.0071
1084 - 34	3.4615	0.1239	0.1244	0.0065
1084 - 35	1.6362	0.1459	0.1832	0.0191
1084 - 36	2.6748	0.1586	0.1244	0.0093
1084 - 37	3.4456	0.1385	0.1244	0.0088
1084 - 38	2.8896	0.1440	0.1503	0.0121
1084 - 39	3.3484	0.3143	0.1173	0.0235
1084 - 4	2.7406	0.1342	0.1218	0.0117
1084 - 40	0.4609	0.0444	0.2020	0.0107
1084 - 41	0.1646	0.0107	0.1968	0.0053
1084 - 42	1.2881	0.1329	0.2267	0.0214
1084 - 44	0.1733	0.0241	0.0945	0.0057
1084 - 46	2.7647	0.2474	0.2245	0.0250
1084 - 47	0.1608	0.0243	0.4608	0.0314
1084 - 48	1.5964	0.1974	0.1648	0.0270
1084 - 49	0.8039	0.0795	0.2446	0.0217
1084 - 5	3.4829	0.1727	0.1064	0.0137
1084 - 50	0.2627	0.0560	0.2371	0.0092
1084 - 51	2.0958	0.6167	0.2233	0.0754
1084 - 53	3.6067	0.1462	0.1098	0.0060
1084 - 54	2.1128	0.1813	0.2615	0.0316
1084 - 55	3.6286	0.1335	0.0994	0.0030
1084 - 56	3.4017	0.1855	0.1161	0.0177
1084 - 57	3.7036	0.2104	0.1010	0.0107
1084 - 58	3.3135	0.3214	0.1178	0.0200
1084 - 59	3.5594	0.2158	0.0959	0.0110
1084 - 6	2.7192	0.1222	0.1236	0.0094
1084 - 60	1.6445	0.1760	0.2060	0.0230
1084 - 7	0.1858	0.0554	0.2380	0.0417
1084 - 8	2.2883	0.1456	0.1102	0.0139
1084 - 9	1.7121	0.2682	0.1556	0.0157
1183 - 1	3.3836	0.2450	0.1215	0.0169
1183 - 10	0.3874	0.1874	0.2287	0.0698
1183 - 11	3.0705	0.1595	0.1027	0.0080
1183 - 12	3.3386	0.2383	0.1285	0.0145
1183 - 13	3.4167	0.1977	0.1016	0.0099
1183 - 14	3.5639	0.1908	0.1123	0.0108

1183 - 15	3.8081	0.5210	0.1572	0.0385
1183 - 16	3.6608	0.1827	0.0991	0.0073
1183 - 17	3.0777	0.1997	0.1575	0.0146
1183 - 18	0.2642	0.0506	0.1573	0.0140
1183 - 19	2.2562	0.1439	0.1321	0.0121
1183 - 2	3.6709	0.3035	0.1219	0.0207
1183 - 20	2.9442	0.3794	0.1114	0.0300
1183 - 24	3.1643	0.2827	0.0978	0.0189
1183 - 26	3.0226	0.2471	0.1730	0.0256
1183 - 27	2.8660	0.1369	0.1629	0.0117
1183 - 28	1.5663	0.2511	0.1262	0.0121
1183 - 29	1.7934	0.1078	0.1225	0.0110
1183 - 3	1.8453	0.3102	0.3491	0.0670
1183 - 30	2.9920	0.1521	0.1286	0.0114
1183 - 31	5.5913	0.4807	0.0985	0.0069
1183 - 32	3.6263	0.1674	0.1010	0.0086
1183 - 33	3.3749	0.1821	0.1019	0.0118
1183 - 34	2.5380	0.1115	0.1075	0.0069
1183 - 35	3.2761	0.1263	0.1178	0.0061
1183 - 36	2.8159	0.1463	0.1236	0.0086
1183 - 37	3.5345	0.1750	0.0941	0.0110
1183 - 38	0.1621	0.1361	0.4710	0.1590
1183 - 4	3.5215	0.2296	0.0905	0.0137
1183 - 40	3.4144	0.1904	0.1263	0.0139
1183 - 42	0.1223	0.0167	0.8145	0.0304
1183 - 43	3.5566	0.1330	0.0983	0.0087
1183 - 44	0.3905	0.1138	0.3556	0.0624
1183 - 46	3.6299	0.1570	0.1002	0.0098
1183 - 47	1.7065	0.0853	0.1100	0.0070
1183 - 49	3.5472	0.1046	0.0950	0.0060
1183 - 5	3.5320	0.2277	0.0957	0.0116
1183 - 52	1.6852	0.1446	0.1608	0.0216
1183 - 53	1.7858	0.1588	0.1807	0.0225
1183 - 54	3.0917	0.0943	0.1380	0.0079
1183 - 55	1.6802	0.1941	0.2056	0.0219
1183 - 56	3.7167	0.1250	0.1080	0.0072
1183 - 58	0.0873	0.0933	0.3427	0.1082
1183 - 59	2.5433	0.7529	0.2173	0.0951
1183 - 6	1.5408	0.1186	0.1212	0.0102
1183 - 61	2.1576	0.1870	0.3581	0.0525
1183 - 64	3.0109	0.5441	0.1667	0.0416
1183 - 65	0.5925	0.1347	0.1713	0.0367
1183 - 67	2.0030	0.1309	0.1572	0.0157

1183 - 68	2.6669	0.1352	0.1867	0.0144
1183 - 7	1.0018	0.1050	0.1380	0.0156
1183 - 71	2.3259	0.0852	0.1152	0.0066
1183 - 9	2.9506	0.1820	0.1462	0.0152
1210 - 10	3.1860	0.1333	0.1095	0.0104
1210 - 12	3.4803	0.2213	0.1070	0.0145
1210 - 13	3.1366	0.2244	0.1425	0.0186
1210 - 14	3.3696	0.1369	0.1195	0.0100
1210 - 16	2.7227	0.1789	0.1348	0.0243
1210 - 17	1.4921	0.1509	0.1379	0.0227
1210 - 18	3.1211	0.2561	0.1010	0.0267
1210 - 2	1.8087	0.1459	0.2152	0.0206
1210 - 20	2.5955	0.1684	0.1239	0.0146
1210 - 21	3.4884	0.1060	0.1022	0.0051
1210 - 23	3.4402	0.8003	0.1042	0.0543
1210 - 24	1.8469	0.6576	0.1316	0.0465
1210 - 25	2.0350	0.1929	0.1330	0.0305
1210 - 26	3.4328	0.1560	0.1193	0.0146
1210 - 28	2.4754	0.1953	0.1329	0.0181
1210 - 3	1.8595	0.2766	0.2546	0.0610
1210 - 33	1.9262	0.1904	0.1182	0.0184
1210 - 36	0.1299	0.0203	0.8504	0.0326
1210 - 38	3.3089	0.1850	0.1062	0.0077
1210 - 39	3.4003	0.1560	0.1271	0.0116
1210 - 42	3.7564	0.3118	0.1333	0.0279
1210 - 45	2.5866	0.2500	0.2495	0.0399
1210 - 46	1.0138	0.1141	0.1500	0.0160
1210 - 47	2.4539	0.3201	0.1931	0.0331
1210 - 48	3.4010	0.1681	0.1031	0.0103
1210 - 5	3.7229	0.0909	0.1093	0.0048
1210 - 52	2.5997	0.1996	0.1296	0.0181
1210 - 54	3.5091	0.1228	0.0997	0.0062
1210 - 58	2.0137	0.5179	0.1184	0.0152
1210 - 59	3.1618	0.1552	0.1025	0.0114
1210 - 6	3.0191	0.1243	0.1288	0.0097
1210 - 60	3.4132	0.1136	0.1129	0.0060
1210 - 61	1.9708	0.2046	0.1942	0.0291
1210 - 62	3.2938	0.0930	0.1213	0.0047
1210 - 65	2.9761	0.1578	0.1313	0.0118
1210 - 66	2.4116	0.2346	0.1573	0.0260
1210 - 67	3.6608	0.1038	0.1000	0.0049
1210 - 68	4.3886	0.1547	0.1068	0.0077
1210 - 69	4.3097	0.4724	0.0782	0.0188

1210 - 7	0.8318	0.0580	0.1959	0.0148
1210 - 70	3.1094	0.2345	0.1433	0.0200
1210 - 71	3.3327	0.1895	0.1225	0.0127
1210 - 72	2.8651	0.2536	0.1150	0.0191
1210 - 73	3.4791	0.1752	0.1085	0.0102
1210 - 74	2.9734	0.1370	0.1454	0.0102
1210 - 75	0.3410	0.1290	0.0988	0.0229
1210 - 76	1.8438	0.1090	0.1125	0.0146
1210 - 8	2.3981	0.1052	0.1217	0.0121
1210 - 9	1.9309	0.2592	0.1366	0.0311
Standards Run 1				
401 - 1	11.5314	0.4874	0.0642	0.0066
401 - 10	11.3616	0.4821	0.0652	0.0067
401 - 11	11.4433	0.4853	0.0851	0.0082
401 - 12	10.2383	0.5527	0.1329	0.0222
401 - 13	11.6925	0.4990	0.0832	0.0078
401 - 14	11.7649	0.5007	0.0636	0.0069
401 - 15	11.8001	0.5022	0.0653	0.0068
401 - 16	11.4702	0.4877	0.0657	0.0068
401 - 17	11.6450	0.4955	0.0673	0.0074
401 - 18	11.8946	0.5057	0.0676	0.0074
401 - 19	11.2799	0.4782	0.0649	0.0067
401 - 2	11.5741	0.4896	0.0650	0.0067
401 - 20	11.5951	0.4934	0.0670	0.0074
401 - 3	11.6035	0.4914	0.0682	0.0086
401 - 4	11.3435	0.4775	0.0650	0.0067
401 - 5	11.6751	0.4959	0.0636	0.0067
401 - 6	11.7615	0.4995	0.0695	0.0090
401 - 7	11.6728	0.4957	0.0711	0.0072
401 - 8	11.4434	0.4830	0.0673	0.0076
401 - 9	11.1706	0.4715	0.0692	0.0071
MAD - 1.csv	13.1137	0.3943	0.0566	0.0050
MAD - 10.csv	12.8489	0.3864	0.0566	0.0050
MAD - 11.csv	12.9832	0.3904	0.0566	0.0050
MAD - 12.csv	13.0146	0.3913	0.0566	0.0049
MAD - 13.csv	13.5084	0.4062	0.0566	0.0050
MAD - 14.csv	13.0640	0.3928	0.0566	0.0050
MAD - 15.csv	13.3526	0.4015	0.0566	0.0051
MAD - 16.csv	13.1763	0.3962	0.0566	0.0049
MAD - 17.csv	13.3356	0.4010	0.0566	0.0050
MAD - 18.csv	13.0739	0.3931	0.0566	0.0050
MAD - 19.csv	13.1819	0.3964	0.0566	0.0049
MAD - 2.csv	13.3542	0.4016	0.0566	0.0050

MAD - 20.csv	12.7293	0.3828	0.0567	0.0049
MAD - 3.csv	12.9625	0.3898	0.0566	0.0049
MAD - 4.csv	12.9433	0.3892	0.0566	0.0049
MAD - 5.csv	13.3308	0.4008	0.0566	0.0049
MAD - 6.csv	13.1299	0.3948	0.0567	0.0049
MAD - 7.csv	13.2663	0.3989	0.0566	0.0049
MAD - 8.csv	12.9467	0.3893	0.0567	0.0049
MAD - 9.csv	13.0078	0.3911	0.0566	0.0050
McClure - 1.csv	8.5824	0.3775	0.2751	0.0156
McClure - 10.csv	8.6333	0.3481	0.2427	0.0121
McClure - 11.csv	10.2450	0.3934	0.1416	0.0091
McClure - 12.csv	4.8330	1.1485	0.2923	0.1075
McClure - 13.csv	9.6898	0.3891	0.1907	0.0107
McClure - 14.csv	10.0203	0.3948	0.1543	0.0090
McClure - 15.csv	Error	Error	0.6242	0.2677
McClure - 16.csv	9.0251	0.4149	0.2527	0.0163
McClure - 17.csv	9.6210	1.3412	0.1782	0.0160
McClure - 18.csv	Error	Error	< DL	0.0075
McClure - 19.csv	10.4586	0.3987	0.1435	0.0093
McClure - 2.csv	9.2612	0.3896	0.2643	0.0152
McClure - 20.csv	8.1701	0.3276	0.3127	0.0146
McClure - 3.csv	9.5460	0.4101	0.1967	0.0124
McClure - 4.csv	9.3492	0.6962	0.2260	0.0264
McClure - 5.csv	10.3365	0.4039	0.1545	0.0100
McClure - 6.csv	9.6052	0.3878	0.1846	0.0125
McClure - 7.csv	9.2891	0.4294	0.2317	0.0156
McClure - 8.csv	8.8968	0.3669	0.2353	0.0139
McClure - 9.csv	8.3893	0.3889	0.2952	0.0199
NIST610 - 1.csv	Error	Error	Error	Error
NIST610 - 10.csv	Error	Error	Error	Error
NIST610 - 11.csv	Error	Error	Error	Error
NIST610 - 12.csv	Error	Error	Error	Error
NIST610 - 13.csv	Error	Error	Error	Error
NIST610 - 14.csv	Error	Error	Error	Error
NIST610 - 15.csv	Error	Error	Error	Error
NIST610 - 16.csv	Error	Error	Error	Error
NIST610 - 17.csv	Error	Error	Error	Error
NIST610 - 18.csv	Error	Error	Error	Error
NIST610 - 19.csv	Error	Error	Error	Error
NIST610 - 2.csv	Error	Error	Error	Error
NIST610 - 20.csv	Error	Error	Error	Error
NIST610 - 3.csv	Error	Error	Error	Error
NIST610 - 4.csv	Error	Error	Error	Error

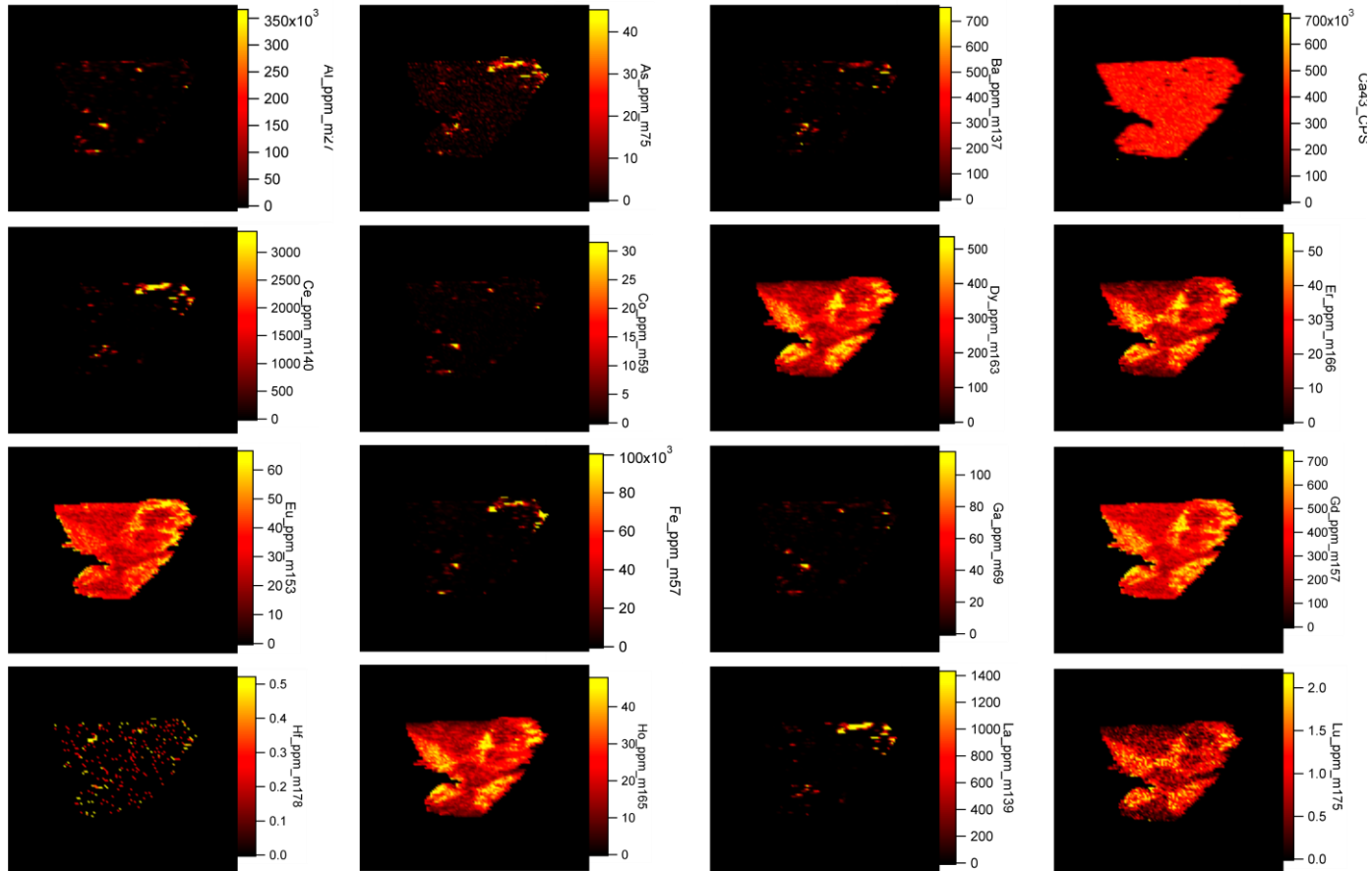
NIST610 - 5.csv	Error	Error	Error	Error
NIST610 - 6.csv	Error	Error	Error	Error
NIST610 - 7.csv	Error	Error	Error	Error
NIST610 - 8.csv	Error	Error	Error	Error
NIST610 - 9.csv	Error	Error	Error	Error
Standards Run 2				
401 - 1.csv	11.58194012	0.543924086	0.066431957	0.007378553
401 - 10.csv	11.75378281	0.585236437	0.067370078	0.008450611
401 - 11.csv	11.50021171	0.487491183	0.064794326	0.007697901
401 - 12.csv	10.92151636	0.499961644	0.085510449	0.014119189
401 - 13.csv	11.81603753	0.392707867	0.0664497	0.00868035
401 - 14.csv	11.54858565	0.386057303	0.073221807	0.009314598
401 - 15.csv	11.92487462	0.428008426	0.059893419	0.009044173
401 - 16.csv	11.19639954	0.395224846	0.063558739	0.007231345
401 - 17.csv	11.50637015	0.425453144	0.093700657	0.009148338
401 - 18.csv	9.820795322	0.557795306	0.146175404	0.029017398
401 - 19.csv	11.41062753	0.416563732	0.064135843	0.00830824
401 - 2.csv	11.7229971	0.55506131	0.061120144	0.008223955
401 - 20.csv	11.34137183	0.41368069	0.062901644	0.007944401
401 - 21.csv	11.82240917	0.451261146	0.061651024	0.006892004
401 - 22.csv	11.40724519	0.433358344	0.065684873	0.007032133
401 - 23.csv	11.65088531	0.436504371	0.073544392	0.009605826
401 - 24.csv	11.52251979	0.430387555	0.069265938	0.00796855
401 - 25.csv	11.99490374	0.421680113	0.068135886	0.008713369
401 - 26.csv	11.90328786	0.414822498	0.064930434	0.007850368
401 - 27.csv	11.89250532	0.407808765	0.072675087	0.007806378
401 - 28.csv	11.23744236	0.378890631	0.064597573	0.006963018
401 - 29.csv	11.70945729	0.404377213	0.066114385	0.00719303
401 - 3.csv	12.14691444	0.461425776	0.06986477	0.007372897
401 - 30.csv	11.63398313	0.400995452	0.061656676	0.006909885
401 - 4.csv	11.64001183	0.449545776	0.064438057	0.007023268
401 - 5.csv	11.82916261	0.444862291	0.069862882	0.007354353
401 - 6.csv	11.38067487	0.425729058	0.069561941	0.009549861
401 - 7.csv	11.73544117	0.531302569	0.069040084	0.008335775
401 - 8.csv	11.6803585	0.530358873	0.065952673	0.007147097
401 - 9.csv	11.80522445	0.588352112	0.069213951	0.007672892
MAD - 1.csv	13.26278791	0.246762455	0.056606887	0.005001347
MAD - 2.csv	12.96432539	0.241209373	0.056566573	0.00500404
MAD - 3.csv	13.10763692	0.230540816	0.056617453	0.005073414
MAD - 4.csv	13.11966081	0.230752295	0.05661066	0.005098634
MAD - 5.csv	13.24834752	0.40661481	0.056571197	0.005126897
MAD - 6.csv	12.97142686	0.398115634	0.056609821	0.005128959
MAD - 7.csv	13.32038537	0.485786644	0.056568415	0.005185368

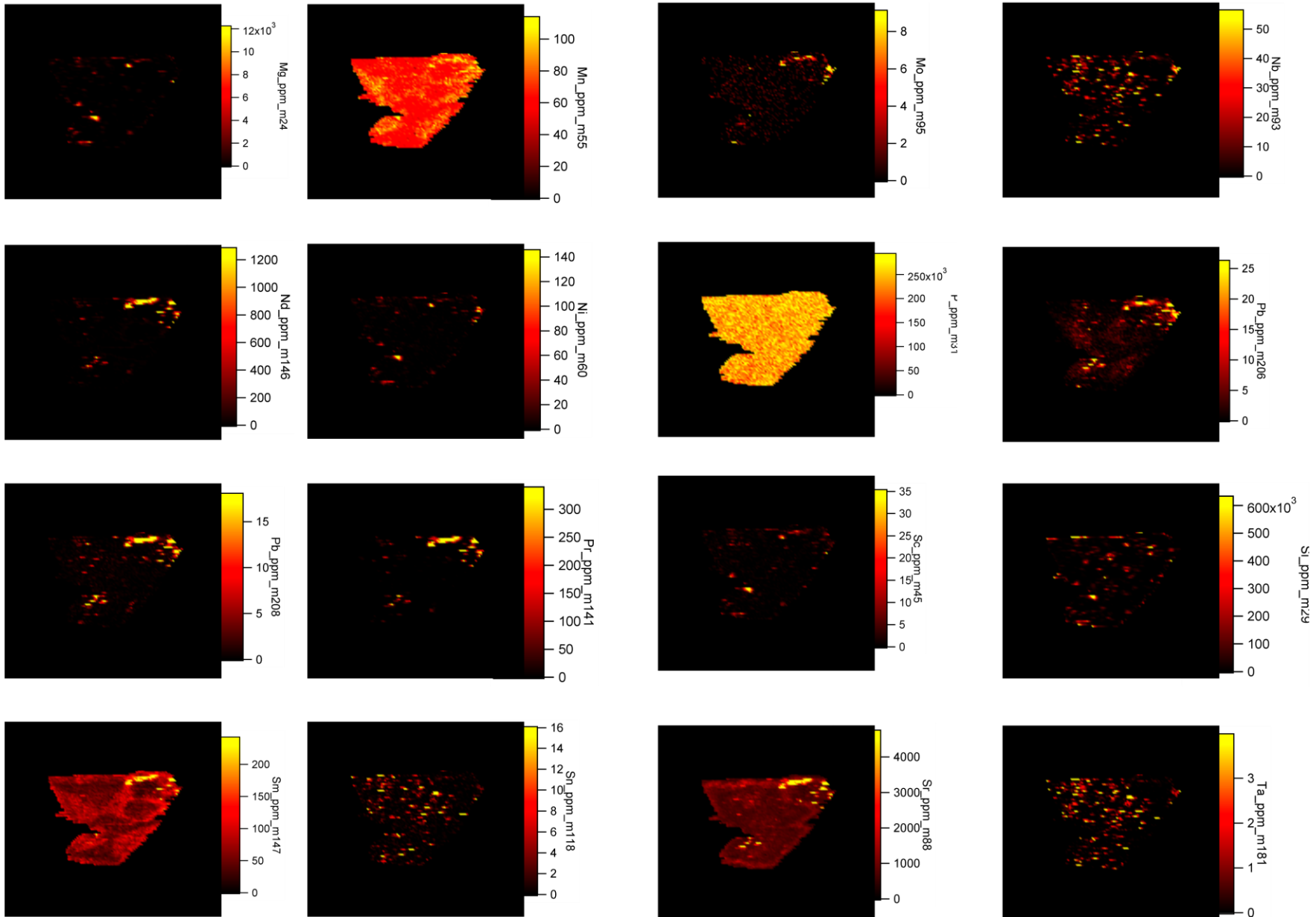
MAD - 8.csv	12.91242644	0.470908621	0.056598393	0.005115163
MAD - 9.csv	12.90920254	0.339386736	0.0566066	0.00511948
MAD - 10.csv	13.33131534	0.350484206	0.056601763	0.005230662
MAD - 11.csv	13.10893996	0.038656667	0.056579312	0.005170577
MAD - 12.csv	13.12459115	0.03870282	0.056619645	0.005152431
MAD - 13.csv	13.10686517	0.16042826	0.056584033	0.005108506
MAD - 14.csv	13.12967544	0.160707458	0.056595982	0.00509978
MAD - 15.csv	13.01817062	0.207164881	0.056627543	0.005116704
MAD - 16.csv	13.22088849	0.210390835	0.056622445	0.005172871
MAD - 17.csv	13.04047334	0.193946846	0.0566027	0.005174781
MAD - 18.csv	13.19821212	0.196292845	0.056611324	0.005249476
MAD - 19.csv	13.02493587	0.239882968	0.056618574	0.005180013
MAD - 20.csv	13.21525886	0.243388186	0.056622293	0.00524913
MAD - 21.csv	13.00922061	0.218699247	0.056620744	0.005173331
MAD - 22.csv	13.22418722	0.222313071	0.056663318	0.005203255
MAD - 23.csv	13.19125807	0.126332617	0.056595346	0.005221003
MAD - 24.csv	13.03802198	0.124865075	0.056597611	0.00520541
MAD - 25.csv	13.12917571	0.073273003	0.056575229	0.005141295
MAD - 26.csv	13.10108724	0.073116243	0.056614941	0.005178121
MAD - 27.csv	13.15625957	0.101538344	0.056580726	0.005215228
MAD - 28.csv	13.07622497	0.100920647	0.056630631	0.00517502
MAD - 29.csv	13.06823037	0.13517966	0.056614415	0.005156985
MAD - 30.csv	13.16416769	0.13617205	0.056585115	0.005197024
McClure - 1.csv	9.517916237	0.371103244	0.213871615	0.014670879
McClure - 10.csv	9.445516628	0.344308186	0.218477067	0.00947479
McClure - 11.csv	8.727976906	0.319907947	0.271073389	0.016845935
McClure - 12.csv	8.438200602	0.296300522	0.28053659	0.016297024
McClure - 13.csv	10.33261328	0.298738213	0.174211306	0.009056643
McClure - 14.csv	9.721976982	0.31948064	0.199752215	0.011655532
McClure - 15.csv	8.869654447	0.384514274	0.259410845	0.018329587
McClure - 16.csv	8.85777572	0.370631502	0.265972431	0.017787028
McClure - 17.csv	9.477066024	0.391081478	0.253058292	0.018118109
McClure - 18.csv	8.706427865	0.366651222	0.237586709	0.016911209
McClure - 19.csv	9.420711786	0.32921805	0.153065447	0.009547755
McClure - 2.csv	9.569247452	0.378763517	0.238683173	0.015081368
McClure - 20.csv	9.851403885	0.655780913	0.158774933	0.013348125
McClure - 21.csv	8.919418511	0.370050887	0.248371797	0.01676516
McClure - 22.csv	9.620174729	0.391682577	0.253033328	0.01735415
McClure - 23.csv	9.44174201	0.302411715	0.230817136	0.012583033
McClure - 24.csv	9.600377891	0.296597568	0.197239312	0.011322806
McClure - 25.csv	9.644129923	0.301103786	0.218991591	0.011515405
McClure - 26.csv	10.99806042	0.26945915	0.147048817	0.008459322
McClure - 27.csv	8.976620632	0.302102249	0.245268165	0.015103835

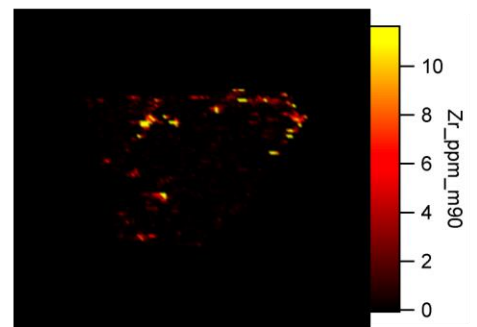
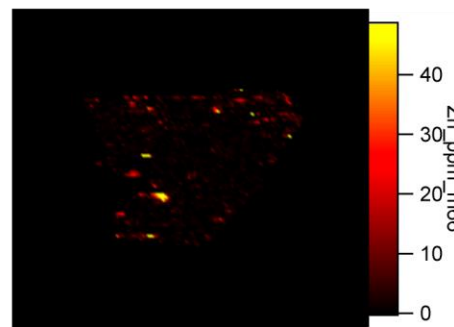
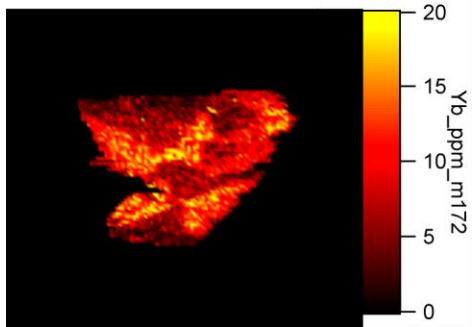
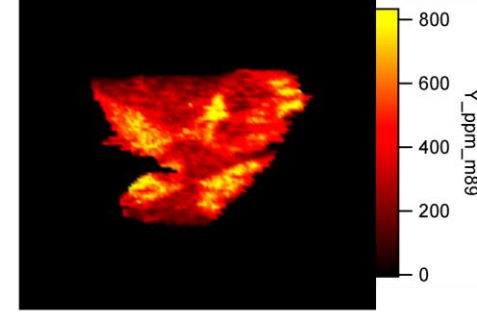
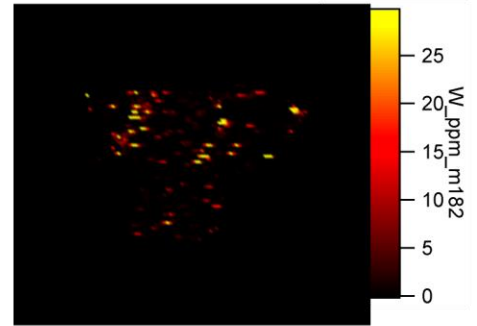
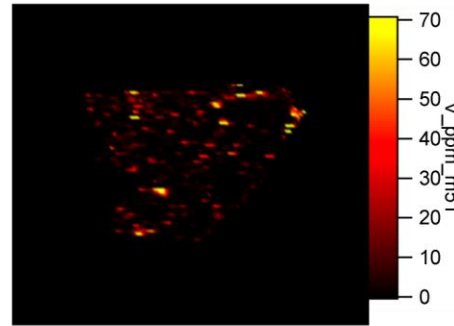
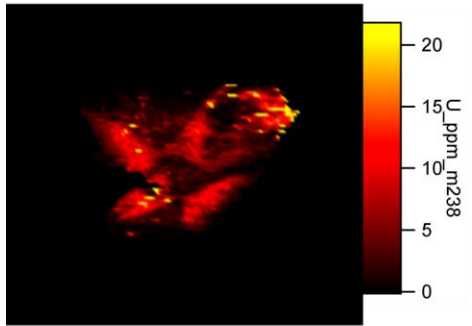
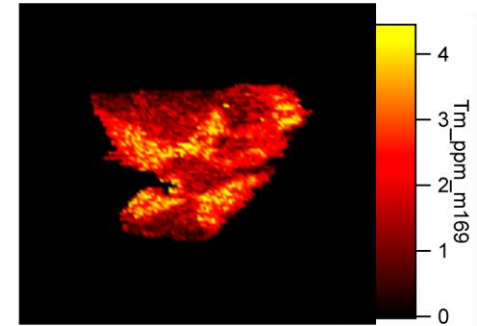
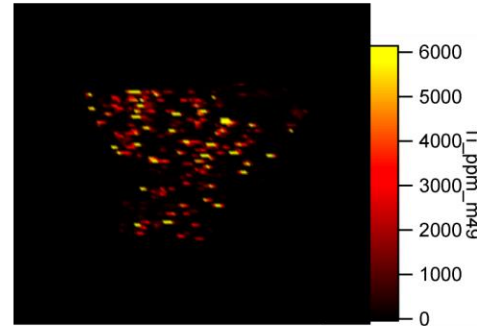
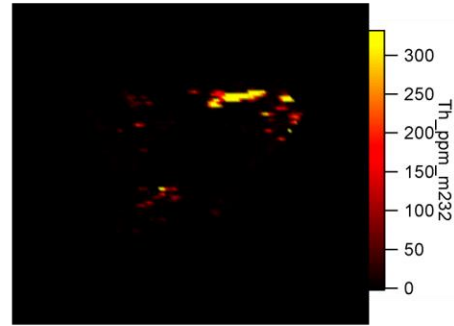
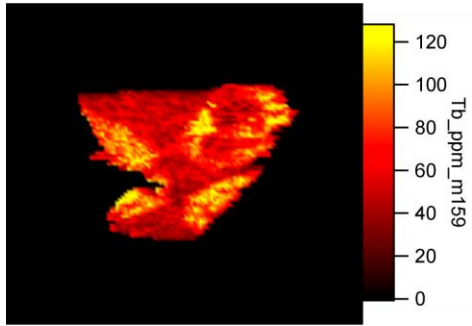
McClure - 28.csv	10.11511063	0.278425711	0.177106873	0.009042963
McClure - 29.csv	9.378500254	0.315677441	0.235655443	0.013224432
McClure - 3.csv	9.667294642	0.358947894	0.204702159	0.012743379
McClure - 30.csv	9.730762018	0.317815759	0.202332384	0.013340564
McClure - 4.csv	8.765519411	0.372496127	0.252246704	0.017317667
McClure - 5.csv	10.7536748	0.421964327	0.116983995	0.006877815
McClure - 6.csv	10.95358539	0.428516856	0.117152992	0.006495794
McClure - 7.csv	10.04605042	0.490015034	0.181174876	0.012716518
McClure - 8.csv	9.646051929	0.484534398	0.196557059	0.013126386
McClure - 9.csv	9.314392015	0.334247774	0.208655289	0.010281518
NIST610 - 1.csv	Error	Error	Error	Error
NIST610 - 2.csv	Error	Error	Error	Error
NIST610 - 3.csv	Error	Error	Error	Error
NIST610 - 4.csv	Error	Error	Error	Error
NIST610 - 5.csv	Error	Error	Error	Error
NIST610 - 6.csv	Error	Error	Error	Error
NIST610 - 7.csv	Error	Error	Error	Error
NIST610 - 8.csv	Error	Error	Error	Error
NIST610 - 9.csv	Error	Error	Error	Error
NIST610 - 10.csv	Error	Error	Error	Error
NIST610 - 11.csv	Error	Error	Error	Error
NIST610 - 12.csv	Error	Error	Error	Error
NIST610 - 13.csv	Error	Error	Error	Error
NIST610 - 14.csv	Error	Error	Error	Error
NIST610 - 15.csv	Error	Error	Error	Error
NIST610 - 16.csv	Error	Error	Error	Error
NIST610 - 17.csv	Error	Error	Error	Error
NIST610 - 18.csv	Error	Error	Error	Error
NIST610 - 19.csv	Error	Error	Error	Error
NIST610 - 20.csv	Error	Error	Error	Error
NIST610 - 21.csv	Error	Error	Error	Error
NIST610 - 22.csv	Error	Error	Error	Error
NIST610 - 23.csv	Error	Error	Error	Error
NIST610 - 24.csv	Error	Error	Error	Error
NIST610 - 25.csv	Error	Error	Error	Error
NIST610 - 26.csv	Error	Error	Error	Error
NIST610 - 27.csv	Error	Error	Error	Error
NIST610 - 28.csv	Error	Error	Error	Error
NIST610 - 29.csv	Error	Error	Error	Error
NIST610 - 30.csv	Error	Error	Error	Error

APPENDIX F: ADDITIONAL ELEMENTAL MAPS

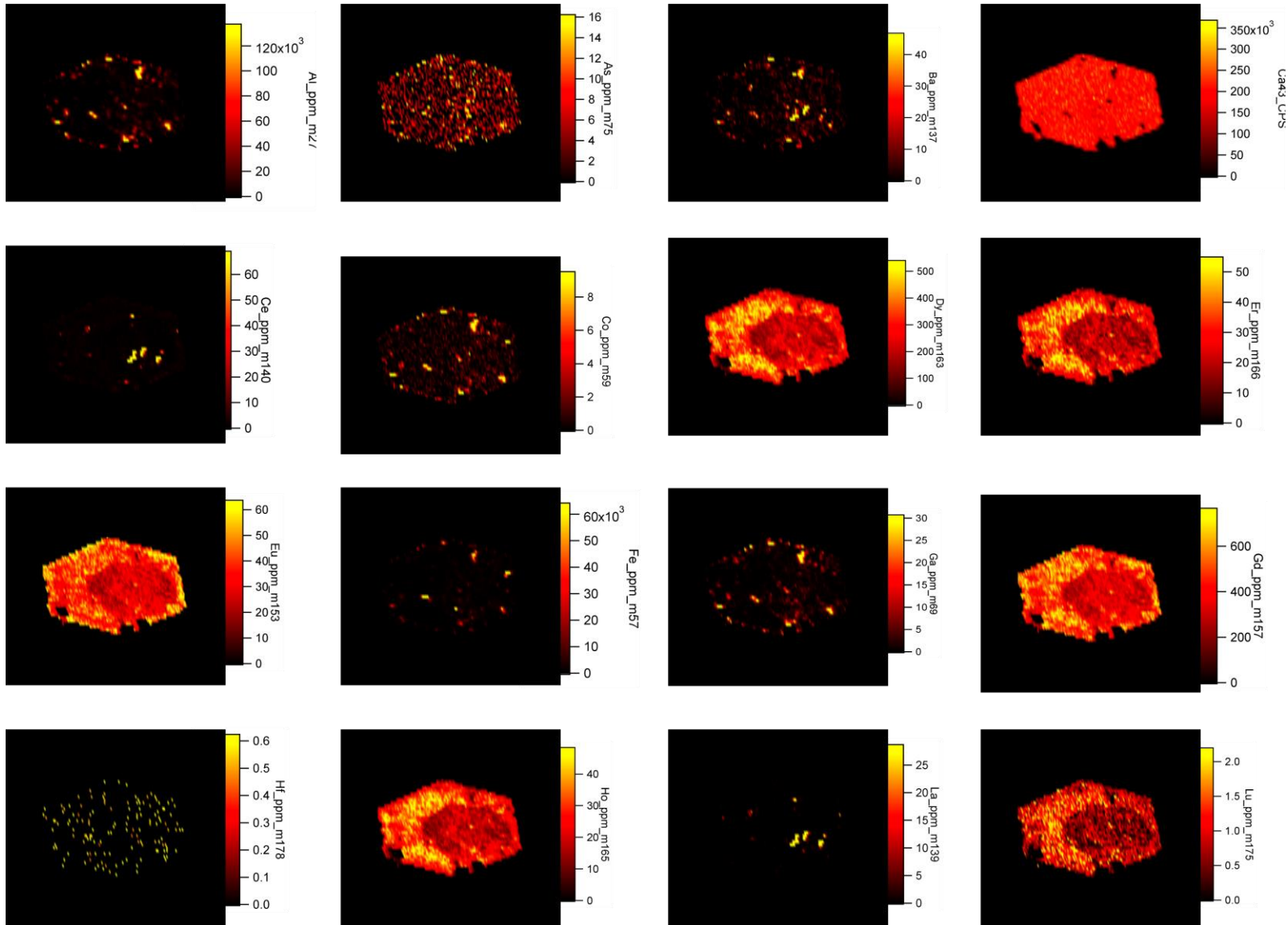
Sample 801 - Apatite 1:

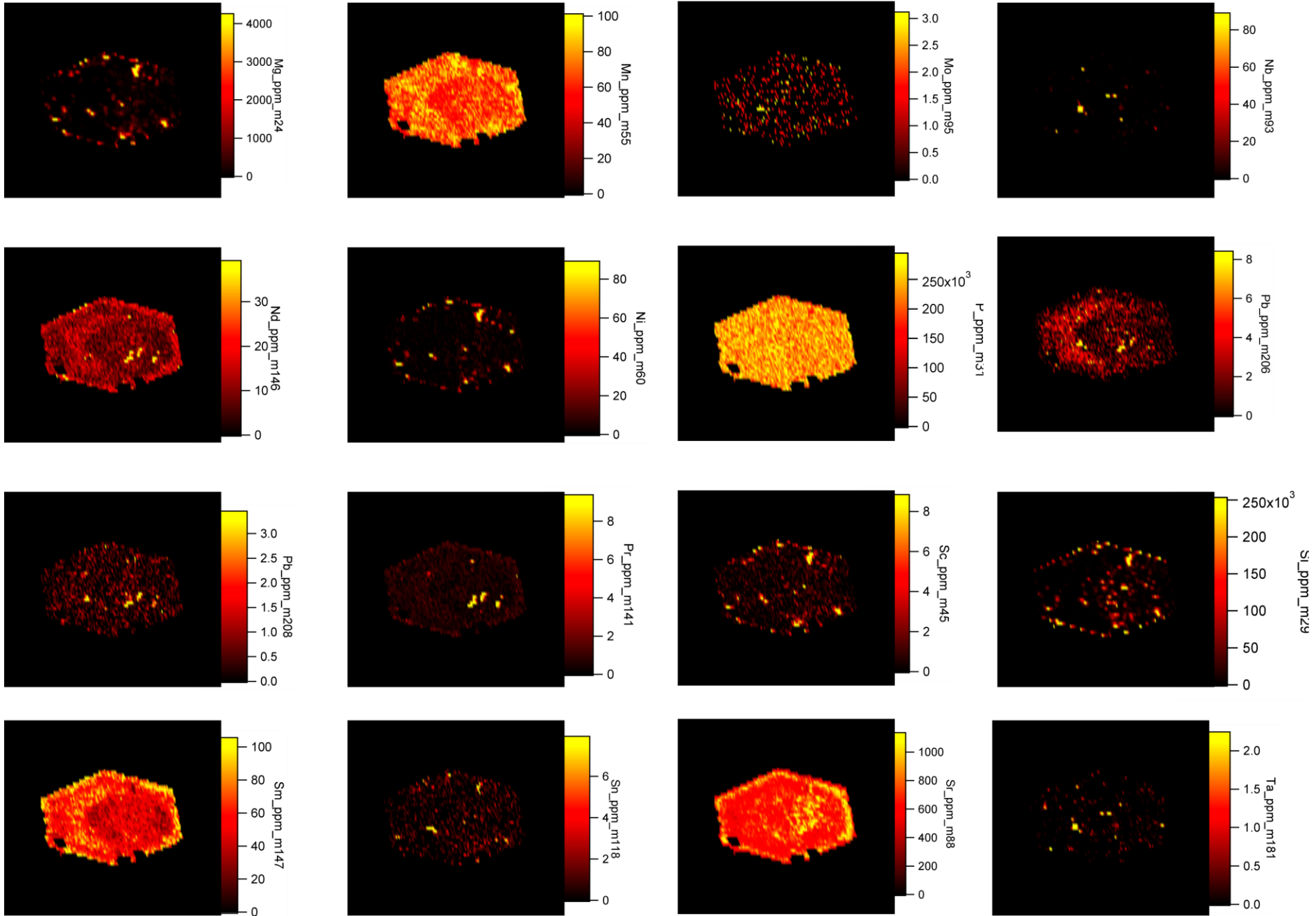


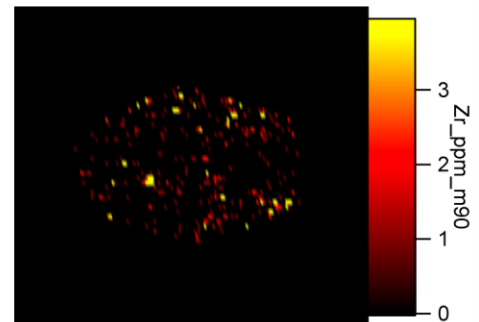
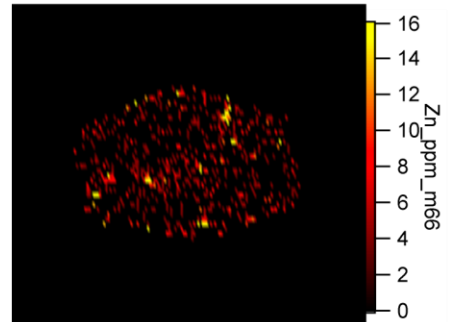
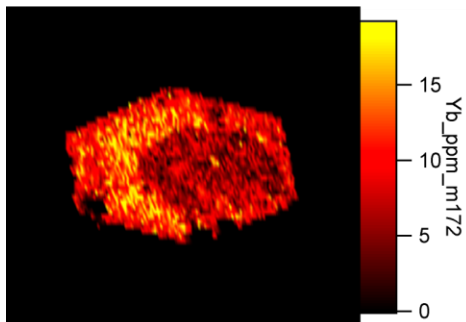
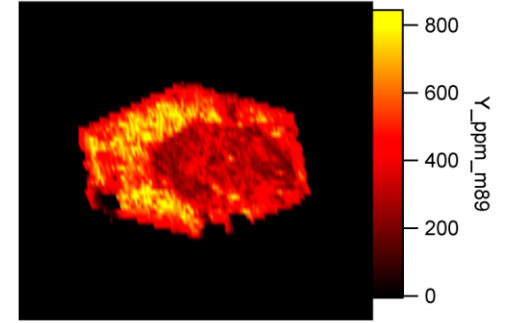
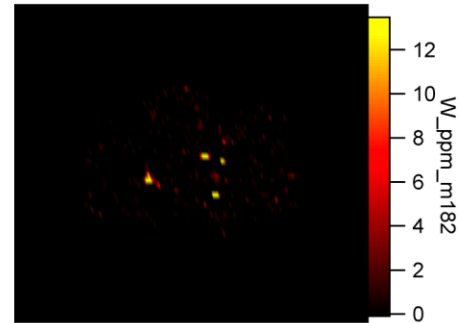
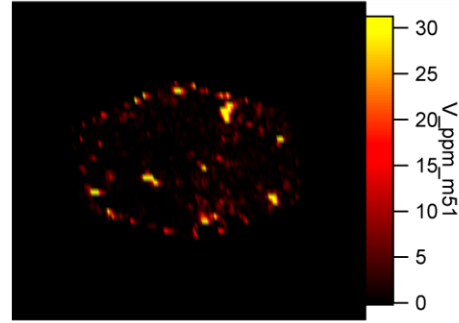
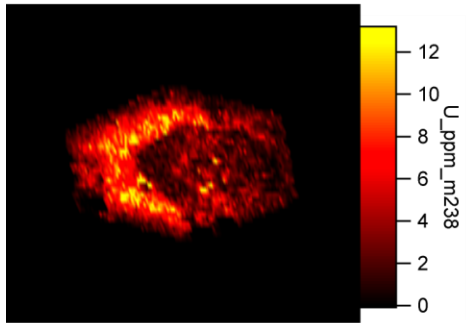
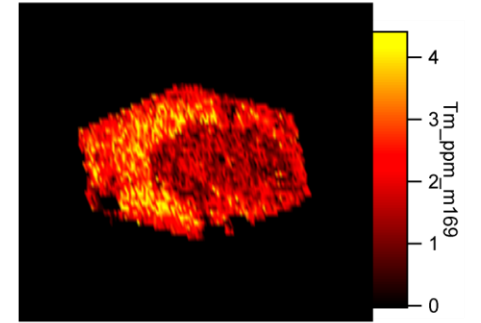
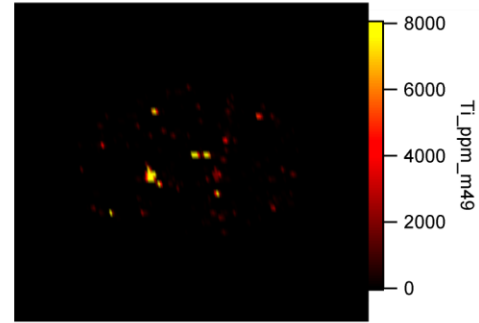
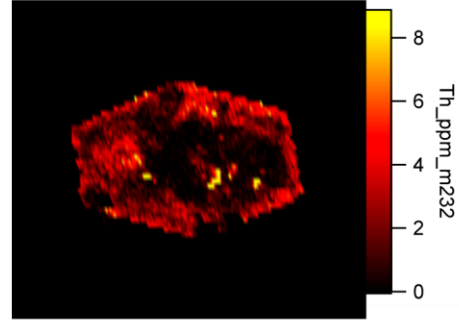
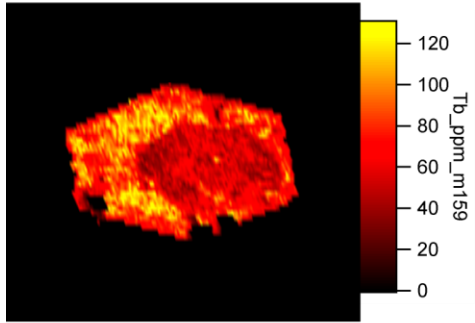




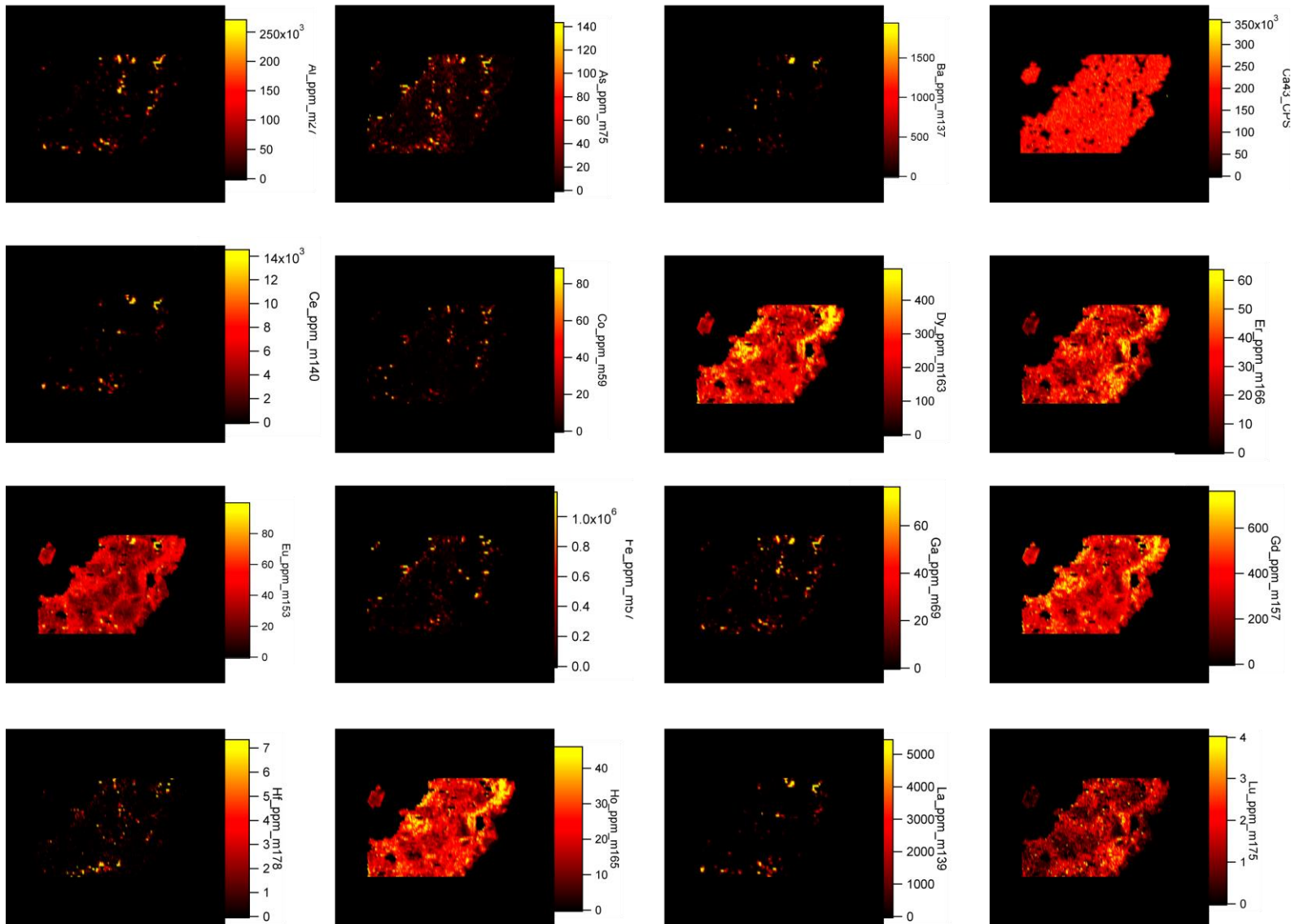
Sample 801 - Apatite 2:

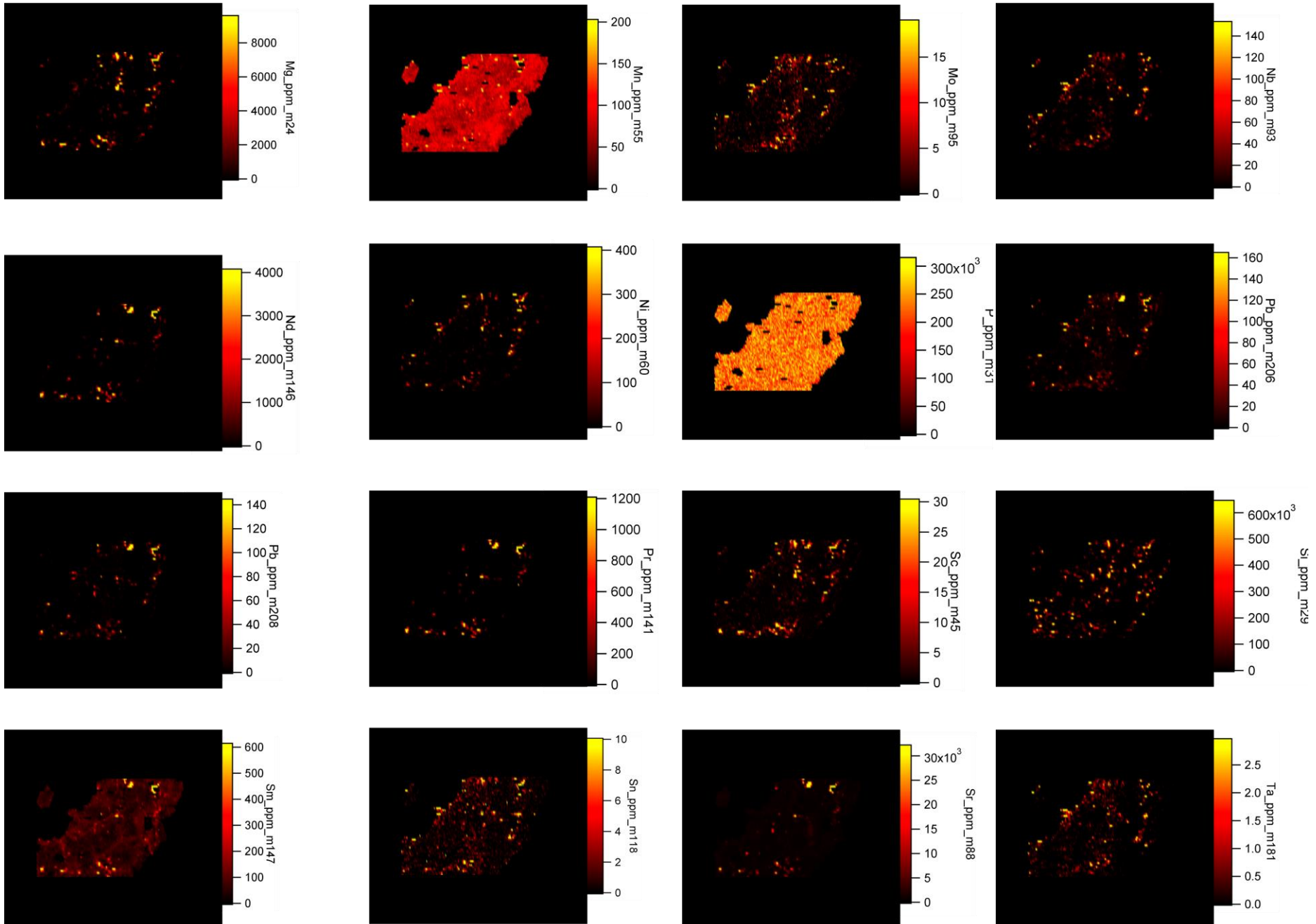


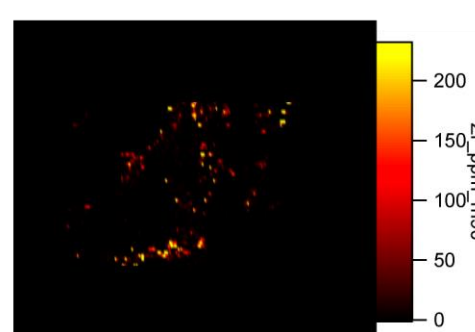
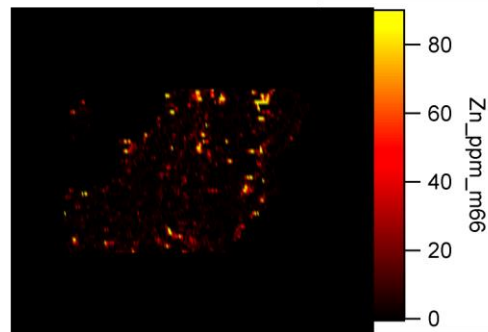
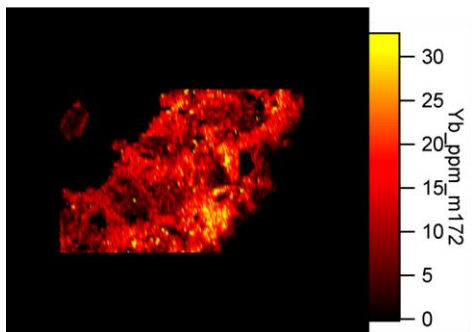
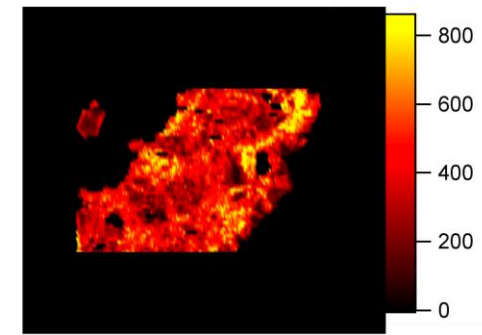
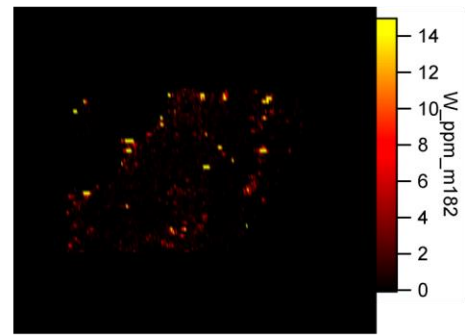
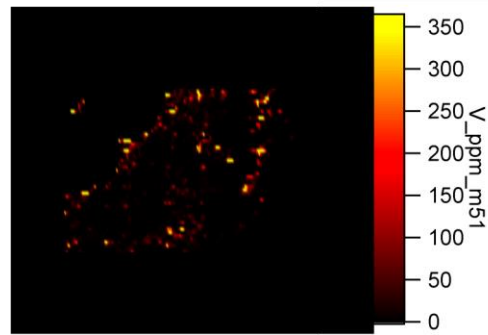
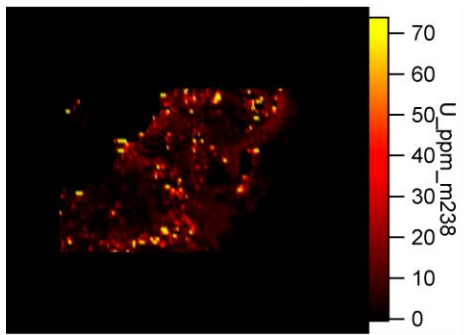
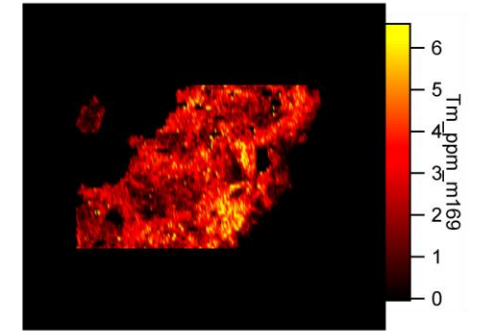
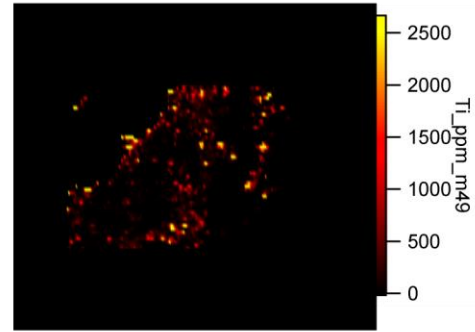
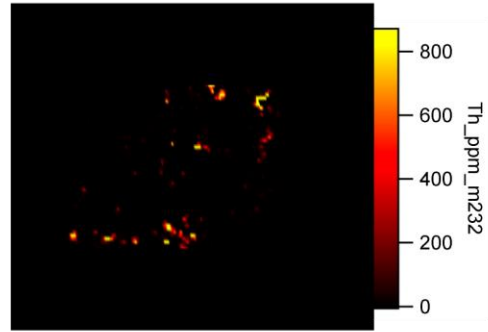
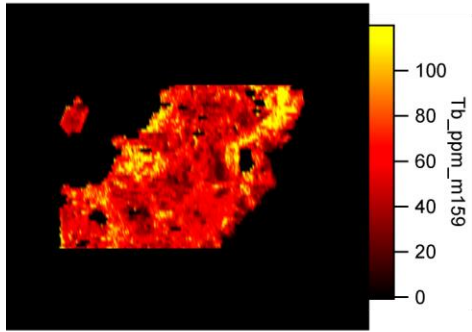




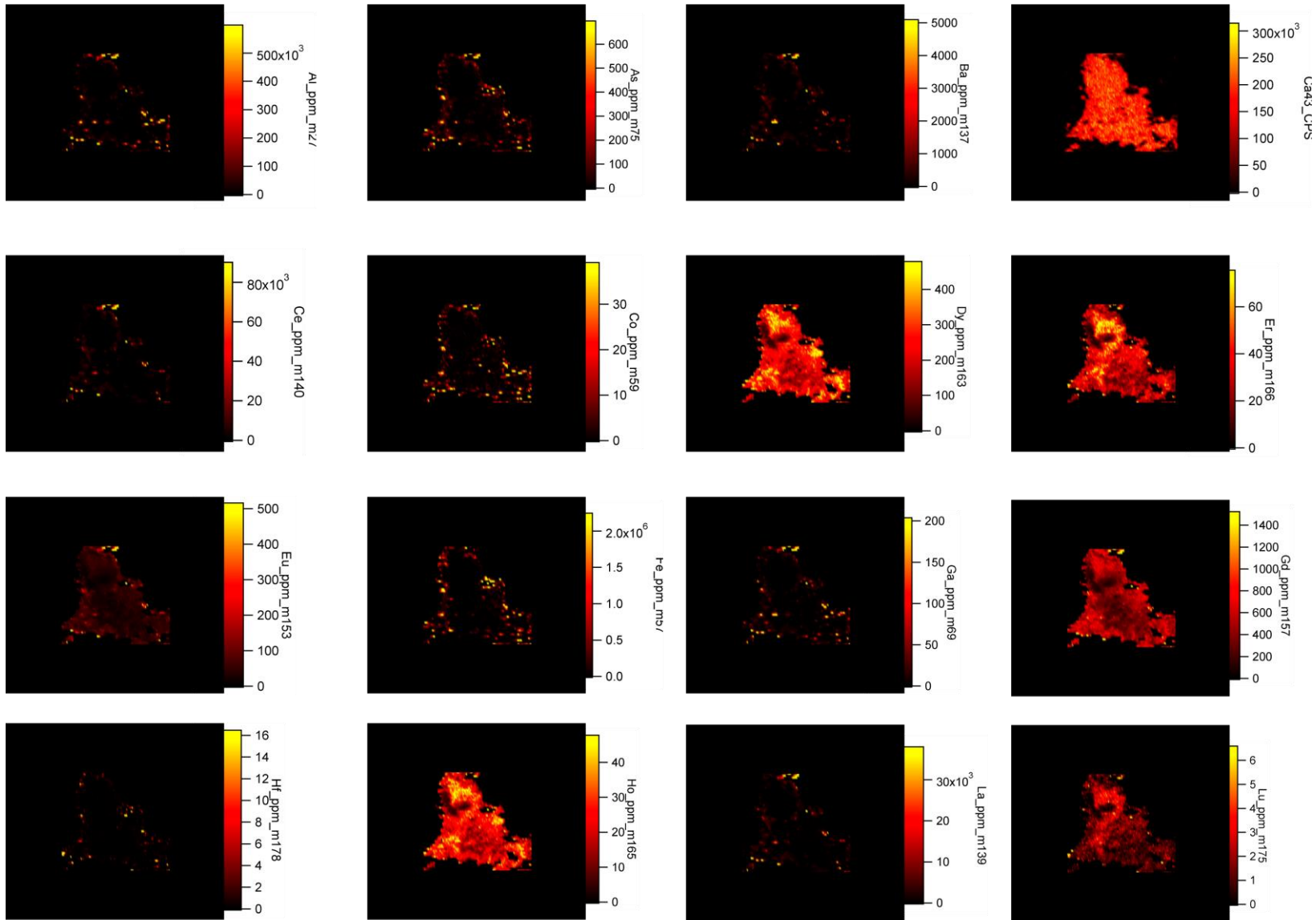
Sample 801 - Apatite 3:

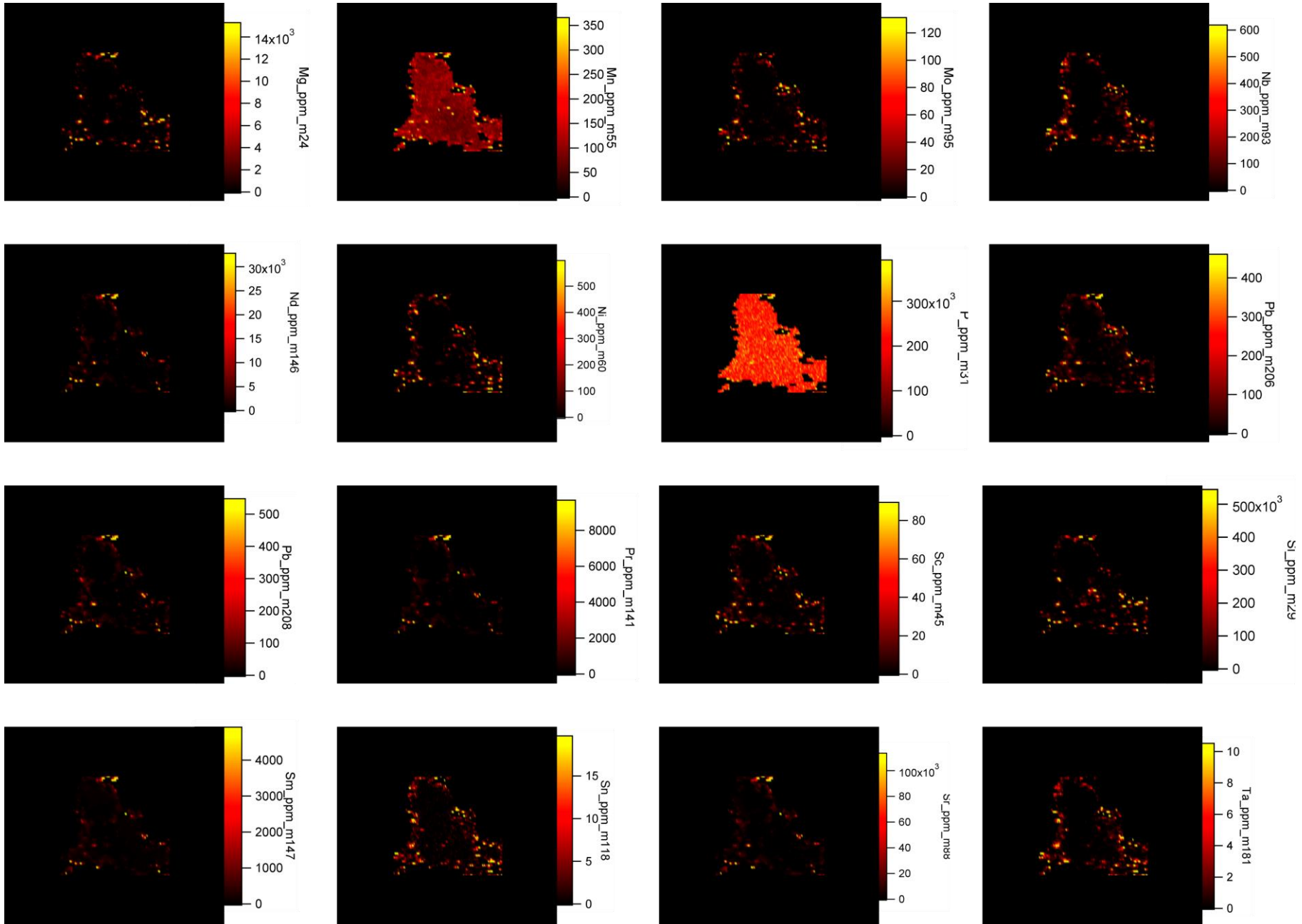


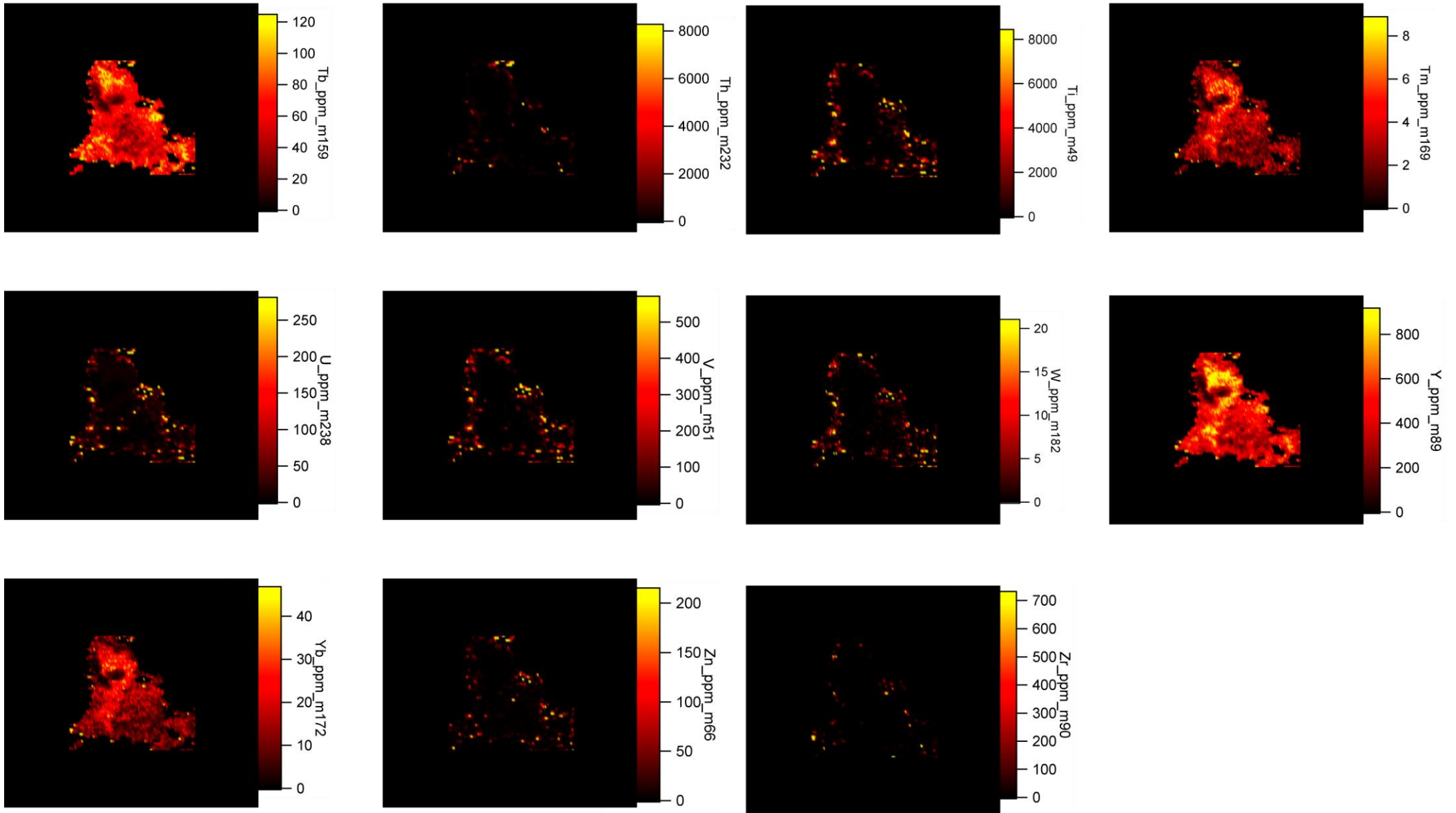




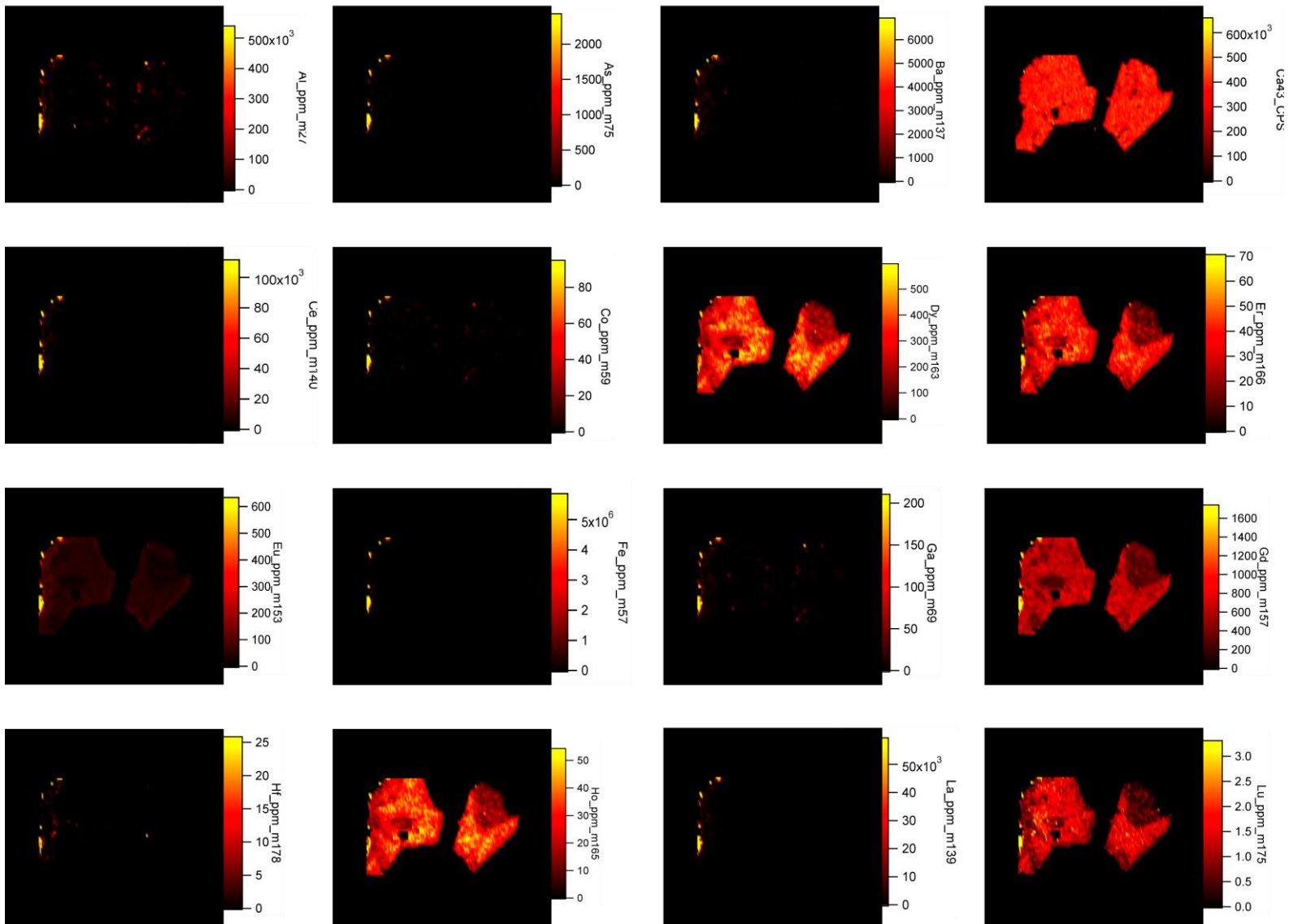
Sample 801 - Apatite 4:

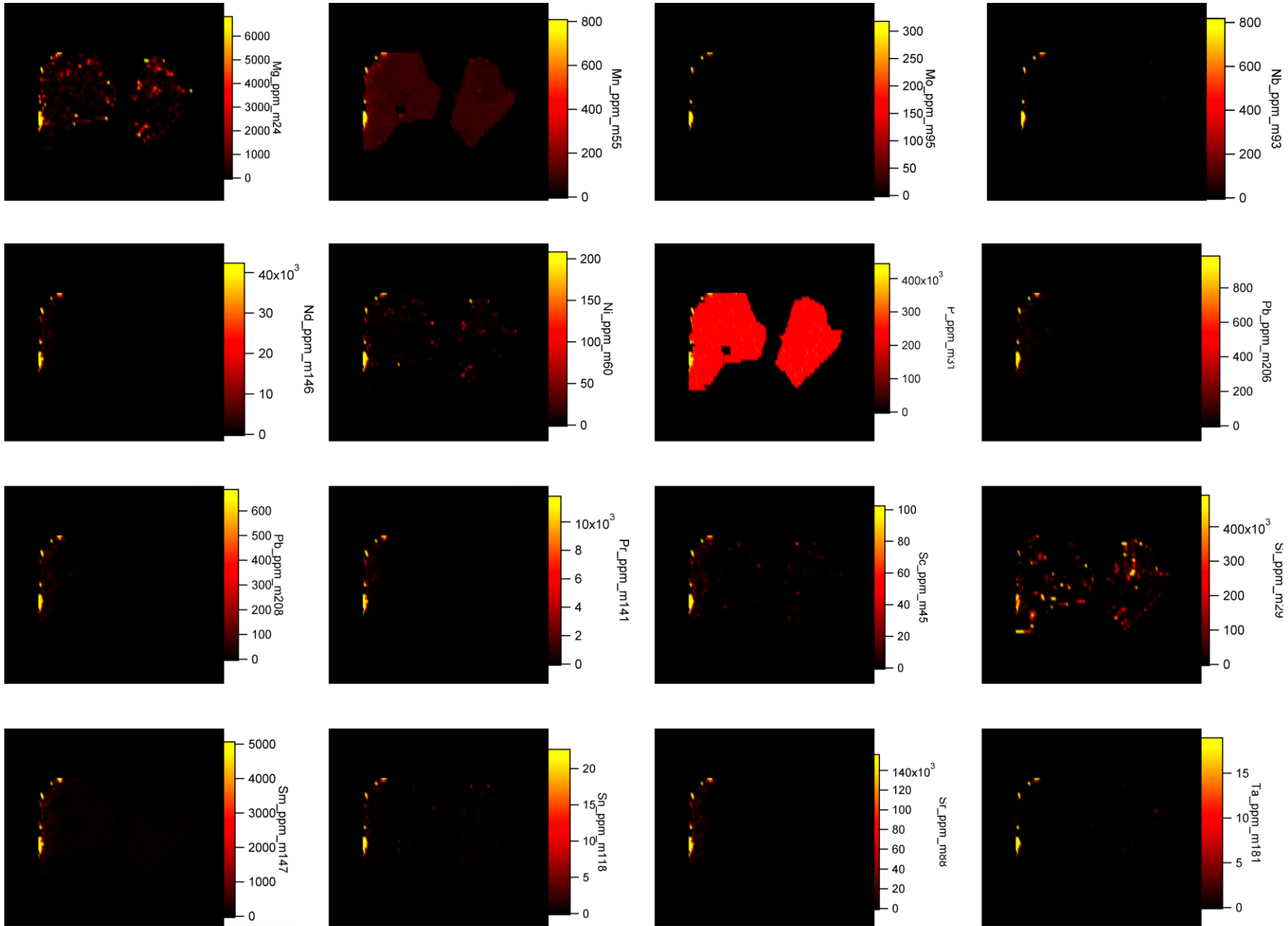


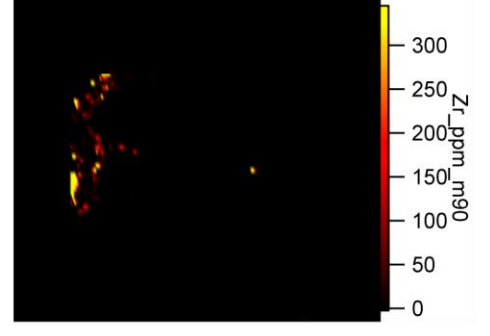
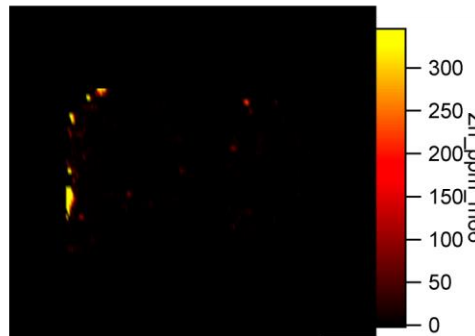
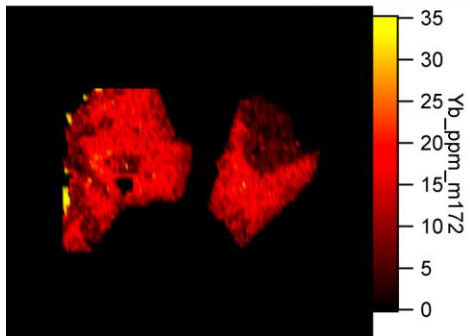
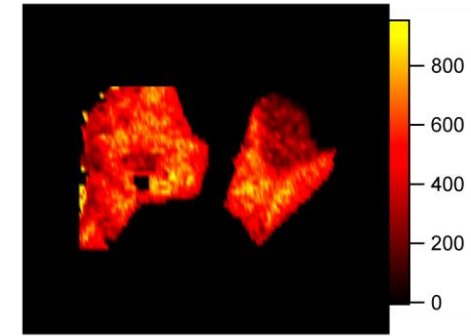
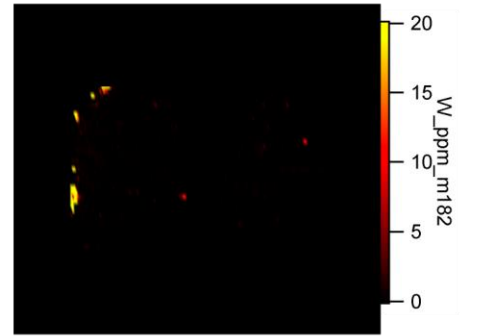
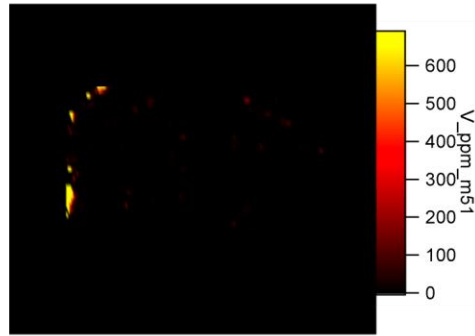
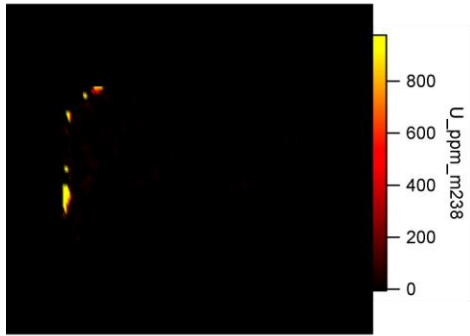
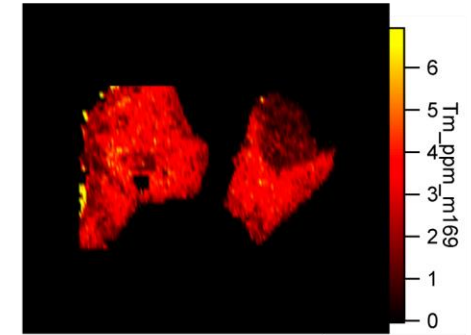
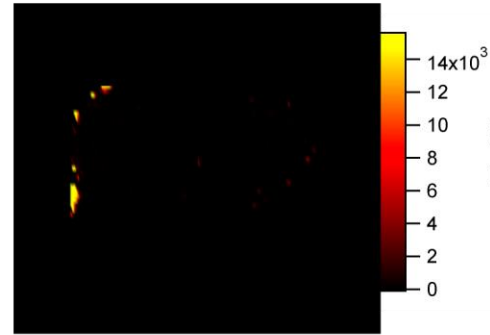
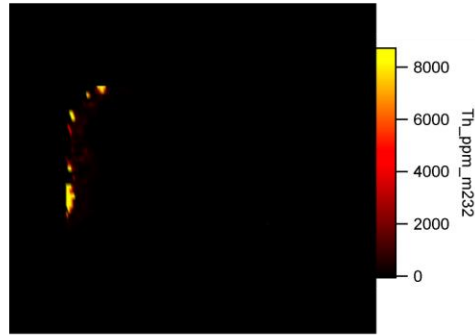
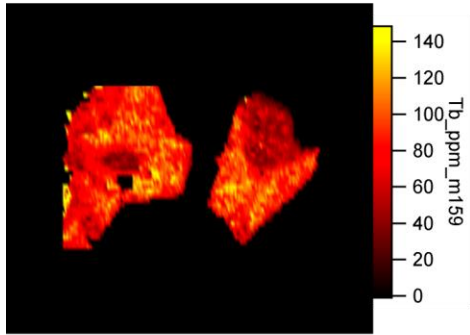




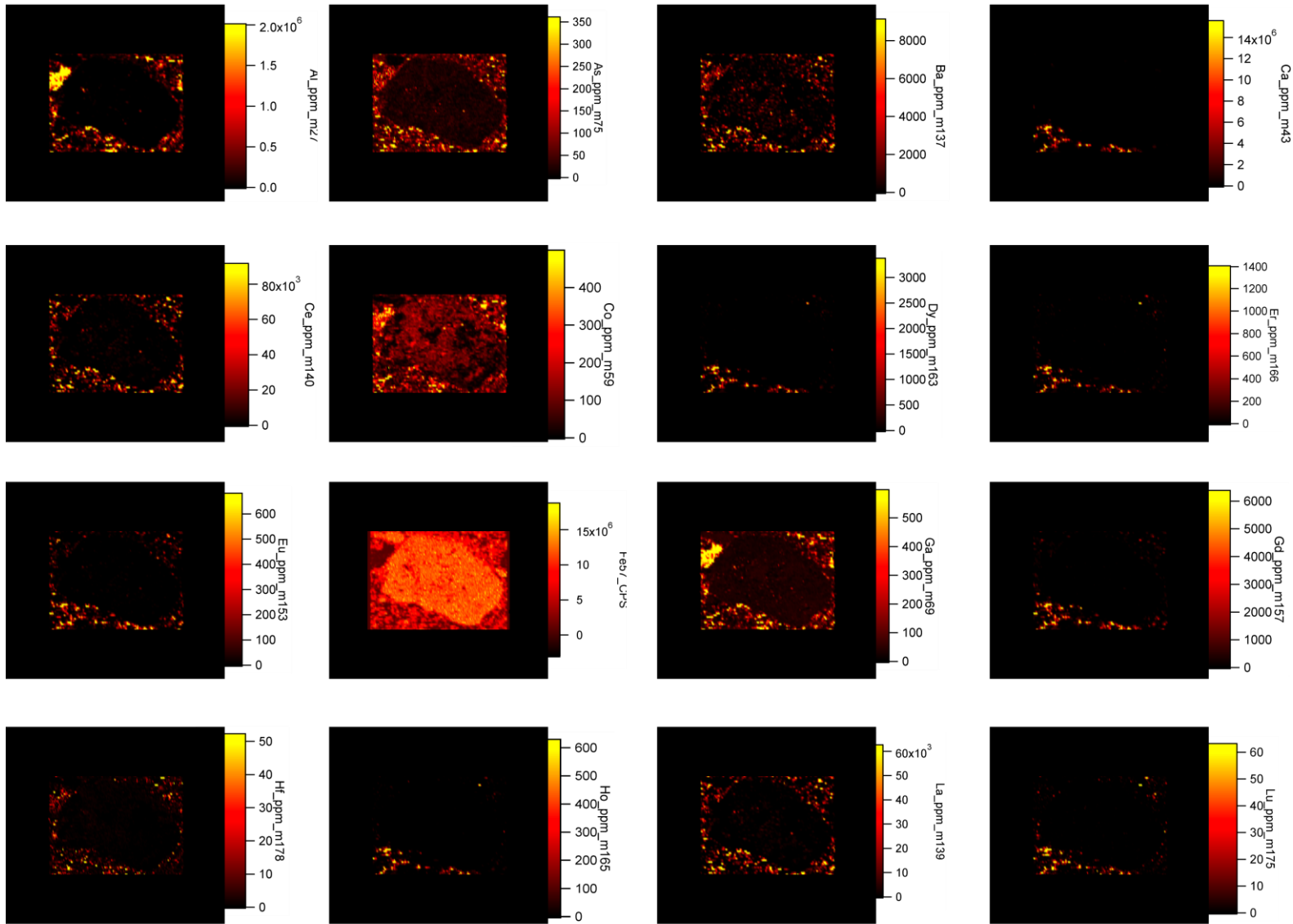
Sample 801 - Apatite 5:

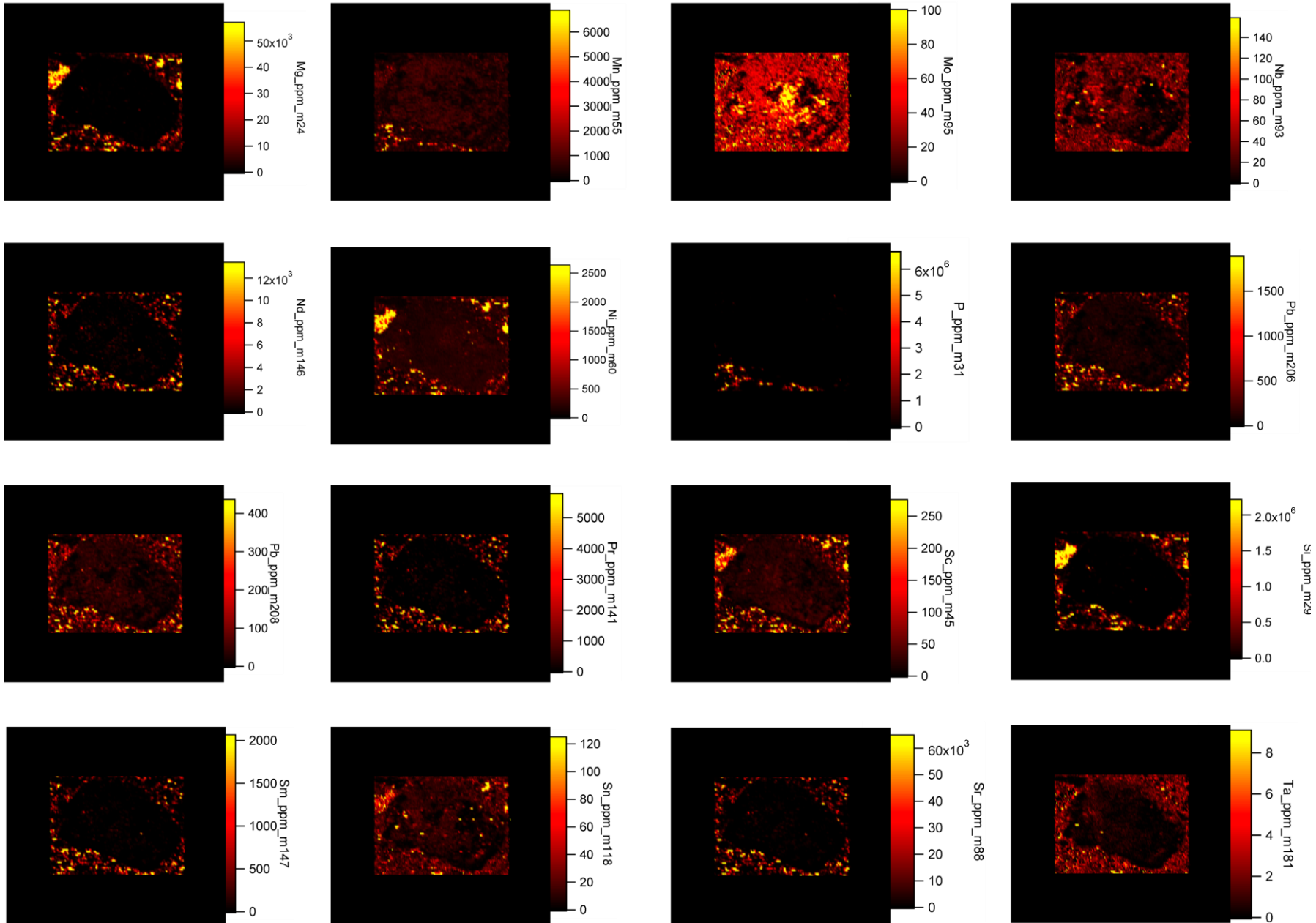


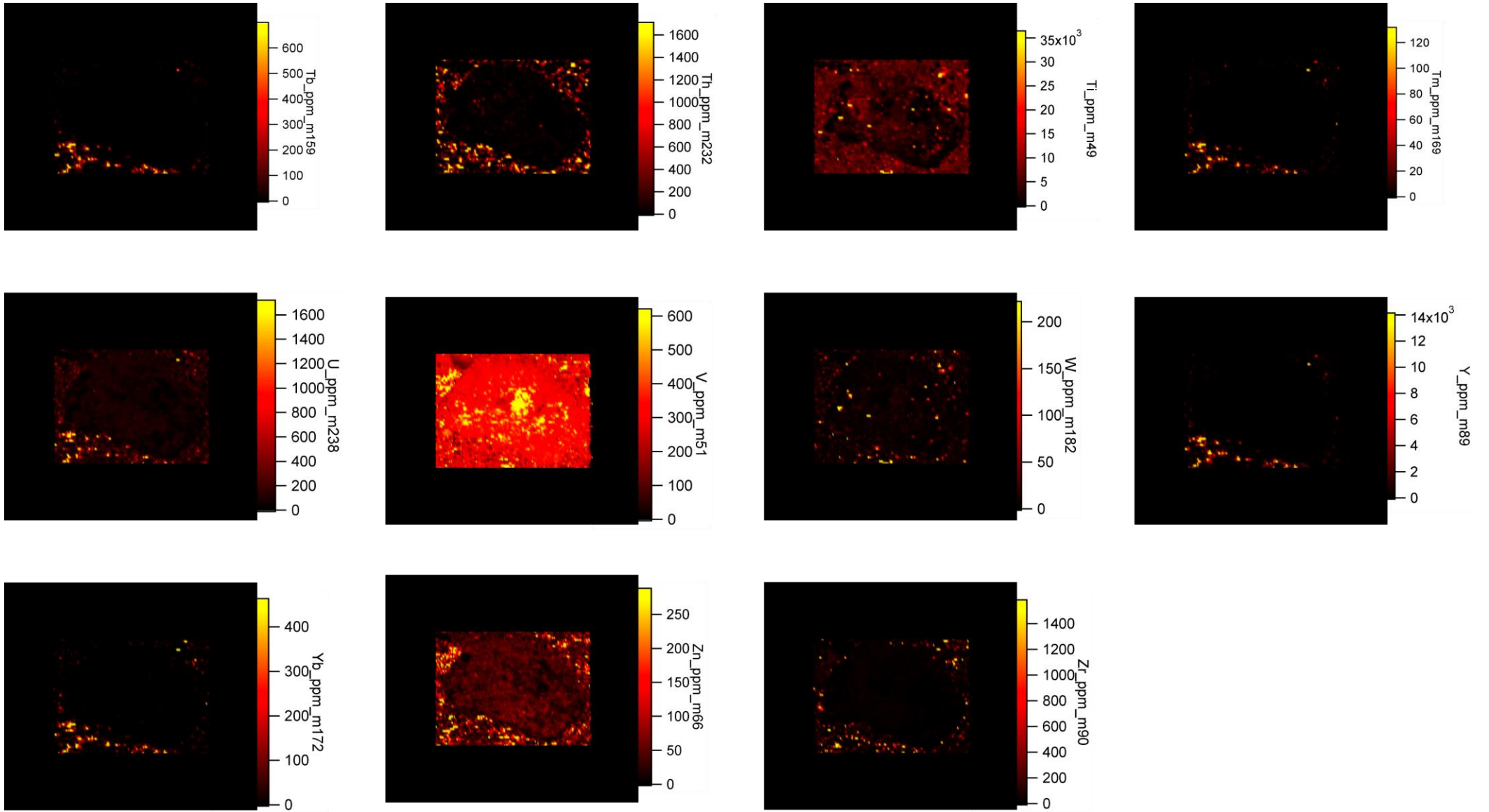




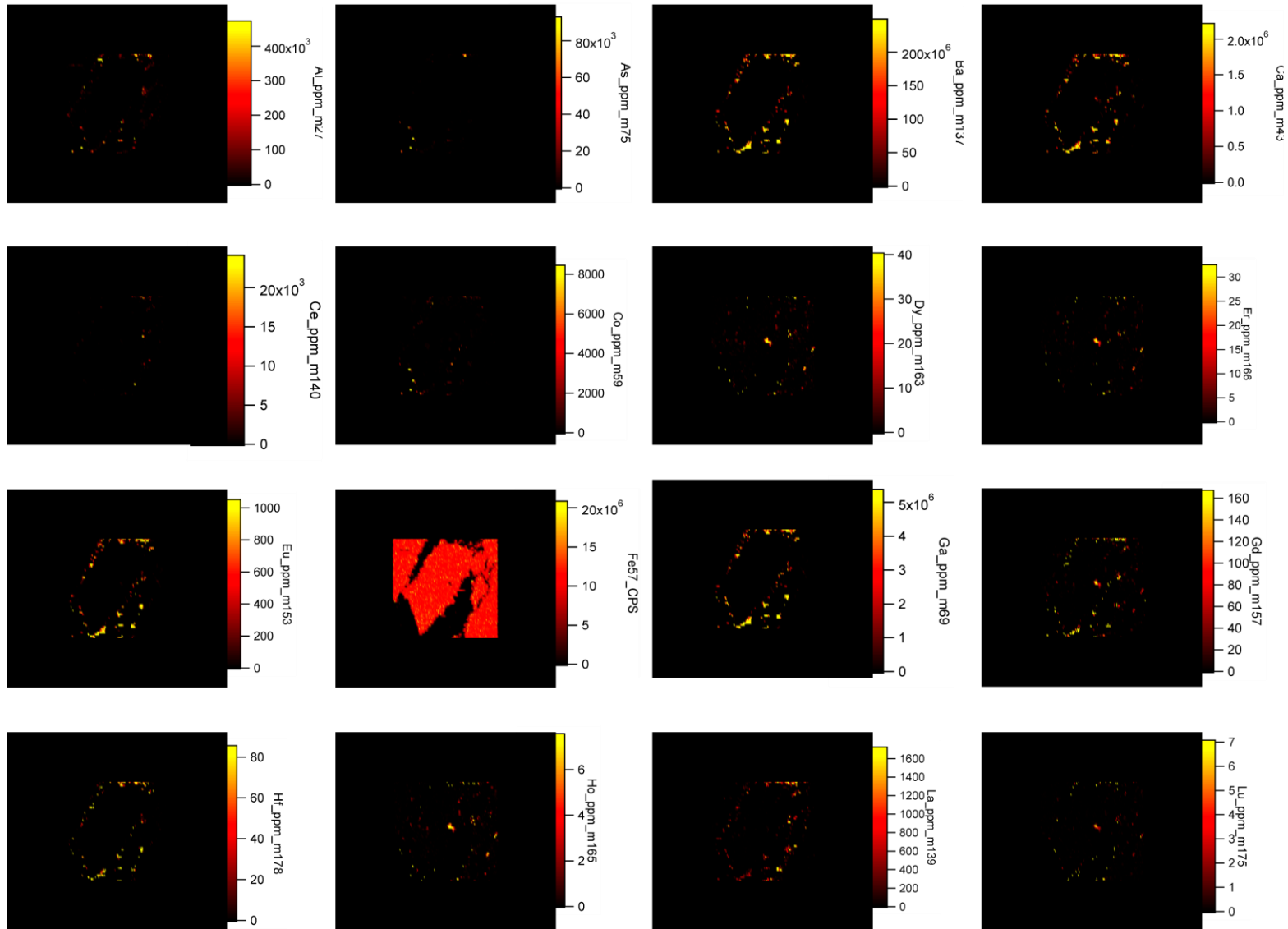
Sample 852 - Hematite Grain 1:

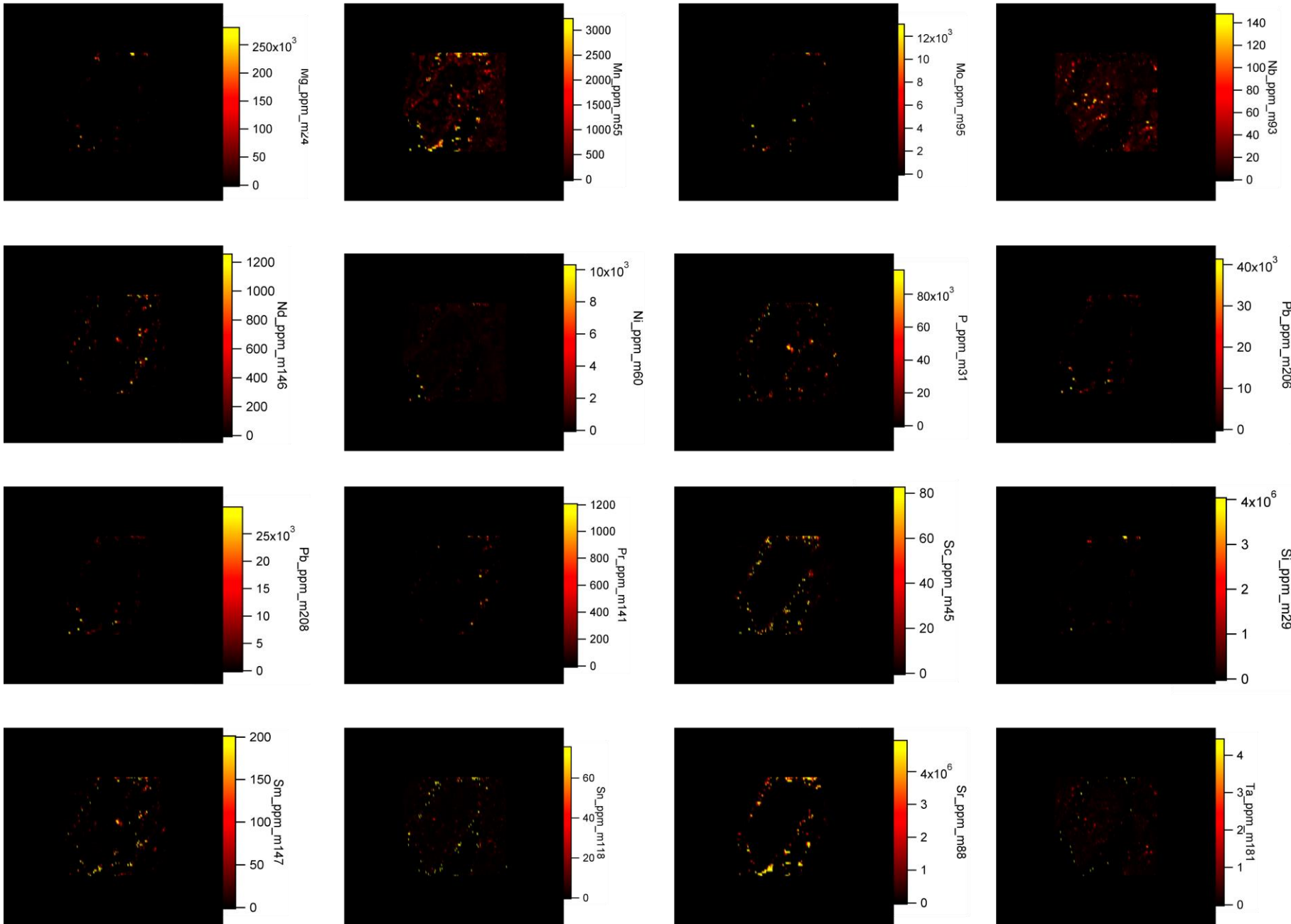


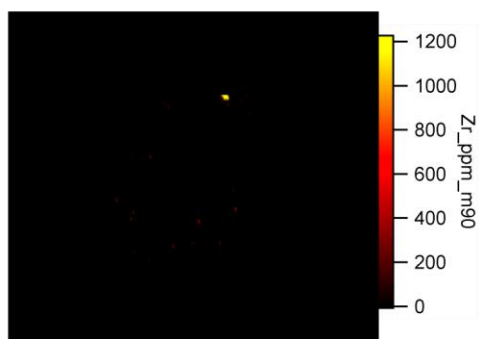
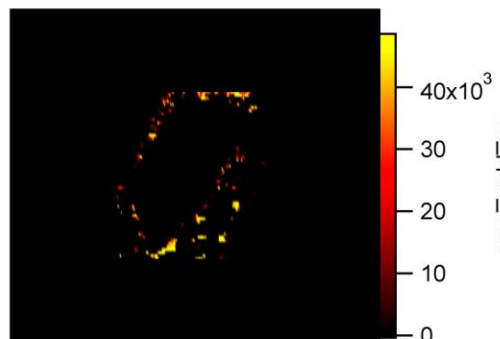
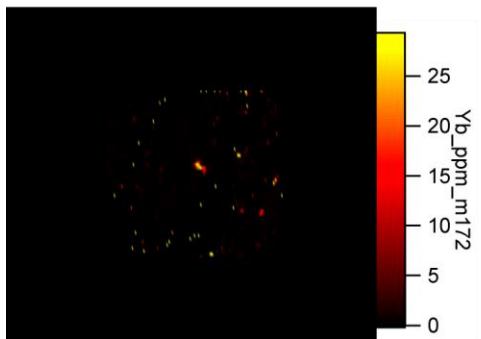
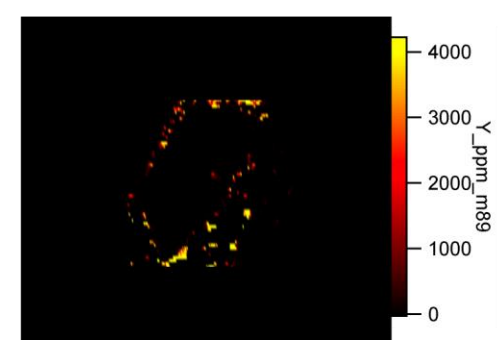
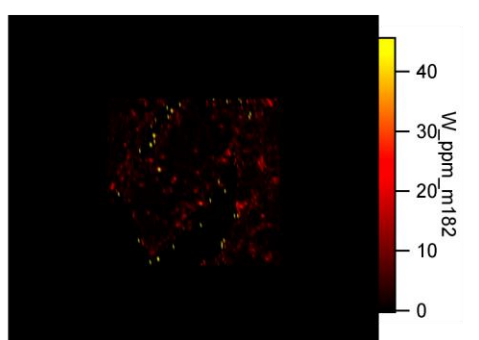
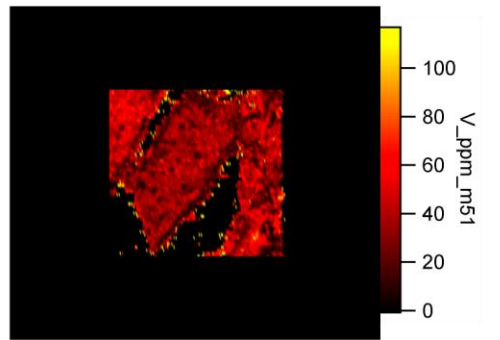
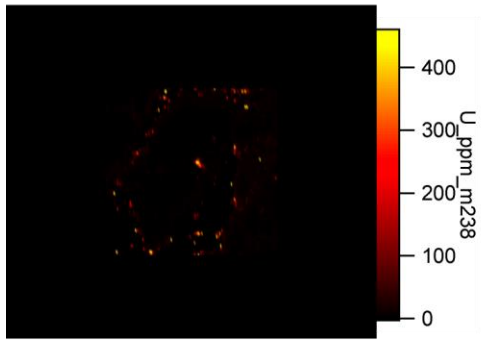
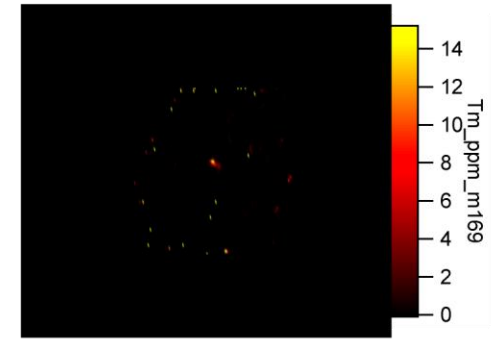
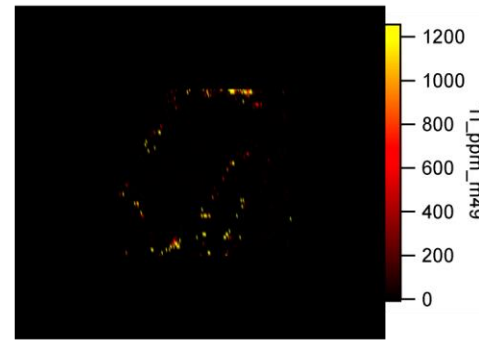
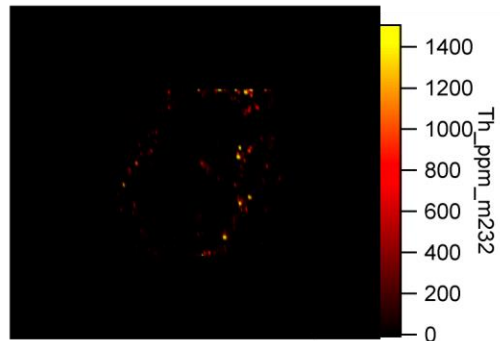
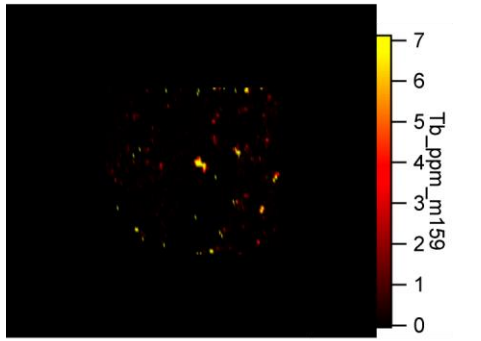




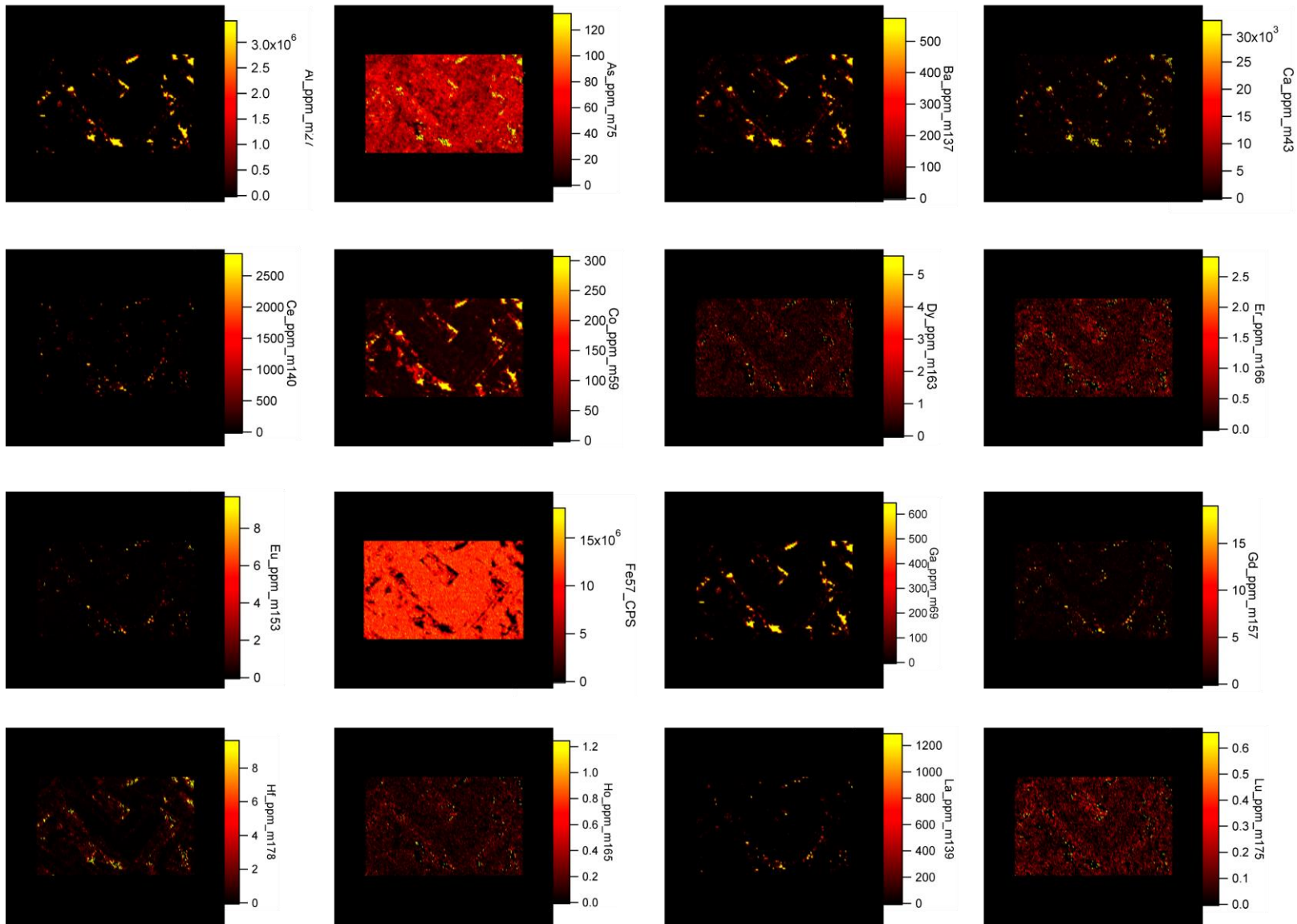
Sample 973 - Hematite Grain 1:

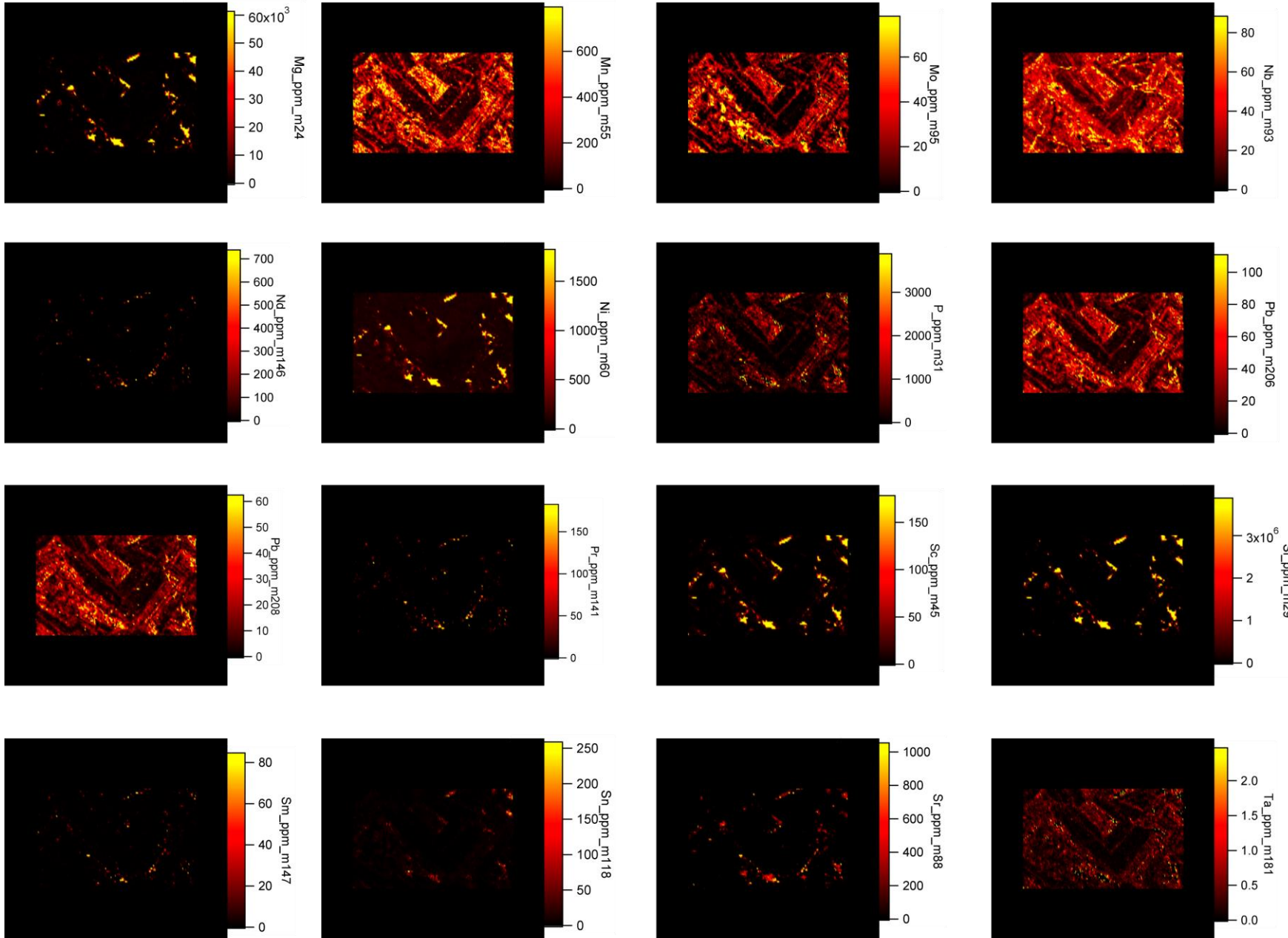


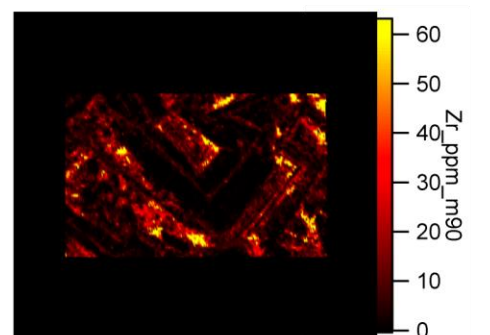
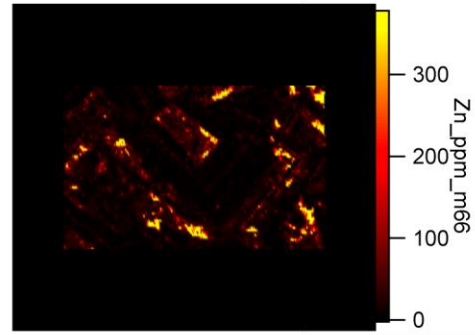
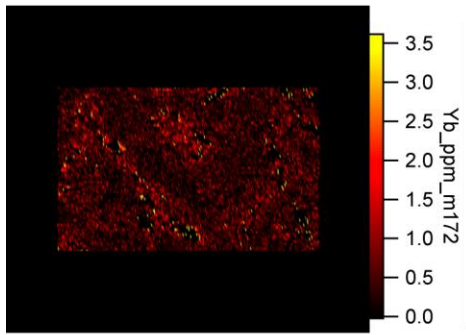
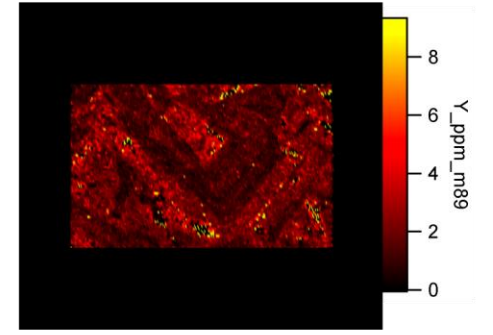
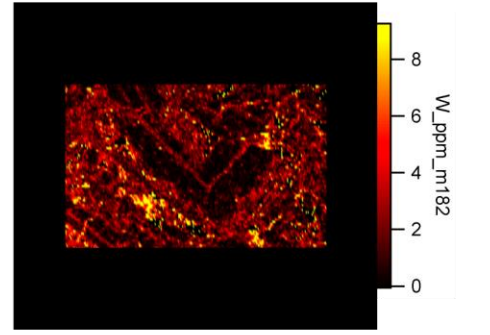
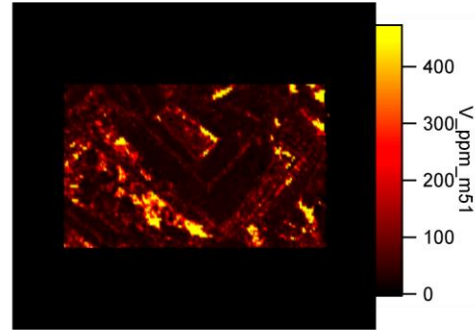
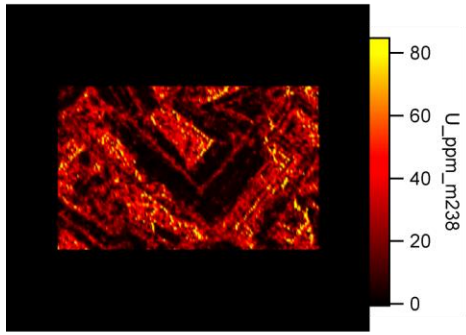
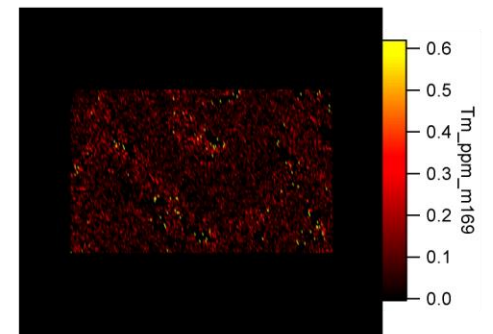
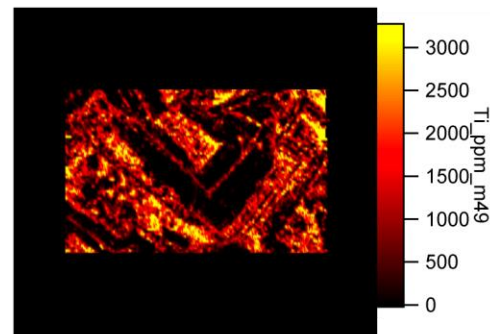
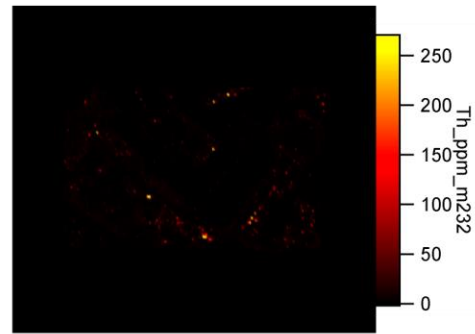
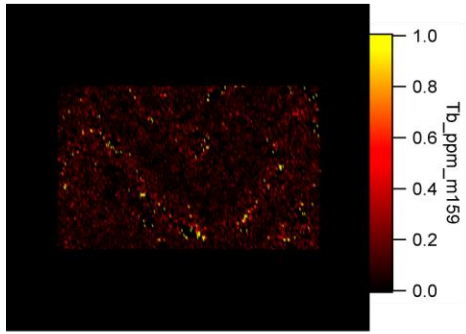




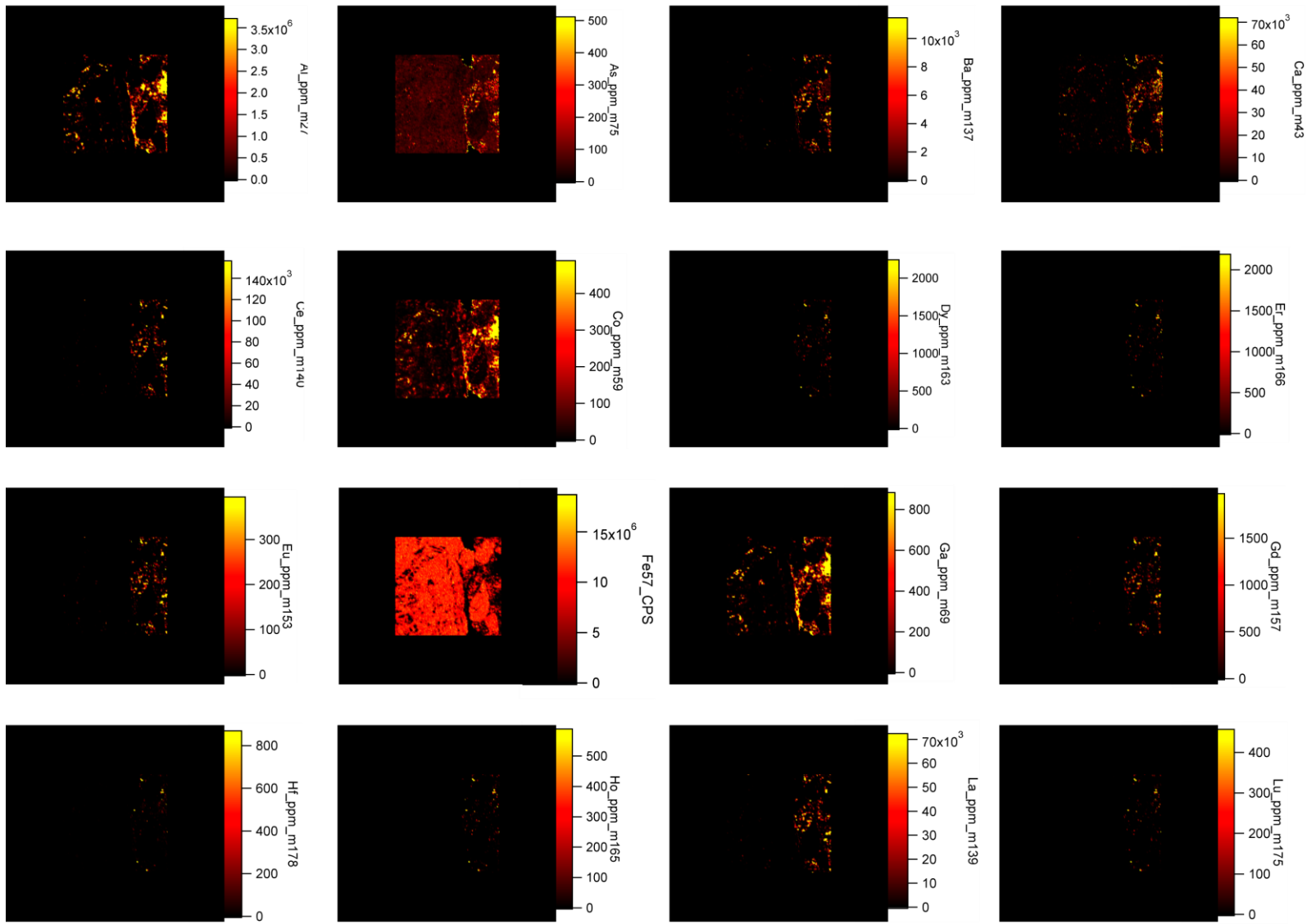
Sample 994 - Hematite Grain 1:

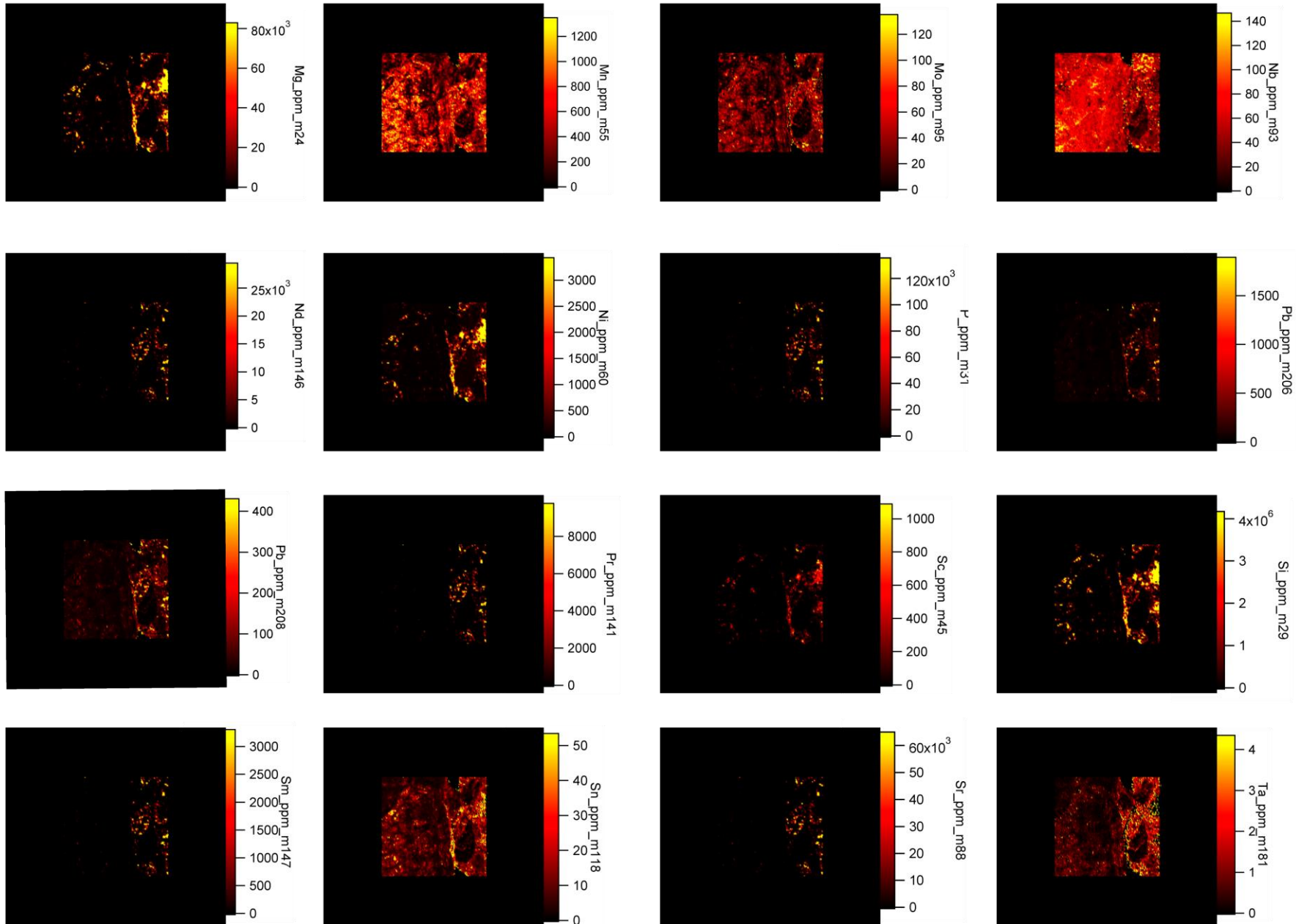


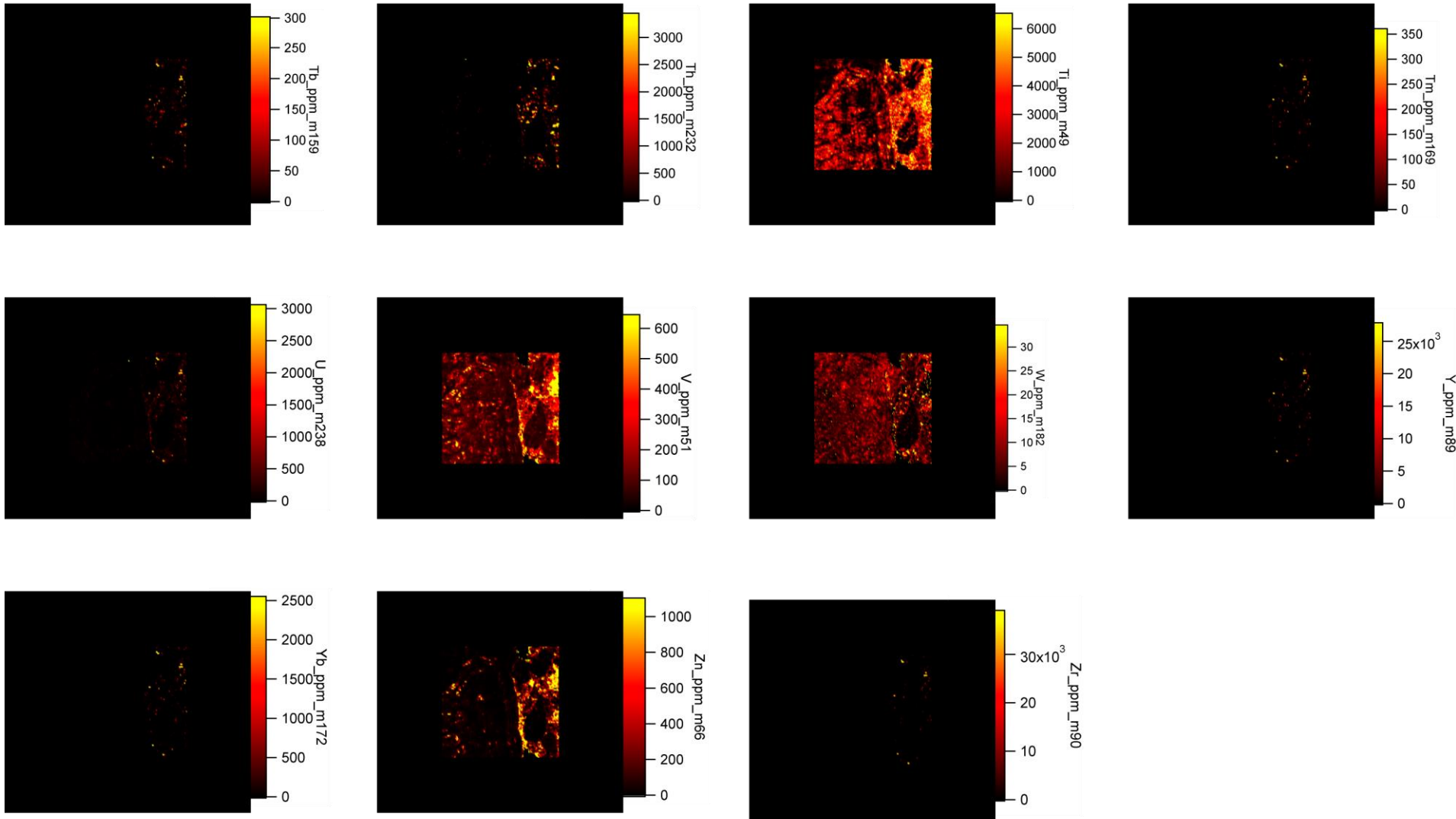




Sample 994 - Hematite Grain 2:







APPENDIX G: HEMATITE TRACE ELEMENT DATA

Sample	La ppm	Ce ppm	Pr ppm	Nd ppm	Sm ppm	Eu ppm	Gd ppm	Tb ppm	Dy ppm	Ho ppm	Er ppm	Tm ppm	Yb ppm	Lu ppm
852(1)-1	1.3103	4.9784	0.8219	4.3269	1.1271	0.1460	1.0437	0.1486	0.7570	0.1624	0.4381	0.0570	0.6194	0.0728
852(1)-10	0.0384	0.1752	0.0321	0.1228	-0.0052	-0.0047	-0.0120	0.0059	-0.0021	0.0024	0.0173	-0.0016	0.0107	0.0054
852(1)-11	0.5846	3.3935	0.7165	3.3508	0.7563	0.1822	0.8897	0.1202	0.9212	0.2050	0.5363	0.0871	0.5454	0.0803
852(1)-12	0.6505	2.3651	0.3470	1.4598	0.4999	0.0382	0.3980	0.0644	0.2678	0.0714	0.1769	0.0210	0.3020	0.0690
852(1)-13	0.4605	2.9742	0.3916	2.5427	0.8776	0.0820	0.6421	0.0666	0.4144	0.1210	0.1819	0.0326	0.2843	0.0451
852(1)-15	0.3856	2.1777	0.4329	2.0633	0.4341	0.1048	0.5714	0.0667	0.3865	0.0764	0.3705	0.0130	0.2517	0.0272
852(1)-16	2.4588	5.2490	0.6219	4.6223	0.4304	0.0399	0.2515	0.0200	0.1865	0.0364	0.1179	0.0088	0.0948	0.0181
852(1)-17	1.2449	4.7157	0.5170	2.5516	0.1710	0.0456	0.2886	0.0384	0.2302	0.0204	0.0891	0.0281	0.0994	0.0053
852(1)-18	11.8134	29.9148	4.2069	16.1171	2.1447	0.2018	1.4619	0.1857	0.7898	0.1899	0.5625	0.0819	0.4295	0.0531
852(1)-19	2.6535	8.4468	1.1203	4.1505	0.6106	0.0577	0.4281	0.0478	0.2485	0.0416	0.1484	0.0329	0.1403	0.0118
852(1)-2	0.5759	3.8108	0.7052	3.3771	0.6842	0.1110	1.1028	0.1672	0.7303	0.1733	0.5817	0.0837	0.7155	0.1000
852(1)-20	2.9120	6.3189	0.8324	2.9472	0.1602	0.0224	0.2992	0.0183	0.1652	0.0377	0.0990	0.0148	0.1540	0.0071
852(1) - 21	1.1304	1.3285	0.1411	0.7182	0.0331	-0.0031	0.0059	0.0048	0.0295	0.0018	0.0209	0.0014	0.0078	0.0016
852(1)-22	0.1174	0.4602	0.0666	0.3125	0.0374	0.0215	0.0280	0.0064	0.0758	0.0077	0.0759	0.0155	0.0216	0.0101
852(1)-23	0.7058	1.9759	0.1862	0.8585	0.1980	0.0124	0.0834	0.0107	0.0752	0.0150	0.0668	0.0039	0.0662	0.0122

852(1)-24	9.2224	32.2423	4.2184	15.5113	2.1782	0.2431	0.7656	0.1058	0.3517	0.0735	0.1549	0.0369	0.1094	0.0165
852(1)-25	8.0701	21.7282	2.7548	9.8377	1.4627	0.1322	0.6976	0.0547	0.2769	0.0394	0.1621	0.0209	0.1639	0.0337
852(1) - 26	0.2287	0.7060	0.1042	0.3329	0.1954	0.0140	0.1262	0.0129	0.2143	0.0236	0.0649	0.0172	0.1364	0.0251
852(1)-27	1.7585	5.5861	0.6781	2.7047	0.5559	0.0829	0.2699	0.0437	0.2113	0.0627	0.1201	0.0215	0.1521	0.0355
852(1)-28	3.0951	8.9103	1.0793	4.1494	0.7285	0.0545	0.3792	0.0269	0.0932	0.0269	0.1108	0.0254	0.1188	0.0141
852(1)-29	0.2097	0.7739	0.1438	0.5913	0.1139	0.0049	0.1950	0.0216	0.1139	0.0338	0.1035	0.0115	0.1491	0.0121
852(1)-3	5.9436	15.1853	2.1145	8.4983	1.7173	0.1625	1.1809	0.0985	0.7940	0.2173	0.7682	0.0837	0.9712	0.0747
852(1)-30	1.2447	4.4860	0.5053	2.5041	0.4148	0.0483	0.1783	0.0282	0.1937	0.0164	0.0877	0.0173	0.2241	0.0490
852(1) - 31	0.6378	2.0187	0.3429	0.9135	0.0875	0.0243	0.1639	0.0077	0.0494	0.0096	0.0292	0.0084	0.0791	0.0132
852(1)-32	0.7000	2.4696	0.2315	0.9596	0.0903	0.0082	0.1513	0.0219	0.1221	0.0276	0.0762	0.0158	0.0648	0.0166
852(1) - 33	0.2274	0.7876	0.0811	0.2852	0.0906	0.0144	0.0060	0.0092	0.0500	0.0070	0.0290	0.0212	0.0423	0.0044
852(1)-35	0.2881	1.9486	0.1613	1.2137	0.2799	0.0296	0.1866	0.0377	0.1566	0.0327	0.1227	0.0116	0.2008	0.0315
852(1)-37	0.3279	0.9589	0.0864	0.3829	0.2005	0.0172	0.0282	0.0134	0.0587	0.0240	0.0819	0.0197	0.0919	0.0110
852(1)-38	0.3323	1.1117	0.1364	0.7101	0.1093	0.0020	0.0646	0.0216	0.1211	0.0080	0.0443	0.0139	0.0452	0.0184
852(1)-39	0.0677	0.5711	0.0942	0.3998	0.0138	0.0080	0.1139	0.0200	0.0550	0.0120	0.0674	0.0174	0.1321	0.0239
852(1)-4	0.1403	0.6638	0.0868	0.4173	0.1158	0.0139	0.1009	0.0206	0.0651	0.0152	0.0720	0.0064	0.0435	0.0120
852(1)-40	1.2168	3.3880	0.3334	1.2270	0.1683	0.0251	0.1357	0.0106	0.1007	0.0273	0.0826	0.0213	0.0893	0.0127

852(1)-41	0.4493	3.7665	0.5777	4.2968	0.9640	0.0768	0.6163	0.0919	0.7326	0.2042	0.5691	0.0984	0.9885	0.1097
852(1)-42	0.3076	1.2847	0.1538	0.4782	0.1822	0.0247	0.0686	0.0200	0.0529	0.0199	0.0950	0.0054	0.0978	0.0147
852(1)-43	14.4694	44.3611	5.1894	21.5436	2.8590	0.2852	1.3131	0.1667	0.7174	0.0995	0.2405	0.0354	0.2875	0.0311
852(1)-44	0.9251	2.7793	0.3710	1.7053	0.3815	0.0207	0.1038	0.0458	0.0975	0.0267	0.0806	0.0250	0.0691	0.0177
852(1)-45	7.2082	21.0409	2.4924	9.0981	1.6886	0.1102	0.8194	0.1483	0.9063	0.1385	0.5540	0.0709	0.3611	0.0450
852(1)-46	0.9078	4.3293	0.6862	3.2210	1.1870	0.1079	0.9002	0.1242	0.7088	0.1319	0.5233	0.0583	0.6696	0.0902
852(1)-47	0.9209	2.8067	0.3441	1.2859	0.1477	0.0154	0.1119	0.0360	0.1744	0.0375	0.1043	0.0104	0.0742	0.0201
852(1)-48	7.6545	24.6292	2.7713	10.4604	1.4526	0.1351	0.6235	0.0588	0.1281	0.0536	0.1074	0.0195	0.2623	0.0254
852(1)-49	5.0248	17.0168	1.9150	6.7510	0.8871	0.0756	0.6810	0.0339	0.1382	0.0452	0.0830	0.0228	0.1520	0.0332
852(1) - 50	0.1379	0.6913	0.0912	0.4004	0.1482	0.0144	0.1907	0.0228	0.0477	0.0322	-0.0025	0.0075	0.0331	0.0032
852(1)-51	0.3776	1.3208	0.1680	0.7308	0.2671	0.0182	0.0562	0.0213	0.0567	0.0261	0.0788	0.0044	0.0503	0.0133
852(1) - 52	0.4535	1.4790	0.1243	1.1720	0.1443	0.0125	0.0825	0.0079	0.0317	0.0060	0.0038	0.0020	0.0163	0.0079
852(1)-53	1.8682	5.7803	0.6464	2.3192	0.2778	0.0410	0.3280	0.0303	0.1414	0.0098	0.0486	0.0214	0.1359	0.0195
852(1)-54	7.8681	19.0531	2.6179	8.3420	1.1613	0.1117	0.5278	0.0335	0.1565	0.0191	0.0804	0.0124	0.0949	0.0135
852(1)-55	4.5622	16.3312	1.6890	7.7330	2.0248	0.2103	1.3680	0.1489	0.7451	0.1559	0.2970	0.0561	0.3402	0.0243
852(1)-56	0.9951	3.0745	0.3751	1.3067	0.2469	0.0219	0.1571	0.0068	0.0520	0.0113	0.0414	0.0042	0.0922	0.0062
852(1)-57	1.2990	3.5901	0.4590	1.6572	0.3379	0.0324	0.1241	0.0179	0.0989	0.0138	0.0638	0.0081	0.0500	0.0211

852(1)-58	2.8972	12.6017	1.3475	6.5452	1.3085	0.1493	1.0211	0.0925	0.5335	0.1394	0.3753	0.0327	0.2416	0.0374
852(1)-59	3.0894	9.1337	1.1427	4.2880	0.6257	0.0699	0.1927	0.0396	0.2297	0.0416	0.1265	0.0025	0.1253	0.0211
852(1)-6	0.5235	2.2662	0.3252	1.2056	0.1963	0.0031	0.3074	0.0111	0.1274	0.0364	0.0884	0.0143	0.1019	0.0171
852(1) - 8	0.0176	0.1522	0.0178	0.1038	0.0157	0.0025	0.0078	- 0.0002	0.0313	0.0020	0.0400	0.0021	0.0088	0.0045
852(1)-9	1.8668	8.1349	1.2464	6.7498	1.4438	0.2601	1.8553	0.2324	1.5680	0.3947	1.0882	0.1552	1.2070	0.1591
973(1)-1	920.4311	1339.725 0	105.596 9	218.6876	26.6903	3.8845	12.528 9	0.6619	2.5217	0.5502	2.3276	0.2771	1.9609	0.2328
973(1)-10	102.7986	152.2331	11.0722	28.2967	3.3613	0.4790	1.1726	0.1151	0.6106	0.1194	0.4089	0.0299	0.3424	0.0593
973(1)-11	28.8280	51.0558	4.2893	11.2756	2.2311	0.1523	0.7909	0.0872	0.6621	0.1054	0.3820	0.0326	0.4505	0.0420
973(1)-12	369.3506	598.7091	45.0119	101.0187	11.9365	1.4374	5.1101	0.2351	1.1439	0.2702	1.1099	0.1032	0.6312	0.0865
973(1)-13	1886.0110	2860.578 5	201.052 3	487.8082	55.7136	8.2347	23.831 1	1.0118	3.7723	0.8658	2.4184	0.2718	1.6632	0.1825
973(1)-14	6.1208	11.6316	1.0283	3.7076	0.4074	0.0279	0.3891	0.0568	0.2699	0.1171	0.3300	0.0760	0.3571	0.0820
973(1)-15	907.0642	1334.536 7	88.4199	218.5523	25.2676	4.2425	12.138 8	0.5912	2.3794	0.7130	2.2362	0.2985	1.4559	0.1461
973(1)-16	14.6923	15.7693	1.4396	4.2493	0.5239	0.0333	0.5642	0.0947	0.7436	0.1393	0.4465	0.0624	0.3289	0.0659
973(1)-17	209.6520	354.9375	33.3924	62.5233	19.1785	3.7000	37.924 6	5.2414	32.126 3	5.9661	14.199 8	1.4033	6.2970	0.6693
973(1)-18	1415.5575	2043.802 9	136.303 1	322.8260	41.7010	4.8117	17.734 6	1.2301	5.0199	0.9319	2.4626	0.3387	1.6572	0.2526
973(1)-19	45.5762	84.3854	7.9260	28.0512	3.1599	0.2806	1.4414	0.1553	0.8916	0.1706	0.6135	0.1314	0.7243	0.1193
973(1)-2	161.9883	206.8790	14.4563	46.2621	4.0531	0.7288	3.0856	0.3195	2.1200	0.5084	1.5094	0.3446	1.6388	0.2453
973(1)-20	3.4278	10.7121	0.3755	0.8231	0.0342	0.0188	0.0210	0.0203	0.1455	0.0317	0.1153	0.0146	0.2355	0.0411

973(1)-21	2.6773	5.0122	0.4194	1.1196	0.1279	0.0267	0.0621	0.0094	0.0664	0.0132	0.1057	0.0286	0.1801	0.0117
973(1)-22	54.5278	85.0576	6.5327	15.7131	1.6894	0.3733	1.2450	0.1003	0.1873	0.0844	0.3552	0.0192	0.2581	0.0443
973(1)-23	139.1514	223.7601	13.2414	33.3340	3.8754	0.5801	1.8835	0.0830	0.3837	0.1331	0.3864	0.0441	0.4543	0.0538
973(1)-24	38.0106	68.5003	4.2807	11.1542	1.3443	0.2371	0.6848	0.0872	0.5147	0.1303	0.6044	0.0690	0.4640	0.0814
973(1)-25	165.5856	210.5158	14.0009	44.8441	4.5224	0.5846	2.1537	0.1485	0.9280	0.1615	0.4903	0.1398	0.6052	0.0793
973(1) - 26	0.6783	1.8884	0.0923	0.3916	0.1279	0.0494	0.0410	0.0160	0.1100	0.0167	0.0597	0.0161	0.1285	0.0354
973(1)-27	29.9921	49.6530	3.9518	9.2740	1.2721	0.6265	3.5653	0.3266	1.4982	0.2570	0.6079	0.0786	0.5539	0.1099
973(1)-28	78.7832	135.2453	12.1776	42.0947	3.6039	0.2050	1.7665	0.2386	1.0601	0.2644	0.6410	0.0612	0.3893	0.0531
973(1) - 29	0.4212	1.1880	0.1423	0.7033	0.1429	0.0185	0.0915	0.0527	0.1359	0.0430	0.1945	0.0352	0.0823	0.0180
973(1)-3	112.7442	187.2795	17.6940	62.0851	4.4511	0.4966	2.7237	0.3507	2.0713	0.3984	1.1549	0.1348	1.1980	0.1925
973(1) - 30	1.0959	1.4516	0.1544	0.4425	0.0724	0.0194	0.0742	0.0126	0.2224	0.0813	0.1893	0.0333	0.2314	0.0488
973(1) - 31	0.0216	0.0711	0.0133	-0.0044	0.0266	-0.0039	-0.0112	0.0019	0.0318	-0.0008	0.0104	0.0029	0.0333	0.0072
973(1) - 32	0.0107	0.0334	0.0024	-0.0045	-0.0049	0.0038	0.0290	0.0016	-0.0020	0.0021	0.0064	-0.0009	0.0093	0.0021
973(1)-33	4186.5005	6263.0757	348.6994	908.8117	84.9611	14.0417	39.6620	1.9176	6.3971	1.2864	3.8953	0.4273	2.9321	0.3804
973(1)-34	6.8916	7.8591	1.1219	2.5477	0.3212	0.1026	0.4209	0.0505	0.1625	0.0457	0.0842	0.0254	0.2556	0.0441
973(1)-35	3.8447	6.7547	0.4556	1.5904	0.3010	0.0355	0.3668	0.0227	0.2749	0.0426	0.1582	0.0155	0.2477	0.0254
973(1)-36	0.7315	1.9397	0.1563	0.5541	0.0975	0.0044	0.0452	0.0253	0.2429	0.0374	0.1335	0.0187	0.2007	0.0387

973(1)-37	128.6159	181.0242	13.4560	30.7904	4.2590	0.6420	3.2964	0.3332	1.8749	0.5365	6.4199	0.2666	1.3980	0.3556
973(1) - 38	0.7735	2.6649	0.0923	0.5635	0.0485	0.0489	0.1383	0.0131	0.3076	0.0351	0.2323	0.0193	0.1227	0.0373
973(1)-39	4784.7217	7369.406 ₃	514.899 ₉	1176.924 ₂	144.020 ₅	28.121 ₂	93.890 ₀	6.8691	21.994 ₀	3.5843	8.6526	0.8852	4.4328	1.2480
973(1)-4	404.8476	610.6054	61.8398	118.2088	15.3904	2.4538	8.8641	1.0458	5.4875	1.0880	5.1328	0.5398	3.1467	0.5141
973(1) - 40	1.0498	2.0412	0.2867	1.1017	0.0360	-0.0005	0.0651	0.0028	0.0828	0.0209	0.0649	0.0092	0.0444	0.0149
973(1)-42	1709.3496	2603.801 ₁	167.591 ₇	456.7073	44.7538	6.5298	24.474 ₉	0.9578	3.6692	0.9215	3.0659	0.3219	1.7749	0.1517
973(1)-43	0.2434	0.7140	0.0338	0.2099	0.0378	0.0011	0.1084	0.0169	0.2544	0.0394	0.1884	0.0280	0.2159	0.0287
973(1)-44	0.7588	1.5445	0.1046	0.2039	0.0536	0.0383	0.1531	0.0313	0.1509	0.0229	0.2016	0.0225	0.1888	0.0413
973(1)-5	6.3325	17.1968	2.5131	7.4278	0.9212	1.0956	0.8490	0.1551	0.9744	0.1675	0.4734	0.1060	0.8000	0.1791
973(1)-6	11.4047	24.6408	2.3595	6.4894	0.9468	1.0691	0.6263	0.0691	0.7148	0.1650	0.6585	0.1371	1.4394	0.2083
973(1) - 7	2.4412	4.0202	0.3199	1.2571	-0.0050	0.1018	0.1506	0.0032	0.2468	0.0506	0.1569	0.0712	0.5386	0.1186
973(1)-8	2048.5671	2929.679 ₀	206.783 ₃	538.4096	63.0739	7.7153	25.940 ₈	0.9704	3.1918	0.4134	1.3013	0.1107	1.2081	0.1615
973(1)-9	18.1768	32.6120	2.0286	5.4818	0.9677	0.0839	0.5158	0.0494	0.4940	0.0866	0.3387	0.0474	0.3059	0.0454
994(1)-1	0.6307	2.1658	0.3303	1.2928	0.1370	0.0258	0.0848	0.0412	0.0764	0.0738	0.1865	0.0219	0.1854	0.0399
994(1)-10	0.6198	2.3926	0.3280	1.2001	0.3927	0.0222	0.1513	0.0311	0.1027	0.0381	0.1163	0.0246	0.1208	0.0193
994(1) - 11	0.1174	0.3856	0.0510	0.3618	0.0994	-0.0019	-0.0108	0.0262	0.0345	0.0038	0.0252	0.0080	0.0565	0.0035
994(1) - 12	0.6240	2.3339	0.3127	2.3122	0.4455	0.0406	0.1780	0.0255	0.1858	0.0227	0.1499	0.0271	0.2827	0.0499
994(1)-13	0.3377	1.8572	0.1990	1.1700	0.3243	0.0370	0.1803	0.0251	0.1583	0.0313	0.1528	0.0422	0.1982	0.0712
994(1)-14	1.5669	4.6823	0.4914	1.9561	0.0665	0.0628	0.1880	0.0415	0.2991	0.0654	0.0981	0.0218	0.4372	0.0535

994(1)-15	3.5929	11.7232	1.4956	7.5345	1.3433	0.1681	0.8083	0.0841	0.3643	0.0717	0.1268	0.0270	0.5591	0.0631
994(1)-16	0.5674	1.6215	0.1636	0.7878	0.1631	0.0166	0.0826	0.0082	0.1035	0.0296	0.1170	0.0275	0.1505	0.0367
994(1)-17	0.6096	2.1997	0.2623	1.0015	0.2589	0.0178	0.1440	0.0265	0.1843	0.0418	0.1376	0.0333	0.2144	0.0275
994(1)-18	0.3659	1.6141	0.1470	0.5237	0.2364	0.0066	0.1531	0.0223	0.1892	0.0225	0.1528	0.0069	0.2218	0.0215
994(1)-19	1.1318	1.4550	0.2050	1.0484	0.2367	0.0052	0.1431	0.0231	0.1925	0.0280	0.1003	0.0332	0.2840	0.0385
994(1) - 2	0.2778	1.0289	0.1708	0.7794	0.2203	0.0094	0.1305	0.0343	0.1255	0.0313	0.1571	0.0170	0.1605	0.0369
994(1)-20	0.2568	0.7726	0.1382	0.5977	0.1818	-0.0032	0.1565	0.0076	0.1303	0.0232	0.2446	0.0223	0.1744	0.0299
994(1)-21	0.2422	1.3018	0.2634	0.9237	0.1866	0.0288	0.0953	0.0339	0.2376	0.0483	0.1481	0.0038	0.2138	0.0418
994(1) - 22	0.4481	1.2640	0.2246	0.7241	0.2332	0.0265	0.1589	0.0390	0.2207	0.0333	0.1856	0.0182	0.2228	0.0320
994(1)-23	2.2588	5.2213	0.6416	1.7778	0.2449	0.0044	0.1929	0.0271	0.1298	0.0492	0.0853	0.0295	0.1388	0.0336
994(1)-24	0.6245	2.3344	0.3494	1.4304	0.2839	0.0240	0.1656	0.0218	0.2349	0.0447	0.1628	0.0299	0.2897	0.0491
994(1)-25	0.3216	1.1276	0.1418	0.7801	0.1422	0.0045	0.0275	0.0477	0.1602	0.0507	0.1558	0.0147	0.1404	0.0358
994(1)-26	1.7338	5.4481	0.6556	2.4506	0.9529	0.0455	0.2752	0.0510	0.3685	0.0397	0.1757	0.0485	0.2271	0.0382
994(1)-27	0.9820	3.4610	0.4374	2.2091	0.2499	0.0560	0.4275	0.0365	0.1803	0.0526	0.2251	0.0419	0.2509	0.0507
994(1) - 28	0.3765	1.1249	0.1328	0.7578	0.1502	0.0262	0.1792	0.0395	0.2001	0.0292	0.1106	0.0328	0.1883	0.0249
994(1)-29	0.5292	1.6421	0.1985	0.9525	0.3011	0.0153	0.2144	0.0465	0.1091	0.0387	0.0829	0.0286	0.2238	0.0144
994(1)-3	0.7128	1.9140	0.2551	0.9453	0.1784	0.0478	0.1325	0.0198	0.1599	0.0273	0.1208	0.0107	0.1385	0.0068

994(1) - 30	0.9443	2.7352	0.2949	1.3866	0.2414	0.0247	0.3289	0.0441	0.2461	0.0533	0.1547	0.0284	0.2501	0.0207
994(1) - 31	0.4568	1.1328	0.1345	0.6687	0.0781	0.0134	0.1925	0.0210	0.1307	0.0207	0.0859	0.0120	0.0756	0.0164
994(1) - 32	0.1496	0.5981	0.0646	0.2513	0.0538	0.0143	0.0695	0.0033	0.0770	0.0106	0.0798	0.0066	0.0636	0.0175
994(1) - 33	2.4150	6.5167	0.8017	2.8346	0.5609	0.0251	0.2654	0.0242	0.1066	0.0318	0.0373	0.0042	0.0240	0.0179
994(1) - 34	24.3754	50.8050	4.6372	11.9980	1.6127	0.1803	0.9197	0.0784	0.5107	0.0673	0.3062	0.0523	0.3801	0.0499
994(1) - 35	0.8905	3.1048	0.4105	1.5528	0.3619	0.0291	0.1880	0.0472	0.3066	0.0746	0.1620	0.0491	0.3549	0.0505
994(1) - 36	1.3562	4.6216	0.5438	2.6779	0.3170	0.0589	0.2068	0.0728	0.0839	0.0198	0.2891	0.0189	0.2729	0.0392
994(1) - 38	0.4870	1.6541	0.2366	0.7249	0.2554	-0.0010	0.1492	0.0103	0.1325	0.0254	0.1022	0.0135	0.1620	0.0318
994(1) - 39	0.6406	2.8841	0.3100	1.2530	0.2740	0.0311	0.1996	0.0385	0.2444	0.0518	0.1710	0.0268	0.2870	0.0500
994(1) - 40	0.6144	2.0891	0.2190	1.0401	0.1423	0.0118	0.1929	0.0302	0.1981	0.0437	0.1359	0.0227	0.1651	0.0207
994(1) - 41	0.2435	0.6870	0.0404	0.3404	-0.0064	0.0274	-0.0149	0.0201	0.0186	0.0145	0.0454	0.0079	-0.0048	0.0038
994(1) - 42	0.7707	2.2947	0.2790	1.5648	0.3281	0.0271	0.2348	0.0457	0.1955	0.0454	0.1329	0.0287	0.1875	0.0271
994(1) - 43	0.7529	4.1430	0.5530	2.1577	0.4564	0.0617	0.3250	0.0522	0.3320	0.0909	0.3242	0.0409	0.3736	0.0635
994(1) - 44	0.2419	1.1351	0.1660	1.0162	0.1534	0.0941	0.0343	0.0525	0.2848	0.0479	0.1808	0.0379	0.4116	0.0503
994(1) - 45	1.2290	4.9397	0.5100	2.2602	0.4019	0.0552	0.1659	0.0744	0.2830	0.0690	0.1199	0.0335	0.4281	0.0533
994(1) - 46	5.9711	19.7879	2.0317	7.7884	1.0710	0.0596	0.5793	0.0731	0.1906	0.0527	0.1967	0.0324	0.2150	0.0201
994(1) - 47	1.1163	2.9960	0.3983	1.3481	0.3368	0.0273	0.1708	0.0230	0.1436	0.0274	0.0858	0.0324	0.1311	0.0332

994(1)-48	0.7166	2.3025	0.3588	1.4013	0.1584	0.0297	0.1180	0.0240	0.1239	0.0418	0.1600	0.0337	0.2922	0.0228
994(1)-49	3.7367	10.1082	1.3774	5.6488	0.8164	0.0580	0.4797	0.0594	0.3093	0.0490	0.1851	0.0330	0.3132	0.0571
994(1)-5	0.3822	2.0132	0.2065	1.1089	0.1894	0.0060	0.1955	0.0253	0.1681	0.0467	0.1432	0.0271	0.1417	0.0340
994(1)-50	0.8899	3.1916	0.4200	2.1082	0.2532	0.0230	0.1986	0.0488	0.3368	0.0628	0.2556	0.0528	0.4044	0.0629
994(1)-51	1.0069	3.1629	0.4261	1.8621	0.3643	0.0152	0.4046	0.0263	0.1752	0.0341	0.1071	0.0180	0.1718	0.0377
994(1)-52	0.3821	1.7539	0.1813	0.9002	0.2020	0.0051	0.1585	0.0296	0.2713	0.0537	0.1791	0.0294	0.1947	0.0240
994(1)-53	0.2126	0.6648	0.0626	0.2906	0.0831	0.0113	0.0426	0.0187	0.0807	0.0203	0.0941	0.0071	0.1360	0.0202
994(1)-54	0.4784	2.3124	0.2936	1.4688	0.3761	0.0064	0.1936	0.0322	0.1863	0.0408	0.2200	0.0254	0.3268	0.0355
994(1) - 55	0.1553	0.7736	0.0841	0.5615	0.0730	0.0059	0.0608	0.0232	0.0233	0.0297	0.1361	0.0269	0.0862	0.0024
994(1)-56	0.6550	2.4020	0.2925	1.3113	0.3291	0.0055	0.2454	0.0178	0.2065	0.0430	0.2390	0.0121	0.3026	0.0594
994(1)-57	0.5136	2.5411	0.3469	1.1526	0.4353	0.0798	0.2495	0.0233	0.2363	0.0776	0.1536	0.0512	0.2929	0.0731
994(1)-58	0.5202	2.0136	0.2099	1.8509	0.3828	0.0253	0.1647	0.0499	0.1645	0.0244	0.1723	0.0268	0.2151	0.0472
994(1)-59	1.1152	3.7627	0.4406	1.6580	0.3483	-0.0009	0.2333	0.0343	0.0938	0.0456	0.1436	0.0370	0.1754	0.0329
994(1)-6	0.4122	1.9923	0.2990	1.1569	0.3277	0.0197	0.1815	0.0399	0.1565	0.0361	0.2335	0.0434	0.1449	0.0505
994(1)-60	0.2492	1.0209	0.1489	0.8203	0.1405	0.0098	0.2552	0.0214	0.0884	0.0182	0.1179	0.0142	0.0802	0.0149
994(1) - 61	0.5041	1.3210	0.1289	0.6214	0.0873	0.0102	0.1015	0.0201	0.0985	0.0236	0.1003	0.0162	0.0950	0.0169
994(1)-62	1.3618	4.8010	0.5332	1.8047	0.2457	0.0523	0.2207	0.0392	0.3108	0.0455	0.1541	0.0150	0.2296	0.0345

994(1)-63	0.3692	1.4949	0.2264	0.6786	0.2407	0.0191	0.0411	0.0070	0.1213	0.0392	0.0763	0.0135	0.1727	0.0161
994(1)-64	2.7583	7.1370	0.9430	4.1045	0.5699	0.0523	0.4178	0.0388	0.2765	0.0483	0.2067	0.0289	0.2777	0.0325
994(1)-65	1.4365	3.0690	0.4448	1.9457	0.2708	0.0305	0.1343	0.0282	0.1804	0.0253	0.2611	0.0263	0.1458	0.0473
994(1)-66	1.2531	5.5080	0.5159	2.1157	0.2881	0.0175	0.2435	0.0349	0.2971	0.0477	0.3420	0.0542	0.2422	0.0462
994(1)-67	0.2028	1.0496	0.1437	0.5815	0.1169	0.0119	0.0773	0.0080	0.1865	0.0251	0.0895	0.0273	0.0818	0.0243
994(1)-68	0.5971	2.6843	0.3093	1.5834	0.2910	0.0362	0.1541	0.0354	0.1709	0.0358	0.1707	0.0267	0.2842	0.0600
994(1)-69	0.9027	3.1268	0.4227	1.6792	0.4789	0.0280	0.2206	0.0507	0.3026	0.0325	0.1692	0.0338	0.2361	0.0409
994(1)-7	0.9166	3.1981	0.3577	1.6168	0.2379	0.0349	0.3429	0.0591	0.4123	0.0839	0.2138	0.0458	0.2157	0.0601
994(1)-70	2.2473	6.2936	0.6325	2.7127	0.4329	0.0260	0.2860	0.0495	0.2369	0.0462	0.1527	0.0124	0.1342	0.0382
994(1)-71	4.1762	10.6379	1.0272	3.3643	0.3671	0.0704	0.3601	0.0431	0.3181	0.0557	0.1980	0.0295	0.1986	0.0334
994(1)-72	0.5956	1.7698	0.2192	0.7962	0.2274	0.0249	0.2687	0.0263	0.1785	0.0356	0.2043	0.0361	0.1968	0.0345
994(1)-73	1.3950	4.8153	0.3120	1.4872	0.4409	0.0220	0.1969	0.0147	0.1580	0.0357	0.0622	0.0203	0.1368	0.0212
994(1)-8	0.6070	1.9775	0.2080	1.4387	0.4104	0.0140	0.0924	0.0280	0.2328	0.0752	0.2079	0.0200	0.2532	0.0443
994(1)-9	1.5153	5.1321	0.7970	3.2331	0.2601	-0.0025	0.1661	0.0479	0.2184	0.0437	0.2241	0.0127	0.3031	0.0465
994(2)-1	0.7594	2.6591	0.3512	1.1552	0.1605	0.0212	0.1125	0.0249	0.2785	0.0830	0.1644	0.0485	0.3170	0.0484
994(2)-10	3.9555	11.4472	0.9051	2.5820	0.2474	0.0430	0.1546	0.0590	0.1534	0.0846	0.2157	0.0204	0.1909	0.0390
994(2)-11	1.6837	3.9425	0.4200	1.3907	0.3345	0.0346	0.2930	0.0298	0.2047	0.0252	0.1876	0.0280	0.1582	0.0191
994(2)-12	0.9137	2.9214	0.2320	1.2588	0.2306	0.0321	0.0806	0.0402	0.2933	0.0489	0.2671	0.0157	0.2948	0.0473

994(2)-14	5.2409	41.5508	0.9448	4.7023	0.5512	0.2087	0.2358	0.0686	0.1588	0.0386	0.1890	0.0235	0.1691	0.0372
994(2)-15	2.7315	4.5784	0.5572	2.1095	0.2804	0.0377	0.2368	0.0429	0.1972	0.0600	0.0947	0.0293	0.2945	0.0375
994(2)-16	1.3802	3.9011	0.5363	1.8213	0.1635	0.0281	0.2354	0.0245	0.2235	0.0492	0.1932	0.0398	0.2163	0.0380
994(2)-17	3.5688	4.1708	0.5548	2.2079	0.4737	0.0348	0.3110	0.0612	0.4730	0.0745	0.3330	0.0399	0.2471	0.0567
994(2)-18	8.5039	17.7724	1.4670	5.2470	0.6191	0.0774	0.5158	0.0716	0.3873	0.0672	0.1783	0.0169	0.1682	0.0304
994(2)-19	1.5935	3.8356	0.4657	1.4146	0.2357	0.0462	0.1854	0.0140	0.1822	0.0249	0.2451	0.0270	0.2316	0.0407
994(2)-2	1.4788	4.8063	0.5834	2.5167	0.3866	0.0463	0.3734	0.0439	0.2120	0.0593	0.1949	0.0520	0.2491	0.0548
994(2)-20	1.8127	5.1422	0.5032	2.2978	0.2657	0.0268	0.2828	0.0583	0.2592	0.0909	0.2320	0.0322	0.2773	0.0261
994(2)-21	2.7086	7.8112	0.9367	3.7370	0.6094	0.0594	0.5410	0.0558	0.2264	0.0774	0.2650	0.0257	0.4135	0.0623
994(2)-22	2.8510	6.0328	0.7654	2.2825	0.4320	0.0604	0.4493	0.0489	0.2457	0.0668	0.1794	0.0316	0.1909	0.0285
994(2)-23	1.5703	4.8848	0.6192	1.9095	0.4285	0.0365	0.4153	0.0551	0.2767	0.0780	0.3992	0.0435	0.4117	0.0628
994(2)-24	5.2659	12.4192	0.7567	2.4210	0.4249	0.0730	0.0934	0.0313	0.1206	0.0986	0.1272	0.0286	0.1563	0.0650
994(2)-25	2.4408	6.4261	0.7942	3.2009	0.6032	0.0353	0.3239	0.0612	0.2873	0.0822	0.2627	0.0391	0.3873	0.0509
994(2)-26	1.8211	6.2420	0.6735	2.2283	0.3356	0.0701	0.2811	0.0453	0.3218	0.0722	0.2313	0.0328	0.2826	0.0489
994(2)-27	0.0446	0.1642	0.0472	0.2561	0.0373	0.0046	0.1477	0.0140	0.0871	0.0470	0.1114	0.0259	0.1570	0.0209
994(2)-28	0.9474	2.3318	0.3052	0.9283	0.0534	0.0276	0.0051	0.0072	0.0622	0.0252	0.0457	0.0070	0.0647	0.0066
994(2)-29	1.9622	5.4981	0.6314	2.9834	0.4716	0.0413	0.2114	0.0471	0.2288	0.0655	0.1742	0.0432	0.3984	0.0603

994(2) - 3	0.3491	1.0079	0.0942	0.4326	0.0332	0.0044	0.0422	0.0172	0.1045	0.0346	0.1089	0.0160	0.1076	0.0408
994(2) - 30	0.3823	1.2196	0.1042	0.4748	0.0702	0.0244	0.0757	0.0147	0.1202	0.0342	0.1060	0.0113	0.1828	0.0112
994(2) - 31	1.6036	6.0271	0.9034	3.3084	0.7089	0.0202	0.3009	0.0804	0.4346	0.0743	0.2826	0.0514	0.3261	0.1042
994(2) - 32	7.2889	18.4714	1.5001	4.9834	0.7270	0.0852	0.4669	0.0599	0.4477	0.0854	0.2317	0.0429	0.1542	0.0583
994(2) - 33	0.7419	2.7185	0.3216	1.2020	0.3790	0.0160	0.2188	0.0377	0.2517	0.0381	0.1925	0.0192	0.2854	0.0339
994(2) - 34	0.2819	0.9731	0.1589	0.5666	0.1146	0.0102	0.0743	0.0346	0.0824	0.0182	0.1064	0.0205	0.1648	0.0300
994(2) - 35	0.3626	1.2542	0.1601	0.5686	0.1338	0.0357	0.1530	0.0155	0.0720	0.0280	0.0624	0.0063	0.1802	0.0168
994(2) - 36	0.2848	0.7564	0.1098	0.3672	0.0622	0.0172	0.0977	0.0216	0.1368	0.0305	0.0945	0.0083	0.1612	0.0112
994(2) - 37	3.1930	8.1279	0.6565	2.7595	0.3875	0.0384	0.4630	0.0451	0.4145	0.0640	0.1885	0.0267	0.2668	0.0337
994(2) - 38	6.1968	14.2122	1.7216	5.5670	0.8154	0.1275	0.6737	0.0696	0.4061	0.1321	0.3870	0.0614	0.4287	0.0945
994(2) - 39	0.2906	0.6223	0.0989	0.2417	0.0418	0.0041	0.0313	0.0098	0.0487	0.0116	0.0069	0.0083	0.0236	0.0051
994(2) - 4	2.1433	5.6144	0.5449	1.8933	0.1632	0.0446	0.2604	0.0361	0.1492	0.0484	0.1395	0.0282	0.2312	0.0409
994(2) - 40	2.7825	6.6809	0.7977	2.9806	0.3439	0.0082	0.2123	0.0179	0.1646	0.0222	0.1254	0.0064	0.0970	-
994(2) - 41	0.7929	3.8125	0.3244	0.7654	0.2431	0.0633	0.1647	0.0249	0.2037	0.0283	0.1443	0.0097	0.0924	0.0274
994(2) - 42	4.4989	12.1618	1.7880	6.3896	0.6795	0.0984	0.6977	0.0454	0.4050	0.0520	0.1805	0.0521	0.3106	0.0381
994(2) - 43	6.6657	15.3891	1.9322	6.2085	1.0126	0.0345	0.3885	0.0385	0.2056	0.0572	0.1078	0.0289	0.2314	0.0423
994(2) - 44	5.3518	11.2127	1.3437	4.1960	0.8979	0.0719	0.3903	0.0336	0.2920	0.0599	0.1687	0.0292	0.2506	0.0297

994(2)-45	3.4745	9.2472	0.9392	4.1751	0.7955	0.0767	0.4294	0.0665	0.2956	0.0764	0.2472	0.0435	0.3059	0.0447
994(2)-46	2.6139	7.5389	0.8355	3.6924	0.4871	0.0422	0.2365	0.0533	0.1881	0.0284	0.1575	0.0291	0.3119	0.0296
994(2)-47	1.6792	4.8054	0.4965	1.8608	0.4073	0.0352	0.1201	0.0084	0.2742	0.0683	0.2579	0.0178	0.2130	0.0468
994(2)-48	0.1858	0.6653	0.0338	0.3648	-0.0047	-0.0028	0.0086	0.0079	0.0543	0.0160	0.0235	0.0040	0.0212	0.0046
994(2)-49	0.8080	2.5755	0.2841	0.9862	0.1555	0.0217	0.2062	0.0231	0.1577	0.0308	0.0545	0.0088	0.1120	0.0169
994(2)-5	8.9606	17.5025	1.4498	4.4111	0.8508	0.0150	0.2861	0.0336	0.3112	0.0543	0.1443	0.0380	0.2855	0.0444
994(2)-50	0.5376	2.1488	0.2179	1.0049	0.1744	0.0166	0.1103	0.0392	0.2353	0.0286	0.1157	0.0188	0.1511	0.0360
994(2)-6	3.0638	9.2908	0.7954	3.7913	0.5509	0.0490	0.4063	0.0419	0.3644	0.0389	0.1693	0.0180	0.1820	0.0208
994(2)-7	2.3571	7.2228	0.6989	2.5160	0.4261	0.0244	0.2532	0.0347	0.1595	0.0569	0.2028	0.0276	0.1510	0.0478
994(2)-8	13.8553	31.3992	2.4939	14.0005	1.1898	0.0789	0.3556	0.0368	0.1628	0.0441	0.1900	0.0288	0.2595	0.0193
994(2)-9	19.0583	18.2601	1.3847	4.1068	0.4368	0.0685	0.3221	0.0191	0.4086	0.0465	0.0902	0.0108	0.1134	0.0106

APPENDIX H: HEMATITE U-PB GEOCHRONOLOGY DATA

Sample	Ca ppm	Pb ppm	U ppm	238U/206Pb	238U/206Pb Uncertainty	207Pb/206Pb	207Pb/206Pb Uncertainty
852(1)-1	3656.0872	14.4502	6.8076	1.3626	0.0931	0.6476	0.0339
852(1)-10	84.0488	12.2828	1.9713	0.5669	0.0626	0.8253	0.0412
852(1)-11	4003.8517	23.1889	6.5334	0.9023	0.1521	0.7319	0.0275
852(1)-12	1303.6052	19.9140	3.6578	0.6078	0.0653	0.7683	0.0276
852(1)-13	1535.3091	29.1510	10.7281	1.0459	0.0570	0.6580	0.0323
852(1)-15	1641.0378	10.3936	5.0621	1.3365	0.1981	0.6475	0.0386
852(1)-16	113.9194	1.8550	2.9259	2.5736	0.2093	0.3602	0.0414
852(1)-17	319.2433	1.2961	1.8124	2.3382	0.1934	0.3727	0.0369
852(1)-18	1617.3723	4.0242	3.7674	2.0508	0.1790	0.4763	0.0283
852(1)-19	641.7647	14.8287	4.4795	0.9091	0.0704	0.7078	0.0300
852(1)-2	3612.7056	23.2413	8.3996	1.0765	0.0490	0.6888	0.0249
852(1)-20	280.5365	6.9310	2.8135	1.0584	0.0822	0.5922	0.0399
852(1) - 21	23.2697	0.4303	1.1736	2.7962	0.2824	0.2313	0.0421
852(1)-22	169.1845	5.0312	2.3434	1.2131	0.1141	0.6027	0.0516
852(1)-23	230.0222	3.6368	2.4719	1.6570	0.2021	0.5469	0.0452
852(1)-24	398.5585	10.3834	4.0354	1.0892	0.1162	0.6414	0.0282
852(1)-25	618.6671	12.6812	4.3219	0.9738	0.0580	0.6390	0.0260
852(1) - 26	99.4710	3.1628	1.9661	1.4333	0.1063	0.5147	0.0370
852(1)-27	661.7932	9.1928	4.2748	1.3063	0.1768	0.6265	0.0283
852(1)-28	273.7172	5.6819	3.6568	1.5470	0.2064	0.5504	0.0478
852(1)-29	392.0719	4.8926	2.3821	1.2852	0.1245	0.6000	0.0389
852(1)-3	1749.6927	7.6704	3.7829	1.2585	0.1227	0.5970	0.0395
852(1)-30	318.1622	2.8485	3.0080	2.0827	0.1264	0.4413	0.0425
852(1) - 31	48.4822	2.0727	2.1898	2.1455	0.1571	0.4449	0.0401
852(1)-32	259.4751	4.2678	2.4188	1.3871	0.0970	0.5570	0.0362
852(1) - 33	91.0225	1.2744	1.3767	2.2933	0.2440	0.4754	0.0637
852(1)-35	324.3519	2.7017	2.1360	1.7144	0.1281	0.4874	0.0552
852(1)-37	275.1615	12.4747	4.4161	1.1784	0.0667	0.6435	0.0336
852(1)-38	213.8735	1.6580	1.0999	1.5559	0.1272	0.5134	0.0480
852(1)-39	212.5839	8.2815	1.9243	0.7205	0.0825	0.7062	0.0423
852(1)-4	179.1991	3.2372	2.2803	1.5909	0.1686	0.5222	0.0582
852(1)-40	232.7106	3.0920	2.8690	1.9309	0.1648	0.4693	0.0401
852(1)-41	4419.3114	17.3269	6.5532	1.3503	0.1597	0.6676	0.0309
852(1)-42	130.4637	2.1769	2.2114	1.9639	0.1931	0.4363	0.0384
852(1)-43	896.9693	15.8327	6.5224	1.1899	0.0862	0.6656	0.0410
852(1)-44	196.7919	1.3619	1.6255	2.2073	0.1825	0.4280	0.0473
852(1)-45	1625.3748	1.1068	1.4984	2.2835	0.2282	0.3901	0.0608

Caelan Charles Grooby
 Geochemistry and Geochronology of an IOCG System: The Vulcan Prospect

852(1)-46	3673.1383	26.5057	7.0597	0.8489	0.0992	0.7312	0.0229
852(1)-47	830.8100	7.5140	1.7879	0.7262	0.1655	0.7039	0.0632
852(1)-48	1229.2746	6.5024	3.3184	1.4429	0.1152	0.6657	0.0744
852(1)-49	692.0619	3.5213	1.7085	1.2311	0.1502	0.5930	0.0798
852(1) - 50	62.8513	7.3730	3.5548	1.2938	0.0815	0.6356	0.0462
852(1)-51	289.5554	7.3278	2.7575	1.0554	0.0857	0.6370	0.0411
852(1) - 52	28.9738	1.0072	1.7291	2.5494	0.1897	0.3143	0.0403
852(1)-53	320.2052	3.7825	2.4620	1.5382	0.1684	0.5283	0.0556
852(1)-54	195.2362	9.3033	3.1199	0.9814	0.0798	0.6700	0.0422
852(1)-55	3236.2983	11.6676	5.0808	1.1864	0.0763	0.6298	0.0275
852(1)-56	159.0270	1.7844	1.9132	1.9240	0.1641	0.4065	0.0619
852(1)-57	166.9016	2.7763	1.8928	1.5184	0.1416	0.5128	0.0519
852(1)-58	2536.5990	13.1459	6.4420	1.6709	0.0996	0.6341	0.0481
852(1)-59	427.4634	9.1624	4.4839	1.3612	0.0931	0.6487	0.0334
852(1)-6	211.5916	1.7101	1.3613	1.6234	0.1355	0.4674	0.0482
852(1) - 8	1.2545	1.8089	1.2674	1.4720	0.1229	0.4903	0.0485
852(1)-9	6856.9225	31.8833	11.1211	1.0323	0.0698	0.6887	0.0258
973(1)-1	612.9059	29.0057	46.6216	1.8073	0.2315	0.2647	0.0099
973(1)-10	199.8951	24.6395	48.2202	2.9099	0.1556	0.3602	0.0123
973(1)-11	885.3140	19.2356	39.9292	3.0776	0.1903	0.3483	0.0140
973(1)-12	307.3281	34.7993	83.4338	3.6806	0.1993	0.3233	0.0084
973(1)-13	939.8941	43.7812	91.1186	2.6403	0.2205	0.2974	0.0098
973(1)-14	334.9391	26.6201	66.5385	3.4064	0.1663	0.3242	0.0134
973(1)-15	709.6251	36.6609	85.1613	3.1665	0.1469	0.3215	0.0093
973(1)-16	259.9121	15.8021	51.4788	4.0966	0.2510	0.2626	0.0131
973(1)-17	#####	22.9859	64.4287	3.4506	0.1916	0.2723	0.0113
973(1)-18	814.9496	41.1337	149.7921	2.7196	0.1664	0.1822	0.0071
973(1)-19	93.1711	21.1071	156.8548	3.6348	0.2166	0.1144	0.0043
973(1)-2	311.8254	13.7052	28.7170	2.9003	0.2247	0.3158	0.0148
973(1)-20	205.4910	6.2050	25.7915	4.6939	0.3400	0.2090	0.0156
973(1)-21	501.8358	2.6896	2.5587	2.0257	0.2142	0.5144	0.0598
973(1)-22	240.9826	19.0024	36.4080	2.8477	0.1551	0.3544	0.0136
973(1)-23	148.7600	33.5452	52.2874	2.6395	0.1345	0.3958	0.0165
973(1)-24	336.5740	25.5478	58.3304	3.1288	0.1879	0.3259	0.0152
973(1)-25	153.6120	14.1241	31.9192	3.0301	0.2247	0.3142	0.0133
973(1) - 26	72.3217	6.7726	29.2050	3.9609	0.1950	0.2139	0.0217
973(1)-27	4332.7971	32.1261	61.8636	3.0999	0.2374	0.3807	0.0188
973(1)-28	147.0934	7.2736	18.9160	3.5479	0.2515	0.3183	0.0188
973(1) - 29	56.2738	4.3321	22.5175	4.0858	0.2141	0.1896	0.0144
973(1)-3	310.6923	40.5999	262.9926	4.1480	0.3349	0.1287	0.0038
973(1) - 30	94.8995	7.9492	42.3498	4.3676	0.2141	0.1834	0.0071
973(1) - 31	-0.9617	0.2922	2.1629	3.8978	0.4269	0.1278	0.0351
973(1) - 32	-11.1026	0.1103	1.3509	3.9852	0.4495	0.0760	0.0268

Caelan Charles Grooby
 Geochemistry and Geochronology of an IOCG System: The Vulcan Prospect

973(1) - 33	1950.4415	55.3580	59.9729	1.0736	0.0611	0.2342	0.0077
973(1) - 34	199.1210	7.2111	14.8591	3.0344	0.1960	0.3456	0.0209
973(1) - 35	152.6950	8.1275	16.8218	3.0490	0.1914	0.3379	0.0169
973(1) - 36	895.7226	12.6129	56.1198	3.9995	0.1923	0.2097	0.0102
973(1) - 37	676.1919	10.0326	23.9927	3.2575	0.3967	0.3180	0.0192
973(1) - 38	21.8860	68.1676	159.3588	3.4930	0.2303	0.3530	0.0092
973(1) - 39	76669.5711	74.4669	76.1629	1.2513	0.0805	0.2824	0.0074
973(1) - 4	328.1296	55.9491	406.8380	3.4503	0.2348	0.1146	0.0064
973(1) - 40	26.4285	6.9718	26.3405	3.9189	0.3570	0.2514	0.0219
973(1) - 42	958.5884	49.8403	93.5051	2.2745	0.1800	0.2816	0.0084
973(1) - 43	100.9240	60.9704	81.4159	2.8121	0.2125	0.4648	0.0111
973(1) - 44	141.3628	11.0885	32.6337	3.9461	0.2465	0.2781	0.0134
973(1) - 5	10.5187	48.8336	424.1443	3.7413	0.2550	0.1010	0.0028
973(1) - 6	112.4929	161.5318	1458.6844	3.8696	0.1539	0.1008	0.0025
973(1) - 7	53.7127	18.2964	142.7489	3.5990	0.4403	0.1118	0.0044
973(1) - 8	1143.9189	39.2319	62.6105	2.0281	0.1580	0.3014	0.0176
973(1) - 9	413.7066	30.3895	63.3701	3.7416	0.2322	0.3514	0.0119
994(1) - 1	186.6328	5.0217	3.2059	1.5738	0.1267	0.5952	0.0361
994(1) - 10	121.0415	2.3724	1.6589	1.5482	0.1733	0.5303	0.0521
994(1) - 11	27.3697	1.5233	2.2875	2.2126	0.3401	0.3624	0.0534
994(1) - 12	30.3907	2.4130	2.1298	1.8368	0.2257	0.4908	0.0435
994(1) - 13	115.1202	2.2368	2.1718	2.0113	0.1642	0.4821	0.0627
994(1) - 14	243.6578	4.3895	6.8463	3.2345	0.2014	0.3839	0.0322
994(1) - 15	167.7928	5.4272	10.1067	2.8107	0.2336	0.3670	0.0300
994(1) - 16	258.2081	2.4640	3.1415	2.5420	0.2919	0.4793	0.0535
994(1) - 17	109.7116	13.4019	37.9491	3.4732	0.2012	0.2892	0.0217
994(1) - 18	104.3519	3.1828	3.5929	2.5994	0.2537	0.4315	0.0469
994(1) - 19	119.0623	7.7899	11.8762	2.8299	0.1371	0.4234	0.0199
994(1) - 2	-0.8608	2.8246	3.0270	1.9904	0.2414	0.4443	0.0321
994(1) - 20	217.2278	3.2366	1.6054	1.7647	0.2030	0.6456	0.0819
994(1) - 21	137.6365	1.1242	1.6986	2.2341	0.3184	0.3535	0.0759
994(1) - 22	53.1732	1.9572	1.9987	1.8208	0.1475	0.4158	0.0463
994(1) - 23	9.4937	1.4617	1.7395	2.0562	0.1919	0.4125	0.0530
994(1) - 24	181.4634	2.9415	2.5956	2.0456	0.2014	0.5175	0.0398
994(1) - 25	120.0389	3.3212	7.5195	3.1040	0.2090	0.3130	0.0235
994(1) - 26	387.9171	3.5139	4.5873	2.7777	0.2086	0.4095	0.0475
994(1) - 27	281.7734	4.5305	4.7670	1.9310	0.1527	0.4363	0.0346
994(1) - 28	88.8818	4.7510	9.3537	3.2456	0.1895	0.3885	0.0268
994(1) - 29	193.3963	4.1703	7.5466	2.8098	0.1589	0.3667	0.0296
994(1) - 3	382.6164	3.5998	4.1390	2.1111	0.1617	0.4551	0.0377
994(1) - 30	65.6392	2.4016	4.3779	2.7219	0.1712	0.3426	0.0613
994(1) - 31	165.9297	2.0512	4.6415	2.9080	0.2105	0.2906	0.0301
994(1) - 32	480.7919	4.3754	3.9562	2.1592	0.3790	0.5056	0.0476

Caelan Charles Grooby
 Geochemistry and Geochronology of an IOCG System: The Vulcan Prospect

994(1)-33	362.3727	12.0952	3.7894	1.1955	0.1271	0.6895	0.0430
994(1)-34	163.5905	7.5450	13.4929	3.5766	0.2358	0.3836	0.0206
994(1)-35	253.5077	5.1693	8.6204	2.8755	0.2359	0.3934	0.0261
994(1)-36	432.4816	5.2766	6.8668	2.9585	0.3372	0.4061	0.0487
994(1) - 38	86.0636	2.2875	2.8947	2.2818	0.1726	0.4208	0.0428
994(1)-39	186.7078	2.1764	3.6435	2.3463	0.1908	0.3276	0.0310
994(1)-40	192.0878	2.6031	1.4149	1.3770	0.1300	0.5867	0.0567
994(1) - 41	91.3436	1.5034	2.9393	3.0695	0.3782	0.2857	0.0401
994(1)-42	324.4153	2.7630	4.3078	2.7240	0.2244	0.3954	0.0355
994(1)-43	248.3045	4.9227	7.9686	2.7689	0.2266	0.3810	0.0243
994(1) - 44	25.8290	4.6991	3.7698	2.0033	0.1527	0.4799	0.0481
994(1)-45	175.1967	9.8169	15.6680	2.9273	0.3543	0.3996	0.0200
994(1)-46	531.1819	3.8173	4.0260	2.3178	0.1709	0.4693	0.0674
994(1) - 47	75.0348	3.4284	5.5162	2.4581	0.1702	0.3418	0.0246
994(1)-48	183.3525	9.7924	13.1697	2.5550	0.1408	0.4364	0.0240
994(1)-49	189.9697	5.3669	8.7364	2.7974	0.3693	0.3792	0.0190
994(1)-5	107.7017	1.6784	2.0054	2.6319	0.3175	0.4271	0.0503
994(1)-50	228.6401	6.3078	15.2622	3.3247	0.1725	0.3035	0.0137
994(1)-51	207.1828	2.3484	2.4463	2.0876	0.1469	0.4557	0.0404
994(1)-52	190.1797	3.2176	6.2475	2.8821	0.2814	0.3450	0.0337
994(1)-53	144.5391	3.7975	6.3352	2.7527	0.1518	0.3637	0.0215
994(1)-54	1622.3644	2.9276	1.5509	1.2825	0.1398	0.5726	0.0706
994(1) - 55	88.6078	1.7119	4.8869	2.9929	0.2074	0.2454	0.0364
994(1)-56	143.4819	6.5672	11.8685	2.9495	0.1944	0.3672	0.0243
994(1)-57	143.8609	8.3315	8.8430	2.0767	0.1599	0.4716	0.0289
994(1)-58	183.2195	2.3838	3.3006	2.5469	0.2702	0.4037	0.0553
994(1)-59	124.0341	4.8138	5.3524	2.0927	0.1446	0.4486	0.0395
994(1)-6	202.5315	3.6946	2.7372	1.7150	0.1174	0.5586	0.0435
994(1)-60	144.3276	2.1528	1.3947	1.9348	0.2607	0.5632	0.0543
994(1) - 61	48.9891	3.3699	3.9020	2.4580	0.2624	0.4435	0.0319
994(1)-62	176.1438	8.4166	5.4340	1.4750	0.0768	0.5424	0.0324
994(1)-63	346.7782	2.6230	2.2455	1.7845	0.2075	0.4734	0.0409
994(1)-64	119.1922	2.2864	2.6085	2.0256	0.1949	0.4050	0.0446
994(1)-65	195.3992	1.8595	1.7581	1.6916	0.1685	0.4092	0.0461
994(1)-66	161.4047	2.3059	3.1821	2.2428	0.1707	0.3714	0.0328
994(1)-67	154.4071	2.2896	1.5814	1.9231	0.2140	0.5399	0.0703
994(1)-68	178.8453	3.6140	6.8595	3.2822	0.2470	0.3971	0.0331
994(1)-69	220.0012	1.9336	2.2648	2.2699	0.1924	0.4040	0.0346
994(1)-7	387.2274	8.6954	14.8051	2.8213	0.1719	0.3997	0.0203
994(1)-70	65.1433	9.9291	14.2182	2.6376	0.1602	0.4079	0.0166
994(1)-71	54.8473	12.0585	18.4380	2.5390	0.1636	0.3847	0.0176
994(1)-72	1897.0471	4.0348	4.2335	2.4444	0.2324	0.4883	0.0329
994(1)-73	314.4448	2.3387	2.0120	1.7042	0.3819	0.4431	0.0518

Caelan Charles Grooby
 Geochemistry and Geochronology of an IOCG System: The Vulcan Prospect

994(1)-8	112.2662	1.9129	2.0136	2.0343	0.1786	0.4641	0.0504
994(1)-9	166.7946	2.7217	2.7054	1.8670	0.1541	0.4526	0.0480
994(2)-1	267.8718	11.9756	12.0307	2.0351	0.1527	0.4570	0.0171
994(2)-10	283.9000	39.5541	42.6052	2.5248	0.2103	0.5243	0.0149
994(2)-11	330.4975	8.5014	10.2630	2.4974	0.1808	0.4512	0.0276
994(2)-12	281.7069	20.8735	16.6287	2.3283	0.1371	0.5432	0.0278
994(2)-14	333.5682	6.1666	4.7545	1.7308	0.1384	0.5380	0.0448
994(2)-15	439.1983	7.1183	6.5183	2.2372	0.1301	0.5116	0.0215
994(2)-16	306.9379	10.8135	7.8194	1.8060	0.1087	0.5469	0.0258
994(2)-17	301.9428	32.2169	26.6460	2.0071	0.1106	0.5509	0.0148
994(2)-18	266.9194	7.4960	11.1924	2.7548	0.1835	0.3947	0.0194
994(2)-19	185.4480	12.3086	13.6303	2.2069	0.1747	0.4463	0.0160
994(2)-2	311.9182	11.2963	13.0955	2.2730	0.1763	0.4479	0.0181
994(2)-20	307.8643	16.5807	14.6703	1.9600	0.1371	0.5081	0.0230
994(2)-21	729.3713	7.3857	7.2202	2.1580	0.1145	0.4864	0.0207
994(2)-22	661.3710	10.7552	11.8434	2.2232	0.1099	0.4566	0.0280
994(2)-23	356.8697	15.9752	21.2468	2.5046	0.1739	0.4328	0.0172
994(2)-24	121.1081	16.1211	19.4957	2.8584	0.1309	0.4385	0.0207
994(2)-25	543.2205	10.1487	11.3008	2.2581	0.0914	0.4553	0.0196
994(2)-26	579.1908	14.2823	11.0796	1.9111	0.1316	0.5411	0.0221
994(2)-27	625.5212	20.3593	33.4098	2.9505	0.1798	0.4157	0.0176
994(2)-28	178.6679	3.2554	2.5591	1.9960	0.1768	0.5158	0.0448
994(2)-29	322.4862	11.5211	15.1463	2.5151	0.1494	0.4463	0.0273
994(2) - 3	47.4717	13.8095	14.8540	2.2550	0.1741	0.4684	0.0260
994(2) - 30	58.6580	13.4683	15.3650	2.3696	0.1412	0.4699	0.0174
994(2)-31	2045.1868	4.6322	3.8058	1.7121	0.1417	0.4805	0.0347
994(2)-32	1156.9097	7.1282	5.8363	1.9004	0.1230	0.5439	0.0429
994(2)-33	527.5188	10.0233	12.4720	2.3474	0.1803	0.4359	0.0212
994(2) - 34	83.2891	8.2814	9.1034	2.5323	0.1737	0.4391	0.0228
994(2) - 35	93.8413	7.6575	10.7690	2.5128	0.1356	0.4048	0.0192
994(2) - 36	27.4702	32.3023	32.7323	2.2204	0.1144	0.5073	0.0179
994(2)-37	420.1033	11.6295	6.5050	1.4952	0.1028	0.6066	0.0282
994(2)-38	441.9751	12.4247	14.2449	2.3579	0.1288	0.4628	0.0222
994(2) - 39	26.8199	1.9564	0.6291	0.9389	0.1397	0.6753	0.0937
994(2)-4	130.1295	12.7536	13.1552	2.5017	0.1520	0.4742	0.0191
994(2)-40	291.3456	1.0711	1.0449	1.8601	0.2735	0.4501	0.0755
994(2)-41	136.0937	5.3004	7.8867	2.9364	0.2881	0.4181	0.0352
994(2)-42	265.8728	6.9090	7.8044	2.6513	0.1899	0.4471	0.0249
994(2)-43	266.4563	7.4802	7.7274	2.3982	0.1857	0.4542	0.0285
994(2)-44	586.4184	12.7487	15.7158	2.4084	0.2327	0.4437	0.0242
994(2)-45	300.7554	12.5448	13.7939	2.0143	0.1301	0.4361	0.0187
994(2)-46	180.8738	12.0489	11.3414	2.0283	0.1277	0.4838	0.0241
994(2)-47	97.7534	13.2378	14.8376	2.7010	0.2197	0.4372	0.0257

Caelan Charles Grooby
 Geochemistry and Geochronology of an IOCG System: The Vulcan Prospect

994(2) - 48	46.9384	4.1864	3.7134	1.8521	0.1559	0.4866	0.0386
994(2) - 49	692.3447	6.3685	6.4536	1.9863	0.2069	0.4466	0.0404
994(2) - 5	535.1678	8.4571	8.2108	2.0532	0.1147	0.4713	0.0221
994(2) - 50	1004.7189	14.1120	11.6832	1.8883	0.0867	0.5305	0.0256
994(2) - 6	602.7431	2.6115	2.9238	2.1721	0.1510	0.4408	0.0388
994(2) - 7	527.3903	9.8405	11.7777	2.3659	0.1784	0.4498	0.0225
994(2) - 8	573.7932	8.6058	9.7239	2.5879	0.1963	0.4760	0.0204
994(2) - 9	336.2015	5.2487	6.9598	2.3897	0.1949	0.4167	0.0250

APPENDIX I: ZIRCON U-PB GEOCHRONOLOGY DATA

Source Filename	238U/206Pb	238U/206Pb Uncertainty	207Pb/206Pb	207Pb/206Pb Uncertainty
801_zircon-1.csv	100.3318	3.819185	0.11391	0.003573
801_zircon-10.csv	78.87553	1.7088	0.101901	0.004862
801_zircon-11.csv	678.7272	25.53716	0.120824	0.00521
801_zircon-12.csv	554.5838	98.69911	0.111368	0.006793
801_zircon-13.csv	23.34528	0.789266	0.093872	0.00252
801_zircon-14.csv	1735.987	80.10269	0.148962	0.01173
801_zircon-15.csv	301.11	12.91291	0.229944	0.008462
801_zircon-16.csv	284.0619	5.574887	0.234034	0.00612
801_zircon-18.csv	7.778063	0.150912	0.146254	0.003812
801_zircon-19.csv	12.77451	0.23703	0.100542	0.002737
801_zircon-20.csv	21.77115	0.449663	0.096881	0.002686
801_zircon-21.csv	84.89113	3.942348	0.115008	0.004602
801_zircon-22.csv	874.367	57.12153	0.15083	0.010465
801_zircon-23.csv	49.37919	1.233772	0.125672	0.006895
801_zircon-24.csv	19.59724	0.760655	0.114135	0.003698
801_zircon-25.csv	156.8141	6.796316	0.136378	0.003694
801_zircon-3.csv	37.57504	2.734355	0.14874	0.010707
801_zircon-4.csv	254.8543	21.92515	0.131778	0.005556
801_zircon-5.csv	7.179905	0.406089	0.117047	0.003764
801_zircon-6.csv	622.0103	15.31154	0.377063	0.011276
801_zircon-8.csv	649.8519	71.42657	0.167263	0.010596
801_zircon-9.csv	307.103	30.4264	0.114226	0.005823
973_zircon - 1.csv	153.4197	17.76577	0.099309	0.00528
973_zircon - 2.csv	36.46765	0.748755	0.098791	0.005364
Standards				
91500 - 1.csv	5.543995	0.127712	0.071023	0.003864
91500 - 2.csv	5.604202	0.131052	0.080413	0.004396
91500 - 3.csv	5.618173	0.128196	0.069737	0.003784

91500 - 4.csv	5.551022	0.125863	0.096476	0.009785
91500 - 5.csv	5.636071	0.147561	0.076282	0.00403
91500 - 6.csv	5.665544	0.147533	0.073513	0.003914
GJ - 1.csv	10.15629	0.09286	0.059032	0.002338
GJ - 2.csv	10.24562	0.093676	0.061978	0.002723
GJ - 3.csv	10.26389	0.093843	0.059312	0.002425
GJ - 4.csv	10.22089	0.09345	0.061291	0.002414
GJ - 5.csv	10.18219	0.093096	0.059099	0.002515
GJ - 6.csv	10.25269	0.093741	0.060231	0.002614
GJ - 7.csv	10.16445	0.142684	0.061501	0.003111
GJ - 8.csv	10.19323	0.143088	0.060366	0.002484
GJ - 9.csv	10.30055	0.144594	0.060785	0.00241
NIST610 - 21.csv	Error	Error	0.909464	0.000886
NIST610 - 22.csv	Error	Error	0.910173	0.000887
NIST610 - 23.csv	Error	Error	0.909627	0.000886
NIST610 - 24.csv	Error	Error	0.908833	0.000886
NIST610 - 25.csv	Error	Error	0.909647	0.000886
NIST610 - 26.csv	Error	Error	0.90981	0.000887
NIST610_20 - 1.csv	4.653156	0.094051	0.907954	0.007464
NIST610_20 - 2.csv	4.660325	0.086134	0.909863	0.008412
NIST610_20 - 3.csv	4.606379	0.106038	0.907072	0.007234
Pleovice - 1.csv	18.90346	0.313311	0.054715	0.002414
Pleovice - 2.csv	18.59186	0.30212	0.054112	0.001944
Pleovice - 3.csv	18.56937	0.285773	0.052662	0.001875
Pleovice - 4.csv	18.8222	0.291296	0.053426	0.002056
Pleovice - 5.csv	18.47182	0.370538	0.053519	0.00215
Pleovice - 6.csv	18.39626	0.379947	0.054031	0.002006

APPENDIX J: FLORENCITE TRACE ELEMENT DATA

Florencite Samples	La	Ce	Pr	Nd	Sm	Eu	Gd	Tb	Dy	Ho	Er	Tm	Yb	Lu
801_florencite - 1	32181.68	49241.1	4979.182	15313.76	1915.734	254.0967	439.8436	15.03206	25.11885	7.747164	9.202133	1.15559	2.510042	0.8849
801_florencite - 10	27398.23	61013.28	7026.374	18807.06	3128.634	380.2409	812.5187	19.51248	23.35935	2.077363	4.362761	0.617226	2.064248	0.15178
801_florencite - 11	18944.82	38429.39	5172.294	16492.67	1788.886	346.1473	534.4441	14.10873	30.56973	2.979774	5.255407	0.524982	2.447157	0.327259
801_florencite - 12	15833.08	37839.35	3719.858	12860.79	1717.768	208.9637	414.0049	14.46064	29.66743	3.319773	5.112	0.701088	1.881191	0.745051
801_florencite - 13	6805.476	13954.85	1131.605	4953.125	712.9776	80.03777	235.1312	4.607603	14.39522	1.063981	1.326603	0.494497	1.321991	0.43215
801_florencite - 14	9253.87	21458.49	2317.112	7534.915	970.7645	134.2027	256.517	8.116147	23.86028	2.879593	5.017353	0.784445	5.179809	0.348474
801_florencite - 15	18064.17	35309.96	3517.094	9704.141	1147.32	125.8645	289.5811	13.11919	46.09623	7.38146	15.8671	1.633672	9.72421	1.997736
801_florencite - 16	4219.205	4600.873	481.8869	2228.746	286.6556	28.72287	68.56281	1.861277	3.084199	1.19727	2.580225	0.09143	0.853387	0.201451
801_florencite - 17	19473.52	36242.11	4509.688	14193.62	1599.385	240.165	400.8417	13.08226	28.26841	2.88473	6.506916	0.511887	2.697999	0.762812
801_florencite - 19	8576.21	18108.74	1915.537	7153.238	722.0934	93.23309	229.8527	8.255887	20.1159	3.180015	7.320492	0.901401	6.976165	0.530436
801_florencite - 2	1700.333	5887.357	921.9377	1645.147	433.1885	30.51671	86.074	3.313268	9.560659	0.91396	2.721676	-0.01098	0.504323	-0.02868
801_florencite - 20	10621	19410.96	1964.968	7244.106	950.9563	114.6808	330.7498	12.19895	24.08557	3.48327	6.842407	0.874457	8.273745	0.340149
801_florencite - 21	11139.75	23428.47	2193.29	6547.36	826.136	94.6391	207.7059	10.64741	29.38818	5.126688	11.73278	1.023026	6.621645	0.780783
801_florencite - 22	20282.16	43069.38	4265.513	13817.5	1889.522	214.6917	423.6823	13.61874	46.66996	5.143665	12.44385	1.660432	6.933555	1.081805
801_florencite - 23	23370.57	43407.29	4542.448	14277.56	2296.242	223.0366	566.43	15.40579	23.14855	1.586554	4.571535	0.184047	2.130144	0.269838
801_florencite - 24	19757.13	46313.14	4920.449	15086.81	1803.043	204.7082	408.2088	14.25738	41.01211	3.640749	6.4005	0.368712	3.403249	0.164859
801_florencite - 25	28832.07	63678.14	8384.692	21428.68	2924.009	348.1342	605.252	23.73142	48.3229	9.394033	14.61892	0.39472	10.38826	0.284574
801_florencite - 26	10267.68	15249.25	1605.523	6805.819	609.7189	85.43828	170.1701	5.482494	8.471118	1.071977	3.192702	0.221564	2.86922	0.28731
801_florencite - 27	470.1144	1391.756	110.3047	336.4194	53.54774	7.826151	21.95543	0.721568	1.097695	0.267007	0.23346	0.164886	0.389389	-0.01975
801_florencite - 28	24447.54	54062.63	5125.12	18520.48	2108.559	292.2519	640.712	17.4375	55.00827	5.366568	12.81216	1.243536	10.63612	0.707285
801_florencite - 29	7606.182	12776.32	1354.85	4936.986	737.6744	79.46909	165.3988	5.847979	12.50109	1.350191	4.413378	0.705514	2.289591	0.334031
801_florencite - 3	4407.182	9159.942	1067.141	3530.71	453.8484	48.41932	136.7392	3.746326	13.90511	1.655527	1.522657	0.236195	3.016976	-0.01489
801_florencite - 30	5449.382	12723.2	1247.119	4300.434	538.5241	68.60563	153.544	6.553807	20.93952	1.162828	3.067862	0.595881	0.888588	0.450619

Caelan Charles Grooby
Geochemistry and Geochronology of an IOCG System: The Vulcan Prospect

801_florencite - 31	20705.14	49527.75	5737.436	16817.21	2408.149	219.0373	600.1385	17.68482	41.04933	4.372114	7.168668	0.493134	4.141668	0.497676
801_florencite - 32	22944.25	56363.38	5183.531	16343.2	2235.989	306.4303	571.6881	18.59136	43.0735	2.751022	6.433388	0.603662	3.657182	0.42902
801_florencite - 33	10017.6	18045.2	1748.226	6012.181	853.1159	83.82198	211.8942	6.660354	14.30613	2.087171	2.37726	0.430842	2.006441	0.248265
801_florencite - 34	7548.318	15629.21	1552.043	5424.807	676.9971	78.35096	181.2421	5.894776	16.61731	1.887254	5.02854	0.42246	2.876225	0.225585
801_florencite - 35	22802.18	45671.47	5688.577	17474.73	2172.776	327.6594	680.3273	19.26186	34.74902	3.461104	5.962899	0.570806	2.558913	0.575884
801_florencite - 36	7355.552	14506.61	1479.03	4642.071	678.4901	87.41057	199.7277	6.352665	13.10397	1.360656	3.032565	0.326735	1.18052	0.108874
801_florencite - 37	14748.14	30587.58	3417.846	10439.65	1596.374	159.3485	391.6787	11.29193	26.72754	3.277994	5.926791	0.411164	1.293929	0.468208
801_florencite - 38	15356.98	32577.87	3417.923	13408.52	1634.638	196.792	492.3385	12.33317	32.8932	3.241437	6.777802	0.481777	3.316532	0.242728
801_florencite - 39	26919.27	65238.42	5973.091	18920.31	2487.603	444.301	729.8922	16.37437	23.51357	2.799093	5.387081	0.375242	2.831807	0.375295
801_florencite - 4	1061.79	1825.6	177.8755	553.9414	98.22978	16.19842	21.34606	1.032731	4.380011	0.346595	1.030476	0.158551	-0.01742	-0.01426
801_florencite - 40	4574.119	9270.313	817.6404	3369.88	349.0488	43.37089	200.4708	3.611264	11.48949	2.689041	1.961654	0.364346	1.727454	0.237131
801_florencite - 5	13351.98	32277.97	3471.414	11300.8	1451.496	185.6428	363.8744	11.49013	33.71352	3.235642	7.785365	0.443726	2.355852	0.209493
801_florencite - 6	22066.71	44678.48	4960.513	16226.81	2028.523	210.1057	572.1357	17.18839	48.39293	7.452715	7.697778	0.799053	4.909661	0.454141
801_florencite - 7	15829.72	31400.02	2927.826	11484.55	1275.269	173.5836	414.3529	13.62433	31.5098	2.986703	4.169812	0.428565	5.405562	0.277871
801_florencite - 9	10616.99	24385.05	3132.395	7644.742	1180.881	142.3726	303.1749	9.676207	18.51533	2.473404	4.269437	0.083608	2.529122	0.764826
852_florencite - 1	18107.65	44428.34	4667.883	14891.45	1352.51	118.5956	393.531	17.98162	60.50182	10.05961	20.45177	2.924983	18.61261	1.331012
852_florencite - 10	33995.79	77363.28	9645.622	30130.35	2956.62	265.7055	750.3623	37.19744	125.6418	19.84539	45.66107	6.822654	41.75565	4.50051
852_florencite - 11	26274.92	72001.15	7775.638	24661.97	2351.565	226.7682	535.3253	20.91327	63.44672	9.340554	32.26376	3.594298	18.99908	2.729766
852_florencite - 12	22967.45	59988.16	8070.666	23698.85	3014.28	211.0709	597.1499	28.21846	104.2971	20.13142	35.73772	7.803559	26.94842	3.85436
852_florencite - 13	30080.56	75960.92	8601.414	28308.83	2918.207	235.4169	655.1109	34.77701	79.01212	12.3724	41.41255	5.019311	26.35382	3.523347
852_florencite - 15	3149.713	7657.656	1007.296	3129.748	338.0139	30.39462	73.12301	2.419838	8.187466	1.799029	1.568417	0.312639	5.265339	0.37974
852_florencite - 16	31740.21	79440.31	8901.647	29044.33	2666.739	223.1601	710.4026	33.30765	132.7943	19.6894	54.38573	6.302928	41.77257	6.629612
852_florencite - 17	32997.35	75321.04	9148.614	28036.32	2664.804	237.3754	704.9121	37.03935	113.6271	23.09218	56.8414	7.682059	40.32012	5.657893
852_florencite - 18	31995.59	74806.28	8982.889	28292.18	2731.262	236.4285	714.7785	40.79723	201.6042	34.84229	95.08075	9.090495	61.5771	9.519763
852_florencite - 19	32607.51	81337.84	9301.438	30027.75	2965.999	260.947	794.671	40.49185	137.3221	22.05572	64.43641	7.020247	55.16988	6.220588
852_florencite - 2	34137.7	81775.16	8891.063	28401.57	2907.114	248.063	776.0258	50.96612	206.5184	31.43628	71.09915	7.262501	41.07818	6.591344
852_florencite - 20	31835.53	78204.8	9156.532	28213.18	2500.38	232.5903	696.8505	30.7042	127.3366	20.49767	54.19899	6.42835	46.45546	4.295554

Caelan Charles Grooby
Geochemistry and Geochronology of an IOCG System: The Vulcan Prospect

852_florencite - 21	32402.26	78530.1	9132.365	29763.28	2610.576	237.1741	708.7474	31.38456	112.9501	17.23494	45.17509	5.515015	28.7042	4.152058
852_florencite - 23	33684.97	77034.08	9314	27709.07	2614.83	214.9437	611.9814	31.08722	106.1905	14.86109	41.75996	5.17333	32.44778	4.571113
852_florencite - 24	4778.78	14312.55	1545.425	3816.643	386.3644	103.8602	54.11047	1.021219	23.448	4.989836	5.944033	0.495115	53.70567	1.28751
852_florencite - 25	25597.58	63451.81	8201.077	25105.43	1910.992	187.9069	521.6165	18.96397	66.40838	8.190249	24.26109	2.395969	18.80874	2.294113
852_florencite - 27	29580.9	78039.79	8841.626	27910.72	2496.57	221.5589	577.829	22.59349	69.40062	11.43784	28.10063	3.325529	20.80146	2.503837
852_florencite - 28	32157.35	72446.51	8746.796	28186.28	2631.529	235.6644	646.5975	22.8886	83.43757	11.54835	27.42006	3.543488	22.68989	2.89391
852_florencite - 29	32735	75617.03	9230.873	29247.93	2716.629	235.5933	639.8521	31.05802	99.35372	18.1588	45.50991	5.807786	30.0192	4.315905
852_florencite - 3	994.698	2510.539	249.4067	805.8161	87.08374	7.260434	24.56539	3.713804	3.134579	0.864481	2.575444	0.716213	1.889392	0.54564
852_florencite - 32	21343.39	54085.99	7235.306	22623.96	2150.625	181.3831	457.2617	17.15196	63.11166	10.91926	49.01275	2.500135	16.2109	2.328853
852_florencite - 33	29646.43	70001.17	8722.179	29645.23	2668.117	236.6711	670.0274	25.86764	85.27581	15.38423	52.77595	6.992868	38.11465	3.549049
852_florencite - 34	30972.29	79114.12	9272.503	26015.11	2634.435	244.6194	753.3902	49.21132	214.2694	43.50812	104.4279	13.46654	93.26286	11.43999
852_florencite - 39	37391.15	74129.11	8551.698	27372.05	2705.67	226.1747	675.2513	33.08995	111.3764	24.57738	45.89779	9.56786	38.53974	4.801171
852_florencite - 4	35478.84	84578.2	9438.903	29903.47	2648.011	229.4572	738.5087	38.97883	125.7587	17.91618	38.9796	5.328762	28.19886	4.045656
852_florencite - 40	24070.38	53764.94	7061.891	25170.42	1964.763	211.205	995.2098	22.94934	100.6412	17.2791	45.00666	5.289087	102.3217	18.11813
852_florencite - 42	38470.35	81233.32	8967.644	26722.55	2203.917	201.1604	616.0036	32.45244	133.9032	21.77446	62.50261	6.806003	56.4411	5.538064
852_florencite - 47	32082.08	76889.04	8626.887	27014.69	2301.626	212.0201	616.232	41.89911	194.6938	29.01179	99.16442	9.812139	73.53006	8.432259
852_florencite - 5	25806.95	73263.82	7368.086	21904.93	2157.361	194.8634	584.0505	25.23839	87.58651	14.43328	35.80639	6.251333	30.83597	4.024728
852_florencite - 50	26609.65	69965.51	7128.141	23243.79	2053.479	199.194	651.7511	44.45521	220.1762	37.2188	94.61971	15.83599	84.78231	11.17191
852_florencite - 51	32956.36	69992.68	8731.776	29222.25	2485.184	221.0918	568.2251	31.14378	109.4074	14.7535	31.90842	6.990239	33.68664	4.860163
852_florencite - 52	29596.9	73296.5	8300.701	28087.41	2714.569	244.7285	728.9906	44.60753	197.19	34.4603	81.31557	12.8416	83.13479	7.874141
852_florencite - 54	28747.06	65858.67	8001.658	23749.65	2271.583	223.2559	566.8468	26.13936	94.93266	19.02785	36.57557	4.352547	22.96231	3.173906
852_florencite - 6	28773.26	74492.57	8286.02	28562.74	2379.317	228.3982	716.9115	48.57456	251.0155	40.031	97.04883	17.24428	74.86423	14.51623
852_florencite - 7	25202.67	60875.15	7240.284	23897.38	2253.472	205.5598	599.4635	32.28085	124.515	20.53379	53.29536	7.944578	57.0851	8.082504
852_florencite - 8	28836.24	75050.42	8985.638	27940.71	2600.885	230.7655	629.4857	24.02533	112.4797	10.69654	33.27187	5.832138	25.03952	2.734105
973_florencite - 1	48934.92	67522.82	4407.206	10632.25	1112.293	153.6272	487.3965	21.97271	70.11998	13.21384	41.60747	4.678557	22.58691	2.622472
973_florencite - 10	31936.45	49507.06	3655.348	8060.631	909.661	141.057	400.1863	17.86233	51.48059	6.491805	10.05847	0.887686	5.732163	0.47141
973_florencite - 11	37250.23	54701.39	3680.26	9600.414	1149.244	168.2612	502.4331	19.59277	48.58848	6.305116	10.54682	1.406491	5.247719	0.368499

Caelan Charles Grooby
Geochemistry and Geochronology of an IOCG System: The Vulcan Prospect

973_florencite - 12	16050.12	24320.14	1684.409	4105.431	489.7974	77.97247	232.5262	8.007453	28.30239	2.518919	7.001427	0.62241	2.694356	0.548976
973_florencite - 13	37345.96	54718.93	3893.626	9906.858	1189.551	158.146	490.8243	21.2421	52.86682	5.88894	11.87735	0.922469	5.068007	0.73107
973_florencite - 14	34259.89	49699.46	3266.423	8037.381	971.2684	127.8078	374.6713	20.25227	51.69669	7.279134	17.64842	1.633868	10.82538	0.815835
973_florencite - 15	36997.45	56828	4127.871	10583.28	1235.078	165.874	522.7001	22.71955	60.34637	7.197598	9.584574	0.971252	3.435567	0.339177
973_florencite - 16	49231.98	70833.26	5132.508	13181.37	1613.193	235.5491	687.797	25.78947	67.57867	6.108141	10.85419	0.645706	4.543899	0.491872
973_florencite - 17	23685.86	33018.15	2324.721	5773.541	664.1963	98.254	260.7034	13.02145	31.35873	4.181509	9.406693	0.724758	5.066537	0.472713
973_florencite - 18	48288	79404.99	5326.041	13156.89	1474.217	218.1603	681.3477	27.21921	71.74808	8.726269	13.41524	1.724506	4.705851	0.736881
973_florencite - 19	27027.55	41410.67	2936.627	7505.832	874.5879	126.8096	382.7681	16.05369	42.95138	4.670926	9.22327	0.858822	5.084012	0.585036
973_florencite - 2	57449.66	78851.91	5486.672	11580.66	1261.015	192.1968	530.581	24.98266	84.41864	18.09076	48.90564	6.035218	32.3932	4.034198
973_florencite - 20	20134.89	29750.35	2083.58	5780.219	681.1568	92.11151	280.5811	13.47757	29.15198	3.843713	6.3708	0.70204	3.625485	0.453738
973_florencite - 21	3290.64	4906.162	377.8252	955.7356	121.7893	12.04264	57.91997	3.038895	9.238339	0.772657	3.607121	0.227346	2.232805	0.109113
973_florencite - 22	4675.545	4740.922	281.6526	742.8355	78.75191	12.01897	27.57081	3.026016	5.4448	0.662318	3.486774	0.143692	2.167598	0.143929
973_florencite - 23	5040.209	7125.835	527.6351	1154.782	160.0253	25.99224	79.19097	2.91943	7.185786	2.145992	3.635779	0.420234	5.925473	0.498175
973_florencite - 24	15065.84	21732.52	1379.925	3579.393	354.31	63.52784	170.4384	8.075499	20.18973	5.362634	13.0547	1.219652	7.6583	0.973334
973_florencite - 25	12592.19	18807.93	1321.186	2867.121	353.3568	54.72204	149.4319	5.805564	19.47964	3.697244	13.29749	0.916585	5.952635	1.302245
973_florencite - 26	33941.26	48191.31	3363.887	8336.527	1024.346	140.3662	406.0664	16.44287	61.88723	15.6799	54.2674	6.992214	35.50628	3.901333
973_florencite - 27	42439.95	59891.26	4071.969	10019.64	1184.129	182.487	515.8626	21.11218	80.41388	16.75344	67.07937	8.36921	44.66275	4.931818
973_florencite - 28	41989.38	59059.94	3994.39	9595.007	1094.153	170.5112	484.1897	21.82829	81.28014	18.92358	62.68339	8.783821	42.78158	5.250211
973_florencite - 29	32338.83	46828.59	3180.598	8115.794	918.2672	134.0419	425.7835	15.19187	47.12052	6.026864	14.17637	2.314445	9.389622	0.81639
973_florencite - 3	35332.13	48857.61	3103.381	7666.926	768.9647	113.3466	335.8528	15.7836	54.33757	12.49768	34.4415	4.441158	18.53837	2.42449
973_florencite - 30	2546.943	4340.054	277.6017	882.6067	84.69265	10.75893	52.09473	3.158938	7.665564	1.698777	6.687448	1.957136	4.372842	0.65208
973_florencite - 31	47944	62516.71	4391.723	10209.94	1134.065	173.3708	530.7389	23.44771	64.93293	10.25295	25.31607	2.743571	16.23809	1.905485
973_florencite - 32	48357.18	66723	4162.46	10032.08	1128.96	152.1338	474.2941	22.51162	82.46332	13.32307	37.23359	4.074502	24.80764	3.807776
973_florencite - 33	43045.63	62616.18	4296.207	9979.586	1073.173	165.8803	470.4581	20.62845	61.81423	10.11782	23.32131	2.671967	14.17877	1.586915
973_florencite - 37	16483.99	21933.53	1458.376	3432.652	383.5979	57.21939	177.4599	8.394201	35.09283	5.700194	24.92109	1.77891	13.82493	1.741288
973_florencite - 38	37928.53	61317.49	4057.996	9800.915	1098.973	172.3835	504.3554	21.6486	54.76897	6.390021	12.28013	1.002398	5.364002	0.650126
973_florencite - 39	11332.11	14573.55	1063.161	2359.696	294.704	51.19594	165.766	5.839366	14.02421	3.13519	9.319942	0.447865	7.163044	1.05044

Caelan Charles Grooby
Geochemistry and Geochronology of an IOCG System: The Vulcan Prospect

973_florencite - 4	44630.19	61951.47	3932.617	9974.938	1105.74	164.7893	488.5001	19.03692	68.39612	13.991	46.56004	5.033539	27.66914	2.758227
973_florencite - 40	11952.91	17697.86	1346.237	3033.002	421.2614	70.90873	159.8562	6.041316	19.31582	3.545194	7.001937	0.576098	2.753595	-0.00513
973_florencite - 41	3184.135	5260.187	360.6318	1029.208	99.86197	21.9115	55.09964	1.729194	6.296613	0.703334	1.912124	0.092813	1.431975	0.011424
973_florencite - 42	38862.4	60752.25	5003.767	10987.13	1107.022	190.2694	495.5105	20.11095	70.64714	13.37666	37.21849	2.826463	14.73725	1.857818
973_florencite - 43	9877.885	15344.94	1104.73	2657.413	337.7063	44.06653	126.3884	7.80729	14.3858	2.427054	9.745391	0.840821	4.465118	0.57206
973_florencite - 44	8104.202	12874.42	924.9621	2571.373	302.0191	51.83008	135.936	7.596552	16.76131	3.445203	6.608292	0.503475	5.173703	0.343811
973_florencite - 45	6528.7	9772.458	882.1817	1319.078	210.0482	32.63627	80.34377	3.437484	14.51833	2.014674	9.476207	1.524111	5.836213	0.518577
973_florencite - 46	57233.93	80106.07	5325.482	11172.64	1453.799	201.3422	633.4553	22.49593	63.21559	11.49537	27.64654	3.354073	11.10848	1.490958
973_florencite - 47	45530.79	70897.28	4995.725	11900.32	1365.321	201.6231	640.8837	21.34696	62.0891	9.798714	21.24131	2.16189	11.10582	1.450899
973_florencite - 48	10252.66	14489.54	972.1418	2642.677	343.6552	35.73407	143.4037	6.528623	20.93164	3.534391	10.826	1.526623	5.950171	0.795947
973_florencite - 49	51395.6	71594.75	4809.969	12914.9	1415.093	212.1785	668.1656	24.63707	55.99459	8.359548	18.39274	1.616384	7.172185	0.81321
973_florencite - 5	23830.34	37363.75	2516.315	6302.385	917.0724	128.9529	618.3505	41.0558	101.4729	15.87875	42.11236	4.612378	20.3337	1.631167
973_florencite - 50	24904.42	40369.59	3040.014	5824.927	740.7519	112.6841	262.4018	18.91339	45.18999	7.529883	16.80599	1.937584	12.69478	2.078487
973_florencite - 52	12796.77	20403.15	1325.788	3307.442	443.3571	65.59788	190.5398	5.866818	15.60417	2.072429	5.196623	0.351371	3.06592	0.224597
973_florencite - 53	56377.77	77065.9	5022.633	12393.23	1513.091	221.8996	637.1275	23.41491	56.92617	7.167993	17.65972	1.681899	9.861997	1.516908
973_florencite - 54	60166.16	84083.15	5378.408	13934.09	1428.464	188.0915	597.7104	26.11208	81.90327	13.78187	34.96617	4.240841	21.84788	2.566039
973_florencite - 55	14601.07	19275.42	1457.881	3182.995	395.7354	56.23037	158.8439	6.298412	26.60845	3.303803	7.996795	1.069744	7.209706	0.132089
973_florencite - 56	60430.46	80218.42	5032.379	12408.35	1261.705	179.2949	525.6873	24.87807	72.58998	9.069626	24.212	2.951387	17.10599	2.176216
973_florencite - 57	55245.5	76565.08	4953.875	11478.85	1256.442	178.2063	529.9514	22.05437	68.38098	10.45691	26.04411	2.81891	14.83125	1.804492
973_florencite - 58	29224.49	42709.64	2806.212	7510.142	910.7421	149.7727	440.6523	18.95467	43.25121	6.305742	14.45939	1.342878	6.92523	1.828065
973_florencite - 6	28182.77	42100.57	2915.733	6991.981	856.8342	123.7323	400.4419	17.34159	39.7376	4.368531	10.4692	0.920289	4.677238	0.409612
973_florencite - 60	12756.21	19036.62	1218.602	2662.864	334.905	62.98713	162.7089	6.57665	21.05588	3.912866	7.849762	1.280867	5.42756	0.612479
973_florencite - 61	45825.31	77885.93	4602.637	13109.66	1433.366	231.3104	684.0412	26.69018	68.119	6.079147	12.45495	0.838339	4.204791	0.48517
973_florencite - 7	30416.85	45122.19	3094.896	7925.988	913.3927	144.54	412.2576	15.84944	46.19612	5.754452	9.208907	1.377938	6.092639	0.535003
973_florencite - 8	25364.3	38914.97	2489.256	6531.669	755.3	105.6956	336.4708	13.33673	35.01082	4.694283	8.955214	0.927309	5.610724	0.29302
973_florencite - 9	31518	49650.11	3397.786	8448.724	958.2719	134.206	449.5199	18.00558	39.28507	6.588936	12.2595	1.374939	4.70134	1.397884
Standards														

NIST610 - 27.csv	439.4771	453	447.0123	430.6843	454.5343	445.1774	451.0738	436.3278	435.4695	447.837	455.7505	434.352	450.3711	438.8765
NIST610 - 28.csv	440.2616	453	448.941	429.9542	453.2955	448.9115	446.6005	436.97	438.5439	450.1955	454.0562	435.6004	449.5595	439.0235
NIST610 - 29.csv	443.0445	453	450.7074	431.5481	458.5339	447.9497	453.0041	439.9073	439.2049	450.1401	458.134	436.7013	450.893	441.3738
NIST610 - 30.csv	437.8755	453	445.1929	427.188	448.6981	446.0032	445.8373	436.1548	434.7511	447.8337	451.7196	433.8098	449.0976	436.4834
NIST610 - 31.csv	439.8126	453	447.5946	428.5887	451.6591	447.2049	448.148	436.0087	435.9029	448.5125	455.2573	434.2044	449.3933	439.883
NIST610 - 32.csv	438.7443	453	448.4207	430.5016	455.4763	446.8367	449.5602	437.186	438.1929	449.4723	454.7525	434.37	450.6328	438.0435
NIST610 - 33.csv	441.6533	453	447.8961	429.0653	453.8779	445.775	449.1238	436.9738	435.8787	449.704	454.4129	435.4406	449.9525	439.5597
NIST610 - 34.csv	439.8921	453	447.9425	433.8648	450.9348	448.1611	449.3218	437.9321	438.0726	448.1969	455.4895	436.0581	449.9781	438.2319
NIST610 - 35.csv	441.4851	453	451.7734	431.757	453.5402	449.583	452.8998	439.1852	439.142	450.5499	457.715	437.6276	451.5712	443.1952
NIST610 - 36.csv	436.7344	453	444.0527	427.1883	445.2765	444.2889	444.6425	433.4559	434.7672	447.3862	452.1758	432.0226	448.3072	434.6139
NIST610 - 37.csv	439.1176	453	448.1227	430.9167	452.4083	447.3852	450.7583	437.3726	437.0402	448.9367	454.8239	435.5063	451.3026	439.1301
NIST610 - 38.csv	441.9237	453	447.8116	428.2926	453.1065	446.5946	445.8509	434.9761	437.0246	449.0672	455.1544	433.741	448.6718	438.8654
NIST610 - 39.csv	440.7034	453	449.3522	429.7033	454.767	447.0326	449.9132	437.2719	435.4256	448.9384	455.5811	435.1862	449.1877	438.9128
NIST610 - 40.csv	440.2026	453	446.624	431.2783	453.9753	447.0175	450.1076	437.02	438.6407	449.0946	454.4307	435.6874	450.7881	439.0588
NIST610 - 41.csv	439.1409	453	447.2612	430.2199	452.5433	445.9497	446.0762	436.6099	437.1892	448.3447	454.2976	434.8607	451.4253	439.7647
NIST610 - 42.csv	439.2316	453	448.7467	428.6858	452.8325	448.091	449.0897	438.4217	436.8094	449.6424	455.7662	434.693	448.4583	438.1089
NIST610 - 43.csv	441.455	453	448.5316	429.9582	454.0399	447.2656	450.9049	438.4215	436.7733	449.8188	454.55	435.7399	450.4905	440.2916
NIST610 - 44.csv	439.2446	453	447.4684	430.605	454.5007	446.7344	449.0875	435.8048	437.2267	448.1812	455.45	434.3988	449.5095	437.7084
NIST610_13 - 1.csv	8193.611	8651.655	8430.561	8103.506	8342.537	8168.685	8205.935	7790.494	7892.256	8004.939	8106.565	7786.907	8161.865	7771.809
NIST610_13 - 10.csv	8110.737	8648.784	8449.384	7900.407	8403.382	8140.891	8144.128	7831.867	7888.296	7967.338	8237.487	7734.813	8138.736	7888.831
NIST610_13 - 11.csv	8040.338	8611.412	8360.369	8058.095	8413.146	8334.506	8195.602	7868.645	7868.856	8075.357	8342.23	7789.21	8071.212	7836.625
NIST610_13 - 12.csv	8134.609	8476.263	8360.276	8238.27	8208.216	8114.346	8194.24	7902.625	7890.424	8074.674	8212.942	7723.997	8096.145	7765.381
NIST610_13 - 13.csv	8181.201	8642.123	8420.486	7904.865	8208.619	8197.331	7921.324	7968.349	8021.459	8079.394	8186.167	7776.112	7987.556	7874.65
NIST610_13 - 14.csv	8117.209	8637.834	8432.446	8236.146	8457.02	8221.624	8147.749	7926.963	7841.388	7998.233	8307.528	7753.554	8139.79	7816.639
NIST610_13 - 15.csv	8195.468	8690.831	8462.301	8111.075	8595.009	8224.942	8119.665	7897.854	7913.998	8078.939	8084.897	7721.538	8017.304	7792.328
NIST610_13 - 16.csv	8052.332	8626.516	8356.489	7795.811	8387.031	8135.648	8067.142	7811.035	7893.342	7955.057	8127.241	7737.261	7960.83	7769.209
NIST610_13 - 17.csv	8191.248	8691.629	8458.26	8204.579	8515.818	8333.776	8258.448	8012.974	7890.619	8037.93	8077.359	7794.46	8087.5	7806.906

NIST610_13 - 18.csv	8155.468	8612.802	8315.553	7816.352	8354.848	8040.923	8379.207	7747.541	7747.736	8035.973	8206.42	7617.269	7874.058	7790.342
NIST610_13 - 2.csv	8264.465	8649.501	8388.811	8102.76	8338.525	8118.012	8083.691	7888.334	7965.119	8110.538	8043.33	7770.238	8030.262	7849.558
NIST610_13 - 3.csv	8288.197	8669.101	8368.356	7878.318	8365.394	8246.289	8061.532	7880.132	7922.612	8001.608	8112.078	7816.133	8095.089	7842.86
NIST610_13 - 4.csv	8094.221	8595.044	8396.999	7876.88	8434.73	8057.317	7835.486	7758.532	7841.829	7947.485	8052.969	7720.573	8161.728	7716.099
NIST610_13 - 5.csv	8195.249	8664.429	8386.003	8013.802	8323.084	8224.405	8123.964	7892.176	7726.031	8107.211	8112.95	7629.457	8057.802	7849.203
NIST610_13 - 6.csv	8172.869	8680.919	8380.111	7851.884	8584.23	8189.195	7965.335	7802.002	7835.854	7972.967	8287.412	7779.788	8013.219	7768.471
NIST610_13 - 7.csv	8176.499	8554.872	8302.852	8110.178	8368.694	8131.728	8057.626	7909.355	7838.748	7957.253	8108.408	7892.199	7950.2	7883.845
NIST610_13 - 8.csv	8198.484	8746.659	8371.16	7994.376	8308.012	8280.28	8042.213	7874.223	7982.494	7966.583	8333.305	7793.554	8113.057	7836.906
NIST610_13 - 9.csv	8306.601	8567.264	8338.873	8157.969	8398.082	8216.827	8118.618	7817.644	7912.498	7969.433	8123.739	7704.579	8083.924	7854.055